Contributions to the robust stabilization of networks of hyperbolic systems

Jean Auriol

université PARIS-SACLAY

Habilitation à diriger des recherches

Contributions to the robust stabilization of networks of hyperbolic systems

Contributions à la stabilisation robuste de réseaux de systèmes hyperboliques

Habilitation à diriger des recherches de l'Université Paris-Saclay

présentée et soutenue à Paris-Saclay, le 10 janvier 2024, par

Jean AURIOL

Composition du jury

Yacine CHITOUR Professeur, Université Paris-Saclay, Laboratoire des Signaux et Systèmes	Rapporteur
Jean-Michel CORON Professeur, Laboratoire Jacques-Louis Lions, Université Pierre et Marie Curie	Rapporteur
Sabine MONDIE Professeur, Departamento de Control Automatico, CINVESTAV	Rapporteure
Christophe PRIEUR Directeur de Recherches CNRS, Gipsa-Lab	Président du jury
Lucie BAUDOUIN Directrice de Recherches CNRS, LAAS CNRS,	Examinatrice
Mohammed CHADLI Professor, Université Paris-Saclay, IBISC, University of Evry Val d'Essone	Examinateur
Wim MICHIELS Professeur, Numerical Analysis and Applied Mathematics (NUMA) Centre	Examinateur
Nathan VAN DE WOUW Professeur, Department of Mechanical Engineering, Eindhoven University of Technology	Examinateur

université PARIS-SACLAY

ÉCOLE DOCTORALE
Sciences et technologies de l'information et de la communication (STIC)

Titre: Contributions à la stabilisation robuste de réseaux de systèmes hyperboliques.
Mots clés: EPDs hyperboliques, réseaux, backstepping, équations à retards intégrales, systèmes à retards, équations intégrales.

Résumé:

Les réseaux de systèmes hyperboliques, éventuellement couplés à des équations différentielles ordinaires (ODE), constituent une représentation essentielle pour décrire une grande variété de systèmes complexes, pouvant modéliser la propagation d'ondes, des systèmes de trafic routier, des dispositifs de forage ou des réseaux de communication. Le contrôle et l'estimation d'état pour de tels systèmes sont des problèmes difficiles en raison de la nature distribuée des différents sous-systèmes composant le réseau (dépendance temporelle et spatiale), de la structure de graphe possiblement intriquée du réseau et de l'impossibilité physique/économique de placer des capteurs et actionneurs en tout point du domaine spatial. Ce manuscrit présente quelques contributions récentes concernant la stabilisation robuste des réseaux de systèmes hyperboliques. Nous montrons d'abord qu'en utilisant des transformations de backstepping appropriées, la classe de réseaux que nous considérons peut-être réécrite comme un ensemble d'équations à retards intégrales. Sous certaines hypothèses structurelles, cette nouvelle forme se prête mieux à la synthèse de lois de commande stabilisantes. Nous nous concentrons ensuite sur les réseaux avec une structure de chaîne afin de proposer de nouvelles méthodologies dépassant les limitations structurelles rencontrées précédemment. Nous considérons dans un premier temps le cas où les actionneurs et les capteurs sont disponibles à une extrémité de la chaîne. En introduisant des prédicteurs d'état, nous présentons une approche récursive permettant de stabiliser l'ensemble de la chaîne. Nous nous intéressons ensuite au cas où les actionneurs et capteurs ne sont disponibles qu'à la jonction entre deux sous-systèmes composant la chaîne. Nous montrons qu'une telle configuration ne garantit pas systématiquement la contrôlabilité de la chaîne. À l'aide de conditions de contrôlabilité/observabilité adéquates, nous proposons des lois de commande stabilisantes simples en utilisant un nouveau type de transformation intégrale. Enfin, nous illustrons comment nos résultats s'appliquent à deux cas d'étude : l'estimation de la vitesse d'une tête de forage et la stabilisation de deux segments d'autoroute en cascade. Nous concluons le manuscrit en donnant quelques perspectives générales.

Title: Contributions to the robust stabilization of networks of hyperbolic systems.
Keywords: hyperbolic PDEs, networks, backstepping, integral delay equations, time-delay systems.

Abstract: Networks of hyperbolic systems, possibly coupled with ordinary differential equations, constitute an essential paradigm to describe a wide variety of large complex systems, including wave propagation, traffic network systems, drilling devices, or communication networks. Controlling and monitoring networks of hyperbolic systems are difficult control engineering problems due to the distributed nature of the different subsystems composing the network (time and space dependency), the possibly involved graph structure of the network, and the physical/economic infeasibility of placing sensors and actuators everywhere along the spatial domain.

This manuscript presents some recent contributions to the robust stabilization of networks of hyperbolic systems. We first show that using appropriate backstepping transformations, the class of networks under consideration can be rewritten as a set of Integral Delay Equations. This new form is more amenable to the design of stabilizing output feedback control laws under structural assumptions. We then focus on networks with a chain structure to derive new methodologies that overcome the previously encountered structural limitations. We first consider the case where the actuators and sensors are available at one end of the chain. Using appropriate state predictors, we present a recursive approach to stabilize the whole chain. Then, we focus on the case where the actuators and sensors are only available at the junction between two subsystems composing the chain. We show that such a configuration does not always guarantee the controllability of the chain. Under appropriate controllability/observability conditions, we will design simple stabilizing control laws using a new type of integral transformation. Finally, we illustrate how our results apply to two test cases: estimating the drill bit source signature in a drilling device and stabilizing two cascaded freeway segments. We conclude the manuscript by giving some general perspectives.

Remerciements

En premier lieu, je tiens à remercier Yacine Chitour, Jean-Michel Coron et Sabine Mondié, qui m'ont fait l'honneur d'accepter d'être rapporteurs de ce manuscrit. Merci également à Lucie Baudouin, Mohammed Chadli, Wim Michiels, Christophe Prieur et Nathan Van de Wouw d'avoir participé à mon jury de soutenance. Vos questions et précieux commentaires ont considérablement contribué à l'amélioration de ce manuscrit et m'ont fourni de nouvelles pistes de recherches.

Je remercie tous les membres du L2S (et son directeur Pascal), en particulier l'équipe administrative et technique : Audrey, Stéphanie, Catherine, Caroline, José, Joëlle, Anne-Elysabeth, Khaldoun, Christian. Je remercie en particulier tous mes collègues du *Pôle Automatique et Systèmes* du L2S : Thiago, Nina, Riccardo, Frédéric, Catherine, Islam, Andrei, Lucas, Antoine, Yacine, Sette, Didier, Stéphane, Antoine, Luca, Alessio, Ziad, Françoise, Hugo, Antonio, Maria, Paolo, Guilherme, Frédéric, Hugues, Silviu, Dorothée, Sorin, Elena, William, Laurent, Dario, Pedro, Guillaume, Adnane, Houria, Cristina, Sihem, Sami, Giorgio et Cristina. Merci à tous les doctorants et postdoctorants du laboratoire. Un grand merci en particulier à tout le groupe des jeunes recrutés auquel j'ai la chance d'appartenir. Soyez assurés que je ne manquerai pas votre pot de soutenance lorsque votre tour viendra. Vous contribuez à faire du L2S un lieu agréable, combinant exigence académique (oui, je pense au Pazy de Riccardo), bonne entente (merci d'avance à celui qui me remplacera sur le prochain TD où je serai absent), et grande convivialité (les gâteaux alsaciens de Laurent et de sa maman en sont un excellent exemple).

Je remercie tous mes collaborateurs qui ont contribué aux travaux présentés dans ce manuscrit : U. J. Aarsnes, L. Brivadis, D. Bou Saba, I. Boussaada, D. Bresch-Pietri, F. Bribiesca-Argomedo, J. Curkan, M. Di Loreto, F. Di Meglio, N. Espitia, I. Gates, K. Innanen, P. O. Lamare, Y. Le Gorrec, N. Kazemi, B. Kulcsar, M. Krstic, P. Martin, K. Morris, S.-I. Niculescu, M. Pereira, J. Redaud, R. Shor, R. Vazquez, Y. Wu, H. Yu. Federico, si tu ne sais pas quoi faire de l'argent restant sur ton projet européen, je suis prêt à t'aider. Je remercie particulièrement Jeanne et Gabriel que j'ai pu encadrer dans leur travail de doctorat et qui m'ont grandement motivé à défendre cette habilitation. Merci également aux postdoctorants (actuels ou futurs collègues !) avec qui j'ai eu le plaisir de collaborer Lucas et Ismaïla. Merci à tous les stagiaires que j'ai pu encadrer. La recherche a besoin de cette force vive !

Mes remerciements vont également à tous ceux qui étaient présents lors de ma soutenance en dépit du froid mordant qui pouvait régner sur le plateau de Saclay ce jour là. Merci en particulier à tous les membres présents du Centre Automatique et Systèmes de l'Ecole des Mines (Pauline, Delphine, Florent et Nicolas) d'avoir quitté pour l'espace d'une journée le 5ème arrondissement pour une petite visite du plateau. Les discussions qui ont suivies lors du pot n'étaient pas sans rappeler mes belles années de thèse. Merci à Marine, d'être venue voir son ancien prof de TD (et accessoirement beau-frère) alors qu'avait lieu une course de biathlon à la même heure ! Merci à Guillaume d'être venu du CEA, quittant ainsi l'espace d'un instant l'univers de la physique pour des questions de théorie des opérateurs. Merci à Céline d'avoir fait l'effort d'assister une présentation mathématique sans même avoir pu profiter du pot ! Mon filleul et son frère ne se rendent pas encore compte du grand sacrifice que leur mère fit pour eux. Merci à Mike qui n'a pu venir en raison d'un genou défaillant et à Jay-Bee occupé à sauver l'OL (et pourtant il n'avait pas bridge ce jour-là). Merci à François qui m'a promis de fêter ça à Fontainebleau. Merci enfin à tous ceux qui étaient connectés en ligne et dont je n'ai pu voir les noms.

Je voudrais remercier les membres de ma famille au sein de laquelle je compte certains de mes plus grands admirateurs scientifiques (malheureusement ce ne sont pas eux qui relisent mes papiers). Si cela n'avait tenu qu'à eux, j'aurais eu ce diplôme sans avoir besoin de rédiger le manuscrit ! Je regrette qu'ils ne soient pas en charge des comités éditoriaux ou des jurys de concours !

Enfin, un immense merci à mon épouse Clotilde, support moral indéfectible. Même si tu ne goûtes pas (encore) aux joies des Lyapunofferies ou des transformations de backstepping, ton écoute quotidienne et ton assistance permanente (je sais que t'es là pour m'aider) font de toi mon rempart et mon salut. Et puis, n'oublions pas que le pot auquel tu as contribué a reçu les louanges des plus grands !

Contents

Notations and symbols

The following list describes several symbols that will be later used within the body of the document. The parameters n, m, p, q are positive integers, while $a < b$ are real numbers. Most of the definitions directly extend for $b = +\infty$.

$\mathbb{R}^n$	n^{th} dimensional Euclidean space.
$\mathbb{C}^n$	n^{th} dimensional complex space.
$\mathbb{R}^{n\times m}$	The set of real-valued matrices of dimensions $n \times m$.
$\mathbb{R}^+$	The set of non-negative real numbers.
$\mathbb{C}^{n\times m}$	The set of complex-valued matrices of dimensions $n \times m$.
$\mathbb{K}^{n\times m}$	Can either be $\mathbb{C}^{n\times m}$ or $\mathbb{R}^{n\times m}$.The associated norm is denoted $\|\|\cdot\|\|$. For any $X \in \mathbb{K}^n$, $\|\|X\|\| = \sqrt{\sum_{i=1}^{p} \|X_i\|^2}$.
$\|a\|$	The absolute value of a.
v_i	For $v \in \mathbb{K}^n$, the i^{th} entry of the vector v.
$\mathsf{Re}(s)$	Real part of $s \in \mathbb{C}$.
$\mathsf{Im}(s)$	Imaginary part of $s \in \mathbb{C}$.
$\mathbb{C}^+$	Open complex right half plane: $\mathbb{C}^+ = \{z \in \mathbb{C},\ \mathsf{Re}(z) > 0\}$.
$\mathbb{C}_a$	The space $\{z \in \mathbb{C},\ \mathsf{Re}(z) \geq -a\}$.
Id_n	The identity matrix of dimension n (denoted Id if no confusion arises).
$M^\top$	The transpose of a matrix $M \in \mathbb{K}^{n\times m}$.
$M_{i,j}$	For $M \in \mathbb{K}^{n\times m}$, the $(i,j)^{\text{th}}$ entry of the matrix M.
$Sp(M)$	The spectral radius of a matrix $M \in \mathbb{K}^{n\times m}$.
$\bar{\sigma}(M)$	The largest singular value of $M \in \mathbb{K}^{n\times m}$.
$\underline{\sigma}(M)$	The smallest singular value of $M \in \mathbb{K}^{n\times m}$.
$\operatorname*{ess\,sup}_{x\in[a,b]} f$	Essential supremum of a function f defined on $[a,b]$.
$C^p([a,b],\mathbb{K}^n)$	Space of $\mathbb{K}^n$-valued functions that are p times continuously differentiable on $[a,b]$.

$L^p([a,b],\mathbb{K}^n)$ Space of $\mathbb{K}^n$-valued functions whose p^{th} power is integrable on $[a,b]$.
The associated norm is denoted $||\cdot||_{L^p}$
For any $f \in L^p([a,b],\mathbb{K}^n)$, $||f||_{L^p} = (\int_a^b ||f(t)||^p dt)^{\frac{1}{p}}$.

$L^\infty([a,b],\mathbb{K}^n)$ Space of $\mathbb{K}^n$-measurable functions bounded almost everywhere on $[a,b]$.
The associated norm is denoted $||\cdot||_{L^\infty}$
For any $f \in L^\infty([a,b],\mathbb{K}^n)$, $||f||_{L^\infty} = \underset{x\in[0,1]}{\text{ess sup}}||f(x)||$.

$H^1([a,b],\mathbb{R})$ One-dimensional Sobolev space: the subset of functions f in $L^2([a,b],\mathbb{R})$ such that f and its weak derivative of order 1 have a finite L^2 norm.
The associated norm is denoted $||\cdot||_{H^1}$.
For any $f \in H^1([a,b],\mathbb{R})$, $||f||_{H^1} = \sqrt{\int_a^b (f(t))^2 + (f'(t))^2 dt}$.

$\mathbb{1}_\Omega$ Characteristic function of the set $\Omega \subseteq \mathbb{R}$: $\mathbb{1}_\Omega(\theta) = \begin{cases} 1 & \text{if } \theta \in \Omega \\ 0 & \text{else.} \end{cases}$

$\partial_y f$ Partial derivative of a function f with respect to the variable y.

$\dot{f}$ Time-derivative of a function of time f.

s The Laplace variable.

$\mathbf{f}(s)$ The Laplace transform of a function $f(t)$ (provided it is well defined).
If no confusion arises, it will be denoted $f(s)$.

$\delta(\cdot)$ The Dirac distribution.

$\mathcal{A}(0)$ Wiener algebra: convolution Banach algebra of BIBO-stable generalized functions in the sense of [Vid72]. A function $f(\cdot)$ belongs to $\mathcal{A}(0)$ if it can be expressed as $f(t) = f_r(t) + \sum_{i=0}^{\infty} f_i \delta(t-t_i)$, where $f_r \in L^1(\mathbb{R}^+,\mathbb{R}), \sum_{i\geq 0} |f_i| < \infty$, $0 = t_0 < t_1 < \dots$.

$\mathcal{A}(\beta)$ If we only have $\mathrm{e}^{-\beta t} g_r \in L^1(\mathbb{R}^+,\mathbb{R})$ (β being a real), then we say that $g \in \mathcal{A}(\beta)$. The associated norm is $||g||_{\mathcal{A}} = ||g_r||_{L^1} + \sum_{i\geq 0} |g_i|$.
An input-output linear system given in the form of a convolution, $y = h \star u$ is BIBO-stable if its kernel h belongs to the class $\mathcal{A}$.

$\hat{\mathcal{A}}(0)$ Banach space of Laplace transforms of elements in $\mathcal{A}(0)$.
The associated norm is $||\hat{g}||_{\hat{\mathcal{A}}(0)} = ||g||_{\mathcal{A}(0)}$.

$\hat{\mathcal{A}}_-(0)$ Subalgebra of $\hat{\mathcal{A}}(0)$ such that $\hat{\mathcal{A}}_-(0) = \{\mathbf{f} \,|\mathbf{f} \in \hat{\mathcal{A}}(\beta), \text{ for some } \beta < 0\}$.

$\hat{\mathcal{A}}_\infty(0)$ Subalgebra of $\hat{\mathcal{A}}(0)$ such that $\hat{\mathcal{A}}_\infty(0) = \{\mathbf{f} \,|\mathbf{f} \in \hat{\mathcal{A}}_-(0), \inf_{s\in\bar{\mathbb{C}}^+, |s|\geq\rho} |\mathbf{f}(s)| > 0 \text{ for some } \rho > 0\}$.

$\hat{\mathcal{B}}(0)$ Callier Desoer class of transfer functions: quotient algebra $\hat{\mathcal{A}}_-[\hat{\mathcal{A}}_\infty(0)]^{-1}$.

diag(a_i) For $1 \leq i \leq n$, $a_i \in \mathbb{R}$, diagonal matrix of dimensions n with diagonal entries given by a_i.

diag(M,N) For $M \in \mathbb{R}^{m\times m}$, $N \in \mathbb{R}^{n\times n}$, the block diagonal matrix of dimensions $m+n$ with diagonal blocks given by M and N.

$\mathcal{T}_u$	Upper unit triangular domain: $\mathcal{T}_u = \{(x,y) \in [0,1]^2,\ x \leq y\}$.
$\mathcal{T}_\ell$	Upper unit triangular domain: $\mathcal{T}_\ell = \{(x,y) \in [0,1]^2,\ x \geq y\}$.
$\mathcal{U}$	Unit square: $\mathcal{U} = \{(x,y) \in [0,1]^2\}$.
$\phi_{[t]}(\theta)$	Partial trajectory of the function $\phi : [-\tau, \infty) \mapsto \mathbb{K}^m$ (with $\tau > 0$ and $-\tau \leq \theta \leq 0$). We have $\phi_{[t]}(\theta) = \phi(t+\theta)$.
$L^2([-\tau,0],\mathbb{K}^n)$	Banach space of L^2 functions mapping the interval $[-\tau,0]$ into $\mathbb{K}^n$. The associated norm is denoted $\|\cdot\|_{L^2_\tau}$ For any $\phi_{[t]} \in L^2([-\tau,0],\mathbb{K}^n)$, $\|\phi_{[t]}\|_{L^2_\tau} = (\int_{-\tau}^0 \|\phi(t+s)\|^2 dt)^{\frac{1}{2}}$. When no confusion arises, this space will be denoted L^2_τ.
$H^1([-\tau,0],\mathbb{R})$	Banach space of H^1 functions mapping the interval $[-\tau,0]$ into $\mathbb{R}$. The associated norm is denoted $\|\cdot\|_{H^1_\tau}$.For any $\phi_{[t]} \in H^1_\tau([-\tau,0]$ $,\mathbb{R}), \|\phi_{[t]}\|_{H^1_\tau} = \sqrt{\int_a^b (\phi(t+s))^2 + (\phi'(t+s))^2 dt}$.
$C^{pw}([-\tau,0),\mathbb{R}^n)$	Banach space of piecewise continuous functions mapping the interval $[-\tau,0)$ into $\mathbb{R}^n$. It will be denoted C^{pw}_τ when no confusion arises.
$D^+v(\varphi_{[t]})$	Dini upper right-hand derivative of a functional $v(\varphi_{[t]})$

Acronyms

ARZ Aw-Rascle-Zhang.

BCS Boundary Control System

BIBO Bounded-Input Bounded-Output

BHA Bottom Hole Assembly

DHCS District Heating and Cooling Systems.

HPDE Hyperbolic Partial Differential Equation.

IDE Integral Delay Equation.

ISS Input-to-State Stability.

LWR Lighthill–Whitham–Richards.

ODE Ordinary Differential Equation.

PDE Partial Differential Equation.

PHS Port-Hamiltonian Systems.

RHF Right Half Plane.

SDE Stochastic differential equations.

SNR Signal-to-Noise Ratio.

SWD Seismic While Drilling

UAV Unmanned Aerial Vehicles

UCS Uniaxial Compressive Strength

Part I

Presentation of the candidate

1 - Curriculum Vitae

Jean AURIOL

1.1 . Contact information

Nationality: French
Phone: +33 6 70 59 18 04
E-mail: jean.auriol@l2s.centralesupelec.fr
Address: Laboratoire des Signaux et Systèmes,
CentraleSupélec, 3 rue Joliot Curie,
91192 Gif-sur-Yvette, France
Web page: https://l2s.centralesupelec.fr/u/auriol-jean/
CV HAL: https://cv.archives-ouvertes.fr/jean-auriol

Civil engineer from Ecole des Mines
Ph.D. in applied mathematics and control theory from Ecole des Mines, PSL Research University.

1.2 . Current Position

CNRS Researcher (Chargé de Recherches Classe Normale, CRCN) since **December 2019**, Université Paris-Saclay, CNRS (UMR 8506), CentraleSupélec, Laboratoire des Signaux et Systèmes (L2S), UMR CNRS 8506, Gif-sur-Yvette, France.

Research interests:

- Practical control of networks of hyperbolic systems.
- Control of underactuated infinite-dimensional systems (hyperbolic equations and time-delay systems of neutral form) using integral equations.
- Efficient and Reliable control of coupled Stochastic and Partial differential Equations.
- Stabilization of mechanical vibrations in drilling devices.
- Neural networks-based estimators for infinite-dimensional systems.
- Adaptive control of neural fields.
- Traffic estimation and regulation.

Keywords: Distributed Parameter Systems, output feedback control, robustness, networks, Lyapunov analysis, time-delay systems, neutral systems, distributed delays, backstepping, mechanical vibrations, drilling, traffic networks, neural fields, integral equations

1.3 . Education

2015-2018 **Ph.D. in Control Theory and Applied Mathematics**
CAS (*Centre Automatique et Systèmes*).
MinesParis, PSL Research University, France.
Title: *Robust design of backstepping controllers for systems of linear hyperbolic PDEs*.
Advisors: Dr. Florent Di Meglio, Prof Nicolas Petit.
Committee: Prof. Y. Le Gorrec (Examiner, President), Prof. K. Morris (Examiner), DR. S.-I. Niculescu (Examiner), Prof. A. Pavlov (Referee), Prof. R. Vazquez (Referee).

2012-2015 **Mines Paris engineer**
MinesParis, PSL Research University, France.
Master in Science and Executive Engineering.
Specialization in Applied Mathematics and Control Theory.
Mention: Excellent (highest honours).
Main courses: control theory, optimization, diff. calculus.

1.4 . Professional experience

10/2018-12/2019 - **Dep. of Chemical and Petroleum Engineering**, University of Calgary, Canada.
Postdoctoral fellow in Roman Shor's team.
Subject: Estimation and control of subsurfaces process during drilling operations.

05/2017-07/2017 - **Dep. of Applied Mathematics**, University of Waterloo, Canada.
Research stay under the supervision of Kirsten Morris.
Subject: Comparison of early-lumping and late-lumping approaches for the design of state-feedback controllers for infinite dimensional systems.

01/2015-06/2015 - **Kelda Drilling Control**, Porsrunn, Norway.
Research internship under the supervision of Glenn-Ole Kaasa.
Subject: Stabilization of the pressure in a drilling device.

06/2014-09/2014 - **UCLA**, Electical Engineering Department, Los Angeles United States of America.
Research internship under the supervision of Paulo Tabuada and Suhas Digavi.
Subject: Observer design for traffic network systems.

09/2013-02/2014 - **Centre Automatique et Systèmes**, Mines ParisTech, France.
Research internship under the supervision of Nicolas Petit.
Joint work with Fluigent.
Subject: Pressure control in a water tank with applications in microfluidics.

1.5 . Publications (quantitative overview)

- **Author/co-author** of **59 publications**:
  - **27 publications** in international journals with reviewing committees (8 additional publications are under review).
  - **27 publications** in international conferences with reviewing committees (2 additional publications is under review).
  - **1 Edited Volume** in the Springer series *Advances in Delays and Dynamics*.
  - **2 chapters** in collaborative books (1 chapter under revision).

- **1 Patent** (US Patent 11725499, accepted in 2023).
- **1 Ph.D. thesis**.

- **H-index:** 14, **Index i10:** 19 , 722 citations (December 20^{th} 2023) according to *Google Scholar* (GS).
- **Most cited publication**: J. Auriol, F. Di Meglio, *Minimum time control of heterodirectional linear coupled hyperbolic PDEs*, Automatica, vol. 71, p.300-307, 2016 (GS: 115 citations).

Category	Published	Submitted	**Total**
International journals	27	8	35
International conferences	27	2	29
Edited Volumes	1	0	1
Book chapters	2	1	3
Patents	1	0	1
Thesis	1	0	1
Total	59	11	70

Table 1.1: Quantitative overview of J. Auriol's publications.

1.6 . Scientific Animation

1.6.1 . Current activities

- **Member** of Equipe de Pilotage du **GDR MACS**, in charge of Young Researchers (2024-2028).
- **Member** of the **IFAC Technical Committee 2.2** on *Linear Control Systems* (2019-now).
- **Member** of the **IFAC Technical Committee 2.6** on *Distributed Parameter Systems* (2019-now).
- **Member** of the **IEEE Technical Committee** on *Distributed Parameter Systems* (2019-now).
- **Organizer** of the *PhD students seminars* of the "pôle Automatique" of the Laboratoire des Signaux et Systèmes.
- **Organizer** of the *Infinite-dimensional workshops* of the "pôle Automatique" of the Laboratoire des Signaux et Systèmes.

1.6.2 . Past activities

- **Member of the International Program Committee** (IPC) for the 4^{th} IFAC Workshop on Control of Systems governed by Partial Differential Equations, CPDE (**2022**).
- **Co-organizer** of the 3^{rd} DECOD workshop, **23-26 November 2021**, Gif-sur-Yvette, France, 70 attendees. Organizing committee: Jean Auriol, Guilherme Mazanti, Giorgio Valmorbida.
- **Founder and Organizer** of the *Distributed Parameters Systems online seminars,* with Federico Bribiesca-Argomedo, and Rafael Vazquez (**2020-2021**).
- **Organizer** of the bi-monthly *laboratory scientific workshops* of Centre Automatique et Systèmes (**2016-2018**).
- **Member** of the *Research Committee* of MinesParis (**2017-2018**).
- **Member** of the *Doctoral School SMI Committee* (Sciences et Métiers de l'Ingénieur) (**2017-2018**).

1.7 . Editorial activities

- **Associate Editor** for *Systems & Control Letters*, SCL (**2023-now**).
- **Associate Editor** for the European Control Conference, ECC (**2023-now**).
- **Associate Editor** for the 4^{th} IFAC Workshop on Control of Systems governed by Partial Differential Equations, CPDE (**2022**).
- **Main Editor** of the volume *Advances in Distributed Parameter Systems* the Springer series *Advances in Delays and Dynamics*, vol 14, **2021**.
- **Associate Editor** for the the 3^{rd} DECOD workshop (**2021**).
- **Associate Editor** for the 24^{th} International Conference on System Theory, Control and Computing, ICSTCC (**2020**).
- **Reviewer** for books, international journals, and international conferences with reviewing committee.
  - **Books:** Springer.
  - **Journals:** Automatica, IEEE Transactions on Automatic Control, Systems & Control Letters, IEEE Transactions on Control Systems Technology, Journal of the Franklin Institute, Journal of Process Control, SIAM Journal of Applied Mathematics, European Journal of Control, International Journal of Robust and Nonlinear Control, Journal of Differential Equations, etc.
  - **Conferences:** IEEE Conference on Decision and Control (CDC), IEEE American Control Conference (ACC), IFAC World Congress, European Control Conference (ECC), International Symposium on Mathematical Theory of Networks and Systems, IFAC Workshop on Control of Systems governed by Partial Differential Equations, etc.
- **Reviewer** for the French Agence Nationale de la Recherche (ANR).

1.8 . Awards and distinctions

- Supervisor of J. Redaud, who was nominated (accessit) for the **Ph.D. award** of the doctoral school STIC of Université Paris Saclay, 2022.
- Supervisor of J. Redaud, who received **TDS 2021 best student paper award** for the paper co-authored with J. Auriol and S.-I. Niculescu entitled *Observer design for a class of delay systems using a Fredholm transform* and presented at the 16^{th} IFAC workshop on time-delay systems, Guangzhou, China, 2021.
- Nominated (finalist) for the **best Ph.D. award** of the GDR MACS and la Section Automatique du Club EEA, 2018.
- **Outstanding Reviewer** of the year 2017 for the journal *Automatica*.

1.9 . Research projects and international collaborations

1.9.1 . Research collaborations

- **35 co-authors** from **11 countries**.
- **22 invitations** to give seminars (in more than seven countries).
- **Main current collaborations:**

- Collaboration with the **International Research Laboratory on Learning Systems** (Canada), on the problems of *physics-informed transformer-based neural networks for estimation of infinite-dimensional systems dynamics* (3 months student exchange, **2022**).
- Collaboration with S. Mondié from **CINVESTAV-IPN**, on the questions of *stability for neutral equations with distributed delays* (student exchanges, **2022**).
- Collaboration with B. Kulcsár from the Automatic Control group of **Chalmers University of Technology**, Sweden, and M. Pereira from the Geostatistics Group of the Geosciences department of **MinesParis**, France, on the questions related to the *stochastic control of traffic networks* (10 days stays in **2022** and **2023**, visit of a Ph.D. student expected, one paper presented during the the IFAC World Congress).
- Collaboration with R. Shor and S. Swaroop Kandala from **University of Calgary**, Canada, on the questions of *adaptive state estimation for drilling devices* (visits in **2019, 2022**, several joint publications).
- Collaboration with N. Kazemi from **Université du Québec à Montréal**, Canada, on the questions of *machine learning-based estimation of drilling parameters*, and *seismic-while drilling estimation techniques* (visits in **2022**, several joint publications).
- Collaboration with M. Krstic and H. Yu from the **University of San Diego**, United States, on the questions related to the *control of traffic networks* (fifteen days long visit in **2020**, three publications). Creation of a CNRS International Research Network (**IRN "PheSTiNS"**).
- Collaboration with K. Morris from the **University of Waterloo**, Canada, on the questions of *model reductions for output-feedback controllers for infinite dimensional systems* (visits in **2017** and **2019**, 5 months in total). Creation of a CNRS International Research Network (**IRN "PheSTiNS"**).
- Collaboration with Y. Le Gorrec and Y. Wu from **FEMTO-ST**, France, on the questions of *damping assignment and performance specifications for infinite-dimensional systems* (regular stays in **2020** and **2021**, two publications + one submission, CNRS project submission).
- Collaboration with N. Espitia from the **CRIStAL** laboratoy, France, on the questions related to *event-triggered control* (visits in **2020** and **2021**, two publications).
- Collaboration with F. Bribiesca-Argomedo and M. Di Loretto from **Ampère laboratoy**, INSA Lyon, France, on the questions related to the *control of networks of Partial Differential Equations* (regular visits in **2017**, **2020-2023**, several joint publications).
- Collaboration with D. Bresch-Pietri from **MinesParis**, France, on the questions of *Lyapunov analysis for neutral time-delay systems*, and *robust stabilization of systems with stochastic input delays* (regular visits in **2022, 2023**, two publications).

1.9.2 . On-going research projects

1. **Coordinator of the Young Researcher Project (JCJC) PANOPLY**

   - Subject: PrActical control of Networks Of hyPerboLic sYstems.
   - Funding: Agence Nationale de la Recherche (ANR), 250k€.
   - Duration: 4 years starting from March 2024.
   - Collaboration: J. Auriol, F. Bribiesca-Argomedo (INSA Lyon), S. Tliba (L2S), L. Brivadis (L2S), Y. Wu (FEMTO-ST).
   - Summary of the proposal: This project aims to develop an advanced systematic framework for the practical control of networks of linear hyperbolic systems. Graphs can describe such networks: each node corresponds to an elementary hyperbolic subsystem, and each edge corresponds to the interconnection between the different subsystems. The first objective is understanding the links between the network structure (nb of cycles, incidence matrix) and its controllability/observability (C/O) properties. We aim to characterize the configurations for a given graph structure that

guarantees C/O. To identify reflections of graph-theoretic notions on the system properties, we will use the concepts of structural controllability and controllability of multi-agent systems as a starting point. The second objective is to develop generic analytical techniques to quantify closed-loop performances with respect to industry-inspired performance indices. This is crucial to optimize actuators/sensors placement and to tune the controllers we will design. Finally, we aim to design modular, scalable, and numerically implementable output feedback controllers for an admissible configuration of actuators and sensors. The design must introduce degrees of freedom to guarantee potential trade-offs with respect to implementation constraints. The proposed methodology will be based on a graph representation of the network and its systematic structural analysis. It will also use recent results obtained for simple networks showing strong relations between spectral controllability and the existence of a solution for a set of appropriate integral Fredholm equations, from which it is possible to derive explicit controllers. To validate our theoretical results and compare them to conventional strategies, we will benchmark them on an experimental test case that presents several specifications. This test case corresponds to the active control of vibrations in mechanical structures equipped with piezoelectric actuators.

2. **Coordinator of the CNRS "Projet Emergence" AURA**

   - Subject: Approche mUltiphysique pour la Recherche de systèmes cibles par bAckstepping.
   - Funding: CNRS, 6500€.
   - Duration: 1 year starting from January 2023.
   - Collaboration: J. Auriol, Y. Le Gorrec (FEMTO-ST), Y. Wu (FEMTO-ST).
   - Summary of the proposal: The main scientific objective of this project is to propose a structural representation of the physical phenomena involved in the dynamics of linear hyperbolic systems using Port Hamiltonian Systems (PHS). Such a representation facilitates stability analysis and will allow the definition of a class of target systems for the backstepping method that are both reachable and easily configurable. This will lead to the introduction of degrees of freedom while designing control laws for infinite-dimensional systems, thus allowing trade-offs between various performance indices. This project implies members of the FEMTO-ST laboratory (in Besançon) with expertise in PHSs. An experimental test device is also available. Funding for the project covers missions between Paris and Besançon, participation in a conference, and an M2 research internship.

3. **Member of the IRN project PheSTInS**

   - Subject: Phénomènes Spatiaux-Temporaux et Interconnexions des Systèmes.
   - Funding: CNRS, 30k€.
   - Role: Coordinator of a *Coordinated Research Action* (CoRA): AI and control of infinite-dimensional systems. Participation in CoRA 1 (Inhomogeneity in space/time and nonlinear control) and CoRA 2 (Delay, Transport, and Propagation).
   - Duration: 5 years starting from January 2024.
   - Collaboration: More than 60 researchers, postdocs, and Ph. D. students from France, the United States, and Canada.
   - Summary of the proposal: The "PheSTInS" network has three objectives. The first consists of making progress in analyzing and controlling infinite dimensional dynamical systems. These topics are at the interface between Automatic Control, Applied Mathematics (Canada), and Engineering and Applied Mathematics (United States). Thus, the related scientific objectives cover a broad thematic spectrum related to dynamic systems in infinite dimensions. The second objective is to promote the rapprochement of the network members and strengthen the collaborations between the French, American, and Canadian teams (research work carried out jointly) in a structured framework (from two angles: themes and scientific objectives associated with each theme). Finally, the last objective is to provide an attractive and flexible framework

for young researchers; depending on the local dynamics and the particularities of the partners involved in the project (Saclay, Toulouse, Lille, Nantes, Grenoble, Nancy), the implementation of theses in joint supervision between French and American or Canadian universities is to be expected. The project is structured in the form of four CoRAs covering a reasonably broad thematic spectrum - control of nonlinear dynamic systems under the assumption of spatial and temporal heterogeneities (CoRA 1), analysis and control of delay systems, propagation phenomena, and transport (CoRA 2), hybrid control and infinite-dimensional dynamic systems (CoRA 3) and finally, Artificial Intelligence (AI) and the control of dynamic systems with distributed parameters (CoRA 4) involving teams with strong thematic complementarity.

4. **Member of a H-CoDe "non thematic" call**

   - Subject: Modélisation des interactions et contrôle par stimulation en boucle fermée des réseaux neuronaux claustro-corticaux.
   - Funding: H-Code, 10k€.
   - Duration: 2 years starting from January 2023.
   - Collaboration: T. Bal, A. Destxhe, S. Jacquir, C. Monier, G. Ouanounou, M. Pananceau, J. Auriol, L. Brivadis, A. Chaillet.
   - Summary of the proposal: The claustrum is a deep brain structure whose function remains mysterious despite a recent resurgence of interest because of its hyperconnected "hub" neuroanatomical organization. It comprises a layer of neurons densely connected to almost all cortical regions. Although works in the literature report the involvement of the claustrum in high-level cognitive functions (attention, consciousness), the participation of different types of claustral neurons and their dynamics within the claustral network and in a closed loop with the cerebral cortex is still subject to discussion. It is, therefore, fundamental to understand both the organization of CL neurons and how this organization is related to the processing of information passing through the claustrum. Work has shown that the claustrum may play a role in synchronizing neuronal oscillations between cortical areas. However, some questions remain open: what is the relationship between claustro-cortical and cortico-cortical synchronizations? Do they occur at the same frequency? What triggers claustrum activity? What process terminates the synchronization generated in the cortex by the claustrum? Considering the different cell types in the claustrum expressing other discharge properties, are local cortical circuits differentially affected by these subpopulations? The work carried out within the framework of this project should make it possible to advance our understanding of signal processing in the claustrum and, consequently, to elucidate how the claustrum contributes to processing cerebral information.

5. **Member of a H-CoDe "non thematic" call ClaControl**

   - Subject: Claustro-Cortical Network Oscillations: mechanisms, modeling, and control.
   - Funding: H-Code, 20k€.
   - Duration: 2 years starting from October 2023.
   - Collaboration: T. Bal (coordinator), G. Ouanounou, M. Pananceau, A. Ledoux, C. Monier, A. Destexhe, S. Jacquir, A. Chaillet, J. Auriol, L. Brivadis, V. Jirsa, D. Depannemaecker.
   - Summary of the proposal: The claustrum holds a central position in the brain hierarchy, being reciprocally connected to all cortical and many subcortical structures. It is phylogenetically preserved from reptiles to humans. The role of this brain hub remains mysterious despite a surge of experimental studies in the last five years (in Europe, the USA, and Japan, but barely in French labs). There are a growing number of proposed functions for the claustrum throughout the sleep-wake cycle: from attention to controlling cognitive functions or slow-wave sleep rhythms. One of the partners has designed a brain slice preparation containing the claustrum synaptically connected to parts of the cerebral cortex. They found that the cla neuronal network is the generator of a new type of slow oscillation in the 0,3-1 Hz range (preliminary data). In

this project, we will experimentally unravel the cellular and network mechanisms of claustrum oscillations and their interactions with cortical networks. They have full expertise in electrophysiology/optogenetic/imaging tools, and they will experiment tools emerging from control theory for the analysis and control of neural network dynamics. Then, we will integrate the biological data obtained before and during the grant (cell types; membrane properties; synaptic circuit structure and properties, oscillatory activities) in spiking computational models of claustral cells and circuits and examine the emergence of oscillatory regimes. A reduction from spiking to mean-field models will then be performed with the goal of inserting the claustrum hub and its dynamics into the connectome-based model of The mouse Virtual Brain (TVBm). The project will therefore bring new knowledge on the claustrum, showing for the first time its oscillatory properties and mechanisms, and its control of cortical networks. On a larger scale, it opens the possibility to examine virtually claustrum functions (and malfunctions) in the existing model of the whole brain.

6. **Member of a H-CoDe "non thematic" call VibRo**

   - Subject: Renouvellement des équipements matériels et logiciels pour les plateformes Vibrations et Robotique (ViBro)
   - Funding: H-Code, 7k€.
   - Duration: 2 years starting from October 2023.
   - Collaboration: S. Tliba, R. Bonalli, J. Auriol, I. Boussaada, K. Ammari.
   - Summary of the proposal: The main objective of this project is to renew some L2S computer hardware and real-time acquisition/computation/control systems. These experimental setups are intended for testing some of the output feedback controllers presented in this manuscript. We will consider, in particular, the non-trivial case of three-dimensional mechanical structures, such as thin mechanical structures of the plate type governed by the PDEs of Kirshoff-Love or Reisner-Mindlin. We will hire a Master's intern to implement these aspects.

1.10 . Synthesis of the research works and description of the main results, projects, and perspectives

Distributed parameter systems provide a natural representation of industrial processes involving the evolution of quantities in time and space. In particular, hyperbolic partial differential equations play a crucial role in the mathematical description of transport phenomena with finite propagation speeds, e.g., transport of matter, sound waves, and information. **Networks of hyperbolic systems** (possibly coupled with Ordinary Differential Equations) constitute an essential paradigm to describe a wide variety of large complex systems, including wave propagation, traffic network systems, electric transmission lines, hydraulic channels, drilling devices, communication networks, smart structures, multiscale and multiphysics systems. These systems are a source of **complex control engineering problems** and often have stringent **environmental safety and economic feasibility constraints**. For instance, oil and gas pipelines can be modeled by networks of conservation laws. Since leaking pipelines cause severe damage to the environment and economic losses, it is, therefore, crucial to detect and find leaks in these pipelines accurately. Similarly, controlling complex traffic networks is essential for reducing contamination and fluidifying the density of cars on the roads. Controlling and monitoring networks of hyperbolic systems is a complex task due to the distributed nature of the different subsystems composing the network (time and space dependency), the possibly involved **graph structure** of the network, and the physical/economic **infeasibility of placing sensors and actuators everywhere** along the spatial domain (they are usually located at some nodes of the network).

During my thesis, I derived robust stabilizing output feedback controllers for elementary hyperbolic systems. These systems are **elementary** in that one boundary of the system is fully actuated or measured. The proposed approaches relied on the **backstepping method**. I also showed strong

connections between hyperbolic systems and **time-delay systems of neutral types with distributed delays**.

In my **"post-thesis"** works, I mainly focused on developing a **systematic framework for the practical control of networks of linear hyperbolic systems and underactuated systems**. I developed new tools (*Fredholm-based time-delay transformations, recursive interconnected frameworks, filtering methods to guarantee robustness*) that strongly rely on the time-delay representation of hyperbolic systems. This explains why I also worked on *time-delay systems of neutral type*. In the meantime, I also considered several application test cases as *traffic networks and drilling vibrations*. Recently, I also considered other classes of infinite-dimensional systems as *neural fields and stochastic systems*. In what follows, the publication references correspond to the publications given in Chapter 4.

1.10.1 . Control of underactuated time-delay integral difference equations

- Description of the main results: Due to the strong connections between hyperbolic and **time-delay systems of neutral type**, it appeared crucial to deeply analyze this latter class of systems as such a representation is often more straightforward and could facilitate the design of controllers or observers. Networks of hyperbolic systems have equivalent stability properties to those of time-delay difference equations with distributed delays, namely, **Integral Delay Equations** (J5). These systems may be underactuated (i.e., there are fewer control inputs than states), and the control action may even be delayed due to the underlying transport phenomenon. We first succeeded in designing **predictors** for this class of systems (J18). In the case of fully actuated systems, we even obtained an **explicit expression** of this prediction, depending only on the state and input history and involving integral kernels, which are the solutions to recursive Volterra equations (J22). We then considered the case of two equations, only one of them being actuated. Under appropriate spectral **controllability conditions**, we could rewrite the system as one equation with distributed actuation. Then, we could introduce a set of candidate control inputs expressed as distributed delayed feedback of the state and the input. A control law from this set will stabilize the system if an associated set of **Fredholm equations admits a solution**. Interestingly, it appeared that the spectral controllability conditions imply the existence of solutions for these integral equations (C10, C16). State observers could be designed following a similar path (C17, J24). In the meantime, we took advantage of this time-delay representation to derive a **filtering technique** that robustifies stabilizing controllers for systems composed of heterodirectional linear first-order hyperbolic Partial Differential Equations (PDEs) interconnected with Ordinary Differential Equations (ODEs) through their boundaries. Assuming that a stabilizing controller is available, we derived simple sufficient conditions under which appropriate low-pass filters can be combined with the control law to **robustify** the closed-loop system.

- Collaborations: L2S, MinesParis, INSA Lyon.

- Perspectives: The central perspective would be to extend the proposed integral approach (requiring solving a Fredholm equation) to the case of an arbitrary number of equations under appropriate controllability conditions. In this context, we should focus on some tools from **operator theory**. One promising path to follow would be to understand the links between the system structure (actuation matrix) and the corresponding Fredholm integral equation. We could take advantage of the structure to simplify the system's description and subdivide it into simpler sub-networks. Another interesting perspective would be to focus on the time-delay representation of hyperbolic systems with **in-domain control**. As they can be rewritten as time-delay systems with distributed actuation, similar techniques could be applied, thus allowing the derivation of explicit feedback laws.

1.10.2 . Practical control of networks of hyperbolic systems

- Description of the main results: Before considering arbitrary networks of hyperbolic systems, we first focused on **chains** with a cascade structure (i.e., the graph representing the network is a straight line, and the actuator is located at one of its extremities). We derived a general backstepping controller for a chain of scalar hyperbolic systems (J12) before proposing a more generalizable

recursive method that combines state prediction and tracking (C15, J17). In both cases, the actuator was at the end of the chain. The proposed approach is **modular** and relies on simple conditions for each subsystem of the chain. Thus, it could be extended to chains that include ordinary differential equations or parabolic systems (as long as the proposed conditions are still verified). We extended this approach to non-scalar systems in J18. We have recently shown that depending on the actuators/sensors locations, the system may not be **controllable/observable**. For instance, considering two hyperbolic systems with actuation at the junction, we obtained spectral controllability conditions under which it was possible to derive stabilizing control laws using **Fredholm operators** (J24). We expect this approach to be generalizable to an arbitrary number of subsystems.

In the meantime, we focus on the **output regulation - output tracking** problem for a hyperbolic system coupled at both boundaries with ordinary differential equations, representing actuator and load dynamics (O1, J23, SJ2). Finally, we recently analyzed simple networks using a Port-Hamiltonian approach (C21, C23). This gave us a **physical framework** to parameterize the closed-loop properties of our system. Introducing **degrees of freedom** in the design is crucial to guarantee potential trade-offs w.r.t implementation constraints.

- Collaborations: L2S (thesis of J. Redaud), FEMTO-ST, MinesParis, INSA Lyon.
- Perspectives: The central objective is to generalize our existing results to more general **network structures**. One first perspective would be to enhance the **qualitative analysis** to understand the links between the network structure (e.g., number of cycles, incidence matrix) and its **controllability/observability** properties for a given position of actuators/sensors. We aim to characterize the **possible actuator/sensor configurations** for a given graph structure that guarantees controllability/observability. To identify reflections of graph-theoretic notions on the system properties, we could take advantage of the concepts of **structural controllability** and **controllability of multi-agent systems.** Then, we could aim to develop **generic analytical techniques** to quantify closed-loop performances with respect to industry-inspired **performance indices** (e.g., sensitivity, robustness margins, data sampling, convergence rate, computational effort). This step is crucial to **optimize actuator/sensor placement** and tune the proposed controllers. Finally, we want to design output-feedback controllers for an admissible configuration of actuators and sensors. The control design methods should be **modular, scalable, and numerically implementable**. Introducing **degrees of freedom** in the design is crucial to guarantee potential trade-offs with respect to implementation constraints. We will consider numerical aspects and model reduction to quantify the computational effort inherent to our approaches.

1.10.3 . Parameters estimation and stick-slip mitigation for drilling devices

- Description of the main results: Extracting resources from the earth's subsurface - oil, gas, minerals, and thermal energy - requires drilling long slender boreholes from the surface to the subsurface target. Drilling devices are the source of **complex dynamic behaviors** as many dynamic phenomena are involved, such as vibrations, bending and twisting quasi-static motion, and bit-rock interactions. The interaction between the drill string and the borehole or between the bit and the rock may generate undesired oscillations, including destructive **stick-slip oscillations**, which may cause fatigue of the equipment, a deterioration of the performance of the process, or a premature failing of the bit. In order to **improve the performance** of drilling systems (Rate Of Penetration), prevent any eventual damage, and reduce safety risks, it is crucial to have a clear understanding of the underlying dynamics. This implies estimating the different physical parameters and monitoring the system's state in real time. These estimations can then be used to design a proper mitigation strategy. Using the backstepping methodology, we first derived an **adaptive observer** for the torsional motion of the drilling device with the bit off-bottom (J8). This observer could estimate Coulomb's friction parameter (one cause of stick-slip) and be validated against **field data**. An alternative estimation procedure was also recently derived in (C19). Then, we derived a procedure to guarantee **closed-loop toolface control** (J11). Recently, using the proposed observer, we derived and compared several advanced control strategies to **eliminate stick-slip oscillations** (C14,

J21). The proposed strategies combined multiplicity-induced dominancy (MID) techniques and our recursive interconnected dynamics framework.

In the meantime, we focused on estimating **torsional and axial vibrations** in the presence of **bit-rock interaction**. We first adjusted our model and the corresponding observer to estimate the states and the new unknown parameters (e.g., intrinsic energy of the rock), thus obtaining a **self-tuning model** (C7). Then, we derived a new recursive methodology using **seismic-while-drilling** data to obtain a reliable estimation of the nature of the rock (J9, J16, C8). This new methodology has been used to improve sensing and imaging for **efficient energy exploration in complex reservoirs** (J13, J15, SJ1, C12, C13, C18). Recently, we focused on **machine-learning-based estimation methods** (C20). The research team includes researchers, postdocs, and Ph.Ds students.

- Collaborations: L2S, University of Calgary, UQAM, MinesParis, Norce.

- Perspectives: Among the different perspectives, we would like first to focus on coupled **axial-torsional dynamics**. A complete analysis will include model validation against field data. We also envisage tests of the proposed techniques on real **drilling devices**. Finally, we would like to focus on **physics-informed transformer-based neural networks** for enhanced estimation of drilling dynamics.

1.10.4 . Robust output-feedback control of traffic flow networks

- Description of the main results: **Freeway traffic modeling** and control have been intensively investigated over the past decades. One crucial control problem consists of the suppression of **stop-and-go traffic oscillations**. Among the traffic management infrastructures, we can cite ramp meterings and varying speed limits (VSL). Ramp meterings can regulate the traffic flow rate entering from the on-ramp to the mainline freeway, while VSL can modify the velocity at a specific location. Following the objective of deriving efficient and reliable control strategies, recent contributions rely on macroscopic models that represent the traffic dynamics at an aggregate level. These models describe freeway traffic dynamics using aggregated state values which are easy to sense and actuate, leading to a particular interest in **freeway traffic management**. They predict the evolution of continuous traffic states in the temporal and spatial domains by employing hyperbolic PDEs describing traffic density and velocity dynamics. Among the most popular models, we can cite the first-order Lighthill–Whitham–Richards (LWR) model and the second-order **Aw–Rascle–Zhang (ARZ)** model. The ARZ model can describe stop-and-go oscillations by adding a velocity PDE to the LWR model. During the last decades, various traffic ramp-metering control strategies have been developed and successfully implemented to suppress the stop-and-go traffic oscillations on the freeway either upstream or downstream of the ramp. In particular, H. Yu and M. Krstic designed **backstepping boundary control** laws for ramp metering. Unfortunately, such a control strategy was inefficient for controlling complex networks or even simple cascaded freeway segments connected by a junction.

  In this context, I started working in 2019 with H. Yu and M. Krstic, and we could develop **boundary output feedback** controllers for traffic flow on **two cascaded freeway segments** connected by a junction (C6, C9, J19). The control strategy and the observer design were adjusted from my recent results on the stabilization of interconnected hyperbolic systems (C4). We later considered a more realistic setting to implement the ramp metering on a digital platform developing an **event-triggered boundary output controller**. Contrary to the continuous control law, we used an event-triggered scheme so that the control signal is only updated when an event-triggering condition is satisfied. The event-triggered control design emulates the backstepping boundary output feedback and uses a dynamic event-triggered strategy to determine the time instants at which the control value must be **updated**. N. Espitia brought his expertise to show the existence of a uniform minimal dwell time (independent of initial conditions), thus avoiding the Zeno phenomenon and guaranteeing the exponential convergence of the closed-loop system under the proposed event-triggered control

scheme. This work was presented at the 3^{rd} DECOD-workshop before being published in O2 and J20.

Finally, in collaboration with M. Pereira and B. Kulcar, we recently showed closed-loop **mean-square exponential stability** of the proposed control strategies under random system parameter perturbations, provided the nominal parameters are sufficiently close to the stochastic ones on average. Indeed, **random variables** would better describe some parameters (such as the drivers' behavior or road parameters). This strongly relates to my recent research interests in stochastic systems.

- Collaborations: L2S, University of California San Diego (USA), CRIStAL (France), Chalmers University of Technology (Sweden).

- Perspectives: Future perspectives include the design of a **periodic event-triggered** control strategy to monitor the triggering condition periodically, saving computational resources. Moreover, we wish to investigate the questions related to **quantized** implementations of event-triggered controllers. They will lay the foundations for digital realizations of boundary-backstepping-based controllers. We then aim to extend the proposed strategies to more **complex networks**. We would also continue to investigate the effect of stochastic disturbances on the control strategy. Another interesting perspective is considering a vehicular platoon both from the macroscopic and microscopic points of view and investigating and quantifying the relations between the two models. To this purpose, a coupled hyperbolic-Ordinary Differential Equation model is of interest. The coupling is generated by considering the impact of **macroscopic variables** for the **microscopic model** in the vehicles' control laws. Consequently, the hyperbolic part will depend on the speed average value of the set of vehicles generated by the finite-dimensional dynamics. Such a mixed model could allow more accurate estimations of the system's global (macroscopic and microscopic) state. Such reliable estimations could be used to design more efficient control algorithms that eliminate stop-and-go oscillations.

1.10.5 . Adaptive control and parameter estimation for neural fields.

- Description of the main results: The central problem of the project is related to the treatment by **deep brain stimulation** (DBS) for Parkinson's disease. The treatment consists of electrically stimulating specific areas of the patient's brain via permanently implanted electrodes. Although the method is effective and commonplace, it needs significant practical and theoretical shortcomings. Currently, the signal transmitted by the electrodes is in an open loop. Therefore, the evolution of the patient's health condition or the progressive electrode deterioration requires manual adaptation of the signal. Many recent works propose to develop **closed-loop stimulation methods** for two reasons. First, to ensure that the signal emitted is **effective**, it allows the alteration of the pathological brain oscillations from which the patient suffers. Second, to ensure that the signal **does not affect the regular brain activity** of the patient, in particular when pathological oscillations are absent. Mathematically, these systems can be described by **non-linear integro-differential equations** (Wilson-Cowan type equations), the integral part corresponding to a **Hilbert-Schmidt operator**. With L. Brivadis (postdoc) and A. Chaillet, we first assumed that we could control/measure a whole neural population. We ensured the existence of an **equilibrium point** for the closed-loop system (J26). Then, we proposed an **online estimation** of the neural field kernels (C22). This estimation could then be used to design an **adaptive controller** (SJ4). The different strategies rely on the operator theory, persistence of excitation, and Lyapunov functions.

- Collaborations: L2S, Institut des Neurosciences Paris-Saclay NeuroPSI (France).

- Perspectives: The first perspective we want to follow is **leveraging** the different assumptions that are currently required. In particular, the proposed estimation/control strategies require the measurements of a whole neuronal population. We aim to consider the case of a finite number of **pointwise** sensors and actuators while focusing on sensor/actuator placement. Then, in collaboration with the NeuroPSI laboratory, we aim to test our estimation techniques on real data. Finally,

the proposed parametric identification techniques we recently developed could be used to **estimate the core of synaptic interconnections between neurons** in the claustrum (ClaControl project).

1.10.6 . Efficient control of stochastic systems

- Description of the main results: Stochastic equations naturally arise when modeling processes whose dominant dynamics are affected by a **probabilistic disturbance**. Recently, we considered with D. Bresch-Pietri and S. Kong the **robustness** of delayed linear integral difference equations with respect to random delays. With M. Pereira and B. Kulcsar, we extended the proposed approach to guarantee closed-loop mean-square exponential stability of **scalar hyperbolic systems** under **random system parameter perturbations**, provided the nominal parameters are sufficiently close to the stochastic ones on average (SC2). Our objective is now to take into account the effect of **stochastic disturbances** (and not simply random parameters) on the global dynamics. With R. Bonnali and I. Boussaada, we hired a Ph.D. student (G. Velho) to design methods for efficient and theoretically guaranteed control of a broad class of **coupled stochastic and partial differential equations**. The proposed approaches must be constructive to obtain a semi-explicit design of the corresponding control laws, enabling performance-efficient numerical paradigms. In SJ5, we submitted some preliminary results for the efficient control of stochastic equations. The proposed methodologies could then be adequately coupled with existing control methods for hyperbolic equations.

- Collaborations: L2S (thesis of G. Velho), MinesParis, Chalmers University of Technology (Sweden).

- Perspectives: Among the possible perspectives, we would like to investigate under which conditions the well-posedness of statistical linearization can be strengthened, enabling **general efficient and reliable numerical methods** for controlling non-linear stochastic equations. We would also like to investigate under which conditions the most recent methods for hyperbolic systems can be extended to a broader class of systems and, in particular, develop techniques that are as much independent as possible from any inherent regularizing property of the system (e.g., optimization methods or modular approaches). Another perspective could be to **leverage statistical linearization** to transform the stochastic part of the interconnection into a (constrained) well-posed equation and leverage the aforementioned improved methods for interconnected hyperbolic/differential equations systems to design efficient control strategies for the original system.

2 - Student Supervision

In what follows, the publication references correspond to the publications listed in Chapter 4. In the publication list, the names of the different students are written using specific colors.

2.1 . Ph.D. Supervision

1. **Mr. Gabriel Velho** (November 2022-present date)

   - Subject: *Efficient and reliable control of coupled stochastic and partial differential equations*. Stochastic differential equations (SDEs), which are coupled with (possibly non-linear) partial differential equations (PDEs), are a class of systems that naturally arise when modeling processes whose dominant probabilistic dynamics are affected by a distributed dynamics (destabilizing second-order convection-diffusion-reaction effects, or transport phenomena for instance). These systems are called SDE+PDE systems. A relevant example of an SDE+PDE system is provided by District Heating and Cooling Systems (DHCSs). DHCSs deliver thermal energy to a network of buildings from an outside source. They offer numerous advantages over individual building apparatus, including greater safety and reliability, reduced emissions, and reliance on alternative fuels such as biomass or waste. However, due to low operating temperatures and limited flow capacity, customer demand can be met only if 1) non-linear SDE-based dynamical models are leveraged to capture as many uncertain weather fluctuations as possible and 2) the aforementioned stochastic models are coupled with sophisticated non-linear PDEs to accurately capture energy losses which often occur along pipelines and hinder performance. In turn, the overall setting requires to efficiently and reliably control a complex SDE+PDE system. Unfortunately, too few specific works on SDE+PDE systems appear in the literature, hence calling for the design of novel tools for the efficient modelization and control of such systems. This thesis aims to design methods for efficient and theoretically guaranteed control of a broad class of SDE+PDE systems. The proposed approaches must be constructive to obtain a semi-explicit design of the corresponding control laws, enabling performance-efficient numerical paradigms.
   - Supervision: J. Auriol (main supervisor, 45%, **dérogation HDR**), R. Bonalli (advisor, 45%), and I. Boussaada (advisor, 10%).
   - Fundings: Contrat doctoral Ministère de l'Enseignement Supérieur et de la Recherche. Ecole Doctorale STIC, L2S, CentraleSupélec.
   - Publications: So far, G. Velho submitted **one journal paper** (SJ5), has submitted one conference paper and is working on one journal paper.

2. **Mrs. Jeanne Redaud** (November 2020-present date)

   - Subject: *Robust control of chains of scalar hyperbolic Partial Differential Equations*.
     Networks of interconnected linear partial differential equations (PDEs) are a class of systems that naturally arise when modeling industrial processes for which the dominant dynamics involve a transport phenomenon. Elementary PDE systems can be connected between themselves or with Ordinary Differential Equations. Related applications include (among others) electrical transmission lines, traffic networks, multiphase flows, or smart grids. Such networks are generally underactuated, which makes their stabilization challenging. This explains why the stabilization of such systems is an active research topic. The main objective of this thesis was to derive general controllability and observability criteria for a class of **scalar interconnected systems with a chain structure**. The proposed approach had to be constructive in order to obtain an explicit design of the corresponding control laws and observers.

Since the beginning of her thesis, Jeanne has contributed to the development of a control method called "recursive interconnected framework," allowing her to stabilize (under general assumptions) chains of systems of scalar interconnected partial differential equations (contributions C15, J17). This approach was applied to stabilizing a drilling device (contribution C19). In the case of simple chains, she also solved the trajectory tracking/disturbance rejection problem (contribution O2, contribution SJ2), a crucial step for real implementation. Jeanne has implemented a new approach for the design of control laws and observers for systems of integral delay equations with distributed actuation and measurement (contributions C16, C17). This approach relied on Fredholm integral transformations and was extended to certain classes of networks of partial differential equations (contribution J24). Undoubtedly, this new tool will be the key to designing stabilizing controllers for underactuated networks of partial differential equations. Recently, Jeanne has been interested in the possibility of going beyond the simple stabilization and the possibility of imposing particular properties on closed-loop systems via the use of a Hamiltonian formalism (submissions C21, C23, and SJ3). Her thesis defense is scheduled for November 2023.

- Supervision: J. Auriol (co-supervisor till 2023, 75%, main supervisor since 2023 (**dérogation HDR**), 100%) and S.-I. Niculescu (main supervisor till 2023, 25%).
- Fundings: Contrat doctoral Ministère de l'Enseignement Supérieur et de la Recherche. Ecole Doctorale STIC, L2S, CentraleSupélec.
- Publications: So far, J. Redaud published **two journal papers** (J17, J24), **eight conference papers** (C16, C17, C19, C21, C23, C24), **one book chapter** (O1). **Two journal papers** (SJ1, SJ3) are under revision. The difference in terms of supervision percentage is manifested by the fact that S.-I. Niculescu did not participate in several contributions (and consequently did not co-authored them).
- Awards:
  - Nominated (accessit) for the **Ph.D. award** of the doctoral school STIC of Université Paris Saclay, 2022.
  - **TDS 2021 best student paper award** for the paper co-authored with J. Auriol and S.-I. Niculescu entitled *Observer design for a class of delay systems using a Fredholm transform* and presented at the 16^{th} IFAC workshop on time-delay systems, Guangzhou, China, 2021.

2.2 . Postdoctoral fellows

1. **Dr. Lucas Brivadis** (October 2021-October 2022)

- Subject: *Adaptive control of neural fields. Application to Parkinson's disease*. During his postdoctorate at L2S, Lucas worked on adaptive control problems for neural field populations. The central problem of the project is related to the treatment by deep brain stimulation (DBS) for Parkinson's disease. The treatment consists of electrically stimulating specific areas of the patient's brain via permanently implanted electrodes. Although the method is effective and commonplace, it needs significant practical and theoretical shortcomings. Currently, the signal transmitted by the electrodes is in an open loop. The evolution of the patient's health condition or the progressive deterioration of the electrode, therefore, requires manual adaptation of the signal. Many recent works propose to develop closed-loop stimulation methods for two reasons. First, to ensure that the signal emitted is effective, in particular, that it allows the alteration of the pathological brain oscillations from which the patient suffers. Second, to ensure that the signal does not affect the normal brain activity of the patient, in particular when pathological oscillations are absent. The objective of the postdoc was to develop adaptive control methods to meet these specifications. Lucas ensured the existence of an equilibrium point of the closed-loop system in J26. He worked on designing new control laws whose objective is to cancel the components of pathological neuronal activity while preserving the asymptotic behavior of the healthy activity. In C22, he proposed an online estimation of the neural field kernels. This estimation can be used to design an adaptive controller (SJ4).

- Supervision: J. Auriol (50%), A. Chaillet (50%).
- Fundings: L2S Postdoctoral Grant, L2S, CentraleSupélec.
- Publications: We collaborated with L. Brivadis on **two journal papers** (J26 and SJ4) and **one conference paper** (C22).
- Current position: L. Brivadis is now a CNRS Researcher (Chargé de Recherches Classe Normale, CRCN) since October 2022, Université Paris-Saclay, CNRS (UMR 8506), Centrale-Supélec, Laboratoire des Signaux et Systèmes (L2S), UMR CNRS 8506, Gif-sur-Yvette, France.

2. **Dr. Ismaïla Balogoun** (October 2023-October 2024)

   - Subject: *Certified stabilization of partial differential equations with prescribed solutions decay rate*.

     It has been shown in [ADM19] that hyperbolic systems have equivalent stability properties as the ones of time-delay difference systems with distributed delays. Thus, it becomes possible to apply appropriate methods developed for time-delay systems to analyze quantitatively and qualitatively the closed-loop system properties or design appropriate and simple stabilizing controllers. Recently, G. Mazanti and I. Boussaada have set a new paradigm of Partial Pole Placement (PPP) for linear time-invariant functional differential equations and some classes of partial differential equations. The PPP relies on two main strategies, themselves certified by the spectral distribution properties of time-delay systems: **multiplicity-induced-dominancy** (MID) and **coexisting-real-roots-induced-dominancy** (CRRID). The objective for Ismaïla will be to extend the MID and CRRID properties to stabilize hyperbolic systems. This would pave the way for a new generation of stabilizing controllers that are simple to implement (and consequently do not require an expensive computational cost) while explicitly taking into account the delays and high-frequency content in the model (which should lead to overall increased performance). This will require analyzing the dominancy properties in the multi-delay and distributed-delay contexts.
   - Supervision: J. Auriol (34%), I. Boussaada (33%), G. Mazanti (33%).
   - Fundings: L2S Postdoctoral Grant, L2S, CentraleSupélec.

2.3 . MSc supervision

1. **Mrs. Lea Prade Njoua Dongmo** (March 2023 - September 2023)

   - Subject: *Machine learning and mixed ODE-PDE for mesoscopic traffic control systems*.
     Disruptive technologies have paved the road for new types of traffic control systems. Two main approaches have been proposed in the literature: 1) traffic management through intelligent infrastructures imposing speed limitations according to traffic conditions, based on a PDE modeling describing the traffic flow from a macroscopic point of view (mainly flow and density of the whole set of vehicles); 2) displacement of autonomous vehicles to reduce stop-and-go waves propagation and traffic oscillations via the concepts of String Stability, based on an ODE modeling describing the traffic flow from a microscopic point of view (every single vehicle-driver unit and the interactions with the others). Recently, new methods targeting exploiting the interaction between the controlled vehicles and the surrounding flow can be used to modify the traffic density to improve congestion and reduce emissions. These methods are based on a mesoscopic approach, introducing macroscopic information in a microscopic framework for improving local control strategies. A state variable describing the macroscopic information in an aggregate formalism is defined. The necessity to investigate the matching between the macroscopic vision and the microscopic one arises to verify the compatibility of the mixed approach. The goal is to consider a vehicular platoon both from the macroscopic and microscopic points of view and to investigate and quantify the relations between the two models. To this purpose, a coupled PDE-ODE model is of interest. The coupling of the ODE model with the PDE is generated by taking into account the impact of macroscopic variables for the microscopic model in the control laws.

Consequently, the PDE will depend on the speed average value of the set of vehicles generated by the ODEs. Such a mixed model could allow more accurate estimations of the system's global (macroscopic and microscopic) state. Such reliable estimations could be used to design more efficient control algorithms that eliminate stop-and-go oscillations.

- Supervision: J. Auriol (50%), A. Iovine (50%).
- Publications: We have submitted one journal paper in IEEE Transactions on Control Systems Technology.
- Fundings: L2S, CentraleSupélec.

2. **Mr. Maxence Lamarque** (December 2022 - March 2023)

   - Subject: *Design of Lyapunov functionals for systems of balance laws*.
     This internship aims to investigate necessary and sufficient Lyapunov conditions for Input-to-State Stability (ISS) of Linear Difference Equations with pointwise and distributed delays subject to an exogenous additive signal. Grounding on recent works in the literature on necessary conditions for the exponential stability of Difference Equations, we aim to propose a quadratic Lyapunov functional involving the derivative of the so-called delay Lyapunov matrix. The objective is to prove that ISS of Linear Integral Difference Equations is equivalent to the existence of an ISS Lyapunov functional. We wish to apply this result to the stability and ISS analysis of hyperbolic Partial Differential Equations of balance laws.
   - Supervision: D. Bresch-Pietri (85%), J. Auriol (15%).
   - Publications: We plan to submit a journal paper before the end of the year.
   - Fundings: Parcours Recherche, Centre Automatique et Systèmes, MinesParis.

3. **Mr. Yun-Ithry Gamrani** (October 2021 - present date)

   - Subject: *Development of a numerical toolbox for the control of partial differential equations*.
     In order to control systems of partial differential equations, different theoretical methods have been proposed in the literature. In general, such approaches require the solution of a complex set of equations to be implemented. Moreover, they may present a certain number of degrees of freedom that are supposed to ensure a compromise between performance, disturbance rejection, robustness to noise, and delays (phenomena that appear naturally during a practical implementation but that are often neglected during theoretical developments). There is yet to be a systematic method in the literature for the numerical solution of such equations or calibrating the associated degrees of freedom. However, these steps are crucial for implementing such control laws on real systems. The main objective of this research project is to develop a numerical toolbox similar in its operation to what has been done for finite dimensional systems (in Matlab and Python, for example), allowing the synthesis of control laws for systems of partial differential equations while respecting the various constraints of the imposed specifications (speed of convergence, robustness or accuracy, for example). So far, Yun-Ithry has developed and compared several numerical algorithms to solve the so-called "kernel equations" that appear when using the backstepping methodology. He also focused on investigating explicit solutions when the coefficients of the kernel equations have an explicit structure. He recently obtained promising results using Fourier analysis.
   - Supervision: J. Auriol (100%).
   - Fundings: Parcours Recherche, CentraleSupélec.
   - Current position: Yun-Ithry is currently taking a gap year during which he will work with myself and B. Kulcsar on a different project. He will complete the current project in 2024.

4. **Mrs.** Jordan Curkain (February 2019 - September 2018)

- Subject: *Impacts and challenges of acoustic seismic while drilling*.
  The oil and gas industry, operating and service companies, and academia are actively searching for ways to look ahead of the drill bit while drilling to reduce the risks and costs of the operation and improve the well-placement process. Optimal drilling in challenging and highly heterogeneous reservoirs, where geological data cannot adequately constrain high-frequency variations in rock properties, requires reliable subsurface information from around and ahead of the drill bit. To provide this, we wanted to develop a seismic-while-drilling (SWD) imaging algorithm using signal processing, drillstring modeling, and prestack wave-equation migration. To extend the visibility ahead of the bit, we use the drill bit as a seismic source and image the changes in acoustic properties of rocks both around and ahead of the drill bit. The common practice is to build reverse vertical seismic profile (R-VSP) gathers. Here, we use a blind deconvolution algorithm to estimate the drill-bit source signature from the data directly. The proposed methodology was tested on the McMurray Formation. Jordan collaborated on journal articles [J13], [J15], and the conference paper [C12]. This work was directly related to my postdoctoral project.
- Supervision: S. Najedi (80%), J. Auriol (20%).
- Fundings: University of Calgary.
- Current position: Jordan is now Geologist in Training at Canadian Natural Resources Limited (CNRL).

5. **Mr. Pierre-François Massiani** (September 2017 - February 2018)

   - Subject: *Parameter estimation in a Rijke tube*.
     The objective of this research project was to design an adaptive estimator for a Rijke tube. The Rijke tube is a simple test case for the analysis of thermoacoustic oscillations. It can be modeled by an ODE sandwiched between two transport equations. Pierre-François first built an experimental setup before designing a theoretical observer that he tested on various experimental test cases. This subject was directly related to my research activities since the Rijke tube corresponds to a simple test case of interconnected systems.
   - Supervision: J. Auriol (75%), F. Di Meglio (25%).
   - Fundings: Parcours Recherche, MinesParis.
   - Current position: Pierre-François is now a 3^{rd} year Ph.D. student at RWTH Aachen University, Germany.

6. **Mr. Hubert Menou** (September 2016-February 2017)

   - Subject: *Passive vibration damping in a washing machine with a CRONE control*.
     The non-uniform distribution of the laundry inside the drum mainly causes washing machine vibrations. The passive controllers currently used (string-damper systems) are only sized for some nominal masses and do not guarantee a constant damping quality regardless of the laundry distribution. This project aimed to strengthen the washing machine vibration damping efficiency with respect to the different possible masses configurations. The proposed control strategy relied on the CRONE method. The supervision of this subject was entrusted to me because of the underlying problems related to mechanical vibrations.
   - Supervision: J. Auriol (50%), F. Di Meglio (50%).
   - Fundings: Parcours Recherche, MinesParis.
   - Current position: Hubert has defended his Ph.D. in 2023, MinesParis, PSL Research University. He is now working at Fairmat.

3 - Teaching activities

Even though teaching is not compulsory due to my status as a CNRS researcher, I have always appreciated this activity of transmitting knowledge. It seems essential to me to bring science to life and to give students a taste of it. This is why I have always sought to maintain a teaching activity. It also allows sharing some of my research interests and meeting with brilliant students who can continue with a thesis. During my career (between 2016 and 2023), I gave more than 550 hours of teaching in French, Moroccan and Canadian establishments (automatics, mathematics, optimization, data analysis, and complex analysis). Below, I briefly describe the courses I taught for each establishment. The complete synthesis of my teaching activities is given in Table 3.1. The different hours are given in ETD (Equivalent TD).

3.1 . Mines Paris, PSL Research University (2016-present date)

1. ***Complex analysis and applications:*** pedagogical responsibility, lectures, tutorials (2021-present date).
   - *Description:* This course is given during the international *Athens week* with students from several universities in Europe. The first part of the course is an introduction that is designed to expose the theory of complex analysis in a short amount of time. The attempts to solve the pain points experienced by attending students over the years explain most of the deviations from standard expositions. We skip some technical proofs (that will still be available for the most motivated students), focusing on the meaning of the different concepts. The second part of the course focuses on use cases of complex analysis in engineering. Numerous modern problems in many unrelated fields (scientific computing, image editing, signal processing, control problems) can be solved by complex analysis even though their statements have nothing to do with this theory.
   - This class is an excellent opportunity to emphasize the links between complex analysis and some current research domains. The concepts introduced during the class are, for instance, crucial for the analysis of time-delay systems (and consequently of hyperbolic systems). Thus, this class can motivate some students to start an internship or a thesis in these domains.
   - 40 Master students (M1/M2), (40h ETD per year)
   - Total: 120h ETD.
2. ***Differential, integral and stochastic calculus:*** tutorials and optional lectures (2020-present date)
   - *Description:* This course introduces the critical concepts of differential calculus (differentials of first and second order, Hessian), integral calculus (Lebesgues' integral, L^p spaces), differential equations, stability, and Lyapunov analysis.
   - This course is a unique opportunity to meet students from MinesParis who can become potential Ph.D. students two years later. Moreover, I have the opportunity to give two lectures on differential calculus in infinite dimensional spaces and an introduction to partial differential equations. These lectures can sensitize the students to my research fields.
   - 20 first year students (L3), (25h ETD per year and 10 hours per year of oral exams).
   - Total: 100h ETD.
3. ***Differential calculus:*** tutorials (2016-2018)
   - *Description:* This class introduced the concept of differential, ordinary differential equations and partial differential equations (conservation laws). It also included some developments related to optimization and calculus of variations.

- I taught this class during my Ph.D. and it was related to my research expertise.
- 25 first year students (L3), (15h ETD per year and 10 hours per year of oral exams).
- Total: 30h ETD.

4. ***Introduction to control theory:*** tutorials (2015-2018)
   - *Description:* The course presents the fundamental tools for controlling dynamic systems. It illustrates the importance of stability, controllability, and observability properties. The numerical aspects of controllers/observers implementation are described.
   - I taught this class during my Ph.D. and it was related to my research expertise. Some students from my tutorial groups joined the Centre Automatique et Systèmes as interns first and then as Ph.D. students.
   - 25 first year students (L3), (16h ETD per year)
   - Total: 48h ETD.
5. ***Mechatronics:*** Invited expert (2016-2018)
   - *Description:* I was selected as an invited expert to help a group of 10 students in their mechatronics project. The project consisted in the design and manufacturing of a Ball-droid (BB8).
   - This expertise mission was a good opportunity to sensitize the students on the difficulties related to the real implementation of the theoretical controllers.
   - 10 Master students (M1), (15h ETD per year including 3h of oral exams).
   - Total: 30h ETD.
6. ***Introduction to complex analysis:*** tutorials (2016-2017)
   - *Description:* This course was an introduction to the main concepts of complex analysis.
   - I taught this class during my Ph.D. as it was related to my research expertise. Some students from my tutorial groups joined the Centre Automatique et Systèmes as Ph.D. students.
   - 20 Master students (M1), (16h ETD per year).
   - Total: 32h ETD.

3.2 . CentraleSupélec (2020-present date)

1. ***Model representations and analysis:*** tutorials (2020-present date)
   - *Description:* The objective is of this course is to represent and analyze the evolution of a system by means of a model that is analytically or numerically exploitable, adapted to the objective of modeling, determined in terms of modeling assumptions, representativeness and level of complexity, and to determine its validity domain.
   - This course allows me to get in touch with CentraleSupelec students and is related to some critical challenges in automatics.
   - 35 first year students (L3), (15h ETD per year). Total: 45h ETD.

3.3 . EMINES, Maroc (2020-present date)

1. ***Dynamical systems and control theory:*** tutorials (2020-present date).
   - *Description:* This course is an introduction to dynamical systems and to control theory. It includes theoretical developments (e.g. Kalman's criterion, LQR) and numerical implementation using Python.

- This course is directly related to my research expertise. Several students from EMINES contacted me to join the Master ATSI in CentraleSupélec.
- 25 second year students (M1), (25h ETD per year).
- Total: 100h ETD

3.4 . Université Paris-Saclay (2020-present date)

1. ***Research initiation seminars:*** lectures.

   - *Description:* This series of Research initiation seminars aims to give students an overview of some current and trendy research fields. My seminar is devoted to *Boundary control of hyperbolic Partial Differential Equations*. I try to give the students some keys to understanding broadly used techniques in the community.
   - Thanks to this course, I can present to Master students some of my most recent research results. Some of them contacted me for an internship.
   - 35 second ATSI Master students (M2), 3 hours per year (4.5h ETD per year).
   - Total: 12.5h ETD.

3.5 . University of Calgary, Canada (2019)

1. ***Introduction to optimization, data analysis and control theory:*** pedagogical responsibility, lectures, tutorials (2019).

   - *Description:* The objective of this series of lectures was to introduce the basic concepts of optimization (gradient algorithms, Newton's algorithm), data analysis (classifications, regressions, unsupervised learning, reinforcement learning), and control theory (pole placement, controllability, observability). Classical algorithms were implemented using Python. Several test cases inspired by the industry were deeply analyzed.
   - I created this course and was entirely in charge of it. Thus, I could sensitize the students to my research interest. Most of the students were from the geophysical or chemistry departments. Thus I focused on examples from these research fields. After my departure at the end of my postdoc, the course was still maintained due to the highly positive feedback.
   - 60 Master students (M1/M2), (50h ETD per year).
   - Total: 50h ETD.

2. ***Introduction to machine learning:*** lectures and tutorials (2019)

   - *Description:* The objective of this series of lectures was to introduce the basic concepts of machine learning (classifications, regressions, unsupervised learning, reinforcement learning). Classical algorithms (e.g., K-means, classifiers) were implemented using Python.
   - 30 Master students (M2), (20h ETD per year).
   - Total: 20h ETD

3.6 . ENSTA ParisTech (2016-2017)

1. ***Control of dynamical systems:*** tutorials (2016-2017).

   - *Description:* The course presents the fundamental tools for controlling dynamic systems. It illustrates the importance of stability, controllability, and observability properties. The numerical aspects of controllers/observers implementation are described.

- I taught this class during my Ph.D. as it was related to my research expertise. Some students from my tutorial groups joined the Centre Automatique et Systèmes as interns.
- 30 second year students (M1), 15 hours (ETD) per year.
- Total: 30h ETD.

Mines Paris		
Complex analysis and applications	2021-2023	120h ETD
1A Differential, integral, stochastic calculus	2020-2023	100h ETD
1A Differential calculus	2016-2018	30h ETD
1A Introduction to control theory	2015-2018	48h ETD
2A Mechatronics	2016-2018	30h ETD
2A Introduction to complex analysis	2016-2018	32h ETD
CentraleSupélec		
1A Model representations and analysis	2020-2023	45h ETD
EMINES		
2A Dynamical systems and control theory	2019-2023	100h ETD
Université Paris-Saclay		
Research initiation seminars	2020-2023	12.5h ETD
University of Calgary		
Optimization, data analysis, control theory	2019	50h ETD
Introduction to machine learning	2019	20h ETD
ENSTA Paris Tech		
2A Control of dynamical systems	2016-2018	30h ETD
Total		**617.5h ETD**

Table 3.1: Synthesis of teaching activities between 2016 and 2023

4 - List of publications

Publications by the author of the manuscript as of January 16, 2023. All the articles are available on HAL. My name is written as J. Auriol, while the name of each student I supervised is written with a specific color.

4.1 . Journal Papers with reviewing committee

J28 J. Redaud, J. Auriol, Y. Le Gorrec, *In domain dissipation assignment of boundary controlled Port-Hamiltonian systems using backstepping*, Systems and Control Letters, 2024, [RALG24].

J27 J. Redaud, F. Bribiesca-Argomedo, J. Auriol, *Output regulation and tracking for linear ODE-hyperbolic PDE-ODE systems*, Automatica, 2024, [RBAA24].

J26 L. Brivadis, C. Tamekue, J. Auriol, *A comment on "Robust stabilization of delayed neural fields with partial measurement and actuation" [Automatica 83 (2017) 262-274]*, Automatica, 2023, [BTA22].

J25 J. Auriol, F. Bribiesca-Argomedo, F. Di Meglio, *Robustification of stabilizing controllers for ODE-PDE-ODE systems: a filtering approach*, Automatica, vol. 147, p.110724, 2023, [ABADM23].

J24 J. Redaud, J. Auriol, S.-I. Niculescu, *Stabilizing Output-feedback control law for Hyperbolic Systems using a Fredholm transformation*, IEEE Transactions on Automatic Control, vol.67 (12), p.6651-6666, 2022, [RAN22c].

J23 J. Auriol, F. Bribiesca-Argomedo, *Observer design for n+m linear hyperbolic ODE-PDE-ODE systems*, IEEE Control Systems Society letters, vol .7, p.283-288, with presentation at the IEEE Conference on Decision and Control, Cancun, 2022, [ABA22].

J22 J. Auriol, S. Kong, D. Bresch-Pietri, *Explicit Prediction-based Control for Linear Difference Equations with Distributed Delays*, IEEE Control Systems Society letters, with presentation at the IEEE Conference on Decision and Control, Cancun, 2022, [AKBP22].

J21 J. Auriol, I. Boussaada, R. Shor, H. Mounier, S.-I. Niculescu, *Comparing advanced control strategies to eliminate stick-slip oscillations in drillstrings*, IEEE Access, vol. 10, p.10949-10969, 2022, [ABS+22].

J20 N. Espitia, J. Auriol, H. Yu and M. Krstic, *Traffic flow control on cascaded roads by event-triggered output-feedback*, International Journal of Robust and Non-linear Control (IJRNC), 2022, [EAYK22b].

J19 H. Yu, J. Auriol, M. Krstic, *Simultaneous Downstream and Upstream Output-Feedback Stabilization of Cascaded Freeway Traffic*, Automatica, vol. 136, p.110044 2022, [YAK22].

J18 J. Auriol, D. Bresch-Pietri, *Robust state-feedback stabilization of an underactuated network of interconnected $n+m$ PDE systems*, Automatica, vol. 136, pp.110040, 2022, [ABP22].

J17 J. Redaud, J. Auriol, S.-I. Niculescu, *Output-feedback control of an underactuated network of interconnected hyperbolic PDE-ODE systems*, Systems and Control Letters, vol. 154, p.104984, 2021, [RAN21b].

J16 J. Auriol, N. Kazemi, S.-I. Niculescu, *Sensing and computational frameworks for improving drillstring dynamics estimation*, Mechanical Systems and Signal Processing, vol. 160, p.107836, 2021, [AKN21].

J15 N. Kazemi, S. Nejadi, J. Auriol, J. Curkan, R. Shor, K. Inannen, S. Hubbard, I. Gates, *Advanced sensing and imaging for efficient energy exploration in complex reservoirs*, Energy Report, vol. 6, p.3104-3118, 2020, [KNA+20].

J14 J. Auriol, U.J.F. Aarsnes, F. Di Meglio, R. Shor, *Robust control design of under-actuated* 2×2 *PDE-ODE-PDE systems*, IEEE Control Systems Society letters, vol. 5, no 2, p.469-474, with presentation at the IEEE Conference on Decision and Control, Jeju Island, Korea, 2020, [AADMS20].

J13 S. Najedi, N. Kazemi, J.A. Curkan, J. Auriol, P.R. Durkin, S.M. Hubbard, K.A. Innanen, R.J. Shor, I.D. Gates, *Look ahead of the bit while drilling: potential impacts and challenges in the McMurray Formation*, SPE Journal, vol. 25, no 05, p.2194-2205, 2020, [NKC+20b].

J12 J. Auriol, *Output-feedback stabilization of an underactuated cascade network of interconnected linear PDE systems using a backstepping approach*, Automatica, vol. 117, 2020, [Aur20].

J11 J. Auriol, R.J. Shor, U.J.F. Aarsnes, F. Di Meglio, *Closed-loop toolface control with the bit off-bottom, Journal of Process Control*, vol. 90, p.35-45, 2020, [ASADM20].

J10 J. Auriol, F. Di Meglio, *Robust output feedback stabilization for two heterodirectional linear coupled hyperbolic PDEs*, Automatica, vol. 115, p.108896, 2020, [ADM20].

J9 J. Auriol, N. Kazemi, R.J. Shor, K.A. Innanen, I.D. Gates, *A sensing and computational framework for estimating the seismic velocities of rocks ahead of the drill bit*, IEEE Transactions on Geoscience and Remote Sensing, vol. 58, no 5, p.3178-3189, 2019, [AKS+19].

J8 U.J.F. Aarsnes, J. Auriol, F. Di Meglio, R.J. Shor, *Estimating friction factors while drilling*, Journal of Petroleum Science and Engineering, vol. 179, p.81-91, 2019, [AADMS19].

J7 D. Bou Saba, F. Bribiesca-Argomedo, J. Auriol, M. Di Loreto, F. Di Meglio, *Stability analysis of linear* 2×2 *hyperbolic PDEs using a backstepping transform*, IEEE Transactions on Automatic Control, vol. 65, no 7, p.2941-2956, 2019, [BSBAA+19].

J6 J. Auriol, K. A. Morris, F. Di Meglio, *Late-lumping backstepping control of partial differential equations*, Automatica, vol. 100, p.247-259, 2019, [AMDM19].

J5 J. Auriol, F. Di Meglio, *An explicit mapping from linear first order hyperbolic PDEs to neutral systems*, Systems and Control Letters, vol. 123, p.144-150, 2019, [ADM19].

J4 J. Auriol, F. Bribiesca-Argomedo, D. Bou Saba, M. Di Loreto, F. Di Meglio, *Delay-robust stabilization of a hyperbolic PDE-ODE system*, Automatica, vol. 95, p.494-502, 2018, [ABABS+18].

J3 J. Auriol, U.J.F. Aarsnes, P. Martin, F. Di Meglio, *Delay-robust control design for two heterodirectional linear coupled hyperbolic PDEs*, IEEE Transactions on Automatic Control, vol. 63, no 10, p.3551-3557, 2018, [AAMDM18].

J2 J. Auriol, F. Di Meglio, *Two-sided boundary stabilization of heterodirectional linear coupled hyperbolic PDEs*, IEEE Transactions on Automatic Control, vol. 63, p.2421-2437, 2018, [ADM18].

J1 J. Auriol, F. Di Meglio, *Minimum time control of heterodirectional linear coupled hyperbolic PDEs*, Automatica, vol. 71, p.300-307, 2016, [ADM16a].

4.2 . Conference Papers with reviewing committee

C27 J. Redaud, J. Auriol, *Backstepping stabilization of a clamped string with actuation inside the domain*, IFAC World Congress, Yokohama, 2023, [RA23].

C26 J. Auriol, M. Pereira, B. Kulcsar, *Mean-square exponential stabilization of coupled hyperbolic systems with uncertain parameters*, IFAC World Congress, Yokohama, 2023, [APK23].

C25 J. Auriol, D. Bresch-Pietri, *On Input-to-State Stability of Linear Difference Equations and Its Characterization with a Lyapunov Functional*, IFAC World Congress, Yokohama, 2023, [ABP23].

C24 J. Redaud, J. Auriol, S.-I. Niculescu, *Characterization of PI feedback controller gains for interconnected ODE - hyperbolic PDE systems*, Joint 8th IFAC Symposium on System Structure and Control, 17th IFAC Workshop on Time Delay Systems, 5th IFAC Workshop on Linear Parameter Varying Systems, Montreal, vol. 55, no 34, p.102-107, 2022, [RAN22a].

C23 J. Redaud, J. Auriol, Y. Le Gorrec, *In-domain damping assignment of a Timoshenko-beam using state feedback boundary control*, IEEE 61st Conference on Decision and Control (CDC), Cancun, pp. 5405-5410, 2022, [RALG22b].

C22 L. Brivadis, A. Chaillet, J. Auriol, *Online estimation of Hilbert-Schmidt operators and application to kernel reconstruction of neural fields*, IEEE 61st Conference on Decision and Control (CDC), Cancun, pp. 597-602, 2022, [BCA22].

C21 J. Redaud, J. Auriol, Y. Le Gorrec, *Distributed Damping Assignment for a Wave Equation in the Port-Hamiltonian Framework*, IFAC CPDE workshop on Control of Systems Governed by Partial Differential Equations, vol. 55, no 26, p.155-161, 2022, [RALG22a].

C20 J. Auriol, R. Shor, S.-I. Niculescu, N. Kazemi, *Estimating Drill String Friction with model-based and data-driven methods*, IEEE American Control Conference, pp. 3464-3469, Atlanta, USA, 2022, [ASNK22].

C19 J. Redaud, J. Auriol, S.-I. Niculescu, *Recursive dynamics interconnection framework applied to angular velocity control of drilling systems*, IEEE American Control Conference, pp. 5308-5313, Atlanta, USA, 2022, [RAN22b].

C18 A. Fathalian, N. Kazemi, J. Auriol, D. O. Trad, K. A. Innanen, R. Shor, *Forward modeling of seismic-while-drilling data in anisotropic viscoelastic media with anisotropic attenuation*, 83rd EAGE annual conference, Madrid, Spain, 2022, [FKA+22]

C17 J. Redaud, J. Auriol, S.-I. Niculescu, *Observer Design for a class of delay systems using a Fredholm transform*, 16th IFAC workshop on Time Delay Systems, Guangzhou, China, vol. 54, no 18, p.84-89, 2021, [RAN21a].

C16 J. Redaud, J. Auriol, S.-I. Niculescu, *Stabilizing Integral Delay Dynamics and Hyperbolic Systems using a Fredholm Transformation*, 60th IEEE Conference on Decision and Control, Austin, Texas, USA, p.2595-2600, 2021, [RAN21c].

C15 J. Auriol, F. Bribiesca-Argomedo, S.-I. Niculescu, J. Redaud, *Stabilization of a hyperbolic PDEs-ODE network using a recursive dynamics interconnection framework*, European Control Conference, Rotterdam, Netherlands, p.2494-2499, 2021, [ABANR21].

C14 J. Auriol, I. Boussaada, H. Mounier, S.-I. Niculescu, *Torsional-vibrations damping in drilling systems: Multiplicity-Induced-Dominancy based design*, MTNS, Cambridge, United Kingdom, vol. 54, no 9, p.428-433, 2021, [ABMN21].

C13 N. Kazemi, J. Auriol, K. Innanen, R. Shor, I. Gates, *Successive Full-waveform inversion of surface seismic and seismic-while-drilling datasets without low frequencies*, 82nd EAGE Annual Conference and Exhibition, Amsterdam, Netherlands, 2021, [KAI+21].

C12 S. Najedi, N. Kazemi, J.A. Curkan, J. Auriol, P.R. Durkin, S.M. Hubbard, K.A. Innanen, R.J. Shor, I.D. Gates, *Look ahead of the bit while drilling: potential impacts and challenges in the McMurray Formation*, the SPE Heavy Oil Conference, Calgary, 2020, [NKC+20a].

C11 J. Auriol, G. A. de Andrade, R. Vazquez, *A differential-delay estimator for thermoacoustic oscillations in a Rijke tube using in-domain pressure measurements*, IEEE Conference on Decision and Control, Jeju Island, Korea, p.4417-4422, 2020, [AdAV20].

C10 J. Auriol, F. Bribiesca-Argomedo, D. Bresch-Pietri, *Stabilization of an underactuated 1+2 linear hyperbolic system with a proper control*, IEEE Conference on Decision and Control, Jeju Island, Korea, 2020, [ABABP20].

C9 H. Yu, J. Auriol, M. Krstic, *Output-feedback PDE control of traffic flow on cascaded freeway segments*, IFAC World Congress, Berlin, Germany, vol. 53, p.7623-7628, 2020, [YAK20a].

C8 J. Auriol, N. Kazemi, K. Innanen, R.J. Shor, *Combining formation seismic velocities while drilling and a PDE-ODE observer to improve the drill-string dynamics estimation*, IEEE American Control Conference, Denver, Colorado, p.3120-3125, 2020, [AKIS20].

C7 J. Auriol, U. J. F. Aarsnes, F. Di Meglio, R.J. Shor, *Self-Tuning Torsional Drilling Model for Real-Time Applications*, IEEE American Control Conference, Denver, Colorado, p.3091-3096, 2020, [AAS20].

C6 H. Yu, J. Auriol, M. Krstic, *Simultaneous stabilization of Traffic Flow on Two Connected Roads Using the Aw-Rascle-Zhang Model*, IEEE American Control Conference, Denver, Colorado, p.3443-3448, 2020, [YAK20b].

C5 J. Auriol, F. Bribiesca-Argomedo, *Delay-robust stabilization of a $n+m$ hyperbolic PDE-ODE system*, IEEE Conference on Decision and Control, Nice, France, p.4996-5001, 2019, [ABA19].

C4 J. Auriol, F. Di Meglio, F. Bribiesca-Argomedo, *Delay-robust stabilization of a network of two interconnected PDE systems*, IEEE American Control Conference, Philadelphia, Pennsylvania, USA, p.593-599, 2019, [ADMBA19].

C3 P-O. Lamare, J. Auriol, U. J. F. Aarsnes, F. Di Meglio, *Robust output regulation of 2×2 hyperbolic systems*: Control law and Input-to-State Stability, IEEE American Control Conference, Milwaukee, Wisconsin, USA, p.1732-1739, 2018, [LADMA18].

C2 J. Auriol, F. Di Meglio, *Trajectory tracking for a system of two linear hyperbolic PDEs with uncertainties*, 20th World Congress of the international Federation of Automatic Control, Toulouse, France, vol. 50, no 1, p.7089-7095, 2017, [ADM17].

C1 J. Auriol, F. Di Meglio, *Two-sided boundary stabilization of two linear hyperbolic PDEs in minimum time*, Proc. of the 55th IEEE Conference on Decision and Control, Las Vegas, Nevada, USA, p.3118-3124, 2016, [ADM16b].

4.3 . Edited Volumes

B1 J. Auriol, J. Deutscher, G. Mazanti, G. Valmorbida, *Advances in Distributed Parameter Systems*, volume in the series *Advances in Delays and Dynamics*, vol. 14, Springer, 2021, [ADMV22].

4.4 . Book chapters

O2 N. Espitia, J. Auriol, H. Yu, M. Krstic, *Event-triggered output feedback control of traffic flow on cascaded roads*, chapter in *Advances in Distributed Parameter Systems*, volume in the series *Advances in Delays and Dynamics*, vol. 14, Springer, 2021, [EAYK22a].

O1 J. Redaud, J. Auriol, F. Bribiesca-Argomedo, *Practical output regulation and tracking for linear ODE-hyperbolic PDE-ODE systems*, chapter in *Advances in Distributed Parameter Systems*, volume in the series *Advances in Delays and Dynamics*, vol. 14, Springer, 2021, [RBAA22].

4.5 . Patents

P1 J. Auriol and R. Shor, *Methods relating to tool face orientation*, US Patent 11725499, 2021.

4.6 . Thesis

T1 J. Auriol, *Robust design of backstepping controllers for systems of linear hyperbolic PDEs*, PhD, MinesParis, PSL Research University, 2018, [Aur18].

4.7 . Submitted papers

SJ1 N. Kazemi, J. Auriol, K. Innanen, R. Shor, I. Gates, *Successive Full-waveform inversion of surface seismic and seismic-while-drilling datasets without low frequencies*, submitted to Geophysical Prospecting journal, 2022.

SJ2 L. P. Njoua Dongmo, J. Auriol, A. Iovine, *Smart traffic manager for speed harmonization and stop-and-go waves mitigation dedicated to connected autonomous vehicles*, submitted to IEEE Transactions on Control Systems Technology, 2023

SJ3 L. Brivadis, A. Chaillet, J. Auriol, *Adaptive control of spatiotemporal delayed neural fields*, submitted to Systems and Control Letters, 2023.

SJ4 G. Velho, J. Auriol, R. Bonalli, *A Gradient Descent-Ascent Method for Continuous-Time Risk-Averse Optimal Control*, submitted to Systems and Control Letters, 2023.

SJ5 Y. Zhang, H. Yu, J. Auriol, M. Pereira, *Mean-Square Exponential Stabilization of Mixed-Autonomy Traffic*, submitted to Automatica, 2023.

SJ6 J. Auriol, *Output-feedback stabilization of an underactuated network of N interconnected $n+m$ hyperbolic PDE systems*, submitted to IEEE Transactions on Automatic Control, 2023.

SJ7 S. Wiersdalen, M. Pereira, A. Lang, G. Szederkenyi, J. Auriol, B. Kulcsár, *Incremental exponential stability of the unidirectional flow model*, submitted to IEEE Transactions on Automatic Control, 2023.

SC1 Y. Zhang, J. Auriol, H. Yu, *Robust Boundary Stabilization of Stochastic Hyperbolic PDEs* , submitted to ACC, 2023.

SC2 G. Velho, R. Bonalli, J. Auriol, I. Boussaada, *Mean-Covariance Steering of a Linear Stochastic System with Input Delay and Additive Noise* , submitted to ECC, 2023.

SO1 J. Auriol, *Some insights on the practical control of hyperbolic systems*, submitted as a chapter for a volume in the series Advances in Delays and Dynamics, 2023.

Part II

Summary of research activities

5 - Introduction: Practical Control of Networks of hyperbolic systems

5.1 . General context

Distributed parameter systems provide a natural representation of industrial processes involving the evolution of quantities in time and space. In particular, hyperbolic partial differential equations play a crucial role in the mathematical description of transport phenomena with finite propagation speeds, e.g., transport of matter, sound waves, and information. **Networks of hyperbolic systems**, possibly coupled with Ordinary Differential Equations (ODEs), constitute an essential paradigm to describe a wide variety of large complex systems, including electric transmission lines [MWTA00], gas flow pipelines [RNM15]-[GD11], heat exchangers [XS02], flexible structures [PH22], traffic flow [AHB08, YK23], oil well drilling [Aam16, AS18], open channel flow [CANB99], [dHPC+03], or multiphase flow [DM11, DBVdHJ10, DBAR12]. Controlling and monitoring networks of hyperbolic systems are **difficult control engineering problems** due to the **distributed** nature of the different subsystems composing the network (time and space dependency), the possibly involved **graph structure** of the network, and the physical/economic **infeasibility of placing sensors and actuators everywhere** along the spatial domain. The stringent operating, environmental and economical requirements and the high mathematical complexity of these systems explain why traditional control methods exhibit a limited range of applicability and have not been successful at high technology readiness levels (TRLs) [ADM20, CZ12]. Thus, the theory of control of distributed parameter systems needs substantial advancements to achieve control and estimation objectives for such network structures.

The analysis of networks of balance laws is motivated by challenging recent engineering problems. For instance, such systems can model oil and gas pipelines. Since leaking pipelines cause economic losses and severe environmental damage, it is crucial to detect and locate leaks accurately [AA22]. Although *internal monitoring methods* (based, e.g., on ultrasound [Qid09]) detect leakages accurately, they are expensive and may require distributed measurements all along the network. This is why external methods based on estimations of the distributed states have been recently developed for **simple network configurations** [AA22]. Similarly, controlling traffic networks is essential in the near future for reducing contamination and fluidifying the density of cars on the roads. The traffic on a single freeway segment can be modeled by a set of hyperbolic equations (known as the ARZ model [YK23]), and stabilizing controllers that suppress stop-and-go oscillations have been designed in [YK23, ZPQ19]. However, when considering a general freeway network configuration, there is an effect on traffic flow stability from freeway branches merging or diverging, from branches looping back or forming a "beltway." Therefore, the **controllability of general networks** of ARZ models, with inputs at various locations along the interconnected freeway branches, is a complex question. Indeed, before designing stabilizing controllers to suppress stop-and-go oscillations, one must determine the input locations and actuation types that make the system controllable. These two challenging examples may explain the tremendous scientific interest in the design of stabilizing controllers for networks of hyperbolic systems.

5.1.1 . Boundary control of elementary hyperbolic systems

Before considering complex network structures, different theoretical approaches have been developed during the last decades to design boundary controllers and observers for one-dimensional linear balance law systems [BC16, Chap. 5]. Among them, one can find flatness-based controllers [MZ04, SDMKR13], optimization controllers [Lio71] or Lyapunov-based controllers [CBdN08, Cor09, PGW12] that have for instance enabled the design of dissipative boundary conditions [CBdN08, Cor09]. In this context, the **backstepping approach** [KS08] is a constructive method with some distinguishing

features. It consists of performing an invertible change of variables (using an integral transformation) to map the original system into a simpler form (called **"target system"**) amenable to analysis, control, and observer design. This results in explicit controllers, similar to classical finite-dimensional counterparts, expressed as functionals of the distributed states. The backstepping approach was initially introduced in [SK04] for a class of parabolic equations before producing results for wave equations [KGBS08] and linear (or quasilinear) hyperbolic systems [CVKB13, ADM16a, CHO17, DG19, ADM18, ADM16b]. A complete history of the backstepping method for Partial Differential Equations (PDEs) and of its extensions has been given in [VK17]. Interestingly, for linear hyperbolic systems, one of the major by-products of the backstepping controllers is to (partially) solve the finite-time stabilization and observability problems stated in [Rus72, Rus78b] and generalized by Tatsien Li in [Li10]. The reader is referred to [CN20, CN21a] for the most recent results on the optimal finite-time stabilization of homogeneous quasilinear hyperbolic systems.

One of the main difficulties with the backstepping method is finding a **suitable target system**. It should be simple enough to allow the design of the control law. Still, in the meantime, one must prove the existence of a transformation mapping the original system to the desired target system. The choice of the target system directly impacts the **closed-loop performance**. The general question of reachable target systems is still an open problem. For hyperbolic equations, they were usually chosen as finite-time stable [CN21a], thereby shadowing the robustness properties of the corresponding closed-loop systems [LRW96, MVZ$^+$09]. These robustness limitations may come from uncertainties in the parameters, disturbances acting on the system, noise on the measurements, neglected dynamics, or delays acting on the actuators. It has been observed (see [DLP86, LRW96]) that for many feedback systems, the introduction of arbitrarily small time delays in the loop may cause instability for any feedback. In particular, the controllers designed to guarantee finite-time stability are usually non-strictly proper and therefore may have zero robustness margins. In [ADM20], the authors introduced tuning parameters in the design, thus guaranteeing potential trade-offs between different specifications (namely delay-robustness and convergence rate). The main idea behind these modifications was to avoid the complete cancellation of the reflection terms at the boundaries of the spatial domain of the PDE. The gained robustness comes at the price of degraded performance. A general robustification procedure was proposed in [ABADM23]. This robustification was achieved by the design of appropriate filters, generalizing the approaches in [BSBADLE19, ABP22]. As it will appear in its manuscript, the questions related to the choice of the target system in terms of closed-loop properties are exacerbated when applying the backstepping methodology to networks of PDEs.

Interestingly, hyperbolic systems of linear balance laws have strong connections with a specific class of **neutral-type time-delay systems**. The earliest link is made through D'Alembert's formula [D'A49] that transforms a wave equation into a difference equation. More generally, using the method of characteristics, systems of linear first-order *uncoupled* hyperbolic PDEs can be transformed into difference equations. In [Rus78a, Rus91], the existence of a mapping between the solutions of potentially coupled linear first-order hyperbolic PDEs and zero-order neutral systems is proved using spectral methods. In [KK14], the mapping is proved to be unique and is explicitly constructed for a single hyperbolic equation with a reaction term. Furthermore, in [KK14], the authors have stated that the stability analysis is easier while converting the PDEs to a time-delay form. Indeed various methods have been proposed for the stability and robustness analysis of neutral systems, such as necessary and sufficient stability conditions based on complex analysis [BC63, HL02]. These connections were being generalized in [ADM19]: using appropriate backstepping transformations, a general class of hyperbolic systems can be rewritten as a set of simpler **Integral Delay Equations** (IDEs). This representation allowed the development of new tools for the analysis and control design of hyperbolic systems [BSBAA$^+$19, Aur18, AdAV20]. Therefore, such a time-delay representation of hyperbolic systems will be a cornerstone of the methods we present in this manuscript.

5.1.2 . From elementary systems to networks

Interconnections of hyperbolic systems (potentially coupled with ODEs) are not a new problem as such networks naturally arise in multiple industrial processes (e.g., electric power transmission systems [SWGR13], or traffic networks [YK23]). In particular, interconnections with a **cascade chain**

structure have received specific attention [AS18]. Indeed, this sub-class of networks can model challenging industrial processes as the propagation of torsional waves in drilling systems [AS18] or deepwater construction vessels [SWS10]. Most constructive control designs for such systems are based on the backstepping approach. Of particular note are results concerning cascaded interconnections of hyperbolic PDE-ODE systems, such as [Aam12, DG21, ABABS+18]. For ODE-PDE-ODE configurations, an output-feedback controller has been designed in [DGK18] based on assumptions that guarantee the existence of a Byrnes–Isidori normal form for one of the ODE. These restrictions are partially avoided in [BSBADLE19], where the control design relies on a *rewriting of the interconnection as a time-delay system*. This approach was later extended in [WK20] to encompass a state observer. Some recent developments have also been obtained for interconnected PDE systems with non-linear ODEs using a modular design of tracking controllers [IGDR21]. In [Aur20], the author designed a stabilizing output feedback controller for a chain composed of an arbitrary number of scalar subsystems using a **recursive backstepping transformation**. This approach was generalized in [RAN21b] by introducing a **new recursive dynamics framework**. This new framework is **modular** since the control law only requires simple properties for each subsystem (controllability, trackability, observability, predictability).

In most (if not all) of the contributions listed above, the actuators (or sensors) were always at one end of the chain. There are several situations in which the actuator may be placed at an arbitrary chain node. For instance, when developing traffic control strategies on vast road networks, the actuator (ramp metering) can be located at a crossroad (junction of two roads) [YK23]. Having an actuator located at one of the intersection nodes of the chain raises challenging **controllability questions**. In most cases, such interconnected systems may not be controllable, and appropriate controllability conditions must be derived [RAN22c]. Under appropriate spectral controllability/observability conditions [Pan76, Mou98], it becomes possible to design a stabilizing control law, as it will be shown in this manuscript. Spectral approaches have been developed for networks of wave equations in a broader configuration detailed below. However, to our knowledge, no existing contributions solve the problem for an arbitrary chain composed of non-scalar balance laws subsystems with arbitrary actuator/sensor locations.

Beyond the (relatively) simple cascade structure, some systems can only be expressed using more general network topologies, such as star-shaped networks (i.e., networks with a central vertex belonging to all edges) [DZ06, GS10], tree-shaped networks (i.e., networks without cycles) [BY15, PR14] or cycles [DZ06]. A graph representation has been proposed in [DZ06] for arbitrary networks of wave equations. Such complex network structures have attracted much research effort [BCG+14, DZ06]. For instance, the exact controllability of nodal profile for quasilinear hyperbolic systems in a tree-like network has been assessed in [GL11] using the method of characteristics. It has been shown that depending on the graph structure, some types of controllability (exact/approximate) may not be obtained [TW09]. To identify reflections of graph-theoretic notions on the system properties, the concept of **structural controllability** has been introduced in [Lin74]. As there is a gap between knowing the controllability properties of the system and the design of constructive control laws, different approaches have been proposed for designing stabilizing controllers. PI boundary controllers have, for instance, been considered in [BCT15] for fully actuated tree-like networks (i.e., with one control input per vertex), establishing stability conditions with quadratic Lyapunov functions. In [SWGR13], the authors consider a flatness-based feedforward control design. For networks of wave equations, most contributions [BY15, DZ06] use spectral methods based on eigenvalues. Although these eigenvalues cannot be explicitly computed, obtaining specific information on their asymptotic behavior is possible. Alternative approaches based on reformulating the systems as non-autonomous difference equations are given in [CMS16].

5.1.3 . General objective

The general objective of this manuscript is to present some recent developments for the **practical control** of **networks of linear hyperbolic systems**. The proposed control strategies are said to be practical in the sense that they are constructive and easily implementable. We will show how to obtain sufficient conditions to guarantee the output-feedback stabilization of a large class of networks of

ODE-PDE-ODE systems. These sufficient conditions correspond to rank conditions for the associated control/observer operators. To go beyond these limitations and investigate more complex networks and underactuated systems that do not necessarily verify these conditions, we show that it is crucial to focus on the structural properties of the network. In particular, we will focus on interconnections of hyperbolic systems with a chain structure and introduce novel and original control strategies. We will also show how to apply these strategies to industry-inspired test cases. In the rest of this chapter, we present the generic mathematical representation we use to describe the class of systems under consideration. We then introduce some elementary properties and definitions that will be required in the rest of the manuscript. We show that the proposed representation covers many examples already considered in the literature. Finally, we present the complete outline of the manuscript.

5.2 . Systems under consideration, well-posedness and control objectives

5.2.1 . Generic representation of interconnected systems

In this section, we give a generic mathematical representation that can describe any arbitrary network configuration of linear hyperbolic equations potentially coupled with ODEs (see Section 5.3 for examples). Although constructive control designs require specific structural assumptions, this representation will allow us to introduce preliminary results that will be **milestones** for the developments we present in this manuscript. More precisely, we consider in this manuscript the following general $n \times m$ linear hetero-directional hyperbolic system coupled through its boundaries with linear ODEs

$$\begin{cases} \dot{X}(t) = A_0 X(t) + E_0 v(t,0) + B_X U(t), \\ u(t,0) = C_0 X(t) + Q v(t,0) + B_u U(t), \\ \partial_t u(t,x) + \Lambda^+ \partial_x u(t,x) = \Sigma^{++}(x) u(t,x) + \Sigma^{+-}(x) v(t,x), \\ \partial_t v(t,x) - \Lambda^- \partial_x v(t,x) = \Sigma^{-+}(x) u(t,x) + \Sigma^{--}(x) v(t,x), \\ v(t,1) = R u(t,1) + C_1 Y(t), \\ \dot{Y}(t) = A_1 Y(t) + E_1 u(t,1), \end{cases} \tag{5.1}$$

which is defined for almost every $(t,x) \in [0,+\infty) \times [0,1]$. The state of the system is denoted $(X(t), u(t,\cdot), v(t,\cdot), Y(t))$ and belongs to the space χ, defined by

$$\chi = \mathbb{R}^p \times L^2([0,1],\mathbb{R}^n) \times L^2([0,1],\mathbb{R}^m) \times \mathbb{R}^q, \tag{5.2}$$

where p, n, m and q are positive integers. The associated $\chi-$norm is defined by

$$||(X(t), u(t,\cdot), v(t,\cdot), Y(t))||_\chi = \sqrt{||X(t)||^2_{\mathbb{R}^p} + ||u(t,\cdot)||^2_{L^2} + ||v(t,\cdot)||^2_{L^2} + ||Y(t)||^2_{\mathbb{R}^q}}, \tag{5.3}$$

i.e., the square of this norm corresponds to the sum of the squares of the usual Euclidean or L^2-norm of each component. The matrices Λ^+ and Λ^- are diagonal and represent the **transport velocities**. We have $\Lambda^+ = \text{diag } (\lambda_i)$ and $\Lambda^- = \text{diag } (\mu_i)$ and we assume that their coefficients satisfy

$$-\mu_m < \cdots < -\mu_1 < 0 < \lambda_1 < \cdots < \lambda_n.$$

These transport velocities are assumed to be constant. However, all the results we present in this manuscript can be easily extended to space-dependent transport velocities at the cost of technical and lengthy computations. We denote τ the maximum transport delay for the PDE system

$$\tau = \max_{i,j}\left(\frac{1}{\lambda_i} + \frac{1}{\mu_j}\right). \tag{5.4}$$

The spatially-varying coupling matrices $\Sigma^{\cdot\cdot}$ are regular matrices (we assume here that each coefficient of the matrix is a continuous function). Without any loss of generality, we can assume that the diagonal entries of Σ^{++} and Σ^{--} are equal to zero, i.e., we have

$$\forall\ x \in [0,1],\ \forall\ 1 \leq i \leq n,\ \forall\ 1 \leq i \leq m,\ \Sigma^{++}_{i,i}(x) = \Sigma^{--}_{j,j}(x) = 0. \tag{5.5}$$

Indeed, these diagonal terms can be transferred to the anti-diagonal terms using an exponential change of variables [CVKB13]. The control input is denoted $U(t) \in \mathbb{R}^r$, where r is a positive integrer. The different **constant** coupling matrices satisfy $A_0 \in \mathbb{R}^{p\times p}$, $E_0 \in \mathbb{R}^{p\times m}$, $B_X \in \mathbb{R}^{p\times r}$, $B_u \in \mathbb{R}^{n\times r}$, $C_0 \in \mathbb{R}^{n\times p}$, $A_1 \in \mathbb{R}^{q\times q}$, $E_1 \in \mathbb{R}^{q\times n}$, $C_1 \in \mathbb{R}^{m\times q}$, $R \in \mathbb{R}^{m\times n}$, $Q \in \mathbb{R}^{n\times m}$. Due to the matrices B_X and B_u, the control input can directly act on the ODE state X or the PDE boundary $u(t,0)$. Nevertheless, in what follows, we do not consider the case where the PDE and the ODE can be simultaneously actuated, which means that either $B_X \equiv 0$ or $B_u \equiv 0$. Finally, we consider the case of uncollocated measurements:

$$y = C_Y Y(t) + C_u u(t,1), \tag{5.6}$$

where $C_Y \in \mathbb{R}^{d\times q}$ and $C_u \in \mathbb{R}^{d\times n}$, where d is a positive integer. Again, we consider that we do not simultaneously measure the PDE and ODE states, which means either $C_X \equiv 0$ or $C_u \equiv 0$. The case of collocated measurements can be solved using analogous methodologies.

5.2.2 . Well-posedness

Throughout the manuscript, we will design controllers that stabilize the system (5.1) in the sense of the χ-norm. However, to simplify the analysis (for instance, in Chapter 9 where we consider the pointwise evaluation of the states u and v), it might be interesting to require stronger regularity properties for the system. More precisely, we will consider that the state of the system remains in the following space

$$\chi_0 = \mathbb{R}^p \times H^1([0,1],\mathbb{R}^n) \times H^1([0,1],\mathbb{R}^m) \times \mathbb{R}^q, \tag{5.7}$$

where the associated χ_0-norm is defined by

$$||(X(t),u(t,\cdot),v(t,\cdot),Y(t))||_{\chi_0} = \sqrt{||X(t)||^2_{\mathbb{R}^p} + ||u(t,\cdot)||^2_{H^1} + ||v(t,\cdot)||^2_{H^1} + ||Y(t)||^2_{\mathbb{R}^q}}. \tag{5.8}$$

We then have the following well-posedness result for the open-loop system.

Theorem 5.2.1.

For every initial condition $(X_0,u_0,v_0,Y_0) \in \chi_0$ that verifies the compatibility conditions

$$u_0(0) = C_0X_0 + Qv_0(0), \quad v_0(1) = Ru_0(1) + C_1Y_0, \tag{5.9}$$

there exists one and one only

$$(X,u,v,Y) \in \mathcal{C}^1([0,\infty),\chi) \cap \mathcal{C}^0([0,\infty),\chi_0),$$

which is a solution to the open-loop Cauchy problem (5.1) (i.e., $U \equiv 0$). Moreover, there exists $\kappa_0 > 0$ such that for every $(X_0,u_0,v_0,Y_0) \in \chi_0$ satisfying the compatibility conditions, the unique solution verifies

$$||(X(t),u(t,\cdot),v(t,\cdot),Y(t))||_{\chi} \leq \kappa_0 \mathrm{e}^{\kappa_0 t}||(X_0,u_0,v_0,Y_0)||_{\chi}, \quad \forall t \in [0,\infty). \tag{5.10}$$

Proof : The proof can be adjusted from [BC16, Theorem A.1, Theorem A.6]. It relies on Lumer-Philipps theorem [LP61, Paz12]. ■

This theorem (and most of the results presented in the manuscript) could be adjusted to deal with weak solutions to the Cauchy problem (5.1), as shown in [BC16]. However, this would be at the cost of involved technical computations. It is important to emphasize that Theorem 5.2.1 only shows the well-posedness in open-loop. The closed-loop well-posedness could be shown using the admissibility of the control operator [Cor09] (since the control law we design will be continuous in time) or adjusting the proof of Theorem 5.2.1. The compatibility condition (5.9) may be changed in closed-loop to

encompass the effect of the feedback law that has been designed. Thus, it may appear artificial and rather stringent, as it requires very specific values of the initial conditions. However, as shown in [CVKB13], it is possible to modify our control laws in a way that, without losing the stabilizing properties, does not require any specific values in the initial values beyond the natural conditions. Moreover, the different control strategies proposed throughout the manuscript rely mainly on the backstepping methodology [KS08]. Using invertible and bounded transformations, the closed-loop system can be mapped to a target system for which usual well-posedness results (as Theorem 5.2.1) can be straightforwardly applied. Consequently, the original and target systems share equivalent regularity and stability properties. This is why the well-posedness of the closed-loop system will not be discussed.

5.2.3 . Stabilization Objectives

Stabilizing controllers

The main objective of this manuscript consists in designing output feedback controllers that stabilize the system (5.1) in the sense of the following definition.

Definition 5.2.1 *The zero equilibrium of the closed-loop system* (5.1) *is exponentially stable if there exist* κ_0 *and* $\nu > 0$ *such that for any initial condition* $(X_0, u_0, v_0, Y_0) \in \chi$*, we have*

$$||(X(t), u(t,\cdot), v(t,\cdot), Y(t))||_\chi \leq \kappa_0 \mathrm{e}^{-\nu t} ||(X_0, u_0, v_0, Y_0)||_\chi \; 0 \geq t$$

Even if the state of the system lies in the space χ_0, we only consider its stability properties in the sense of the χ-norm, which can somehow be related to the global energy of the system. Several contributions in the literature considered the stabilization of (5.1) using various techniques, e.g., Byrnes–Isidori normal in [DGK18], inversion of the ODE dynamics in [BSBADLE17]. However, a large number of the proposed controllers feature vanishing robustness margins. Indeed, as detailed in [LRW96, CZ12, HL02], controls laws designed to stabilize hyperbolic systems can result in unstable closed-loop systems in the presence of arbitrarily small delays in the feedback loop or uncertainty in some parameters. To design stabilizing control laws for the class of system (5.1), it may be convenient either to cancel the reflection terms in the PDE or to inverse the ODE dynamics using high-order derivatives. Although such approaches considerably simplify the design, the resulting control laws are not *strictly proper*, which may result in vanishing robustness margins [ABABS+18] (which is a major difference with finite-dimensional linear time-invariant systems). In this manuscript, we aim to design **robust stabilizing controllers**.

Stability and robustness concepts

We now introduce some stability and robustness concepts useful in the whole manuscript. In particular, we emphasize the links between exponential stability in the sense of Definition 5.2.1 and the transfer function associated to (5.1) (see [CM09]). In what follows, the multivariable extensions of the Wiener algebra or the Callier Desoer functions (as well as the corresponding Laplace transforms) will be denoted with a $\mathcal{M}$ (e.g. $\mathcal{M}(\hat{\mathcal{B}}(0))$). We refer the reader to the *Notation* section for a proper definition of the different algebras we use in the rest of this section. For the Callier-Desoer class, we have the following simple representation:

$$\hat{\mathcal{B}}(0) = \hat{\mathcal{A}}_-(0)[\mathcal{R}_\infty(0)]^{-1},$$

where

$$\mathcal{R}_\infty(0) = \{\mathbf{f} \in \mathbb{C}_p(s) \mid \mathbf{f} \text{ has no poles in } \mathbb{C}_0 \text{ and is nonzero at } \infty\},$$

where $\mathbb{C}_p(s)$ denotes the algebra of proper rational transfer functions with complex coefficients. We now recall several results adjusted from [CM09].

Definition 5.2.2 *If a system maps every input* U *in* $L^2(0,\infty)$ *to an output* y *in* $L^2(0,\infty)$*, and if* $\sup_{U\neq 0} \frac{||y||_2}{||U||_2} < \infty$*, the system is* ***stable****. A transfer function* $G(s)$ *is* ***proper*** *if for sufficiently large* ρ*,* $\sup_{Re(s)\geq 0, |s|>\rho} |G(s)| < \infty$*. If the limit of* $G(s)$ *at infinity exists and is 0, G is said to be* ***strictly proper****.*

Theorem 5.2.2.

A linear system is stable if and only if its transfer function G belongs to $H_\infty = \{G : \mathbb{C}^+ \to \mathbb{C} \,|\, G \text{ analytic and } \sup_{Re(s)>0} |G(s)| < \infty\}$, with the norm $||G||_\infty = \sup_{Re(s)>0} |G(s)|$. In this case, the function G is called a stable transfer function.

Consider now a feedback controller $K \in \mathcal{M}\hat{\mathcal{B}}(\beta)$. We have the following definition from [CZ12].

Definition 5.2.3 *The feedback system (G, K) (where G, $K \in \mathcal{M}\hat{\mathcal{B}}(\beta)$), is said to be* $\beta-$input-output stable *if and only if*

1. *There exists a $\rho > 0$ such that*

$$\inf_{s\in\mathbb{C}_{-\beta},\ |s|\geq\rho} |\det(Id - G(s)K(s))| > 0;$$

2. *The transfer matrices $S = (Id - GK)^{-1}$, KS, SG, and $I + KSG$ are in $\mathcal{M}\hat{\mathcal{A}}_-(\beta)$.*

K is called a $\beta-$stabilizing controller for G. If $\beta = 0$, we use the expression input-output stable, and we call K a stabilizing controller.

Recall that $f \in \hat{\mathcal{A}}_-(\beta)$ is holomorphic and bounded on $\mathbb{C}_{-\beta}$ and $\sup_{s\in\mathbb{C}_{-\beta}} \leq ||f||_\beta$. In the Laplace domain, the closed-loop stability properties for a given controller may then be analyzed by focusing on the characteristic equation. In particular, it is crucial to show that S does not have any poles in the closed right-half plane. The reader is referred to [LGM99] for the links between the spectral radius and the spectral bound of the associated semigroup (the so-called spectrum-determined growth condition). However, as shown in the next sections, specific properties exist for time-delay systems of neutral type. Finally, we recall different robustness concepts

Definition 5.2.4 (w-stability [CZ12]) *Consider a plant transfer function $G \in \mathcal{M}\hat{\mathcal{B}}(0)$ and a feedback controller $K \in \mathcal{M}\hat{\mathcal{B}}(0)$. The closed-loop system is* w-stable *if and only if for any approximate identity I_δ (where $0 \leq \delta < \mu$), the closed-loop transfer function $GK\,(I + I_\delta GK)^{-1}$ is stable. An approximate identity is a family of transfer functions $I_\delta \in \mathcal{M}\hat{\mathcal{A}}_-(0)$ such that*

1. $\|I_\delta\|_\infty < 1$, $I_0 = I$;
2. *On every compact set of $\mathbb{C}_0^+$, I_δ converges to I when δ goes to zero.*

Suppose that (G, K) is input-output stable. Then (G,K) is w-stable *if there exists a $\rho > 0$ such that*

$$\sup_{\{s\in\ \mathbb{C}_0^+|\ |s|>\rho\}} ||G(s)K(s)|| < 1. \tag{5.11}$$

Approximate identities may include more general transfer functions than the ones stemming from uncertainties on the delays. Thus, w-stability implies delay-robust stability in the sense of [LRW96]. It also includes robustness with respect to some uncertainties (but not all, since it has been shown in [ADM20] that approximate identities cannot model uncertainties in the transport velocities).

Definition 5.2.5 *Let G and G_Δ be transfer matrices in $\mathcal{M}\hat{\mathcal{B}}(0)$. A perturbation $\Delta_a \in \mathcal{M}\hat{\mathcal{B}}(0)$ is an* admissible multiplicative uncertainty *if $G_\Delta = (I+\Delta_a)G$, if Δ_a has no poles on the imaginary axis, and if G and G_Δ have the same number of unstable poles in $\bar{\mathbb{C}}^+$. It is an* admissible additive uncertainty *if $G_\Delta = G + \Delta_a$ and if either Δ_a is a transfer matrix satisfying the previous requirements, which is strictly proper on $\bar{\mathbb{C}}^+$, or it is a stable perturbation. If $G = \tilde{M}^{-1}\tilde{N}$ is a left-coprime factorization of G over $\mathcal{M}\hat{\mathcal{A}}_-(0)$ [CZ12], a perturbation $(\Delta_N, -\Delta_M) \in \mathcal{M}\hat{\mathcal{A}}_-(0)$ is an admissible left-coprime-factor uncertainty if $\det(\tilde{M} + \Delta_M) \in \hat{\mathcal{A}}_\infty(0)$ and $G_\Delta = (\tilde{M} + \Delta_M)^{-1}(\tilde{N} + \Delta_N)$.*

Toward robust stabilization

The objective of this manuscript consists in designing stabilizing controllers for the system (5.1) in the sense of Definition 5.2.1, but that also are w-stable and robust in the sense of Definition 5.2.5. Several solutions have been proposed in the literature to overcome possible robustness issues while designing stabilizing controllers. A first solution was to cancel only a part of the reflection terms in the PDE, using a convolutional procedure as performed, e.g., in [AA19, Woi13, MZ04]. Although somehow standard, this approach presents the drawback of not distinguishing the effects of high and low frequencies in terms of stability and robustness. In addition, such an approach can be challenging when considering chains with many subsystems. An alternative approach has been proposed in [BSBADLE19, ABP22]. It combines the proposed non-proper control law with a well-tuned low-pass filter. The resulting control law then becomes strictly proper, which guarantees the existence of robustness margins. We will show in the next chapter how this approach can be generalized to obtain a filtering methodology that robustifies stabilizing control laws for the system (5.1). This filtering technique will simplify the design of stabilizing controllers for the proposed class of systems as it dissociates the stabilization problem from the robustness problem.

5.3 . Examples of networks and stabilizing control laws

The framework proposed by the representation (5.1) is extremely broad and can describe various interconnected systems. Under specific structural assumptions, system (5.1) corresponds to simple configurations for which the control design becomes simple. In this section, we give some examples that have either been studied in the literature or will be analyzed in the manuscript. These examples are crucial as they allow the development of specific techniques that can be generalized to complex networks.

5.3.1 . Heterodirectional linear coupled hyperbolic PDEs

Choosing $A_0 \equiv E_0 \equiv C_0 \equiv B_X \equiv A_1 \equiv E_1 \equiv C_1 \equiv 0$, $B_u = I_n$, $X(0) = 0$ and $Y(0) = 0$, system (5.1) can be rewritten as a system of heterodirectional linear coupled hyperbolic PDEs:

$$\begin{aligned}
&\partial_t u(t,x) + \Lambda^+ \partial_x u(t,x) = \Sigma^{++}(x)u(t,x) + \Sigma^{+-}(x)v(t,x),\\
&\partial_t v(t,x) - \Lambda^- \partial_x v(t,x) = \Sigma^{-+}(x)u(t,x) + \Sigma^{--}(x)v(t,x),\\
&v(t,1) = Ru(t,1),\ u(t,0) = Qv(t,0) + U(t).
\end{aligned}$$

This class of system corresponds to balance laws [BC16] and can model wave propagation, traffic network systems [YK23], electric transmission lines [LLM+16], hydraulic channels [dHPC+03], or communication networks. It is schematically pictured in Figure 5.1.

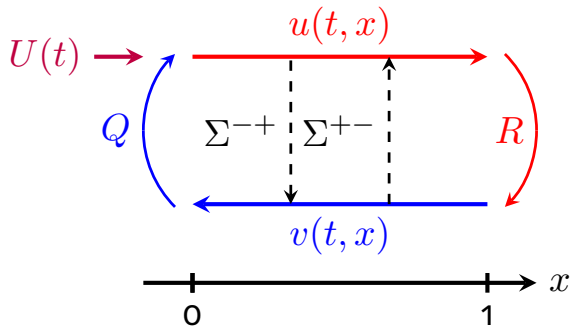

Figure 5.1: Schematic representation of a heterodirectional linear hyperbolic PDE system.

For this class of systems, stabilizing control laws have been designed in [HDMVK16, ADM16a, CHO17] using the backstepping approach [KS08]. The proposed controllers guarantee finite-time

stabilization. However, they require the cancellation of the reflection term $Qv(t,0)$, which results in a non-strictly-proper controller. This raises some robustness issues with respect to small delays in the loop [AAMDM18]. Modifications have been proposed in [ADM19] (by canceling only a part of the reflection terms) to guarantee the existence of robustness margins.

5.3.2 . ODE-PDE-ODE system with scalar hyperbolic states

In the case where $n = m = 1$ and $B_u \equiv 0$, system (5.1) corresponds to an ODE-PDE-ODE system with scalar hyperbolic states. This structure naturally arises when considering linear systems of balance laws with finite-dimensional actuators and load dynamics. It is the case of drilling devices where the PDE part of the system corresponds to the propagation of the mechanical wave, while the actuated ODE corresponds to the top drive and the unactuated ODE models the Bottom Hole Assembly (BHA) at the end of the drilling pipe. We consider such a system in Chapter 10. Similarly, Unmanned Aerial Vehicles (UAV)-cable-payload structure [WK20], or mining cable elevators [WK22] can be modeled by ODE-PDE-ODE systems. A schematic representation of such a configuration is given in Figure 5.2.

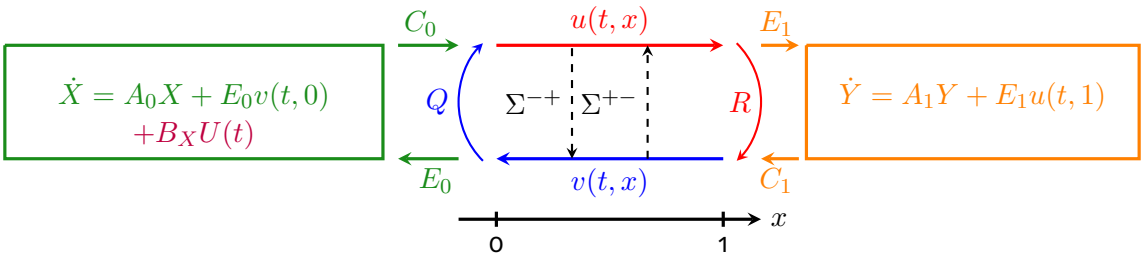

Figure 5.2: Schematic representation of an ODE-PDE-ODE system.

For this class of systems, stabilizing controllers have been designed in [WKP18, DGK18] or in [BSBADLE19]. However, most of the proposed designs, even though mathematically correct, possess a zero robustness margin. In [BSBADLE19], the proposed control law combines the backstepping approach with a Laplace analysis. Several assumptions were required to guarantee exponential stability. A low-pass filter has been added to the control law to make it strictly proper, thus guaranteeing the existence of robustness margins.

5.3.3 . Cascade network of interconnected PDEs

In [Aur20], we detailed the design of a robust stabilizing output feedback control law for an underactuated cascade network of n systems of two heterodirectional linear first-order hyperbolic Partial Differential Equations interconnected through their boundaries, only one of the subsystems being actuated. Such a network is pictured in Figure 5.3. This class of system may appear when considering oil production systems made of networks of pipes (whose principal line is known as the manifold) [MJ17] or traffic network systems [YAK22]. Such a system can be recast under the form (5.1) using a technique referred to as folding (see [Aur20, ABP22] for details). The control strategy proposed in [Aur20] combines successive backstepping transformations with a specific cascade structure. However, it is hardly generalizable to other types of interconnections. An extension for two coupled $n+m$ hyperbolic systems has been proposed in [ABP22], combining the backstepping approach with a flatness-based feedforward tracking control design. The case of a cascade of $n+m$ hyperbolic systems will be deeply analyzed in Chapter 8.

5.3.4 . Interconnected PDE-ODE systems

The framework proposed by system (5.1) can describe interconnections of ODEs and PDEs subsystems in a cascade structure. Each subsystem may be actuated. Such a configuration is described in Figure 5.4 in the case of N subsystems.

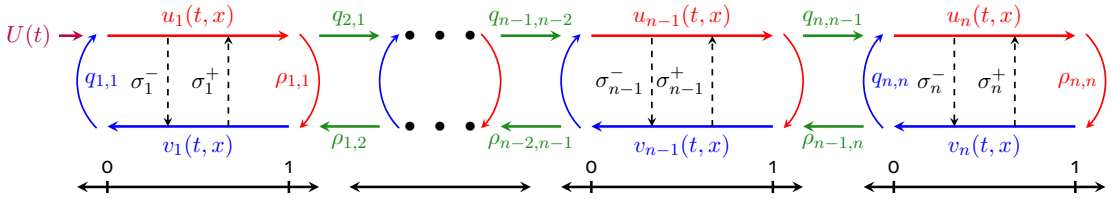

Figure 5.3: Schematic representation of a chain of linear PDE subsystems.

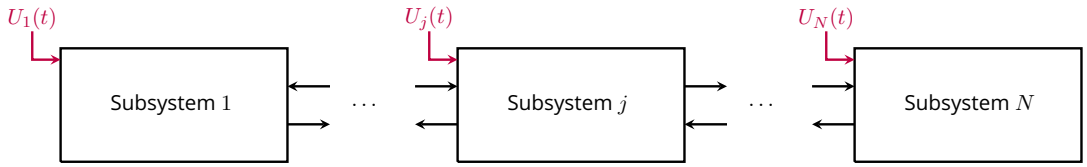

Figure 5.4: Schematic representation of a chain of ODEs/PDEs subsystems.

5.4 . Organization of the manuscript

The framework proposed in system (5.1) can describe complex networks composed of interconnected *elementary* hyperbolic/ODEs subsystems. The different subsystems are called elementary in that if taken alone, we already know how to design stabilizing output-feedback control laws for such subsystems. In that sense, the framework given by equations (5.1) is comprehensive and can describe various interconnected systems. Therefore, it legitimates the investigation of the controllability/observability properties of the system (5.1) in its most generic form. In **Chapter 6**, we present two important technical results used in the whole manuscript. First, we will show that the system (5.1) has equivalent stability properties to those of a time-delay system of neutral type. This representation will simplify the design of stabilizing controllers. Then, we will present a robustifying methodology that will simplify the design of robust stabilizing controllers for the proposed class of systems as it dissociates the stabilization problem from the robustness problem.

In **Chapter 7**, we give general assumptions under which it becomes possible to design stabilizing output feedback controllers. However, we will show that these assumptions are restrictive as we will exhibit some simple examples that do not fulfill them and for which we can still design stabilizing controllers. Indeed, it is essential to emphasize that equations (5.1) give a general representation that may not always be the most suitable for all systems since it could hide specific network/cascade structures of the system that could be leveraged in the control design. In particular, we will focus in **Chapter 8** on chains of subsystems actuated at one extremity of the chain. We will give generic conditions to design stabilizing control laws using a *recursive interconnected framework*. These conditions are less restrictive than those proposed in **Chapter 7** but require a specific cascade structure.

Beyond the network's structure, the available actuators/sensors' location is crucial to design an appropriate stabilizing output feedback law. It has been recently shown that depending on the actuators/sensors' locations, the system may not be controllable/observable [RAN22c]. In **Chapter 9**, we will consider the case of interconnected scalar hyperbolic systems but with the actuator located at one junction (and not at the extremity of the chain). We will prove that under appropriate spectral controllability conditions, designing a stabilizing control law is possible based on Fredholm integral equations.

These specific cases only cover some of the possible configurations. However, the different theoretical tools we introduce in the manuscript for stabilizing cascade systems and simple underactuated systems can become milestones to designing output feedback controllers for more complex networks with arbitrary actuators/sensor locations. Moreover, the proposed approaches can be used to solve challenging application cases. In particular, we will focus in **Chapter 10** on estimating the drill bit source signature in a drilling device. In **Chapter 11**, we will consider the stabilization of stop-and-go

oscillations in traffic networks.

Finally, we will conclude the manuscript with some perspectives to develop a systematic framework for the practical control of networks of linear hyperbolic systems. More precisely, a network could be described as a **graph**: each node corresponding to an elementary subsystem and each edge corresponding to the interconnection laws (boundary conditions) between the different subsystems. Therefore, the objective will be to enhance the **qualitative analysis** and generalize the proposed techniques to understand the links between the structure of the network (e.g., number of cycles, incidence matrix) and its **controllability/observability properties** for a given position of actuators/sensors. We aim to characterize the **possible actuators/sensors configurations** for a given graph structure that guarantee controllability/observability. We will also discuss introducing tuning parameters in the design to guarantee potential trade-offs with respect to implementation constraints. This will also emphasize the need for generic analytical techniques to quantify closed-loop performances with respect to industry-inspired performance indices (e.g., sensitivity, robustness margins, data sampling, convergence rate, and computational effort). We will also propose some discussions related to numerical integration and model reduction questions.

6 - Time-delay representation and robustification

It has been long noticed that some linear hyperbolic systems of Partial Differential Equations can be represented as difference time-delay systems. The earliest links were made through D'Alembert's formula [D'A49] that transforms a wave equation into a difference equation. More generally, using the method of characteristics, systems of linear first-order uncoupled hyperbolic PDEs can straightforwardly be transformed into difference equations. In [Rus91, Rus78a], the existence of a mapping between the solutions of potentially coupled hyperbolic PDEs and zero-order difference systems is proved using spectral methods. In [KK14], the mapping is proved to be unique and is explicitly derived for a single hyperbolic equation with a reaction term. Furthermore, the authors have stated that the stability analysis is easier when converting the first-order hyperbolic PDEs to a delay equation. These connections were extended in [ADM19] where it was shown that hyperbolic systems of linear balance laws could be rewritten as a set of simple neutral-type time-delay systems, namely **Integral Delay Equations** (IDEs). This representation has allowed the extension of time-delay systems methods (see [HVL93, Nic01]) to hyperbolic systems, thus simplifying the control design or the robustness analysis [ADM19]. In this chapter, we first show that such a time-delay representation can be obtained for the class of system (6.1). Introducing appropriate backstepping transformations [KS08], we show that the networks under consideration share equivalent stability properties to those of (IDEs). This time-delay representation will be crucial in the design of stabilizing controllers we propose in the following chapters.

Throughout this manuscript, we want to design **practical control strategies** in the sense that the associated controllers should be constructive, easily implementable, and guarantee the existence of robustness margins. It has been observed in [LRW96, CZ12, AAMDM18] that introducing arbitrarily small time delays in the loop may cause instability for many hyperbolic systems. In most cases, such a lack of robustness is induced by the fact that the proposed controller is not **strictly proper** [AAMDM18, Aur18]. Indeed, classical control strategies may require canceling reflection terms or inverting dynamics to simplify the design. Therefore, in the second part of this chapter, we introduce a **robustifying technique** that will simplify the control design by decoupling the design of a stabilizing control law from its robustification. This robustification is achieved by introducing appropriate filters that, when applied conjointly with the (possibly) non-strictly proper controller, will ensure robust stability of the closed-loop dynamics. This technique will considerably simplify the design we propose in the following chapters. It extends the approach derived in [Mor94, Mor95] for wave equations. Below, we rewrite system (6.1) for the sake of completeness

$$\begin{cases} \dot{X}(t) = A_0 X(t) + E_0 v(t,0) + B_X U(t), \\ u(t,0) = C_0 X(t) + Q v(t,0) + B_u U(t), \\ \partial_t u(t,x) + \Lambda^+ \partial_x u(t,x) = \Sigma^{++}(x) u(t,x) + \Sigma^{+-}(x) v(t,x), \\ \partial_t v(t,x) - \Lambda^- \partial_x v(t,x) = \Sigma^{-+}(x) u(t,x) + \Sigma^{--}(x) v(t,x), \\ v(t,1) = R u(t,1) + C_1 Y(t), \\ \dot{Y}(t) = A_1 Y(t) + E_1 u(t,1), \end{cases} \tag{6.1}$$

the different parameters being defined in Section 5.2. This chapter is inspired by the results of [ADM19, ABADM23].

6.1 . Time-delay formulation

In this section, we adjust the results from [ADM19] to rewrite (6.1) as a time-delay system. The proposed approach relies on successive backstepping transformations [KS08] that will move in-domain

coupling terms from the PDE equations. Using the method of characteristics, obtaining the desired time-delay system will then become possible.

6.1.1 . Integral transformations

First integral transformation: removing in-domain coupling terms

Inspired by [CHO17], we first combine two integral transformations to move the local coupling terms $\Sigma^{\cdot\cdot}$ to the actuated boundary (in the form of integral terms). Due to these transformations, non-local coupling terms and ODE terms will appear in the system. Consider the following Volterra transformation, similar to the one introduced in [CHO17, HDMVK19, ADM19].

$$\left\{\begin{array}{ll} X(t) & = \bar{X}(t) - \int_0^1 L_1(y)\alpha(t,x)dy - \int_0^1 L_2(y)\beta(t,x)dy, \\ u(t,x) & = \alpha(t,x) - \int_x^1 L^{\alpha\alpha}(x,y)\alpha(t,y)dy - \int_x^1 L^{\alpha\beta}(x,y)\beta(t,y)dy + \gamma_\alpha(x)Y(t), \\ v(t,x) & = \beta(t,x) - \int_x^1 L^{\beta\alpha}(x,y)\alpha(t,y)dy, - \int_x^1 L^{\beta\beta}(x,y)\beta(t,y)dy + \gamma_\beta(x)Y(t), \end{array}\right. \tag{6.2}$$

where the kernels $L^{\cdot\cdot}$ are bounded piecewise continuous functions defined on $\mathcal{T}_u = \{(x,y) \in [0,1]^2,\ x \leq y\}$, while the kernels L_1, L_2, γ_α and γ_β are bounded functions defined on $[0,1]$. They satisfy the following set of equations on their respective domains of definition

$$\left\{\begin{array}{l} \Lambda\partial_x L(x,y) + \partial_y L(x,y)\Lambda = \Sigma(x)L(x,y), \\ \Lambda\partial_x \gamma(x) = \Sigma(x)\gamma(x) - \gamma(x)^\top \bar{A}_1, \\ \partial_x L_1(x)\Lambda^+ = A_0 L_1(x) + E_0 L^{\beta\alpha}(0,x) - D_0(L^{\alpha\alpha}(0,x) - QL^{\beta\alpha}(0,x) - C_0 L_1(x)), \\ \partial_x L_2(x)\Lambda^- = -A_0 L_2(x) - E_0 L^{\beta\beta}(0,x) + D_0(L^{\beta\alpha}(0,x) - QL^{\beta\beta}(0,x) - C_0 L_2(x)), \end{array}\right. \tag{6.3}$$

with the boundary conditions

$$\left\{\begin{array}{l} \Lambda L(x,x) - L(x,x)\Lambda = \Sigma(x),\ \gamma_\alpha(1) = D_1,\ \gamma_\beta(1) = RD_1 + C_1, \\ L_1(0) = D_0(\Lambda^+)^{-1},\ L_2(0) = (D_0 Q + E_0)(\Lambda^-)^{-1}, \end{array}\right. \tag{6.4}$$

where $\Lambda = \text{diag}(\Lambda^+, -\Lambda-)$, $\Sigma = \begin{pmatrix} \Sigma^{++} & \Sigma^{+-} \\ \Sigma^{-+} & \Sigma^{--} \end{pmatrix}$, $L = \begin{pmatrix} L^{\alpha\alpha} & L^{\alpha\beta} \\ L^{\beta\alpha} & L^{\beta\beta} \end{pmatrix}$, $\gamma = (\gamma_\alpha, \gamma_\beta)$. The matrices D_0 and D_1 are **arbitrary matrices** of appropriate dimensions. They will be chosen later to simplify the design of stabilizing controllers or state observers. For instance, if the pair (A_1, E_1) is stabilizable, the matrix D_1 can be chosen such that $\bar{A}_1$ is Hurwitz. We define the matrices $\bar{A}_0$ and $\bar{A}_1$ by

$$\bar{A}_0 = A_0 + D_0 C_0,\ \bar{A}_1 = A_1 + E_1 D_1. \tag{6.5}$$

Finally, we define $L_{ij}^{\alpha\alpha}$ for $i \leq j$ by

$$L_{ij}^{\alpha\alpha}(0,y) = QL^{\beta\alpha}(0,y) + C_0 L_1(y). \tag{6.6}$$

To this set of equations, we add arbitrary continuous values for $L_{ij}^{\alpha\alpha}(x,1)$ (when $i > j$), and $L_{ij}^{\beta\beta}(x,1)$ (when $i > j$), and $L_{ij}^{\beta\beta}(0,y)$ ($i \leq j$). The following lemma assesses the existence of the kernels $L^{\cdot\cdot}$, γ_α, and γ_β.

Lemma 6.1.1 *The set of equations* (6.3)-(6.6) *has a unique solution* $(L^{\alpha\alpha}, L^{\alpha\beta}, L^{\beta\alpha}, L^{\beta\beta},\ L_1, L_2,\ \gamma_1, \gamma_2)$ *in* $(\mathcal{T}_u)^4 \times [0,1]^4$*, which is bounded and piecewise continuous.*

Proof : The proof follows from [DMBAHK18, Theorem 3.2]. The main idea consists of reinterpreting the ODEs in (6.3)-(6.6) as PDEs evolving in the triangular domain $\mathcal{T}_u$ with horizontal characteristic lines (since there is only an evolution along the x-axis). ■

The transformation (6.2) is a Volterra transformation and, therefore, invertible [Yos60]. It maps the original system (6.1) to the target system

$$\left\{\begin{array}{l} \dot{\bar{X}}(t) = \bar{A}_0\bar{X}(t) + G_3\alpha(t,1) + G_4 Y(t) + B_X U(t) + D_0 B_u U(t), \\ \alpha(t,0) = C_0\bar{X}(t) + Q\beta(t,0) + Q\gamma_\beta(0)Y(t) + B_u U(t) - \gamma_\alpha(0)Y(t) \\ \qquad + \int_0^1 F^\alpha(y)\alpha(t,y)dy + \int_0^1 F^\beta(y)\beta(t,y)dy, \\ \partial_t\alpha(t,x) + \Lambda^+\partial_x\alpha(t,x) = G_1(x)\alpha(t,1), \\ \partial_t\beta(t,x) - \Lambda^-\partial_x\beta(t,x) = G_2(x)\alpha(t,1), \\ \beta(t,1) = R\alpha(t,1), \quad \dot{Y}(t) = \bar{A}_1 Y(t) + E_1\alpha(t,1), \end{array}\right. \tag{6.7}$$

where the functions G_1 and G_2 verify the following Volterra integral equations (the existence of solutions are guaranteed in [Yos60]).

$$G_1(x) = \int_x^1 L^{\alpha\alpha}(x,y)G_1(y) + L^{\alpha\beta}(x,y)G_2(y)dy - L^{\alpha\alpha}(x,1)\Lambda^+ + L^{\alpha\beta}(x,1)\Lambda^- R - \gamma_\alpha(x)E_1, \tag{6.8}$$

$$G_2(x) = \int_x^1 L^{\beta\alpha}(x,y)G_1(y) + L^{\beta\beta}(x,y)G_2(y)dy - L^{\beta\alpha}(x,1)\Lambda^+ + L^{\beta\beta}(x,1)\Lambda^- R - \gamma_\beta(x)E_1. \tag{6.9}$$

The matrices G_3 and G_4 are defined by

$$G_3 = L_2(1)\Lambda^- R - L_1(1)\Lambda^+ + \int_0^1 L_1(y)G_1(y) + L_2(y)G_2(y)dy, \tag{6.10}$$

$$G_4 = E_0\gamma_\beta(0) + D_0(Q\gamma_\beta(0) - \gamma_\alpha(0)). \tag{6.11}$$

Finally, the matrices F^α and F^β are defined by

$$F^\alpha(y) = L^{\alpha\alpha}(0,y) - QL^{\beta\alpha}(0,y) - C_0L_1(y), \tag{6.12}$$

$$F^\beta(y) = L^{\alpha\beta}(0,y) - QL^{\beta\beta}(0,y) - C_0L_2(y). \tag{6.13}$$

Note that F^α is **strictly lower triangular** due to equation (6.6). We have the following theorem

Theorem 6.1.1 *There exists an invertible bounded linear map $\mathcal{F}_o : \chi \to \chi$ such that for every initial condition $(X_0, u_0, v_0, Y_0) \in \chi$, if $(\bar{X}, \bar{\alpha}, \beta, Y) \in \mathcal{C}^0([0,+\infty), \chi)$ denotes the solution to (6.7) satisfying the initial data $(\bar{X}(0), \alpha(0,\cdot), \beta(0,\cdot), Y(0)) = \mathcal{F}_o^{-1}(X, u_0, v_0, Y_0)$, then $(X, u, v, Y) = \mathcal{F}_o(X, \alpha, \beta, Y)$ is the solution to (6.1) satisfying $(X(0), u(0,\cdot), v(0,\cdot), Y(0)) = (X_0, u_0, v_0, Y_0)$. Moreover, if the state $(\bar{X}, \alpha, \beta, Y)$ exponentially converges to zero in the sense of the χ-norm, so does the state (X, u, v, Y), solution of (6.1).*

Proof : The proof is a consequence of the invertibility of the backstepping transformations and the boundedness of the different kernels [KS08]. ■

Remark 6.1.1 *The transformation $\mathcal{F}_o$ depends on the design parameters D_0 and D_1 that have not been chosen yet. We now denote it $\mathcal{F}_o(D_0, D_1)$ to emphasize this dependency.*

The target system (6.7) will be of specific interest for designing state observers. However, in terms of control purposes, it may be convenient to transform the coupling term $G_1(x)\alpha(t,0)$ by a term that depends on $\alpha(t,1)$.

Second integral transformation:

Consider the following transformations defined by

$$\alpha(t,x) = \check{\alpha}(t,x) - \int_x^1 \check{L}(x,y)\check{\alpha}(t,y)dy \tag{6.14}$$

$$\check{\alpha}(t,x) = \bar{\alpha}(t,x) - \int_0^1 \bar{L}(x,y)\bar{\alpha}(t,y)dy, \tag{6.15}$$

The kernel $\check{L}$ is a lower triangular matrix (i.e., $(\check{L})_{ij} = 0$ if $i < j$) whose components are bounded piecewise continuous functions. The kernel $\bar{L}$ is a strictly upper-triangular matrix (i.e., $\bar{L}_{ij} = 0$ if $i \geq j$) whose components are bounded piecewise continuous functions. The invertibility of the transformation is a consequence of its triangular structure. The kernel $\check{L}$ satisfies the following set of equations if $i \geq j$

$$\Lambda^+\partial_x\check{L}(x,y) + \partial_y\check{L}(x,y)\Lambda^+ = 0, \tag{6.16}$$

$$\Lambda^+\check{L}(x,x) - \check{L}(x,x)\Lambda^+ = 0, \tag{6.17}$$

$$(\check{L}(x,1))_{ij} = (G_1(x)(\Lambda^+)^{-1})_{ij} + \int_x^1 \sum_{k=1}^{n} \check{L}_{ik}(x,y)\check{G}_{kj}(y)\frac{1}{\lambda_j}dy, \tag{6.18}$$

where the matrix $\check{G}(x)$ is strictly upper-triangular (i.e. $\check{G}_{i,j}(x) = 0$ if $i \geq j$) and satisfies for all $x \in [0,1]$

$$(\check{G}(x))_{ij} = (G_1(x))_{ij} + \int_x^1 \sum_{k=1}^{n} \check{L}_{ik}(x,y)\check{G}_{kj}(y)dy \quad \text{if } i < j. \tag{6.19}$$

Lemma 6.1.2 *The set of equations* (6.16)-(6.19) *has a unique solution in $\mathcal{T}_u$, which is bounded and piecewise continuous.*

Proof : The proof is a consequence of the triangular structure of the different matrices appearing in the equations. For $j = 1$, equation (6.18) can be rewritten as

$$(\check{L}(x,1))_{i1} = (G_1(x)(\Lambda^+)^{-1})_{i,1}.$$

Combining this boundary condition with equation (6.17), we can solve equation (6.16) to compute $\check{L}_{i1}$ on its domain of definition. For $j = 2$, equation (6.19) can be rewritten as

$$(\check{G}(x))_{12} = (G_1(x))_{12} + \int_x^1 \check{L}_{11}(x,y)\check{G}_{12}(y)dy,$$

which is a Volterra equation that can be solved to obtain $\check{G}_{12}(y)$ [Yos60]. This in turns gives the kernels $\check{L}_{i2}$ using (6.18). Iterating the process allows us to compute the kernel matrix $\check{L}$ and the function $\check{G}$. ■

The kernel $\bar{L}$ satisfies the following set of equations

$$\Lambda^+\partial_x\bar{L}(x,y) + \partial_y\bar{L}(x,y)\Lambda^+ = 0, \ \bar{L}(1,y) = 0, \tag{6.20}$$

$$(\bar{L}(x,1))_{ij} = (\check{G}(x)(\Lambda^+)^{-1})_{i,j} \text{ if } i < j, \tag{6.21}$$

Due to its triangular structure, we can obtain a direct expression of $\bar{L}$ (and consequently show its existence) using the method of characteristics. This yields the following lemma

Lemma 6.1.3 *The set of equations* (6.20)-(6.21) *has a unique solution in $\mathcal{U}$, which is bounded and piecewise continuous.*

The invertibility of the transformation (6.15) is a consequence of the triangular structure of the kernel $\bar{L}$. The transformations (6.14)-(6.15) map the system (6.7) to the target system

$$\begin{cases} \dot{\bar{X}} = \bar{A}_0\bar{X} + G_3\bar{\alpha}(t,1) + G_4Y(t) + B_XU(t) + D_0B_uU(t), \\ \bar{\alpha}(t,0) = C_0\bar{X}(t) + Q\beta(t,0) + Q\gamma_\beta(0)Y(t) + B_uU(t) - \gamma_\alpha(0)Y \\ \qquad + \int_0^1 \bar{F}^\alpha(y)\bar{\alpha}(t,y)dy + \int_0^1 F^\beta(y)\beta(t,y)dy, \\ \partial_t\bar{\alpha}(t,x) + \Lambda^+\partial_x\bar{\alpha}(t,x) = G_5(x)\bar{\alpha}(t,0), \\ \partial_t\beta(t,x) - \Lambda^-\partial_x\beta(t,x) = G_2(x)\bar{\alpha}(t,1), \\ \beta(t,1) = R\bar{\alpha}(t,1), \quad \dot{Y} = \bar{A}_1Y + E_1\bar{\alpha}(t,1), \end{cases} \tag{6.22}$$

where

$$\begin{aligned} \bar{F}^\alpha(y) =& F^\alpha(y) + \bar{L}(0,y) + \check{L}(0,y) + \int_0^1 \check{L}(0,\nu)\bar{L}(\nu,y)d\nu - \int_0^1 F^\alpha(\nu)\bar{L}(\nu,y)d\nu \\ & - \int_0^y F^\alpha(\nu)\check{L}(\nu,y)d\nu + \int_0^1\int_1^\eta F^\alpha(\nu)\check{L}(\nu,\eta)\bar{L}(\eta,y)d\nu d\eta. \end{aligned}$$

The upper-triangular matrix function G_5 is defined by

$$G_5(x) = \bar{L}(x,0)\Lambda^+ + \int_0^1 \bar{L}(x,y)G_5(y)dy.$$

The initial condition of the system (6.22) is denoted $(\bar{X}, \bar{\alpha}_0, \beta_0, Y) \in \chi$. It is obtained by applying the different inverse backstepping transformations on the initial condition (X, u_0, v_0, Y_0) of the system (6.1). The original system (6.1) and the target system (6.22) have equivalent stability properties. In particular, we have the following lemma

Theorem 6.1.2 *There exists an invertible bounded linear map $\mathcal{F}_c : \chi \to \chi$ such that for every initial condition $(\bar{X}, u_0, v_0, Y_0) \in \chi$, if $(\bar{X}, \bar{\alpha}, \beta, Y) \in \mathcal{C}^0([0, +\infty), \chi)$ denotes the solution to* (6.22) *satisfying the initial data $(\bar{X}(0), \bar{\alpha}(0, \cdot), \bar{\beta}(0, \cdot), Y(0)) = \mathcal{F}_c^{-1}(X_0, u_0, v_0, Y_0)$, then $(X, u, v, Y) = \mathcal{F}_c(\bar{X}, \bar{\alpha}, \beta, Y)$ is the solution to* (6.1) *satisfying $(X(0), u(0, \cdot), v(0, \cdot), Y(0)) = (X_0, u_0, v_0, Y_0)$. Moreover, if the state $(\bar{X}, \bar{\alpha}, \beta, Y)$ exponentially converges to zero in the sense of the χ-norm, so does the state (X, u, v, Y), solution of* (6.1).

Proof : The transformation $\mathcal{F}_c$ corresponds to the composition of the transformations (6.2) and (6.14)-(6.15). The rest of the proof is a simple consequence of the invertibility of the backstepping transformations and the boundedness of the different kernels [KS08]. ■

This theorem implies that the system (6.22) can be used for stability analysis and control design. Again, the transformation $\mathcal{F}_c$ depends on the design parameters D_0 and D_1. To emphasize this dependency, we now denote it $\mathcal{F}_c(D_0, D_1)$. Although the target system (6.22) may appear more complex than the original system (6.1) it presents the advantage that the right part of the PDE equations does not contain any local in-domain coupling terms but only terms that depend on $\bar{\alpha}(t, 1)$ and $\bar{\alpha}(t, 0)$. Note that similar transformations can be applied without the ODEs (i.e., $X \equiv Y \equiv 0$).

6.1.2 . Target system in delay form

Using the method of characteristics, it is possible to express $\bar{\alpha}(t, x)$ and $\beta(t, x)$ as functions of (delayed values of) $\bar{\alpha}(t, 0)$. Consequently, denoting $z(t) = \bar{\alpha}(t, 0)$, we can show that z is the solution of an IDE [ADM19]. More precisely, we have the following lemma

Lemma 6.1.4 *There exist an integer $N > 0$, positive delays $\tau_i \leq \tau$, constant matrices F_i^z, F_i^X and F_i^Y and piecewise continuous bounded functions H_z, H_X, H_Y such that for all $t > \tau$, we have*

$$z(t) = \sum_{i=1}^{N} F_i^z z(t - \tau_i) + \int_0^\tau H_z(\nu) z(t - \nu) d\nu + C_0 \bar{X}(t) + (Q\gamma_\beta(0) - \gamma_\alpha(0)) Y(t) + B_u U(t) \tag{6.23}$$

$$\dot{\bar{X}}(t) = \bar{A}_0 \bar{X} + \sum_{i=1}^{n} F_i^X z(t - \frac{1}{\lambda_i}) + \int_0^\tau H_X(\nu) z(t - \nu) d\nu + G_4 Y(t) + B_X U(t) + D_0 B_u U(t), \tag{6.24}$$

$$\dot{Y}(t) = \bar{A}_1 Y(t) + \sum_{i=1}^{n} F_i^Y z(t - \frac{1}{\lambda_i}) + \int_0^\tau H_Y(\nu) z(t - \nu) d\nu. \tag{6.25}$$

Proof : The proof can be found in [ABADM23] and is similar to the one given in [ADM19]. The different matrices $F_i^\cdot$ and $H_\cdot$ can be explicitly computed following the methodology of [ADM19]. They only depend on the kernels of the backstepping transformations and the parameters of the system. ■

On the interval $[0, \tau]$ the function $z(t)$ could be expressed as a function of the initial conditions $(\bar{\alpha}_0, \beta_0)$ of the system (6.22). The proof of this result is technical but relies on the ideas developed in [BSBAA+19]. Thus, performing a translation, the function $z(t) = \bar{\alpha}(t, 0)$ could alternatively be seen as a function that belongs to $H^1([0, \tau], \mathbb{R}^n)$ or $H^1([-\tau, 0], \mathbb{R}^n)$. Without the ODEs, the z-equation corresponds to an **Integral Delay Equation** (IDE): a difference equation with a distributed-delay term. The analysis of the principal part of the IDE (i.e., the difference equation alone, without the integral term) has been the purpose of extensive investigation, particularly to characterize the root distribution for the associated characteristic equation [AH80, Hen87]. We will recall some of these properties below. Difference equations or IDEs can model a wide variety of systems in biology [CKG96], chemistry, epidemiology [CK76], or in engineering sciences [Nic01]. They are particularly useful to model electric networks [Bra68, Sle71, Ras74, CK68]. For all $0 < r \leq \tau$, let us define the space χ_r as

$$\chi_r = \mathbb{R}^p \times L^2([-r, 0], \mathbb{R}^n) \times \mathbb{R}^q$$

and define the associated χ_r-norm as

$$||(X(t), z_{[t]}, Y(t))||_{\chi_r} = \sqrt{||X(t)||_{\mathbb{R}^p}^2 + ||z_{[t]}||_{L_r^2}^2 + ||Y(t)||_{\mathbb{R}^q}^2}. \tag{6.26}$$

The following theorem shows how the stability properties of $(\bar{X}, z, Y)$ relate to those of $(\bar{X}, \bar{\alpha}, \beta, Y)$.

Theorem 6.1.3 *There exists two constants κ_0 and κ_1, such that for any linear bounded state-feedback law $U(t)$, for any $t > \tau$*

$$\kappa_0 ||(\bar{X}(t), z_{[t]}, Y(t))||^2_{\chi_{\frac{1}{\lambda_n}}} \leq ||(\bar{X}(t), \bar{\alpha}(t,\cdot), \beta(t,\cdot), Y(t))||^2_{\chi} \leq \kappa_1 ||(\bar{X}(t), z_{[t]}, Y(t))||^2_{\chi_\tau}. \quad (6.27)$$

Moreover, if $U(t) = 0$ for all $t < 2\tau$, the exponential stability of $(\bar{X}, z_{[t]}, Y)$ in the sense of the χ_τ norm is equivalent to the exponential stability of $(\bar{X}, \bar{\alpha}, \beta, Y)$ in the sense of the χ norm.

Proof : Inequality (6.27) follows with minor adjustments from [ADM19]. Let us now prove the second part of the theorem. There exists $M \in \mathbb{N}$ and $0 \leq t_0 \leq \frac{1}{\lambda_n}$ such that $\tau = \frac{M}{\lambda_n} + t_0$. For all $t \geq \tau$, we have

$$\begin{aligned}\int_0^\tau (z(t-\nu))^T z(t-\nu) d\nu = &\sum_{k=1}^{M-1} \int_0^{\frac{1}{\lambda_n}} (z(t-\nu-\frac{k}{\lambda_n}))^T z(t-\nu-\frac{k}{\lambda_n}) d\nu \\ &+ \int_0^{t_0} (z(t-\nu-\frac{M}{\lambda_n}))^T z(t-\nu-\frac{M}{\lambda_n}) d\nu. \quad (6.28)\end{aligned}$$

Assume that the state $(\bar{X}, z_{[t]}, Y)$ is exponentially stable in the sense of the χ_τ norm. Combining the definition of exponential stability with the right-hand-side of inequality (6.27), there exist $C_0 > 0$ and $\nu_0 > 0$ such that for all $t > \tau$,

$$||(\bar{X}(t), \bar{\alpha}(t,\cdot), \beta(t,\cdot), Y(t))||^2_{\chi} \leq C_0 \mathrm{e}^{-\nu t} ||(\bar{X}(\tau), z_{[\tau]}, Y(\tau))||^2_{\chi_\tau}.$$

Then, using equation (6.28), we obtain

$$||(\bar{X}(\tau), z_{[\tau]}, Y(\tau))||^2_{\chi_\tau} \leq \sum_{k=1}^{M-1} ||(\bar{X}(\tau), z_{[\tau-\frac{k}{\lambda_n}]}, Y(\tau))||^2_{\chi_{\frac{1}{\lambda_n}}} + ||(\bar{X}(\tau), z_{[\tau-\frac{M}{\lambda_n}]}, Y(\tau))||^2_{\chi_{t_0}}.$$

Consequently, using the left-hand-side of inequality (6.27) we have

$$\begin{aligned}||(\bar{X}(t), \bar{\alpha}(t,\cdot), \beta(t,\cdot), Y(t))||^2_{\chi} &\leq C_0 \mathrm{e}^{-\nu t} \sum_{k=1}^{M} ||(\bar{X}(\tau), \alpha(\tau-\frac{k}{\lambda_n},\cdot), \beta(\tau-\frac{k}{\lambda_n},\cdot), Y(\tau))||^2_{\chi} \\ &\leq C_1 \mathrm{e}^{-\nu t} ||(\bar{X}(0), \alpha(0,\cdot), \beta(0,\cdot), Y(0))||^2_{\chi},\end{aligned}$$

where we have used the well-posedness of the open-loop system (equation (5.10)) to obtain the last inequality. A similar inequality can be obtained using (5.10) for $t \leq \tau$. This implies the exponential stability of the state $(\bar{X}, \bar{\alpha}, \beta, Y)$ in the sense of the χ-norm. Let us now assume that the state $(\bar{X}, \bar{\alpha}, \beta, Y)$ is exponentially stable in the sense of the χ-norm. Due to equation (6.28) and inequality (6.27), we have for all $t > \tau$

$$||(\bar{X}(t), z_{[t]}, Y(t))||^2_{\chi_\tau} \leq \sum_{k=1}^{M} ||(\bar{X}(t), \alpha(t-\frac{k}{\lambda_n},\cdot), \beta(t-\frac{k}{\lambda_n},\cdot), Y(t))||^2_{\chi}.$$

Consequently, using the exponential stability of $(\bar{X}, \bar{\alpha}, \beta, Y)$, there exists $C_0 > 0$ and $\nu > 0$ such that for all $t > 2\tau$

$$||(\bar{X}(t), z_{[t]}, Y(t))||^2_{\chi_\tau} \leq C_0 \mathrm{e}^{-\nu t} ||(\bar{X}(\tau), \alpha(\tau,\cdot), \beta(\tau,\cdot), Y(\tau))||^2_{\chi}.$$

The right-hand-side of inequality (6.27) implies

$$||(\bar{X}(t), z_{[t]}, Y(t))||^2_{\chi_\tau} \leq \kappa_1 C_0 \mathrm{e}^{-\nu t} ||(\bar{X}(\tau), z_{[\tau]}, Y(\tau))||^2_{\chi}.$$

A similar inequality can be obtained $\tau \leq t \leq 2\tau$, due to [HVL93, Chapter 9, Theorem 3.4]. This concludes the proof. ■

The fact that the norms are different on the two sides of the inequality is related to the structure of the difference equation (see, for instance, the design of converse Lyapunov-Krasovskii functions [PK13]). Note that the equivalence regarding exponential stability has only been proved under $U(t) = 0$ for all $t < 2\tau$. This last condition is not restrictive regarding a stabilization objective as it only affects the transient. In what follows, we will assume that the delays τ_i are **rationally independent**. Indeed, as shown in [HVL93], extending the variable z (and increasing its dimension), it is always possible to rewrite the system in a framework where the delays are rationally independent. System (6.23)-(6.24) can be seen as a **comparison system** for the PDE system (6.22) (see, e.g., [Nic01] and the references therein). Note that any feedback law expressed in terms of $(\bar{X}, z, Y)$ can, in the end, be expressed as a function of $(\bar{X}, u, v, Y)$ using the invertible transformation $\mathcal{F}_c(D_0, D_1)$.

6.1.3 . Equations in the Laplace domain

To analyze the stability properties of the system (6.23)-(6.25), it may be easier to consider a frequential approach (using the Laplace transform). Without any loss of generality (in terms of asymptotic stability analysis), we assume all-zero initial conditions. The Laplace transform applied to (6.23)-(6.24) leads to

$$z(s) = F(s)z(s) + P_{11}(s)z(s) + P_{12}(s)\bar{X}(s) + P_{13}(s)Y(s) + B_u U(s), \tag{6.29}$$
$$(s\mathsf{Id} - \bar{A}_0)\bar{X}(s) = P_{21}(s)z(s) + P_{23}(s)Y(s) + B_X U(s) + D_0 B_u U(s), \tag{6.30}$$
$$(s\mathsf{Id} - \bar{A}_1)Y(s) = P_{31}(s)z(s), \tag{6.31}$$

where

$$F(s) = \sum_{i=1}^{N} F_i^z \mathrm{e}^{-\tau_i s},\ P_{11}(s) = \int_0^\tau H_z(\nu)\mathrm{e}^{-\nu s}d\nu,\ P_{12}(s) = C_0, \tag{6.32}$$

$$P_{21}(s) = \sum_{i=1}^{n} F_i^X \mathrm{e}^{-\tau_i s} + \int_0^\tau H_X(\nu)\mathrm{e}^{-\nu s}d\nu,\ P_{13}(s) = Q\gamma_\beta(0) - \gamma_\alpha(0), \tag{6.33}$$

$$P_{31}(s) = \sum_{i=1}^{n} F_i^Y \mathrm{e}^{-\frac{s}{\lambda_i}} + \int_0^\tau H_Y(\nu)\mathrm{e}^{-\nu s}d\nu,\ P_{23}(s) = G_4. \tag{6.34}$$

Let us denote $\Delta(s)$ the matrix defined by

$$\Delta(s) = \begin{pmatrix} \mathsf{Id} - F(s) - P_{11}(s) & -P_{12}(s) & -P_{13}(s) \\ -P_{21}(s) & (s\mathsf{Id} - A_0) & -P_{23}(s) \\ -P_{31}(s) & 0 & (s\mathsf{Id} - \bar{A}_1) \end{pmatrix}. \tag{6.35}$$

The next theorem shows how the properties of the matrix Δ relate to the stability properties of (6.23)-(6.24).

Theorem 6.1.4 *The open-loop system (i.e. $U \equiv 0$)* (6.23)-(6.24) *is exponentially stable in the sense of the χ_τ-norm if and only if there exists $\eta > 0$ such that all solution of the* ***characteristic equation*** $\det(\Delta(s)) = 0$ *satisfy* $Re(s) < \eta$.

Proof : The proof is obtained from [HVL93, Theorem 3.5] and [Hen74]. ■

This theorem can be adjusted in closed-loop, including the feedback terms added by $U(s)$ in the matrix Δ.

6.1.4 . A remark on robustness

As Section 5.2.3 explains, we want to stabilize the PDE system (6.1) robustly. Considering the time-delay system (6.23)-(6.24), the notion of delay-robust stabilization has to be compared to the one of strong stabilization [HVL93, HL02, MN07, MVZ+09]. Let us consider that $(Q\gamma_\beta(0) - \gamma_\alpha(0)) \equiv C_0 \equiv B_u \equiv 0$. Then, equation (6.23) rewrites

$$z(t) = \sum_{i=1}^{N} M_i z(t - \tau_i) + \int_0^\tau H_1(\nu)z(t - \nu)d\nu. \tag{6.36}$$

We can introduce the following concept of strong stability.

Definition 6.1.1 (Strong stability [HL02]) *The system* (6.36) *is said to be strongly stable if it is stable in the sense of the $L^2([-\tau, 0], \mathbb{R}^n)$-norm and if it remains stable in the presence of small variations acting on the delays τ_i and τ.*

One can notice that the problem of strong stability is related to the problem of robustness with respect to uncertainties in the transport velocities or to delay-robustness. Depending on the matrix M_i, the principal part of the difference equation (6.36) (i.e., the function $\mathsf{Id} - F(s)$) may have an infinite number of roots in $\mathbb{C}^+$. More precisely, we have the following lemma

Lemma 6.1.5 *If the delays τ_i are rationally independent and if*

$$\sup_{\theta_p \in [0,2\pi]^N} Sp\,(\sum_{k=1}^{N} M_k \exp(i\theta_k)) > 1, \tag{6.37}$$

then there exists $\eta < 0$ such that the equation $\det(Id - F(s)) = 0$ has an infinite number of solutions in $\mathbb{C}_\eta$.

Proof : Theorem 2.1 in [HL02] guarantees the existence of a solution in $\mathbb{C}_\eta$ for some $\eta < 0$. We can then apply a continuity argument [AH80, Corollary 3.3]. ■

Unfortunately, if $\det(\mathrm{Id} - F)$ has an infinite number of zeros in $\mathbb{C}_\eta$, so does $\det(\Delta)$, as stated below.

Lemma 6.1.6.

Let $\eta < 0$. If the function $\det(\mathrm{Id} - F)$ has an infinite number of zeros on $\mathbb{C}_\eta$, then the function $\det(\Delta)$ (where Δ is defined by equation (6.35)) has an infinite number of zeros whose real parts are strictly positive.

Proof : The proof of this lemma can be adjusted from [Aur18, Lemma 6.1.4] and relies on arguments from [Lev40, Theorem VIII] and [Boi13]. It can also be obtained using [Hen74]. ■

Consequently, if equation (6.37) is verified, it implies (in the case of rationally independent delays) that the function $\det(\Delta)$ has an infinite number of solutions in $\mathbb{C}^+$. It has been shown in [LRW96] that having an open-loop transfer function with a non-finite number of poles in the open right-half plane makes delay-robust stabilization impossible. This is consistent with [CZ12, Corollary 9.1.4]. Thus, to avoid such a case, we make the following assumption.

Assumption 6.1.1 *We have*

$$\sup_{\theta_p \in [0,2\pi]^N} Sp\,(\sum_{k=1}^{N} F_k^z \exp(i\theta_k)) < 1. \tag{6.38}$$

Then, there exists $\eta_0 > 0$ such that $Id - F(s)$ does not vanish on $\mathbb{C}_{\eta_0}$.

In the case of rationally independent delays, Assumption 6.1.1 corresponds to a necessary condition for delay-robust stabilization and prevents the characteristic equation $\det(\mathrm{Id} - F(s)) = 0$ from having an infinite number of poles on $\mathbb{C}^+$. As shown in [ADM19], this condition implies the exponential stability of the open-loop PDE system (u, v) in (6.1) in the absence of the coupling terms $\Sigma^{\cdot\cdot}$ and of the ODE-states. This property still holds in the case of rationally dependent delays. However, in that case, it is possible to simplify condition (6.38). Furthermore, since the spectral radius of a matrix is upper-bounded by any matrix norm, easy-to-compute sufficient conditions for this spectral radius condition to hold can be derived using different norms of the matrices involved at the cost of increased conservatism [CBdN08]. This spectral condition has since been considerably analyzed in the literature (see [MVZ+09, HV12, SOB10, Car96, DDLM15, Fri02, Nic01, Pep05]). Alternatively, Lyapunov–Krasovskii functionals with prescribed derivative defined by the so-called Lyapunov delay matrix have also been proposed in [KZ03, EM14]. In the rest of the manuscript, we will consider that Assumption 6.1.1 is satisfied.

6.2 . A filtering approach for the robustification of stabilizing controllers

The problem of designing a stabilizing control for the system (6.1) has not been solved in the general case and will be the purpose of the next chapters. In most cases considered in the literature (see the examples given in Section 5.3), it appears convenient for the control design to cancel some of the PDE boundary reflection terms or to invert a part of the ODE dynamics. However, this may result in a non-strictly proper control law, which implies robustness issues [ABABS+18]. Here, we

give general conditions under which it is possible to low-pass filter the (potentially non-strictly proper) control law to make it strictly proper, thus preserving suitable robustness properties while keeping the controller design simple. Indeed, the proposed approach separates the stabilization problem from the robustness problem. This robustification will be achieved by the design of appropriate filters, generalizing the approaches in [BSBADLE19, ABP22], that robustify the controller with respect to delays and parameter uncertainties. More precisely, when applied conjointly with the existing controller, they will ensure strong stability of the closed-loop dynamics. The filters will be designed by leveraging the fact that robustness issues appear at high frequencies. We give sufficient conditions that ensure strong stabilization provided the original control laws ensure exponential stabilization. This strategy can be considered as a generalization of the PI controllers calibrated for drilling applications such as SoftSpeed [KN09] or Z-torque, which aim at canceling the boundary reflection only on a portion of the frequency domain, as detailed in [ADMS18b].

Consider the dynamical system expressed in the Laplace domain by the set of equations (6.29)-(6.31). Let us denote $\bar{\ell}_0$ (resp. $\bar{\ell}_1$) the largest eigenvalue (in modulus) of $(sI - \bar{A}_0)$ (resp. $(sI - \bar{A}_1)$). To simplify the analysis, we consider that $D_0 = 0$. Let us define $\mathbb{C}_u = \{s \in \mathbb{C}^+,\ |s| > \max(\bar{\ell}_0, \bar{\ell}_1)\}$, so that the functions $(sI - \bar{A}_0)^{-1}$ and $(sI - \bar{A}_1)^{-1}$ are properly defined in $\mathbb{C}_u$. Consider a feedback law $U(s)$ of the form

$$U(s) = K_z(s)z + K_X(s)\bar{X} + K_Y(s)Y, \tag{6.39}$$

where the operators K_z, K_X, and K_Y are holomorphic functions that will satisfy some conditions given later. They belong to the Callier-Desoer class of transfer functions. Most (if not all) the feedback laws that have been designed in the literature [CHO17, DMBAHK18, ABABS+18, BSBADLE19] to stabilize systems of the form (6.1) have this expression in the Laplace domain. However, a non-strictly-proper control may not guarantee the existence of robustness margins [ABABS+18]. This is why we will give general conditions under which it becomes possible to low-pass filter the control law to obtain a strictly proper control law, thus allowing the existence of robustness margins. The closed-loop characteristic equation associated to (6.29)-(6.31) with the feedback law (6.39) reads as

$$\det(Q(s)) = \det(I_1(s) - P_0(s) - BK(s)) = 0$$

where the matrix $I_1(s)$ is defined by $I_1(s) = \text{diag}\,(\text{Id} - F(s), s\text{Id} - \bar{A}_0, s\text{Id} - \bar{A}_1)$, while the matrix $P_0(s)$ is defined by

$$P_0(s) = \begin{pmatrix} P_{11}(s) & P_{12}(s) & P_{13}(s) \\ P_{21}(s) & 0 & 0 \\ P_{31}(s) & 0 & 0 \end{pmatrix}.$$

The matrices B and $K(s)$ are defined by

$$B = \begin{pmatrix} B_u & B_X & 0 \end{pmatrix}^T,\ K(s) = \begin{pmatrix} K_z(s) & K_X(s) & K_Y(s) \end{pmatrix}.$$

We consider that the proposed feedback law has been designed to stabilize the system exponentially, i.e., we make the following assumption

Assumption 6.2.1 *The system* (6.29)-(6.31) *with the feedback law* (6.39) *is exponentially stable. Then, there exist* $\eta_1 > 0$ *and* $\epsilon > 0$ *such that* $|\det(Q(s))| > \epsilon$ *for all* $s \in \mathbb{C}_{\eta_1}$. *Moreover, we assume that the explosion rate of the function* $K(s)$ *is, at worst, polynomial.*

In what follows, we denote $\eta = \min\{\eta_0, \eta_1\}$ (where η_0 is defined in Assumption 6.1.1).

6.2.1 . Low-pass filter design

We now give general results that guarantee the possibility to low-pass filter the control $U(s)$ and make it strictly proper while stabilizing the system (6.29)-(6.31). We distinguish the two cases $B_X \equiv 0$ (only the PDE is actuated) and $B_u \equiv 0$ (only the ODE is actuated) as the requirements slightly differ depending on the considered case. We first rewrite Assumption 6.1.1 in a more amenable form.

Assumption 6.2.2 *There exists* $0 < \epsilon_0 < 1$ *such that* $\bar{\sigma}(F(s)) < \epsilon_0 < 1$ *on* $\mathbb{C}_\eta$.

We start with the case where only the PDE is actuated (i.e. $B_X \equiv 0$).

Theorem 6.2.1.

Consider the system (6.29)-(6.31) with the stabilizing feedback control law $U(s)$ given by (6.39). Consider that Assumption 6.2.1, and Assumption 6.2.2 are satisfied. Assume that $B_X \equiv 0$ and that

1. The controller gains are such that the functions $B_u K_Y(s)(s\mathrm{Id} - \bar{A}_1)^{-1}P_{31}(s)$, $B_u K_X(s)\,(s\mathrm{Id} - \bar{A}_0)^{-1}P_{21}(s)$, and $B_u K_X(s)(s\mathrm{Id} - \bar{A}_0)^{-1}P_{23}(s)(s\mathrm{Id} - \bar{A}_1)^{-1}$ are strictly proper
2. The function $K_z(s)$ is defined by $K_z(s) = K_z^p(s) + K_z^u(s)$, where $K_z^p(s)$ is strictly proper and K_z^u satisfies $K_z^u(s) = -H_0(s)F(s)$, such that $B_u H_0(s)$ is similar to a diagonal matrix whose components belong to [0,1].

For any $M > 0$ and any integer $N > 0$, define $w(s)$ a low-pass filter (i.e. $w(s) \to 1$ as $|s| \to 0$ and $|w(s)| \to 0$ as $|s| \to +\infty$) with relative degree N, such that we have on $\mathbb{C}_\eta$, $|1 - w(s)| < 1, |w(s)| < 1$ and the following additional condition if $|s| \leq M$:

$$|1 - w(s)| < \frac{\underline{\sigma}(Q(s))}{\bar{\sigma}(\begin{pmatrix} B_u & 0 & 0 \end{pmatrix}^T K(s)) + 1}. \tag{6.40}$$

Then, there exists $M > 0$ and $N > 0$ such that the filtered control law $w(s)U(s)$ stabilizes the system (6.29)-(6.31) with $w(s)K(s)$ being strictly proper.

Proof : Let us consider a constant $M > 0$ and define a low pass-filter $w(s)$ that satisfies $|1 - w(s)| < 1$, $|w(s)| < 1$ and equation (6.40). The relative order of this filter is denoted N and is chosen such that $w(s)K(s)$ is strictly proper (which is possible since the growth rate of $K(s)$ is, at worst, polynomial). Our objective is to prove that we can choose the constant M such that the new filtered control law $w(s)U(s)$ still guarantees the stabilization of (6.29)-(6.31). Plugging this filtered control law into the system (6.29)-(6.31), we obtain the characteristic equation:

$$\det(I_1(s) - P_0(s) - w(s)BK(s)) = 0. \tag{6.41}$$

In what follows, we denote $\bar{Q}(s) = I_1(s) - P_0(s) - w(s)BK(s)$. For the sake of contradiction, assume that equation (6.41) admits a solution $s \in \mathbb{C}_0$. Consider in a first time that $s \in \mathbb{C}_u$ so that $\det(s\mathrm{Id} - \bar{A}_0)$ and $\det(s\mathrm{Id} - \bar{A}_1)$ do not vanish. Since s is a solution of equation (6.41), there exists $\zeta \neq 0$ (where $\zeta = (\zeta_1, \zeta_2, \zeta_3)$) such that $\bar{Q}(s)\zeta = 0$. We obtain

$$\begin{aligned} F_0(s)\zeta_1 =& (P_{12}(s) + w(s)B_u K_X(s))\zeta_2 + (P_{13}(s) + w(s)B_u K_Y(s))\zeta_3, && (6.42)\\ (s\mathrm{Id} - \bar{A}_0)\zeta_2 =& P_{21}(s)\zeta_1 + P_{23}(s)\zeta_3, && (6.43)\\ (s\mathrm{Id} - \bar{A}_1)\zeta_3 =& P_{31}\zeta_1, && (6.44) \end{aligned}$$

where $F_0(s) = \mathrm{Id} - F(s) - P_{11}(s) - w(s)B_u K_z(s)$. Multiplying equation (6.44) by $(s\mathrm{Id} - \bar{A}_1)^{-1}$ and equation (6.43) by $(s\mathrm{Id} - \bar{A}_0)^{-1}$ and injecting them into equation (6.42), we obtain

$$\bar{F}(s)\zeta_1 = 0, \tag{6.45}$$

where $\bar{F}(s) = F_0(s) - P_{13}(s)(s\mathrm{Id} - \bar{A}_1)^{-1}P_{31}(s) - w(s)B_u K_Y(s)(s\mathrm{Id} - \bar{A}_1)^{-1}P_{31}(s) - P_{12}(s)(s\mathrm{Id} - \bar{A}_0)^{-1}P_{21}(s) - w(s)B_u K_X(s)(s\mathrm{Id} - \bar{A}_0)^{-1}P_{21}(s) - (P_{12}(s) + w(s)B_u K_X(s))(s\mathrm{Id} - \bar{A}_0)^{-1} \cdot P_{23}(s)(s\mathrm{Id} - \bar{A}_1)^{-1}$. Due to condition (2) in the statement of the Theorem, and Assumption 6.2.2, we have

$$\bar{\sigma}(F + w(s)B_u K_z^u) \leq \bar{\sigma}(\mathrm{Id} - w(s)B_u H_0(s))\epsilon_0 \leq \epsilon_0,$$

since $B_u H_0(s)$ is similar to a diagonal matrix whose component belong to $[0, 1]$ and since for all $d \in [0, 1], |1 - w(s)d| < 1$ (due to the requirements on the filter). Moreover, due to condition (1) and the definitions of the different matrices, the remaining functions that appear in the definition of $\bar{F}$ (except the identity in $F_0(s)$) are strictly proper. Thus, equation (6.45) can be rewritten as

$$(Id + R_1(s) + R_2(s) + w(s)R_3(s))\zeta_1 = 0,$$

where R_2 and R_3 are strictly proper and where $R_1(s)$ satisfies $\bar{\sigma}(R_1(s)) \leq \epsilon_0 < 1$. Consequently, using the fact that $|w(s)| < 1$, there exist $\epsilon_1 > 0$ and $M_1 > 0$ that do not depend on the choice of w such that if $|s| > M_1$, we have $\bar{\sigma}(R_1(s) + R_2(s) + w(s)R_3(s)) < 1 - \epsilon_1$, which implies $\underline{\sigma}(\bar{F}(s)) > \epsilon_1$. Due to equation (6.45), we must have $\zeta_1 = 0$ which in turns implies $\zeta_2 = \zeta_3 = 0$ due to equations (6.43)-(6.44)

(since $s \in \mathbb{C}_u$). This is a contradiction. Thus, the characteristic equation does not admit a solution in $\mathbb{C}_u$ if $|s| > M_1$. Let us now consider the case $|s| < M_1$. Set $M = M_1$ in the definition of the filter given by equation (6.40). The closed-loop system (6.29)-(6.31) can be rewritten as

$$Q(s) = -(1 - w(s)) \begin{pmatrix} B_u & 0 & 0 \end{pmatrix}^T K(s).$$

We have $(1-w(s))\bar{\sigma}(\begin{pmatrix} B_u & 0 & 0 \end{pmatrix}^T K(s)) < \underline{\sigma}(Q(s))$, due to equation (6.40). This results in a contradiction. Consequently, the characteristic equation has no zeros in $\mathbb{C}_0$. The proof could be adjusted to show that the asymptotic vertical chain of zeros of $\bar{Q}(s)$ cannot be the imaginary axis and that $\bar{Q}(s)$ does not have any zeros on $\mathbb{C}_{\eta_1}$. This proves the exponential stability of the closed-loop system [HVL93, CZ12]. ■

The proof of Theorem 6.2.1 provides a suitable value for the constant M (that depends on N). The constant N is chosen such that $w(s)K(s)$ is strictly proper (which is always possible as the explosion rate of the function $K(s)$ is, at worst, polynomial). Although the different conditions given in the statement of Theorem 6.2.1 may appear complex at first sight, they are simple to verify. The first condition is always satisfied for bounded feedback gains. In particular, this condition is satisfied for all the cases currently considered in the literature (see [ABP22] for instance, where $X \equiv 0$). The second condition (on the feedback gain K_z^u) is always satisfied when we cancel all the reflection terms at the actuated boundary of the PDE (as it is done in [CHO17]). The requirements on the function K_z^u could be lowered by considering a matrix filter instead of a scalar one. This would allow canceling the reflection terms arbitrarily. However, in terms of stabilization objective, it appears relevant to cancel as many reflection terms as possible for each line where a control input is available. In pathological cases (for instance, a case for which the same control input acts on two boundary conditions), it may be necessary to perform a change of variables to write the system in a more amenable form. Overall, we believe that condition (2) is not restrictive in its present form. The following lemma gives a constructive way to design the filter w.

Lemma 6.2.1 *There exists $\nu_0 > 0$ such that the low-pass filter defined for all $s \in \mathbb{C}^+$ by $w_{\nu_0}(s) = \frac{1}{(1+\nu_0 s)^N}$ satisfies the requirements of Theorem 6.2.1.*

Proof : We immediately have $|w_{\nu_0}| < 1$ and $|1 - w_{\nu_0}| < 1$. The set $\mathcal{S} = \{s \in \mathbb{C}^+,\ |s| \leq M\}$ is compact. Thus, we can define $\tilde{M} = \inf_{s\in\mathcal{S}} \underline{\sigma}(Q(s))(\bar{\sigma}(\begin{pmatrix} B_u & 0 & 0 \end{pmatrix}^T K(s)) + 1)^{-1} > 0$. Choosing $\nu_0 = \tilde{M}^{\frac{1}{N}}(2M)^{-1}$, we directly obtain $|1 - w_{\nu_0}(s)| < \tilde{M}$, which implies that condition (6.40) is always satisfied. The order of the filter can be chosen arbitrarily high to make the filtered control law strictly proper. ■

Note that such a filter only has an illustrative purpose and may not be the most relevant choice. Butterworth filters may have more amenable properties while satisfying the required conditions.

In the second theorem, we consider the case where only the ODE is actuated (i.e., $B_z \equiv 0$). To simplify the analysis, we assume that $K(s) = K^u(s) + K^b(s)$, where K^b somehow corresponds to the bounded parts of K while the functions K^u may not be proper (as it is the case in [BSBADLE19] when using a dynamical inversion of the ODE). We have the following result.

Theorem 6.2.2.

Consider the system (6.29)-(6.31) with the stabilizing feedback control law $U(s)$ given by (6.39). Consider that Assumptions 6.2.1 and 6.2.2 are verified. Assume that $B_z \equiv 0$. Assume that there exists a matrix $\check{A}_0$ such that $(s\mathrm{Id} - \check{A}_0)^{-1}$ is properly defined on $\mathbb{C}_u$. Consider that

1. The function $K_X^u(s)$ satisfies $K_X^u(s) = \bar{K}^u(s)C_0$. Moreover, the functions $C_0(s\mathrm{Id} - \check{A}_0)^{-1}B_X\bar{K}^u(s)$, $C_0(s\mathrm{Id} - \check{A}_0)^{-1}B_XK_z^u(s)$, and $C_0(s\mathrm{Id} - \check{A}_0)^{-1}\ B_XK_Y^u(s)P_{31}(s)$ are strictly proper.

2. The function $K_X^b(s)$ satisfies $B_XK_X^b(s) = \bar{K}^b(s)C_0 + \check{A}_0 - \bar{A}_0$. Moreover, the functions $(s\mathrm{Id} - \check{A}_0)^{-1}\ B_XK_z^b(s)$, $(s\mathrm{Id} - \check{A}_0)^{-1}B_XK_Y^b(s)(s\mathrm{Id} - \bar{A}_1)^{-1}\ P_{31}(s)$, and $(s\mathrm{Id} - \check{A}_0)^{-1}B_X\bar{K}_X^b$ are strictly proper.

For any $M_0 > 0$ and any $N_0 > 0$ define $w_0(s)$ a low-pass filter with sufficiently high rela-

tive degree N_0, that satisfies for all $s \in \mathbb{C}_{\eta_1}$, $|w_0(s)| < 1$, $|1 - w_0(s)| < 1$ and the additional condition

$$|1 - w_0| < \frac{\underline{\sigma}(Q(s))}{\bar{\sigma}(\begin{pmatrix}0 & B_X & 0\end{pmatrix}^T K^u(s)) + 1}, \tag{6.46}$$

if $|s| \leq M_0$. For any $M_1 > 0$ define $w_1(s)$ a low-pass filter with sufficiently high relative degree N_1, that satisfies for all $s \in \mathbb{C}_{\eta_1}$ $|w_1(s)| < 1$, $|1 - w_1(s)| < 1$ and the additional condition when $|s| \leq M_1$

$$|1 - w_1| < \frac{\underline{\sigma}(\bar{Q}(s))}{\bar{\sigma}(\begin{pmatrix}0 & B_X & 0\end{pmatrix}^T K^b(s)) + 1} \tag{6.47}$$

where $\bar{Q}(s) = I_1 - P_0 - \begin{pmatrix}0 & B_X & 0\end{pmatrix}^T (w_0 K^u + K^b)$. Then, there exists M_0, M_1, N_0, N_1 such that the filtered control law defined by

$$\begin{aligned} U_f(s) =& w_1(s)K_z^b(s)z(s) + w_1(s)K_Y^b(s)Y(s) + w_1(s)K_X^b(s)\bar{X}(s) + w_0(s)K_z^u(s)z(s) \\ &+ w_0(s)K_X^u(s)\bar{X}(s) + w_0(s)K_Y^u(s)Y(s), \end{aligned} \tag{6.48}$$

is strictly proper and stabilizes the system (6.29)-(6.31).

Proof : We consider in a first time that $w_1 \equiv 1$ and that w_0 is a low-pass filter that satisfies $|w_0(s)| < 1$, $|1 - w_0(s)| < 1$, and equation (6.46). Consider that the control law is now $U_f(s) = w_0(s)K_z^u z(s) + w_0(s)K_X^u\bar{X}(s) + w_0(s)K_Y^u Y(s) + K_z^b(s)z(s) + K_Y^b(s)Y(s) + K_X^b(s)\bar{X}(s)$. For the sake of contradiction, assume that the characteristic equation of the system admits a solution $s \in \mathbb{C}_{\eta_1}$. Consider in a first time that this solution belongs to $s \in \mathbb{C}_u$. Thus, there exists $\zeta \neq 0$ (where $\zeta = (\zeta_1, \zeta_2, \zeta_3)$) such that

$$(\mathsf{Id} - F(s) - P_{11}(s))\zeta_1 = P_{12}(s)\zeta_2 + P_{13}(s)\zeta_3, \tag{6.49}$$

$$\begin{aligned} (s\mathsf{Id} - \bar{A}_0)\zeta_2 =& (P_{21}(s) + B_X K_z^b(s))\zeta_1 + w_0(s)B_X K_X^u(s)\zeta_2 + B_X K_X^b(s)\zeta_2 \\ &+ w_0(s)B_X K_z^u(s)\zeta_1 + w_0(s)B_X K_Y^u(s)\zeta_3 + (P_{23}(s) + B_X K_Y^b(s))\zeta_3, \end{aligned} \tag{6.50}$$

$$(s\mathsf{Id} - \bar{A}_1)\zeta_3 = P_{31}(s)\zeta_1. \tag{6.51}$$

Multiplying equation (6.51) by $(s\mathsf{Id} - \bar{A}_1)^{-1}$ and injecting it into equation (6.49), we obtain

$$\bar{F}(s)\zeta_1 = P_{12}(s)\zeta_2 = C_0\zeta_2, \tag{6.52}$$

where $\bar{F}(s) = \mathsf{Id} - F(s) - P_{11}(s) - P_{13}(s)(s\mathsf{Id} - \bar{A}_1)^{-1}P_{31}(s)$. Due to Assumption 6.2.2, there exist $\epsilon_F > 0$ and $M_F > 0$ such that if $|s| > M_F$, we have $\underline{\sigma}(\bar{F}(s)) > \epsilon_F$. Consequently, if $|s| > M_F$, we can multiply equation (6.52) by $(\bar{F}(s))^{-1}$ and inject it into (6.50). Using conditions (1) and (2), equation (6.50) can be rewritten as

$$\begin{aligned} (s\mathsf{Id} - \check{A}_0)\zeta_2 =& w_0(s)B_X\bar{K}^u(s)C_0\zeta_2 + w_0(s)B_X K_z^u(s)\bar{F}^{-1}(s)C_0\zeta_2 \\ &+ w_0(s)B_X K_Y^u(s)(s\mathsf{Id} - \bar{A}_1)^{-1}P_{31}(s)\bar{F}^{-1}(s)C_0\zeta_2 + (R(s) + B_X\bar{K}_X^b)C_0\zeta_2, \end{aligned} \tag{6.53}$$

where the function $R(s)$ is defined by $R(s) = [P_{23}(s)(s\mathsf{Id} - \bar{A}_1)^{-1}P_{31}(s) + P_{21}(s) + B_X K_Y^b(s)(s\mathsf{Id} - \bar{A}_1)^{-1}P_{31}(s) + B_X K_z^b(s)]\bar{F}^{-1}(s)$. Note that the function $(s\mathsf{Id} - \check{A}_0(s))^{-1}(R(s) + B_X\bar{K}_X^b)$ is strictly proper due to the different requirements given in the statement of the theorem. Multiplying equation (6.53) by $C_0(s\mathsf{Id} - \check{A}_0)^{-1}$, and denoting $\bar{\zeta}_2 = C_0\zeta_2$ we obtain

$$\begin{aligned} \bar{\zeta}_2 =& w_0(s)C_0(s\mathsf{Id} - \check{A}_0)^{-1}B_X(\bar{K}^u(s) + K_z^u(s)\bar{F}^{-1}(s) + K_Y^u(s)(s\mathsf{Id} - \bar{A}_1)^{-1}P_{31}(s)\bar{F}^{-1}(s))\bar{\zeta}_2 \\ &+ C_0(s\mathsf{Id} - \bar{A}_0)^{-1}(R(s) + B_X\bar{K}_X^b(s))\bar{\zeta}_2 = G(s)\bar{\zeta}_2. \end{aligned} \tag{6.54}$$

Due to the second requirement of the theorem, $G(s)$ is strictly proper. There exists $\bar{M}_0 > M_F$ (that does not depend on the choice of w_0) such that if $|s| > \bar{M}_0$, $\bar{\sigma}(G(s)) < 1$. This implies $\bar{\zeta}_2 = 0$.Injecting into equation (6.53), we obtain $(s\mathsf{Id} - \bar{A}_0)\zeta_2 = 0$. There exists $M_0 > 0$ such that if $s > M_0$ $\underline{\sigma}((s\mathsf{Id} - \bar{A}_0)) > 1$. It implies $\zeta_2 = 0$ which in turns results in $\zeta_1 = \zeta_3 = 0$. This is a contradiction.

Let us now consider the case $|s| < M_0$. Let us choose this M_0 for the definition of equation (6.46). The closed-loop system (6.29)-(6.31) can be rewritten as $Q(s) = -(1 - w_0(s))B\begin{pmatrix}K_z^u(s) & K_X^u(s) & K_Y^u(s)\end{pmatrix}$. In the meantime, we have $(1 - w_0(s))\bar{\sigma}(B\begin{pmatrix}K_z^u(s) & K_X^u(s) & K_Y^u(s)\end{pmatrix}) < \underline{\sigma}(Q(s))$, due to equation (6.46).

This results in a contradiction. Consequently, the characteristic equation cannot be verified in $\mathbb{C}_\eta$. Thus, the system is exponentially stable. Moreover, the order of the filter w_0 can always be chosen to make the function $w_0(s)B_X K^u(s)$ strictly proper (see Lemma 6.2.1). Thus, we have that the function $(s\mathrm{Id} - \bar{A}_0)^{-1}\begin{pmatrix}0 & B_X & 0\end{pmatrix}^T K^u(s)C_0 w_0(s))$ is strictly proper. Consider now that $w_1(s)$ is a low-pass filter that satisfies $|w_1(s)| < 1$, $|1 - w_1(s)| < 1$, and equation (6.47). Consider that the control law is now $U_f(s) = w_0(s)K_z^u z(s) + w_0(s)K_X^u \bar{X}(s) + w_0(s)K_Y^u Y(s) + w_1(s)[K_z^b(s)z(s) + K_Y^b(s)Y(s) + K_X^b(s)\bar{X}(s)]$. For the sake of contradiction, assume that the system's characteristic equation admits a solution $s \in \mathbb{C}_{\eta_1}$. Consider in a first time that this solution belongs to $s \in \mathbb{C}_u$. Thus, there exists $\zeta = (\zeta_1, \zeta_2, \zeta_3) \neq 0$ such that

$$(\mathrm{Id} - F(s) - P_{11}(s))\zeta_1 = P_{12}(s)\zeta_2 + P_{13}(s)\zeta_3, \tag{6.55}$$

$$\begin{aligned}(s\mathrm{Id} - \bar{A}_0)\zeta_2 &= (P_{21}(s) + w_1(s)B_X K_z^b(s))\zeta_1 + w_0(s)B_X K_X^u(s)\zeta_2 + w_0(s)B_X K_z^u(s)\zeta_1 \\ &\quad + w_0(s)B_X K_Y^u(s)\zeta_3 + w_1(s)B_X K_X^b(s)\zeta_2 + (P_{23}(s) + w_1(s)B_X K_Y^b(s))\zeta_3,\end{aligned} \tag{6.56}$$

$$(s\mathrm{Id} - \bar{A}_1)\zeta_3 = P_{31}(s)\zeta_1. \tag{6.57}$$

In a similar way to what has been done above, we obtain (when $|s| > M_F$)

$$\begin{aligned}(s\mathrm{Id} - \check{A}_0)\zeta_2 &= w_0(s)B_X(K_X^u(s) + K_z^u(s)\bar{F}^{-1}(s) + K_Y^u(s)(s\mathrm{Id} - \bar{A}_1)^{-1}P_{31}(s)\bar{F}^{-1}(s))\zeta_2 \\ &+ (R_w(s) + w_1(s)B_X K_X^b(s))C_0\zeta_2 - (1 - w_1(s))(\bar{A}_0 - A_0),\end{aligned} \tag{6.58}$$

where $R_w(s) = [P_{23}(s)(s\mathrm{Id} - \bar{A}_1)^{-1}P_{31}(s) + P_{21}(s) + w_1(s)B_X K_Y^b(s)(s\mathrm{Id} - \bar{A}_1)^{-1}P_{31}(s) + B_X w_1(s) K_z^b(s)]\bar{F}^{-1}(s)$. Multiplying the right-hand side of equation (6.58) by $(s\mathrm{Id} - \check{A}_0)^{-1}$, we obtain strictly proper functions (since $w_0(s)B_X K_\cdot^u(s)$ is strictly proper). Thus, there exists $M_1 > M_F$ (that does not depend on the choice of w_1 since $|w_1(s)| < 1$ and $|1 - w_1(s)| < 1$) such that if $|s| > M_1$, $\zeta_2 = 0$. This, in turn, implies $\zeta = 0$, which is a contradiction. The rest of the proof (when $|s| < M_1$) is a consequence of equation (6.47). ■

Condition (1) is inspired by [BSBADLE19] and naturally appears when dealing with dynamical inversions of ODE dynamics. The functions K^u correspond to the unbounded parts of the control input and must grow slower at high frequencies than the ODE part of the dynamics $(s\mathrm{Id} - \bar{A}_0)$. Condition (2) is always satisfied in that case. Note that two filters are required (one for the unbounded part and one for the bounded part of the control input). This two-steps procedure is needed since the filter w_1 corresponding to the (bounded) ODE state-feedback needs to be *fast enough* with respect to the resulting closed-loop PDE-distal ODE subsystem (the dynamic of which already depending on the filter w_0).

6.2.2 . Robustness properties

We can now show that having a strictly proper control operator (obtained using adequate low-pass filters) leads to robustness margins. In what follows, we denote $G(s)$ the input-output (the output being here the state) transfer functions associated to (6.29)-(6.31) and $K(s)$ the controller transfer matrix, we have that (G, K) is input-output stable, and that GK is strictly proper (since G is bounded).

Theorem 6.2.3.

Consider system (6.29)-(6.31) with the stabilizing feedback control law (6.39) (i.e. Assumption 6.2.1 is verified). Assume that the functions $K_z(s)$, $K_X(s)$ and $K_Y(s)$ are *strictly proper*. Then, the closed-loop system is $w - stable$. Moreover, K stabilizes $G + \Delta$ for any admissible additive perturbation that verifies on $\bar{\mathbb{C}}^+$

$$||\Delta(s)|| < (||K(s)(\mathrm{Id} - G(s)K(s))^{-1}||)^{-1}. \tag{6.59}$$

Then, K stabilizes $(\mathrm{Id}+\Delta)G$ for any admissible multiplicative perturbation that verifies on $\bar{\mathbb{C}}^+$

$$||\Delta(s)|| < (||G(s)K(s)(\mathrm{Id} - G(s)K(s))^{-1}||)^{-1}. \tag{6.60}$$

Finally, if $G = \tilde{M}^{-1}\tilde{N}$ is a left-coprime factorization of G over $\mathcal{M}\hat{\mathcal{A}}_-(0)$, then K stabilizes $(\tilde{M} + \Delta_M)^{-1}(\tilde{N} + \Delta_N)$ for any left-coprime-factor perturbation $\Delta = (\Delta_N, -\Delta_M)$ that verifies on $\bar{\mathbb{C}}^+$, $||\Delta_M(s)|| < ||\tilde{M}(s)||$ and

$$||\Delta|| < ||\begin{pmatrix}K(s)(\mathrm{Id} - G(s)K(s))^{-1}\tilde{M}^{-1} \\ (\mathrm{Id} - G(s)K(s))^{-1}\tilde{M}^{-1}\end{pmatrix}||^{-1} \tag{6.61}$$

Note that the right hand sides of equations (6.59) (6.60) and (6.61) are well defined since GK is continuous and strictly proper, since (G, K) is exponentially stable, and since $\det(\tilde{M}) \in \hat{\mathcal{A}}_\infty(0)$ (left-coprime factorization).

Proof : The proof is adjusted from [CZ12, Theorem 9.2.6]. The w-stability is a consequence of Definition 5.2.4 as equation (5.11) is verified since GK is strictly proper. Consider now an admissible additive perturbation that verifies (6.59). Denote $G_\Delta = G + \Delta$. We have $\det(\mathsf{Id} - G_\Delta K) = \det(\mathsf{Id} - GK)\det(\mathsf{Id} - \Delta(K(\mathsf{Id} - GK)^{-1}))$. Denote p_K (resp. p_G) the number of poles of K (resp. G) counted according to their McMillan degree. Since K stabilizes G, $\det(\mathsf{Id} - GK)$ has a well defined Nyquist index (ind) equal to $-p_K - p_G$ [CZ12, Th. 9.1.8]. Consider the function $f(s) = \det(\mathsf{Id} - G_\Delta K)(s)$. We have

$$\mathsf{ind}(f) = \mathsf{ind}(\mathsf{Id} - GK) + \mathsf{ind}(\mathsf{Id} - \Delta(K(\mathsf{Id} - GK)^{-1})).$$

The function $g_1(s) = \det(\mathsf{Id} - \Delta(K(\mathsf{Id} - GK)^{-1})$ has a well defined nonzero limit at infinity in $\bar{\mathbb{C}}^+$. Since K is a stabilizing controller for G, the function g_1 is meromorphic on some open set containing $\bar{\mathbb{C}}^+$. So g_1 has a well defined Nyquist index. Since Δ is an admissible perturbation that verifies (6.59), we have that

$$\sup_{\omega \in \mathbb{R}} ||\Delta(j\omega)(K(j\omega)(\mathsf{Id} - G(j\omega)K(j\omega))^{-1})|| < 1.$$

Define $h(s,t) : (-j\infty, j\infty) \times [0,1] \to \mathbb{C}$ by

$$h(j\omega, t) = \det(\mathsf{Id} - t\Delta(j\omega)K(j\omega)(\mathsf{Id} - G(j\omega)K(j\omega))^{-1}).$$

The function h is continuous and $h(j\omega, t)$ and $h(\infty, t)$ are nonzero for every $t \in [0,1]$. This implies that the Nyquist index of g_1 is equal to zero [CZ12, Lemma A.1.18]. Consequently, K stabilizes G_Δ. The proof can be easily adjusted to deal with the case of multiplicative perturbations. For the case of left-coprime-factor perturbations, the proof can be adjusted noticing that $\det(\mathsf{Id} - G_\Delta) = \det(\mathsf{Id} - GK)\det(\mathsf{Id} + \Delta_M M^{-1}))\det(\mathsf{Id} - (K(\mathsf{Id} - GK)^{-1}\tilde{M}^{-1}, (\mathsf{Id} - GK)^{-1}\tilde{M}^{-1})^T)$. See [CZ12, Th 9.2.6] for additional details.

■

Theorem 6.2.3 guarantees the existence of robustness margins for a broad class of perturbations: input delays, uncertainties on the ODE parameters, uncertainties on the transport velocities. Provided we have a stabilizing control law that fulfills the different requirements of Theorem 6.2.1 or Theorem 6.2.2, it is possible to low-pass filter it to make it strictly proper. This, in turns, implies the robustness of the closed-loop system (Theorem 6.2.3). The proposed approach dissociates the stabilization problem from the robustness analysis, considerably simplifying the design. In particular, this allows the cancellation of the PDE reflection terms or the inversion of the ODE dynamics, thus overcoming the limitations highlighted in [ABABS+18]. The robustness results given in Theorem 6.2.3 do not depend on the model of the disturbances but on their bounds (that must be small enough). One significant advantage of such an approach is that, even for complex systems, it guarantees the existence of non-zero robustness margins using a simple low-pass filter that can be characterized by a single degree of freedom (its bandwidth). This bandwidth must verify some constraints that can be easily computed using the norms of the different functions. Qualitatively, increasing the bandwidth would imply reducing the robustness (at least with respect to delays). It is worth mentioning that such an analysis would be necessary to understand how the available degrees of freedom can be exploited to design a robust controller with optimal behavior for a given uncertainty model for some industry-inspired constraints (similarly to what is done with H_∞-based approaches).

Remark 6.2.1 *Having a strictly proper control law is sufficient to guarantee the existence of robustness margins. However, it is not a necessary condition. As seen in [ABABS+18], canceling a part of the reflection terms while guaranteeing robustness margins is possible. However, the proof, in this case, may become technical.*

Finally, it is essential to mention that such a strictly proper controller can be combined with a state-observer (a crucial step for practical implementation) and that the resulting output-feedback law can be made strictly proper by increasing the order of the filter.

6.3 . Conclusions and perspectives

In this chapter, we have proposed a time-delay representation of the class of networks we consider in this manuscript. More precisely, using the method of characteristics, we could rewrite system (6.1) as an Integral Delay Equation coupled with ODEs. This representation will appear helpful in the design of stabilizing controllers throughout the following chapters. We have shown in this chapter one possible application of such a representation by introducing a filtering methodology to robustify (possibly non-strictly proper) stabilizing control laws. More precisely, assuming that a stabilizing controller is available for the system (6.1), we have derived simple sufficient conditions under which appropriate low-pass filters can be combined with the proposed control law to obtain a strictly proper controller, thus enabling the existence of robustness margins. This filtering technique will simplify the design of stabilizing controllers for the class of systems described by equations (6.1) as it dissociates the stabilization problem from the robustness problem. From now, we will not have to consider the robustness properties of the closed-loop system as we know that it is possible to low-pass filter the controller to make it strictly proper, thus guaranteeing the existence of robustness margins in the sense of Theorem 6.2.3. However, it is essential to emphasize that the proposed approach is **qualitative** for now, as only a sufficient robustness condition has been given on the design of the low-pass filters. The impact of the tuning of the filter on performance and robustness margins remains unstudied. In the next chapter, we focus on stabilizing system (6.1) under general assumptions.

7 - Some insights in the output-feedback stabilization for generic interconnection configurations

The main objective of this manuscript is to design stabilizing output-feedback controllers for the general class of ODE-PDE-ODE networks described by the following set of equations

$$\begin{cases} \dot{X}(t) = A_0 X(t) + E_0 v(t,0) + B_X U(t), \\ u(t,0) = C_0 X(t) + Q v(t,0) + B_u U(t), \\ \partial_t u(t,x) + \Lambda^+ \partial_x u(t,x) = \Sigma^{++}(x) u(t,x) + \Sigma^{+-}(x) v(t,x), \\ \partial_t v(t,x) - \Lambda^- \partial_x v(t,x) = \Sigma^{-+}(x) u(t,x) + \Sigma^{--}(x) v(t,x), \\ v(t,1) = R u(t,1) + C_1 Y(t), \\ \dot{Y}(t) = A_1 Y(t) + E_1 u(t,1), \end{cases} \tag{7.1}$$

the different parameters being defined in Section 5.2. As explained in the introductory chapter (Chapter 5), most of the existing results in the literature require **specific structural assumptions** to design appropriate stabilizing controllers. For instance, several contributions do not consider fully interconnected PDE systems but **chains** (i.e., the matrices $\Sigma^{\cdot\cdot}$ have a block diagonal structure), as it is the case of the multi-step approach introduced in [DG20]. Moreover, the control strategy may change depending on whether the ODE or the PDE is actuated/measured (i.e., if $B_X \equiv 0$ or $B_u \equiv 0$). In the case of an actuated PDE (i.e., $B_X \equiv 0$), most of the contributions do not consider the X-ODE and assume that $B_u = \mathrm{Id}_n$. It is the case, for instance, of the backstepping controllers designed in [ABABS+18, dAVP18, AA19]. For such a framework, disturbance rejection procedures were also considered in [Aam12, HAK16]. Recently, the output regulation problem was solved in [DG21] in the case of a wave equation. In the case of an actuated ODE (i.e., $B_u \equiv 0$), a stabilizing observer-controller robust to delays has been proposed for a scalar X-ODE in [DMLA20]. In [DGK18], an output-feedback controller was designed based on assumptions that guarantee the existence of a Byrnes–Isidori normal form for the X-ODE and a relative degree one condition. These restrictions were partially avoided in [BSBADLE17] for the case of a scalar PDE system, as the actuated ODE was simply assumed to be minimum phase for the output that affects the PDE. In [BSBADLE19], a strictly-proper control law was proposed using less restrictive assumptions on the structure of the ODE components. This approach was later extended in [WK20] to encompass a state-observer (thus allowing the design of an output-feedback controller). However, this work still assumed the PDE subsystem to be scalar.

In this chapter, we introduce generic assumptions under which we can design stabilizing output-feedback controllers for the network system (7.1). We distinguish the case of an actuated/measured ODE (Section 7.1) and the case of an actuated/measured PDE (Section 7.2). The proposed design assumptions are essentially made on the **structure of the ODE components** and are less restrictive than those existing in the literature. We do not make in this chapter specific requirements on the structure of the PDE system (this will be the purpose of the following chapters) and will consequently require $B_u = \mathrm{Id}_n$ or rank conditions on the matrices E_0, C_0, C_1, E_1 to avoid the configurations of under-actuated and under-measured PDEs. In the rest of this manuscript, we consider that Assumption 6.1.1 is verified. As explained in Chapter 6, this assumption implies that in the absence of the ODEs and coupling terms $\Sigma^{\cdot\cdot}$, the open-loop system (7.1) is exponentially stable. It is **necessary** to guarantee the existence of robustness margins in closed-loop.

The results of this chapter generalize the results presented in [RBAA22, RBAA24, ABADM23, AA19].

7.1 . Output Regulation and Tracking in the case of an actuated/measured ODE

Let us consider the ODE-PDE-ODE system (7.1) and assume that only the ODE state X is actuated, i.e., $B_u = 0$. The output of the system is given by $y(t) = C_Y Y(t)$, where $C_Y \in \mathbb{R}^{d\times q}$. We consider that $d \geq n$, which means that the number of measurements is greater than the dimension of the PDE state u. Without this assumption, it may not be possible to reconstruct the value of the function $u(t,1)$. It is a reasonable assumption because no result currently exists for under-measured hyperbolic PDE systems. The proposed configuration has been considered in [BSBADLE19] in the case of a scalar PDE subsystem, and a state-observer was proposed in [WK20]. We here design an output-feedback controller that guarantees the robust stabilization of (7.1) under generic structural assumptions. Besides this robust stabilization objective, we consider an **output regulation-output tracking** problem. More precisely, we consider that the distal ODE subsystem is dynamically augmented by an exo-system, whose state is denoted $Y_2(t) \in \mathbb{R}^{q_2\times 1}$, such that

$$Y(t) = \left(Y_1^\top(t)\ ,\ Y_2^\top(t)\right)^\top \in \mathbb{R}^{(q_1+q_2)\times 1},$$

with $q_1 + q_2 = q$. The exogenous input can be considered either as a **disturbance** Y_{pert} and/or as a **known reference trajectory** Y_{ref}. The additional control objective is to stabilize a virtual output $\epsilon(t)$ defined by

$$\epsilon(t) \doteq C_e Y(t), \tag{7.2}$$

with $C_e = [C_{e1}\ C_{e2}]$. In most cases, $\epsilon(t)$ is a scalar function, such that $C_{e1} \in \mathbb{R}^{1\times q_1}, C_{e2} \in \mathbb{R}^{1\times q_2}$ and we can only stabilize a linear combination of components of the extended state. The regulation to zero of this virtual input ϵ fulfills the trajectory tracking and disturbance rejection objectives. Two simple examples of possible outputs are given below.

- **Output regulation problem:** choosing $C_{e1} \not\equiv 0$, and $C_{e2} \equiv 0$, we want to regulate to zero a linear combination of components of $Y_1(t)$ in the presence of a disturbance $Y_2(t)$.
- **Output tracking problem:** choosing $C_{e1,i} - C_{e2,j} = 0$, (and the other components of the extended state equal to zero), we want the i^{th} component of the output Y_1 to converge towards the j^{th} component of a known trajectory Y_2,

For the trajectory tracking problem, we consider that the reference trajectory is known and measured. To emphasize the effect of the exogenous signal (that cannot be controlled), we rewrite the Y-ODE in (7.1) as

$$\dot{Y}(t) = A_1 Y(t) + \begin{pmatrix} E_1 \\ 0_{q_2\times n}\end{pmatrix} u(t,1), \text{ with } A_1 = \begin{pmatrix} A_{11} & A_{12} \\ 0_{q_2\times q_1} & A_{22}\end{pmatrix}, \tag{7.3}$$

where $A_{11} \in \mathbb{R}^{q_1\times q_1}$, $A_{12} \in \mathbb{R}^{q_1\times q_2}$ and $A_{22} \in \mathbb{R}^{q_2\times q_2}$. Note that these two output regulation and output tracking objectives make the complete stabilization at zero impossible in the sense of the χ-norm of the state (X, u, v, Y) in (7.1), and we will only be able to guarantee its boundedness.

7.1.1 . Structural assumptions

The proposed approach to design appropriate output-feedback controllers requires several sufficient yet non-very restrictive assumptions gathered in this subsection. We give some insights regarding their conservatism.

Assumption 7.1.1 *The pairs (A_0, B_0) and (A_{11}, E_1) are stabilizable, i.e. there exist $F_0 \in \mathbb{R}^{r\times p}$, $F_1 \in \mathbb{R}^{n\times q_1}$ such that $\bar{A}_0 \doteq A_0 + B_X F_0$ and $\bar{A}_{11} \doteq A_{11} + E_1 F_1$ are Hurwitz.*

Assumption 7.1.1 is a classical requirement found in most of the papers dealing with ODE-PDE-ODE systems [Geh22, DGK18]. It is not overly conservative since without the stabilizability of (A_{11}, E_1),

it becomes impossible to stabilize the Y state independently of the PDE or interconnection structure. The stabilizability condition on (A_0, B_X) simplifies the design as no mode of X is stabilized indirectly through the PDE system. This condition allows us to obtain constructive control formulations with assumptions that can be easily checked based only on the ODE coefficients and basic finite-dimensional control tools known to any control engineer.

Assumption 7.1.2 *For all $s \in \mathbb{C}_0$, the matrices (A_0, B_X, C_0) satisfy*

$$\textit{rank} \begin{pmatrix} s\mathrm{Id} - A_0 & B_X \\ C_0 & 0_{n\times r} \end{pmatrix} = p + n.$$

This last assumption serves multiple purposes. It implies that the matrices C_0 and B_X are not identically zero. This is crucial for stabilizing the PDE and the Y_1 subsystems through X. Under Assumption 7.1.2, we have that the function $P_0(s) = C_0(s\mathrm{Id} - \bar{A}_0)^{-1}B_X$ does not have any zero in $\mathbb{C}^+$ common to all its components. Thus, the function $P_0(s)$ admits a right inverse whose entries have no unstable poles (such a right inverse is not necessarily proper) [Moy77]. We denote P_0^+ any such right inverse. A possible starting point for the search of such an inverse is given by the Moore-Penrose right inverse $\bar{P}_0^+(s) = P_0^T(s)(P_0(s)P_0^T(s))^{-1}$ (which should be verified to be stable a posteriori). A more involved stable inversion procedure is needed if this is not stable. Such a procedure is given in Section 7.1.2.

Assumption 7.1.3 *The matrix A_{22} is marginally stable, i.e., all its eigenvalues have zero real parts. For all initial conditions, the zero-input trajectories remain uniformly bounded with respect to the norm of the initial condition and in time. Also, there exist matrices $T_a \in \mathbb{R}^{q_1\times q_2}, F_a \in \mathbb{R}^{n\times q_2}$ solutions to the* ***regulator equations****:*

$$\begin{cases} -A_{11}T_a + T_aA_{22} + A_{12} = -E_1F_a, \\ -C_{e1}T_a + C_{e2} = 0. \end{cases} \tag{7.4}$$

This assumption gives a sufficient structural condition for the existence of a solution for the output regulation problem [FW75]. It can be related to the non-resonance condition. This is a condition on the plant's invariant zeros and the exosystem spectrum at low frequencies. More precisely, A_{11} and A_{22} have disjoint spectra, and the number of outputs we regulate (one in the case of a scalar ϵ) is coherent with the number of inputs. The matrices T_a, F_a can be easily computed using a Schur triangulation.

Due to the duality between observation and stabilization, we have analogous assumptions to design the corresponding state observer.

Assumption 7.1.4 *The pairs (A_0, C_0), (A_1, C_Y) are detectable (i.e. there exist $L_X \in \mathbb{R}^{p\times d}$ and $L_Y \in \mathbb{R}^{q\times m}$ such that $\tilde{A}_0 \doteq A_0 + L_XC_0$ and $\tilde{A}_1 \doteq A_1 + L_YC_Y$ are Hurwitz).*

As before, Assumption 7.1.4 is not overly conservative since without the detectability of (A_0, C_0), it becomes impossible to reconstruct the Y-state independently of the PDE or interconnection structure. The detectability condition on (A_1, C_Y) simplifies the observer design (no modes of Y are reconstructed indirectly through the PDE). It results in a set of conditions that can be easily tested.

Assumption 7.1.5 *For all $s \in \mathbb{C}_0$, the matrices (A_1, E_1, C_Y) satisfy*

$$\textit{rank} \begin{pmatrix} s\mathrm{Id} - A_1 & E_1 \\ C_Y & 0_{d\times n} \end{pmatrix} = q + n.$$

The transfer matrix $P_1(s) \doteq C_Y(s\mathrm{Id} - \tilde{A}_1)^{-1}E_1$ has no zeros in the right-half complex plane and admits a stable left-inverse, not necessarily proper.

7.1.2 . Stable left-inversion algorithm

In constructing the controller and the observer, a stable left-inverse is required for the ODE system. This section presents a simple procedure to construct a stable left-inverse for $P_1(s)$. This procedure is adjusted from [ABA22] and is given here to present a complete, self-contained method which is an alternative, in many cases simpler, to the computation of a Hermite normal form of a matrix. We present the procedure in the case of the left-inversion, but it can be easily adjusted to obtain a stable right-inverse.

Preliminary Definitions

Recall that Assumption 7.1.5 guarantees that $P_1(s)$ is full-column rank for all $s \in \mathbb{C}^+$. Furthermore, taking $\det(s\mathsf{Id} - \tilde{A}_1)$ as a common denominator (of degree p, with all its roots in the complex open left half-plane), we can factor $P_1(s)$ as $P_1(s) \doteq \frac{1}{\det(s\mathsf{Id}-\tilde{A}_1)} P_1^{\text{num}}(s)$, where $P_1^{\text{num}}(s)$ has real polynomial entries of degree at most $p-1$ (it is a $d \times m$ matrix over a Principal Ideal Domain, which is in fact a Euclidean Domain, see, e.g., [AW92]). The full-column rank property for $s \in \mathbb{C}_0$ also applies to $P_1^{\text{num}}(s)$. Given a list of real polynomials $\mathcal{P} = (l_1(s), l_2(s), ...l_j(s))$, we will denote by $\gcd(l_1, l_2, ...l_j)$ the polynomial greatest common divisor of the elements of $\mathcal{P}$, and by $(a_1(s), a_2(s), ..., a_j(s)) \doteq \text{bezout}(l_1, l_2, ...l_j)$ a corresponding list of real polynomial coefficients such that $\sum_{k=1}^{j} a_k(s) l_k(s) = \gcd(l_1, l_2, ...l_j)$. To construct a left-inverse for $P_1^{\text{num}}(s)$, we will first transform it into an upper-triangular form. One possible upper-triangular form is the Hermite normal form, see, for instance, Theorem 2.9, in [AW92, Ch. 5]. However, in practice, we do not require the uniqueness provided by this normal form, and it might be simpler to find a different upper-triangular form with the right properties. We provide a simple method that allows for one such construction. We begin defining some matrices that we will use to operate on the rows of $P_1^{\text{num}}(s)$ to construct the desired upper-triangular form. The first matrix, a $d \times d$ upper-triangular matrix with *real polynomial* entries (of degree at most $p-1$), will allow us to replace the i^{th} row of a matrix by a combination of that row and the following ones and allow us to place a "pivot" element in the diagonal of the transformed matrix:

$$T_p^i[c_i, ..., c_d](s) \doteq \begin{bmatrix} \mathsf{Id}_{i-1} & 0_{i-1,d-i+1} \\ 0_{d-i+1,i-1} & U[c_i, ..., c_d](s) \end{bmatrix}, \tag{7.5}$$

where $U[c_i, ..., c_d](s)$ is *any* $d-i+1 \times d-i+1$ polynomial matrix with full rank for $s \in \mathbb{C}^+$ and having as first row the polynomials $[c_i, ..., c_d]$. Note that a *particular* choice for this matrix would be the unimodular (invertible) matrix used to construct the Hermite normal form (see, for instance, the matrix U_1 in the inductive proof of Theorem 2.9 in [AW92, Ch. 5]), it is also worth mentioning that, unlike the construction of the Hermite normal form, we do not require the elements above the diagonal to belong to a set of residues modulo the element on the diagonal. We believe that for the application considered in this paper, this formulation simplifies the necessary computations since, in many cases, one can complete the first line with $d-i$ adequately chosen rows of the identity Id_{d-i+1}, as long as one avoids rank deficiencies in $\mathbb{C}^+$ (trivial if at least one of the c_k polynomials has no roots in $\mathbb{C}^+$). A second, $d \times d$ lower-triangular matrix with with *real polynomial* entries, $T_l^i[p_{i+1}, ..., p_d](s)$, will allow us eliminate the elements under the previously constructed "pivot". It is constructed by replacing all the elements below the diagonal on the i'th column of a $d \times d$ identity matrix, by the column of polynomials $[p_{i+1}, ..., p_d]^T$.

Construction of a stable left-inverse

A stable left-inverse of $P_1(s)$ can be found by a method similar to Gaussian elimination, as detailed in Algorithm 1. Let us remark that a completely analogous algorithm can be used to find a stable right-inverse in the control case (simply acting on the columns of the transfer matrix instead of the rows or transposing the system). If the reader already knows $P(s)$, the Hermite normal form of $P_1^{\text{num}}(s)$ and associated unimodular matrix $T(s)$ such that $P(s) = T(s)P_1^{\text{num}}(s)$, they can skip directly to step 11 of the algorithm. Remark that we do not require the classical condition of the Hermite normal form of having the elements above the diagonal (in the full column rank case) belonging to a complete

set of residues modulo the elements of the diagonal (see [AW92, Ch. 5]), which also simplifies the procedure.

Algorithm 1

$P(s) \leftarrow P_1^{\text{num}}(s)$
$T(s) \leftarrow I_d$
for $i = [1, 2, ..., m]$ **do**
  $(c_i, ..., c_d) \leftarrow \text{bezout}(P_{i:d,i}(s))$
  $P(s) \leftarrow T_p^i[c_i, ..., c_d](s)P(s)$
  $T(s) \leftarrow T_p^i[c_i, ..., c_d](s)T(s)$
  $(p_{i+1}, ..., p_d) = -P_{i+1:d,i}(s)/P_{i,i}(s)$
  $P(s) \leftarrow T_l^i[p_{i+1}, ..., p_d](s)P(s)$
  $T(s) \leftarrow T_l^i[p_{i+1}, ..., p_d](s)T(s)$
end for At the end of this loop, we obtain an upper triangular polynomial matrix $P(s)$ with Hurwitz polynomials on the diagonal and zeros below the diagonal.
$P(s) \leftarrow \begin{bmatrix}\text{Id}_m & 0_{m,d-m}\end{bmatrix} P(s)$ ▷ We extract the first n rows of the matrix $P(s)$, which are full rank in $\mathbb{C}^+$.
$T(s) \leftarrow P^{-1}(s) \begin{bmatrix}\text{Id}_n & 0_{m,d-m}\end{bmatrix} T(s)\ P$, at this step a square, triangular matrix with Hurwitz polynomial entries in the diagonal, has a trivial stable inverse, and $T(s)$ is, therefore, a stable, left inverse of $P_1^{\text{num}}(s)$
$P_1^-(s) \leftarrow \det(s\text{Id}_q - \tilde{A}_1)T(s)$ ▷ $P_1^-(s)$ now contains a stable, left-inverse of $P_1(s)$

7.1.3 . State-feedback control design

In this section, we design a state-feedback controller that will stabilize the virtual output $\epsilon(t)$ (defined by equation (7.2)). The feedback law will be designed by means of frequential analysis.

Time-delay formulation

We first rewrite our system as a time-delay system by following the methodology proposed in Section 6.1. The parameters D_0 and D_1 introduced in equation (6.4) are here chosen as

$$D_0 = 0, \quad D_1 = \begin{pmatrix} F_1 & F_a + F_1 T_a \end{pmatrix},$$

where the matrices F_1, F_a, T_a are defined in Assumption 7.1.1 and Assumption 7.1.3. Consequently, the matrix $\bar{A}_1$ now verifies

$$\bar{A}_1 = \begin{pmatrix} \bar{A}_{11} & \bar{A}_{12} \\ 0_{q_2 \times q_1} & A_{22} \end{pmatrix}, \quad \bar{A}_{12} = A_{12} + E_1(F_a + F_1 T_a),$$

where $\bar{A}_{11}$ is defined in Assumption 7.1.1. Consider $(\bar{X}, \bar{\alpha}, \beta, Y) = \mathcal{F}_c(D_0, D_1, X, u, v, Y)$, where $\mathcal{F}_c$ is defined in Theorem 6.1.2. Let us introduce the intermediate control input $\bar{U}$ such that $U(t) = \bar{U}(t) + F_0 \bar{X}(t)$. Adjusting the computations given in Section 6.1, the time-delay system (6.29)-(6.31) now rewrites in the Laplace domain

$$z(s) = F(s)z(s) + P_{11}(s)z(s) + P_{12}(s)\bar{X}(s) + P_{13}^1(s)Y_1(s) + P_{13}^2(s)Y_2(s), \tag{7.6}$$
$$(s\text{Id} - \bar{A}_0)\bar{X}(s) = P_{21}(s)z(s) + P_{23}^1(s)Y_1(s) + P_{23}^2(s)Y_2(s) + B_X\bar{U}(s), \tag{7.7}$$
$$(s\text{Id} - \bar{A}_{11})Y_1(s) = \bar{A}_{12}Y_2(s) + P_{31}(s)z(s), \tag{7.8}$$
$$(s\text{Id} - A_{22})Y_2(s) = 0, \tag{7.9}$$

where the different matrices are defined by equations (6.32)-(6.34) and where the matrices P_{13}^i and P_{23}^i are such that

$$P_{13} = \begin{pmatrix} P_{13}^1 & P_{13}^2 \end{pmatrix}, \quad P_{23} = \begin{pmatrix} P_{23}^1 & P_{23}^2 \end{pmatrix}.$$

This distinction is made to emphasize the contributions of the Y_1 terms (that we want to stabilize) and of the Y_2 terms (on which we cannot act, due to equation (7.9)). Note that since $D_0 = 0$, we have $P_{23} = E_0\gamma_\beta(0)$, due to equation (6.11). Notice that in the absence of the disturbance signal, the stabilization of z would imply the stabilization of the whole system provided that $\bar{U}(s)$ can be rewritten as a stable, dynamic state feedback of z. This is a consequence of the cascade structure of (7.6)-(7.8).

Frequency analysis

Since the matrices $\bar{A}_0$ and $\bar{A}_1$ are Hurwitz, there exists $\eta > 0$ such that we can invert $(s\mathsf{Id} - \bar{A}_0)$ and $(s\mathsf{Id} - \bar{A}_1)$ on $\mathbb{C}_\eta$. Injecting the corresponding terms into (7.6), we obtain

$$\begin{aligned} z(s) &= (F(s) + G(s))z(s) + H(s)Y_2(s) + C_0(s\mathsf{Id} - \bar{A}_0)^{-1}B_X\bar{U}(s) \\ &= F(s)z(s) + G(s)z(s) + H(s)Y_2(s) + P_0(s)\bar{U}(s), \end{aligned} \tag{7.10}$$

where

$$\begin{aligned} G(s) =& P_{11}(s) + P^1_{13}(s\mathsf{Id} - \bar{A}_{11})^{-1}P_{31}(s) + C_0(s\mathsf{Id} - \bar{A}_0)^{-1}P_{21}(s) \\ &+ C_0(s\mathsf{Id} - \bar{A}_0)^{-1}P^1_{23}(s\mathsf{Id} - \bar{A}_{11})^{-1}P_{31}(s), \end{aligned} \tag{7.11}$$

$$\begin{aligned} H(s) =& P^2_{13}(s) + P^1_{13}(s)(s\mathsf{Id} - \bar{A}_{11})^{-1}\bar{A}_{12} + C_0(s\mathsf{Id} - \bar{A}_0)^{-1}P^2_{23}(s) \\ &+ C_0(s\mathsf{Id} - \bar{A}_0)^{-1}P^1_{23}(s\mathsf{Id} - \bar{A}_{11})^{-1}\bar{A}_{12}, \end{aligned} \tag{7.12}$$

and where $P_0(s)$ is defined after Assumption 7.1.2. Using the superposition principle, the control law is decomposed into two parts: $\bar{U}(s) = U_z(s) + U_{Y_2}(s)$. We can use each component of the control law to compensate for the inner dynamics. First, define the transfer function

$$F_Y(s) \doteq -P_0^+(s)H(s), \tag{7.13}$$

such that, knowing the values of Y_2, the control law $U_{Y_2}(s) = F_Y(s)Y_2(s)$ cancels the effect of the disturbance on the output of the target system. The resulting transfer function is not proper in general. However, we can use our prior knowledge of the disturbance or trajectory dynamics to regularize it and design a strictly proper transfer function $\bar{F}_Y(s)$, following the procedure described in Section 7.1.2. We then define

$$\bar{U}_{Y_2}(s) = \bar{F}_Y(s)Y_2(s). \tag{7.14}$$

Once we canceled the effects of the disturbance on the dynamics or took into account the given trajectory, equation (7.10) rewrites

$$z(s) = G(s)z(s) + P_0(s)U_z(s).$$

Next, we introduce the transfer function

$$F_z(s) = -P_0^+(s)G(s) \tag{7.15}$$

and define $U_z(s) = F_z(s)z(s)$. Consequently, we obtain $z(s) = F(s)z(s)$, which implies the stabilization of z due to Assumption 6.1.1. However, the transfer function $F_z(s)$ may not be strictly proper. To make it strictly proper and guarantee the existence of robustness margins, we can use the filtering technique presented in Section 6.2. We have the following theorem

Theorem 7.1.1.

Consider system (7.1) with $B_u \equiv 0$ under Assumptions 7.1.1, 7.1.2 and 7.1.3. Consider the state $z(s)$ defined by $z(s) = \bar{\alpha}(s, 0)$, the state $\bar{\alpha}$ being defined through the backstepping

transformation $\mathcal{F}_c(D_0, D_1)$. Consider the functions $G(s)$ defined by equation (7.11) and $\bar{F}_Y(s)$ defined by equation (7.14). There exist two low pass filters $w_0(s)$ and $w_1(s)$ that satisfy equations (6.46) and (6.47) such that the control law

$$U(s) = w_1(s)F_0\bar{X}(s) - w_0(s)P_0^+(s)G(s)z(s) - \bar{F}_Y(s)Y_2(s) \tag{7.16}$$

is strictly proper and guarantees the exponential convergence of the virtual output $\epsilon(t)$ (defined in equation (7.2)) to zero. Furthermore, the control action $U(t)$ and the trajectories of X, u, v, and Y remain bounded.

Proof : The different conditions of Theorem 6.2.2 are verified with $\bar{C} = C_0$, $K_X^b = F_0$, $K_X^u = K_Y^u = [0,\ \bar{F}_Y]$, $K_Y^b = 0$, and $K_z^u(s) = -P_0^+(s)G(s)$. The operator K_z^b is more difficult to express since $\bar{X}$ depends on integral terms of z due to the transformation (6.2). We have $B_X K_X^b = \bar{A}_0 - A_0$, and $C_0(s\mathrm{Id} - \bar{A}_0)^{-1}B_X K_z^u(s) = -G(s)$, that is strictly proper. It implies that the filtered control law exponentially stabilizes the state $z(t) = \bar{\alpha}(t, 0)$. Consequently, due to the transport structure of the $\bar{\alpha}$ and β equations in (6.22), we obtain the exponential convergence to zero of $\bar{\alpha}$ and β in the L^2-norm. Let us now show that $C_{e1}Y_1 + C_{e2}Y_2 \longrightarrow 0$. The dynamics of Y_1 rewrites

$$\begin{aligned}\dot{Y}_1(t) &= (A_{11} + E_1F_1)Y_1(t) + (A_{12} + E_1(F_a + F_1T_a))Y_2(t) + E_1\bar{\alpha}(t, 1),\\ &= (A_{11} + E_1F_1)Y_1(t) + (-E_1F_a + A_{11}T_a - T_aA_{22})Y_2(t) + E_1(F_a + F_1T_a)Y_2(t) + E_1\bar{\alpha}(t, 1),\end{aligned}$$

where we have used Assumption 7.1.3 to obtain the last equality. This yields

$$\dot{\overbrace{(Y_1 + T_aY_2)}}(t) = \bar{A}_{11}(Y_1 + T_aY_2) + \underbrace{E_1\alpha(t, 1)}_{\longrightarrow 0}.$$

Therefore, the dynamics of $Y_1 + T_aY_2$ is exponentially stable. It implies that $C_e(Y_1 + T_aY_2)(t) = C_{e1}Y_1(t) + C_{e2}Y_2(t) = \epsilon(t)$ converges to zero. The boundedness of the control input is guaranteed by the fact that functions $\tilde{F}_\xi, \tilde{F}_\eta$ are strictly proper (as $z(s)$ exponentially converges to zero and $Y_2(s)$ is bounded). The boundedness of the state comes from the invertibility and the boundedness of the backstepping transformation $\mathcal{F}_c(D_0, D_1)$. ■

Without the exogenous system, the proposed controller solves the classical stabilization problem. Indeed, the filtered control law exponentially stabilizes the system (6.29)-(6.31). The exponential stability of $(\bar{X}, z, Y)$ implies the exponential stability of $(X, \bar{\alpha}, \beta, Y)$ due to Theorem 6.1.3. This, in turn, implies the exponential stability of (X, u, v, Y) due to the invertibility of the backstepping transformation $\mathcal{F}_c(D_0, D_1)$.

Remark 7.1.1 *So far, we have not discussed the time-domain realization of such a feedback law. Nevertheless, the components of our feedback law are of two types: (i) distributed or pointwise delays of the states of the system and (ii) transfer matrices. The time-domain realization of the distributed delays corresponds to an integral operator with delayed values of the states, whereas a suitable state-space realization of the transfer matrices can be easily found. Thus the control law* (7.16) *is causal (it does not require future state values) and can be suitably approximated for implementation.*

7.1.4 . Observer design and output-feedback controller

To design our observer, we will use the intermediate system (6.7), where the state $(\bar{X}, \alpha, \beta, Y)$ is obtained from the state (X, u, v, Y) using the transformation $\mathcal{F}_o(L_X, 0)$ (defined in Theorem 6.1.1). The matrix L_X is defined in Assumption 7.1.4. We emphasize that the matrix $\bar{A}_0$ now corresponds to $\tilde{A}_0$. The observer state $(\hat{\bar{X}}, \hat{\alpha}, \hat{\beta}, \hat{Y})$ is the solution of a set of equations that is a copy of the original dynamics (6.7) to which we add dynamical output injection gains. We denote $\tilde{y}(t) = y(t) - C_Y\hat{Y}(t)$, the difference between the real output and the observer output. The observer equations read as

$$\left\{\begin{array}{l}\dot{\hat{\bar{X}}}(t) = \tilde{A}_0\hat{\bar{X}}(t) + G_3\hat{\alpha}(t, 1) + G_4\hat{Y}(t) - \mathcal{O}_X(\tilde{y}),\\ \hat{\alpha}(t, 0) = Q\hat{\beta}(t, 0) + C_0\hat{\bar{X}}(t) + (Q\gamma_\beta(0) - \gamma_\alpha(0))\hat{Y}(t)\\ \qquad + \int_0^1 F^\alpha(y)\hat{\alpha}(t, y) + F^\beta(y)\hat{\beta}(t, y)dy - \mathcal{O}_0(\tilde{y}(t)),\\ \partial_t\hat{\alpha}(t, x) + \Lambda^+\partial_x\hat{\alpha}(t, x) = G_1(x)\hat{\alpha}(t, 1) - \mathcal{O}_\alpha(x, \tilde{y}(t)),\\ \partial_t\hat{\beta}(t, x) - \Lambda^-\partial_x\hat{\beta}(t, x) = G_2(x)\hat{\alpha}(t, 1) - \mathcal{O}_\beta(x, \tilde{y}(t)),\\ \hat{\beta}(t, 1) = R\hat{\alpha}(t, 1),\ \dot{\hat{Y}}(t) = A_1\hat{Y}(t) + E_1\hat{\alpha}(t, 1) - L_YC_Y\tilde{y}(t),\end{array}\right. \tag{7.17}$$

with any (arbitrary) initial conditions in χ. The **stable** operators $\mathcal{O}_i$ still have to be defined. We denote with a $\tilde{\cdot}$ the difference between the real and estimated states. Subtracting the observer dynamics from the real one, we obtain the error system

$$\begin{cases} \dot{\tilde{X}}(t) = \tilde{A}_0\tilde{X}(t) + G_3\tilde{\alpha}(t,1) + G_4\tilde{Y}(t) + \mathcal{O}_X(\tilde{y}(t)), \\ \tilde{\alpha}(t,0) = C_0\tilde{X}(t) + Q\tilde{\beta}(t,0) + (Q\gamma_\beta(0) - \gamma_\alpha(0))\tilde{Y}(t) \\ \qquad + \int_0^1 F^\alpha(y)\tilde{\alpha}(t,y) + F^\beta(y)\tilde{\beta}(t,y)dy + \mathcal{O}_1(\tilde{y}(t)), \\ \partial_t\tilde{\alpha}(t,x) + \Lambda^+\partial_x\tilde{\alpha}(t,x) = G_1(x)\tilde{\alpha}(t,1) + \mathcal{O}_\alpha(x,\tilde{y}(t)), \\ \partial_t\tilde{\beta}(t,x) - \Lambda^-\partial_x\tilde{\beta}(t,x) = G_2(x)\tilde{\alpha}(t,1) + \mathcal{O}_\beta(x,\tilde{y}(t)), \\ \tilde{\beta}(t,1) = R\tilde{\alpha}(t,1),\ \dot{\tilde{Y}}(t) = \tilde{A}_1\tilde{Y}(t) + E_1\tilde{\alpha}(t,1). \end{cases} \tag{7.18}$$

The objective is now to tune the different operators $\mathcal{O}_i$ such that the error system exponentially converges to zero. It is sufficient to show the convergence of $\tilde{X}$, $\tilde{\alpha}(t,1)$, and $\tilde{Y}$ to zero. More precisely, we have the following lemma

Lemma 7.1.1 *If $(\tilde{X}(t),\ \tilde{\alpha}(t,1),\ \tilde{Y}(t))$ is exponentially stable in the sense of the χ_τ-norm, then the state $(\tilde{X},\tilde{\alpha},\tilde{\beta},\tilde{Y})$ is exponentially stable in the sense of the χ-norm. This implies the convergence of the observer state to the real state.*

Proof : Due to the stability of the observer operators and using the transport structure of $\tilde{\alpha},\tilde{\beta}$ PDEs, the exponential convergences of $\tilde{Y}$ and $\tilde{\alpha}(t,1)$ to zero imply the exponential convergence of the states $\tilde{\alpha}(t,x)$ and $\tilde{\beta}(t,x)$. The stability is a consequence of the well-posedness of the system. It can also be proved by adjusting the proof of Theorem 6.1.3. ■

Design of the operators $\mathcal{O}_i$

We now want to define the operators $\mathcal{O}_i$ such that $\tilde{X}$, $\tilde{\alpha}(t,1)$, and $\tilde{Y}$ exponentially converge to zero. The analysis will be done in the Laplace domain. The Laplace transform of the last equation of (7.18) yields

$$(s\mathrm{Id} - \tilde{A}_1)\tilde{Y}(s) = E_1\tilde{\alpha}(s,1). \tag{7.19}$$

Due to Assumption 7.1.4, the matrix $(s\mathrm{Id} - \tilde{A}_1)$ is invertible in $\mathbb{C}^+$. This gives $\tilde{y}(s) = C(s\mathrm{Id} - \tilde{A}_1)^{-1}E_1\tilde{\alpha}(s,1)$. Thus, we obtain $\tilde{\alpha}(s,1) = P_1^-(s)\tilde{Y}(s)$, where P_1^- is a left-inverse of P_1 in Assumption (7.1.5). This, in turn, implies

$$\tilde{Y}(s) = (s\mathrm{Id} - \tilde{A}_1)^{-1}E_1P_1^-(s)\tilde{y}(s).$$

This means that the terms that are functions $\tilde{Y}$ and $\tilde{\alpha}(s,1)$ and that appear in the error system can directly be compensated using the observer gains. In particular, we can define $\mathcal{O}_X$ as

$$\mathcal{O}_X(\tilde{y}(s)) = -(G_3P_1^-(s) + G_4(s\mathrm{Id} - \tilde{A}_1)^{-1}E_1P_1^-(s))\tilde{y}(s) \tag{7.20}$$

so that equation (7.18) can be rewritten as $(s\mathrm{Id} - \tilde{A}_0)\tilde{X}(s) = 0$, which implies the exponential convergence of X to zero due to Assumption 7.1.1. Similarly, to get rid of the terms G_1 and G_2, we define the operators $\mathcal{O}_\alpha(x,\tilde{y})$ and $\mathcal{O}_\beta(x,\tilde{y})$ by

$$\mathcal{O}_\alpha(x,\tilde{y}) = -G_1(x)P_1^-(s)\tilde{y}(s),\ \mathcal{O}_\beta(x,\tilde{Y}) = -G_2(x)P_1^-(s)\tilde{y}(s), \tag{7.21}$$

such that the PDE equations in (7.18) rewrite as transport equations. Indeed, for $t > \frac{1}{\lambda_1} + \frac{1}{\mu_1}$, for every $1 \le i \le n$ and every $1 \le j \le m$, we have for every $x \in [0,1]$

$$\tilde{\alpha}_i(t,x) = \tilde{\alpha}_i(t - \frac{x}{\lambda_i}, 0),\ \tilde{\beta}_j(t,x) = \sum_{k=1}^{n} R_{jk}\tilde{\alpha}_k(t - \frac{1-x}{\mu_j}, 1). \tag{7.22}$$

In what follows, we consider that $t > \frac{1}{\lambda_1} + \frac{1}{\mu_1}$. The design of the operator $\mathcal{O}_0$ is more involved since this operator must compensate almost all the terms that appear in the boundary condition of $\tilde{\alpha}(t,0)$ (including the integral terms). To design this observer operator, we will omit the term $C_0\tilde{\xi}$ since this term exponentially converges to zero. We define the operator $\mathcal{O}_0$ as follows

$$(\mathcal{O}_0(\tilde{y}))_i = -((Q\gamma_\beta(0) - \gamma_\alpha(0))(s\mathsf{Id} - \tilde{A}_1)^{-1}E_1P_1^-(s)\tilde{y}(s))_i - \sum_{j=1}^{i}\sum_{k=1}^{m}\sum_{\ell=1}^{n}\int_0^1 F_{ij}^{\alpha}(\nu)$$
$$Q_{jk}R_{k\ell}\mathrm{e}^{-\frac{s\nu}{\lambda_j}}\mathrm{e}^{-\frac{s}{\mu_k}}d\nu(P_1^-(s)\tilde{y}(s))_\ell - \sum_{k=1}^{m}\sum_{\ell=1}^{n}\int_0^1 F_{1k}^{\beta}(\nu)R_{k\ell}\mathrm{e}^{-\frac{s(1-\nu)}{\mu_k}}d\nu\cdot(P_1^-(s)\tilde{y}(s))_\ell. \tag{7.23}$$

It has been shown in [ABA22] that with this operator, we obtain

$$\tilde{\alpha}_i(t,0) = \sum_{k=1}^{m}\sum_{\ell=1}^{n} Q_{ik}R_{k\ell}\tilde{\alpha}_\ell(t - \frac{1}{\mu_k} - \frac{1}{\lambda_\ell}, 0), \tag{7.24}$$

which is exponentially stable due to Assumption 6.1.1. We have the following theorem

Theorem 7.1.2 *Consider the operators $\mathcal{O}_X$, $\mathcal{O}_\alpha$, $\mathcal{O}_\beta$, $\mathcal{O}_0$, respectively defined by equations* (7.20), (7.21) *and* (7.23). *Define the observer states $(\hat{X},\hat{u},\hat{v},\hat{Y}) = \mathcal{F}_o(L_X,0,\hat{\tilde{X}},\hat{\alpha},\hat{\beta},\hat{Y})$, where the transformation $\mathcal{F}_o$ is defined in Theorem 6.1.1, and where $(\hat{\tilde{X}},\hat{\alpha},\hat{\beta},\hat{Y})$ is the solution of the system* (7.17). *Then the state $(\hat{X},\hat{u},\hat{v},\hat{Y})$ exponentially converges to (X,u,v,Y) in the sense of the χ-norm.*

Proof : With this choice of operators, we have already shown that $\tilde{Y}$ and $\tilde{X}$ exponentially converge to zero. Moreover, the recursive design of $\mathcal{O}_0$ implies that for all $t > \frac{1}{\lambda_1} + \frac{1}{\mu_1}$, all $i \leq n$, $\tilde{\alpha}_i(t,0)$ is solution of $\tilde{\alpha}_i(t,0) = \sum_{k=1}^{m}\sum_{\ell=1}^{n} Q_{ik}R_{k\ell}\tilde{\alpha}_\ell(t - \frac{1}{\mu_k} - \frac{1}{\lambda_\ell}, 0) + \mathcal{O}(\tilde{\xi})$, where $\mathcal{O}$ is a linear bounded operator. Thus, $\tilde{\alpha}(t,0)$ exponentially converges to zero, which implies the exponential convergence of $\tilde{\alpha}(t,1)$. Consequently, Lemma 7.1.1 implies that the state $(\tilde{X},\tilde{\alpha},\tilde{\beta},\tilde{Y})$ exponentially converges to zero for the χ-norm. We conclude the proof by using the invertibility and boundedness of the linear transformation $\mathcal{F}_o$. ■

Remark 7.1.2 *Similarly to what has been done for the controller, it is possible to low-pass filter the measured output signal $y(t)$ to use only strictly proper observer operators. Indeed, without filtering, the observer operators $\mathcal{O}_i$ may not be strictly proper (due to the use of the left inverses), and the observer system may consequently be sensitive to measurement delays. Low-pass filtering of the measurement will lead to strictly proper observer operators while still guaranteeing the convergence of the estimated states towards the real states. This will consequently allow the existence of robustness margins.*

Output-feedback controller

We can now design a stabilizing output-feedback controller.

Theorem 7.1.3.

Consider system (7.1) with $B_u \equiv 0$ under Assumptions 7.1.1, 7.1.2 and 7.1.3. Consider the operators $\mathcal{O}_X$, $\mathcal{O}_\alpha$, $\mathcal{O}_\beta$, $\mathcal{O}_0$, respectively defined by equations (7.20), (7.21) and (7.23). Define the observer states $(\hat{X},\hat{u},\hat{v},\hat{Y}) = \mathcal{F}_o(L_X,0,\hat{\tilde{X}},\hat{\alpha},\hat{\beta},\hat{Y})$, where the transformation $\mathcal{F}_o$ is defined in Theorem 6.1.1, and where $(\hat{\tilde{X}},\hat{\alpha},\hat{\beta},\hat{Y})$ is the solution of the system (7.17). Define the state $(\bar{X}_c,\bar{\alpha}_c,\beta_c,Y_c) = \mathcal{F}_c(0,(F_1\ F_a + F_1T_a),\hat{X},\hat{u},\hat{v},\hat{Y})$, where the transformation $\mathcal{F}_c$ is defined in Theorem 6.1.2. Denote $z_c(s) = \bar{\alpha}_c(s,0)$. Consider the functions $G(s)$ defined by equation (7.11) and $\bar{F}_Y(s)$ defined by equation (7.14). There exist two low pass filters $w_0(s)$ and $w_1(s)$ that satisfy equations (6.46) and (6.47) such that the control law

$$\hat{U}(s) = w_1(s)F_0\bar{X}_c(s) - w_0(s)P_0^+(s)G(s)z_c(s) - \bar{F}_Y(s)(Y_c)_2(s) \tag{7.25}$$

is strictly proper and guarantees the exponential convergence of the virtual output $\epsilon(t)$ (de-

fined in equation (7.2)) to zero. Furthermore, the control action $U(t)$ and the trajectories of X, u, v, and Y remain bounded.

Proof : Due to Theorem 7.1.2, the observer state exponentially converges to zero. We can express the control law (7.25) in terms of (7.16) and the error states. This last contribution exponentially converges to zero. Thus, we can adjust the proof of Theorem 7.1.1 to conclude. ■

7.1.5 . Simulation results

In this section, we illustrate the performance of our output feedback controller in two test cases. The first test case corresponds to a disturbance rejection problem (exogenous sinusoidal disturbance), while we consider a trajectory tracking problem in the second case. In both cases, the original open-loop system is unstable. The system, the observer, and the controller were implemented using Matlab and Simulink. The evolution of the PDE systems was simulated using an explicit in time, first-order, upwind finite difference method. The ODE states were simulated using a Runge-Kutta solver (order 4) with fixed timesteps. The transfer functions in the control law were transformed into a state-space representation for implementation. The evolution of the systems was computed on a 100s time scale, with a CFL number equal to 0.5. Consider system (7.1) with the following numerical values: $n = 1, m = 1,\ \Lambda^+ = 2,\ \Lambda^- = 0.7,\ \Sigma^{+-} = 0.3,\ \Sigma^{-+} = 0.2,\ \Sigma^{--} = \Sigma^{++} = 0\ R = 0.5,\ Q = 0.6$. The ODE dynamics are in dimension $p = 4, q_1 = 3, q_2 = 2$, and defined by the matrices

$$A_0 = \begin{pmatrix} 0 & 0.14 & 0 & 0.1 \\ 0 & 0 & 0.14 & 0 \\ 0.29 & -0.43 & 0.57 & 0.2 \\ 0 & 0 & 0 & -1.1 \end{pmatrix}, B_0 = \begin{pmatrix} 0 & 0 \\ 0 & -1 \\ 1 & -1 \\ 0 & 0 \end{pmatrix}, E_0 = \begin{pmatrix} 2 \\ -1 \\ 0.1 \\ 0 \end{pmatrix}, E_1 = \begin{pmatrix} 0.1 \\ -0.05 \\ 0 \end{pmatrix}$$

$$C_0 = \begin{pmatrix} 1 & 0 & 0 & -0.5 \end{pmatrix},\ C_{11} = \begin{pmatrix} 3 & -0.6 & 0 \end{pmatrix},\ A_{11} = \begin{pmatrix} 0.1 & 0 & 0 \\ 0.05 & -0.1 & -0.02 \\ 0 & 0 & -0.2 \end{pmatrix}.$$

The exogenous system is a sinusoidal signal that only acts on the Y-ODE subsystem (i.e., $C_{12} = [0, 0]$) through the matrix A_{12}. We have

$$\dot{Y}_2(t) = A_{22} Y_2(t) = \begin{pmatrix} 0 & \pi \\ -\pi & 0 \end{pmatrix} Y_2,\ A_{12} = \begin{pmatrix} 0 & 0.2 & 0.05 \\ 0.1 & 0 & 0 \end{pmatrix}^T.$$

The virtual input is defined by $C_e = \begin{pmatrix} 1 & 0 & 0 & 0 & 0 \end{pmatrix}$, such that $\epsilon(t) = Y_{1,1}(t)$. Thus the control objective is to stabilize the first component of $Y_1(t)$ in the presence of an exogenous sinusoidal disturbance. We can verify that the different assumptions are satisfied. Notice in particular that $A_{12} \notin Im(E_1)$ (unmatched disturbance), $C_0 B_0 = 0$, $E_0 \notin Im(B_0)$ and (A_0, B_0) is not controllable but is stabilizable. In our simulations, we used

$$F_0 = \begin{pmatrix} 41.71 & 5.43 & -1.93 & 0 \\ 42 & 5 & 0.14 & 0 \end{pmatrix}, F_1 = \begin{pmatrix} -5 & -15 & 0 \end{pmatrix},$$

$$L_X = \begin{pmatrix} -2.45 & -0.21 \\ -0.22 & -3.49 \\ -15.34 & 187.6 \\ -129.5 & 20.2 \end{pmatrix}, L_1 = \begin{pmatrix} -0.72 \\ 0 \\ -0.1 \end{pmatrix}, L_2 = \begin{pmatrix} -21.2 \\ 27.9 \end{pmatrix},$$

and $L_Y = \begin{pmatrix} -0.72 & 0 & -0.1 & -21.1 & 27.9 \end{pmatrix}^T$. We used a space step of 0.0025. An input delay of 0.1s was introduced in the control action to show the robustness of the design to small delays in the loop. We used simple low-pass filters of 4th order with different bandwidths. The observer is initialized with values corresponding to 60% of the real values. As illustrated in Figure 7.1a, the norm of the unstable open-loop system explodes. However, as shown in Figure 7.1b, the virtual output $\epsilon(t)$ converges to zero with the output-feedback control law, even in the presence of the disturbance signal. The control inputs are pictured in Figure 7.2a. Finally, the evolution of the norm

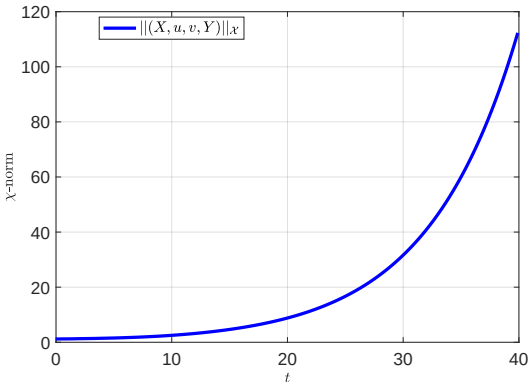

(a) Evolution of the χ-norm of the open-loop system (7.1) in the presence of a disturbance signal.

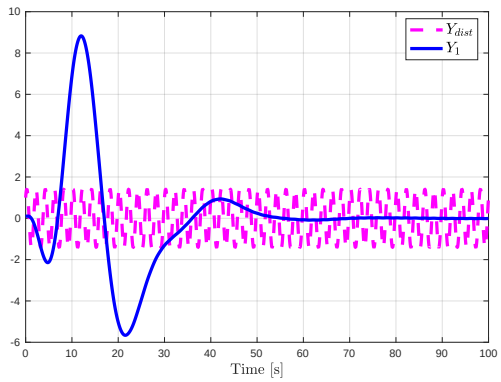

(b) Evolution of the state $Y_1(t)$ (blue) in closed-loop, in the presence of a disturbance (dotted pink).

Figure 7.1: Time evolution of the norm of the Open-Loop system (a), and time evolution of the state Y_1 in closed-loop (b).

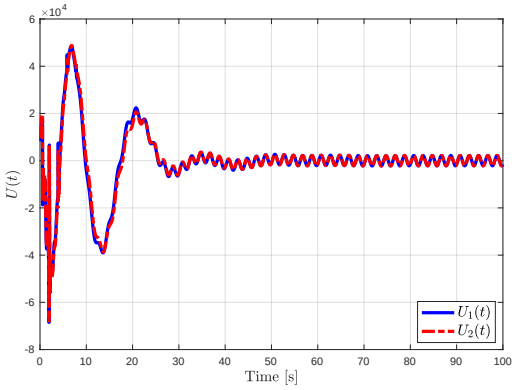

(a) Evolution of the control inputs $U_1(t)$ (blue) and $U_2(t)$ (red).

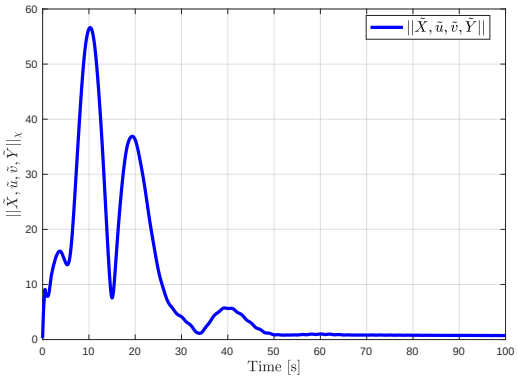

(b) Evolution of the $\chi-$norm of the error state $(\tilde{X},\tilde{u},\tilde{v},\tilde{Y})$.

Figure 7.2: Time evolution of the norm of the Control input (a), and of the $\chi-$norm of the error state (b).

of the error state is represented in Figure 7.2b. As expected, the error seems to converge to zero after the transient. However, the final value is not precisely zero. Even if this discrepancy does not prevent the stabilization of the virtual output in closed loop, it means that some of our states are not correctly reconstructed. This mismatch is due mainly to numerical issues since we noticed that reducing the space step (and consequently the time step due to the CFL condition) implied getting better estimates. Indeed, when performing the backstepping transformations, some kernels or some states may have large values compared to others, which could explain the sensitivity when performing the change of coordinates. Reducing the space step may slow the computations, which is a problem in a real implementation. It could be interesting to consider implicit solvers or use the Simpson method to compute the different integral terms instead of the trapezoidal method to overcome this numerical problem. Finally, it is essential to mention that this numerical issue occurs because of the strong instability of the open-loop system chosen as an example.

More precisely, we illustrated our approach with a complicated academic example (i.e., one where we are fully exploiting all of the assumptions to their fullest). This is a worst-case scenario where all the subsystems are independently unstable, only stabilizable, etc. The controller has to compensate for all the instabilities in the system (in particular those in the distal ODE system) and takes very high values, which is also an explanation for the numerical limitations observed. The resulting system is numerically very stiff and takes an important effort to simulate. The delay margin is non-zero but

might be small in this highly unstable case. We can reasonably expect better simulation behavior and delay margins for less unstable systems. In a practical application, and in particular, for a heavy industrial system, we would not expect all of the components (subsystems) to be independently unstable and simply stabilizable (in particular, the PDE would most likely be destabilized by the interconnection with the ODE and not by itself, and the actuator would not be an unstable ODE), and the actuation will likely require a lot less energy. Furthermore, we would expect a system with a smaller bandwidth (slow system) to naturally have a higher delay margin. Optimizing the filter could increase the delay margin, yet, without a theoretical bound for this, it is outside of the scope of this paper. We do not believe it would have been productive to do so for only one specific example. To illustrate this statement, we present below simulation results for a simple case. We have chosen the following numerical values: $\lambda = 2$, $\mu = 0.7$, $\sigma^+(x) = 0.5 + 0.1\sin(x)$, $\sigma^- = 0.5$, $\rho = 0.5$, $q = 0.6$. The ODE dynamics are in dimension $n = 4, m = 3, c = 2$, and defined by the matrices

$$A_0 = \begin{pmatrix} 0 & 0.014 & 0 & 0.01 \\ -4.2 & -0.5 & 0 & 0 \\ 0 & 0 & -0.15 & 0.2 \\ 0 & 0 & 0 & -0.11 \end{pmatrix}, B_0 = \begin{pmatrix} 0 & 0 \\ 0 & -1 \\ 1 & -1 \\ 0 & 0 \end{pmatrix}, E_0 = \begin{pmatrix} 0.2 \\ -0.1 \\ 0.01 \\ 0 \end{pmatrix},$$

$$C_0 = \begin{pmatrix} 0.1 & 0 & 0 & -0.05 \end{pmatrix}, \; C_1 = \begin{pmatrix} 0 & 1 & 0.5 & 0.1 & 0 & 0 \end{pmatrix}, \; E_1 = \begin{pmatrix} -0.1 \\ -0.1 \\ 0 \end{pmatrix},$$

$$A_{11} = \begin{pmatrix} -0.29 & 0.14 & 0 \\ -0.14 & 0 & 0.1 \\ 0 & 0 & -0.9 \end{pmatrix}, A_{21} = \begin{pmatrix} 0 & 0 & 0 \\ 0 & 0 & 0 \\ 0 & 0 & 0 \end{pmatrix}, A_{12} = \begin{pmatrix} 1 & 0 & 0 \\ 0 & 0 & 0 \\ 0 & 0 & 0 \end{pmatrix}, A_{22} = \begin{pmatrix} 0 & 0 & 0 \\ 0 & 0 & 1 \\ 0 & -1 & 0 \end{pmatrix}.$$

With this choice of coefficients, the two ODE subsystems are independently exponentially stable (as A_0 and A_1 are Hurwitz). However, the interconnection with the PDE makes the whole system unstable, as seen in Figure 7.3a. The reference signal is a sinusoidal function, and the system is subject to constant disturbance. We used a mesh of 101 points for the space domain. We chose small observer and controller gains to avoid numerical problems. The observer state slowly converges to the expected values. The control input is subject to a $0.1s$ delay, which would be closer to delay values encountered in real systems. The simulations are now obtained in less than one minute, and the proposed control strategy guarantees the convergence of the virtual output to zero. As seen in Figure 7.3b, the signal Y_1 converges to the reference signal. The control effort is pictured in Figure 7.4a. As expected, it shows smaller values than the ones given in Figure 7.2a. Finally, a 3D representation of $v(t,x)$, which keeps on oscillating in non transient time, is given in Figure 7.3b.

7.2 . Output-feedback stabilization in the case of an actuated/measured PDE

We now consider the case where the control input acts at the connection point between the u-PDE and the X-ODE (i.e., $B_X \equiv 0$). We make the simplifying assumption that $B_u = \mathrm{Id}$. Similarly, we consider that we measure the PDE state $u(t,1)$ (i.e., $C_Y = 0$ and $C_u = \mathrm{Id}$). As explained in the introduction of this chapter, the problem of stabilizing an ODE-PDE-ODE system when the PDE is actuated has not been well studied in the literature. Indeed, most contributions do not consider the ODE state X [ABABS+18, ADM20, dAVP18]. In this section, we show how we can use the time-delay representation to design a stabilizing output-feedback controller.

7.2.1 . State-feedback controller

Consider the variables $(\bar{X}, \bar{\alpha}, \beta, Y)$ obtained from the initial state (X, u, v, Y) using the transformation $\mathcal{F}_c(0,0)$. Consider the time-delay formulation given by equations (6.23)-(6.25) and define the intermediate control input $\bar{U}(t)$ as

$$\bar{U}(t) = U(t) + \sum_{i=1}^{N} F_i z(t-\tau_i) + \int_0^\tau H_z(\nu) z(t-\nu) d\nu + C_0 \bar{X}(t)$$

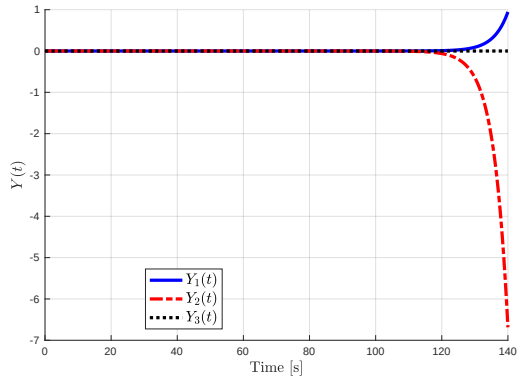

(a) Evolution of the different components of the distal ODE state $Y(t)$ in open-loop.

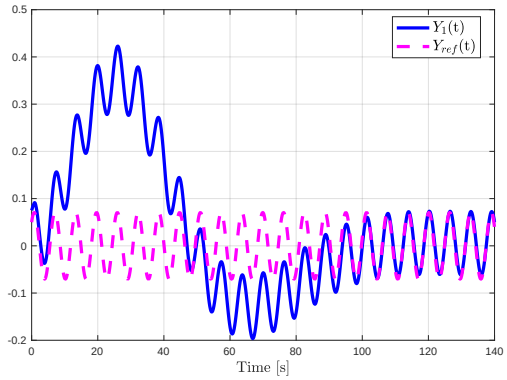

(b) Evolution of the state $Y_1(t)$ (blue) in closed-loop, in the presence of a disturbance (pink).

Figure 7.3: Time evolution of the norm of the state Y in open-loop (a), and time evolution of the state Y_1 in closed-loop (b).

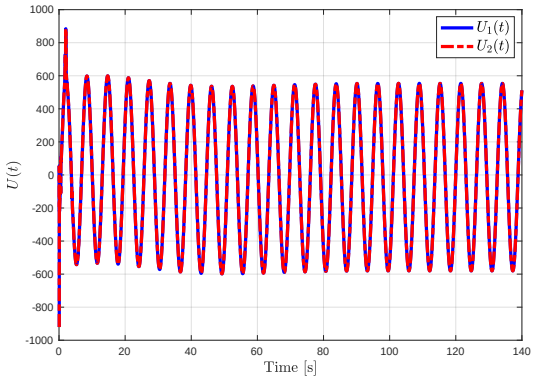

(a) Evolution of the control inputs.

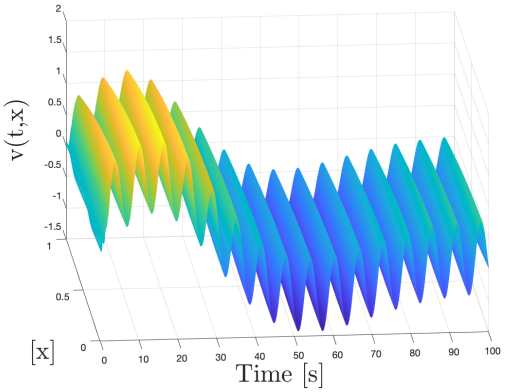

(b) 3D-evolution of PDE state $v(t,x)$.

Figure 7.4: Time evolution of the norm of the Control input (a), and of the PDE state $v(t,x)$ (b).

$$+ (Q\gamma_\beta(0) - \gamma_\alpha(0))Y(t). \tag{7.26}$$

Define $z(t) = \bar{\alpha}(t,0)$. Due to equation (7.26), we have $z(t) = \bar{U}(t)$. Following the computations of Section 6.1.2, we obtain for all $t > \tau$,

$$z(t) = \bar{U}(t) \tag{7.27}$$

$$\dot{\bar{X}}(t) = A_0\bar{X}(t) + \sum_{i=1}^{n} F_i^X \bar{U}(t-\tau_i) + \int_0^\tau H_X(\nu)\bar{U}(t-\nu)d\nu + E_0\gamma_\beta(0)Y(t), \tag{7.28}$$

$$\dot{Y}(t) = A_1 Y(t) + \sum_{i=1}^{n} F_i^Y \bar{U}(t-\frac{1}{\lambda_i}) + \int_0^\tau H_Y(\nu)\bar{U}(t-\nu)d\nu. \tag{7.29}$$

Note that, due to the cancellation of the reflection term $\sum_{i=1}^{N} F_i z(t-\tau_i)$, the control law $U(t)$ will not be strictly proper. Consequently, it will be necessary to low-pass filter it to guarantee the robustness of the closed-loop system. Inspired by [BLK10], we define the following change of coordinates

$$\bar{Y}(t) = Y(t) + \tau^2 \int_0^1 \Big(\int_0^x \mathrm{e}^{-A_1\tau(x-y)} H_Y(\tau(1-y))dy \Big) \bar{U}(t-(1-x)\tau)dx, \tag{7.30}$$

$$\bar{X}_1(t) = \bar{X}(t) + \tau^2 \int_0^1 \Big(\int_0^x \mathrm{e}^{-A_0\tau(x-y)} \bar{H}_X(\tau(1-y))dy \Big) \bar{U}(t-(1-x)\tau)dx, \tag{7.31}$$

where $\bar{H}_X(\nu) = H_X(\nu) - E_0\gamma_\beta(0)\tau\int_0^{\frac{1-\nu}{\tau}} \mathrm{e}^{-A_1(\tau(1-y)-\nu}H_Y(\tau(1-y))dy$. We obtain

$$\dot{\bar{X}}_1(t) = A_0\bar{X}_1(t) + E_0\gamma_\beta(0)\bar{Y}(t) + \sum_{i=1}^{n} F_i^X\bar{U}(t-\tau_i) + \bar{E}_0\bar{U}(t) \tag{7.32}$$

$$\dot{\bar{Y}}(t) = \bar{A}_1\bar{Y}(t) + \sum_{i=1}^{n} F_i^Y\bar{U}(t-\frac{1}{\lambda_i}) + \bar{E}_1\bar{U}(t) \tag{7.33}$$

where $\bar{E}_1 = \tau\int_0^1 \mathrm{e}^{-A_1\tau(1-y)}H_2(\tau(1-y))dy$ and $\bar{E}_0 = \tau\int_0^1 \mathrm{e}^{-A_0\tau(1-y)}\bar{H}_3(\tau(1-y))dy$. Let us denote

$$X_c(t) = \begin{pmatrix}\bar{X}_1(t)\\ \bar{Y}(t)\end{pmatrix},\ A_c = \begin{pmatrix}A_0 & E_0\gamma_\beta(0)\\ 0 & A_1\end{pmatrix}.$$

Inspired by [Art82], we finally define the state Z as

$$\begin{aligned} Z(t) = X_c(t) &+ \sum_{i=1}^{n}\int_{t-\tau_i}^{t} \mathrm{e}^{A_c(t-s-\tau_i)}\begin{pmatrix}F_i^X\\ 0\end{pmatrix}\bar{U}(s)ds \\ &+ \sum_{i=1}^{n}\int_{t-\frac{1}{\lambda_i}}^{t} \mathrm{e}^{A_c(t-s-\frac{1}{\lambda}_i)}\begin{pmatrix}0\\ F_i^Y\end{pmatrix}\bar{U}(s)ds. \end{aligned} \tag{7.34}$$

Consequently, we obtain $\dot{Z}(t) = A_cZ(t) + \bar{B}\bar{U}(t)$, with

$$\bar{B} = \begin{pmatrix}\bar{E}_0\\ \bar{E}_1\end{pmatrix} + \sum_{i=1}^{n}\begin{pmatrix}\mathrm{e}^{-A_c\tau_i}F_i^X\\ \mathrm{e}^{-A_c\frac{1}{\lambda_i}}F_i^Y\end{pmatrix}.$$

We are led to the following assumption

Assumption 7.2.1 *The pair $(A_c, \bar{B})$ is stabilizable, i.e., there exists K_c such that $A_c + \bar{B}K_c$ is Hurwitz.*

We have the following theorem

Theorem 7.2.1.

Consider system (7.1) with $B_u = \mathrm{Id}$. Consider that Assumptions 6.1.1 and 7.2.1 are verified. Consider the control law $U(t)$ defined by equation (7.26) where $\bar{U}(t) = K_cZ(t)$, where Z is defined from $\bar{X}$ and Y using transformations (7.31)-(7.30) and (7.34). Then, there exists a low pass filter $w_0(s)$ that satisfies equation (6.40) such that the control law $U_f(s) = w_0(s)U(s)$ is strictly proper and exponentially stabilizes the system (7.1).

Proof : The exponential stability of Z implies that $\bar{U}$ converges to zero. This implies the exponential stability of the state X (using (7.31)) and Y (using (7.30)). This, in turn, implies the exponential convergence of the state $\alpha(t,0)$ and consequently of (X,u,v,Y). Finally, since the controller gains K_X, K_Y are bounded and since $K_z = -F(s)$, the conditions of Theorem 6.2.1 are verified and the strictly proper controller U_f exponentially stabilizes the system (7.1). ■

7.2.2 . State observer

Analogously to what we have done in Section 7.1.4, we use the intermediate system (6.7) to design our observer. The state $(\bar{X}, \alpha, \beta, Y)$ is obtained from the state (X,u,v,Y) using the transformation $\mathcal{F}_o(0,0)$. Consequently, $y(t) = u(t,1) = \alpha(t,1)$. Following the methodology proposed in Section 6.1.2, we can apply the method of characteristics to obtain for $t > \tau$

$$\alpha(t,1) = \sum_{i=1}^{N}\bar{F}_i^z\alpha(t-\tau_i,1) + \sum_{i=1}^{n}\bar{F}_i^XX(t-\frac{1}{\lambda_i}) + \bar{F}_i^YY(t-\frac{1}{\lambda_i})$$

$$+\int_0^\tau \bar{H}(\nu)\alpha(t-\nu,1)d\nu + \sum B_i^U U(t-\frac{1}{\lambda_i}), \tag{7.35}$$

where the matrices $\bar{F}_i^z$, $\bar{F}_i^X$, $\bar{F}_i^Y$, B_i^U and $\bar{H}$ can be explicitly computed following the methodology of [ADM19]. Since the functions $\alpha(t,1)$ and $U(t)$ are both known, we can consider $y_1(t) = \sum_{i=1}^n \bar{F}_i^X \bar{X}(t-\frac{1}{\lambda_i}) + \bar{F}_i^Y Y(t-\frac{1}{\lambda_i})$ as an available measurement. Define Z as the concatenation of the vector $\bar{X}$ and Y and introduce the matrix $A_o = \begin{pmatrix} A_0 & G_4 \\ 0_{q\times p} & A_1 \end{pmatrix}$. We obtain

$$\dot{Z}(t) = A_0 Z(t) + G_Z y(t), \tag{7.36}$$

where $G_Z = \begin{pmatrix} G_3 \\ E_1 \end{pmatrix}$. Defining $F_i^o = \begin{pmatrix} \bar{F}_i^X & \bar{F}_i^Y \end{pmatrix}$, we have $y_1(t) = \sum_{i=1}^n F_i^o Z(t-\frac{1}{\lambda_i})$. Applying Duhamel's formula to equation (7.36), we obtain for $t > \frac{1}{\lambda_1}$

$$y_1(t) = \sum_{i=1}^n F_i^o \mathrm{e}^{-\frac{A_o}{\lambda_i}} \big(Z(t) - \int_{t-\frac{1}{\lambda_i}}^t \mathrm{e}^{A_o(t-\nu)} G_z y(\nu) d\nu\big). \tag{7.37}$$

We now make the following assumption

Assumption 7.2.2 *There exists L_o such that $A_o + L_o \sum_{i=1}^n F_i^o \mathrm{e}^{-\frac{A_o}{\lambda_i}}$ is Hurwitz.*

This assumption is the dual condition of Assumption 7.2.1. It can be seen as a detectability condition. We can now properly define the observer system. Let us denote $(\hat{\bar{X}}, \hat{\alpha}, \hat{\beta}, \hat{Y})$ as the observer state. We also define $\hat{Z}$ as the concatenation of $\hat{\bar{X}}$ and $\hat{Y}$. They are solutions of the following system

$$\begin{cases} \dot{\hat{Z}}(t) = A_o \hat{Z}(t) + G_Z y(t) - L_o(y_1(t) - \sum_{i=1}^n F_i^o \mathrm{e}^{-\frac{A_o}{\lambda_i}} \hat{Z}(t)) \\ \qquad -L_o \sum_{i=1}^n F_i^o \int_{t-\frac{1}{\lambda_i}}^t \mathrm{e}^{A_o(t-\nu)} G_z y(\nu) d\nu, \\ \hat{\alpha}(t,0) = Q\hat{\beta}(t,0) + C_0 \hat{\bar{X}}(t) + (Q\gamma_\beta(0) - \gamma_\alpha(0))\hat{Y}(t) + B_u U(t) \\ \qquad + \int_0^1 F^\alpha(y)\hat{\alpha}(t,y) + F^\beta(y)\hat{\beta}(t,y)dy - \mathcal{O}_0(\tilde{y}(t)), \\ \partial_t \hat{\alpha}(t,x) + \Lambda^+ \partial_x \hat{\alpha}(t,x) = G_1(x) y(t), \\ \partial_t \hat{\beta}(t,x) - \Lambda^- \partial_x \hat{\beta}(t,x) = G_2(x) y(t), \\ \hat{\beta}(t,1) = R\hat{\alpha}(t,1), \end{cases} \tag{7.38}$$

with any (arbitrary) initial conditions in χ. The operator $\mathcal{O}_o$ still has to be defined. We denote with a $\tilde{\cdot}$ the difference between the real and estimated states. The error system is obtained by subtracting the observer dynamics from the real one. We obtain

$$\begin{cases} \dot{\tilde{Z}}(t) = A_o \tilde{Z}(t) + L_o \sum_{i=1}^n F_i^o \mathrm{e}^{-\frac{A_o}{\lambda_i}} \tilde{Z}(t), \\ \tilde{\alpha}(t,0) = C_0 \tilde{\bar{X}}(t) + Q\tilde{\beta}(t,0) + (Q\gamma_\beta(0) - \gamma_\alpha(0))\tilde{Y}(t) \\ \qquad + \int_0^1 F^\alpha(y)\tilde{\alpha}(t,y) + F^\beta(y)\tilde{\beta}(t,y)dy + \mathcal{O}_0(\tilde{y}(t)), \\ \partial_t \tilde{\alpha}(t,x) + \Lambda^+ \partial_x \tilde{\alpha}(t,x) = 0, \\ \partial_t \tilde{\beta}(t,x) - \Lambda^- \partial_x \tilde{\beta}(t,x) = 0, \\ \tilde{\beta}(t,1) = R\tilde{\alpha}(t,1). \end{cases} \tag{7.39}$$

Note that Lemma 7.1.1 still holds. Thus, we want to define the operator $\mathcal{O}_o$ such that $\tilde{\bar{X}}$, $\tilde{\alpha}(t,1)$, and $\tilde{Y}$ exponentially converge to zero. Since $A_o + L_o \sum_{i=1}^n F_i^o \mathrm{e}^{-\frac{A_o}{\lambda_i}}$ is Hurwitz due to Assumption 7.2.2, we already have the exponential stability of $\tilde{\bar{X}}$ and $\tilde{Y}$. Following the methodology proposed in Section 6.1.2, we can apply the method of characteristics to obtain for $t > \tau$

$$\tilde{\alpha}(t,1) = \sum_{i=1}^N \bar{F}_i^z \tilde{\alpha}(t-\tau_i,1) + \sum_{i=1}^n \bar{F}_i^X \tilde{\bar{X}}(t-\frac{1}{\lambda_i}) + \bar{F}_i^Y \tilde{Y}(t-\frac{1}{\lambda_i})$$

$$+\int_0^\tau \bar{H}(\nu)\tilde{\alpha}(t-\nu,1)d\nu + \mathcal{O}_0(\tilde{y}(t)), \tag{7.40}$$

where the matrices $\bar{F}_i^z$, $\bar{F}_i^X$, $\bar{F}_i^Y$ and $\bar{H}$ are identical to the ones given in equation (7.35) and can be explicitly computed following the methodology of [ADM19]. Thus, we choose $\mathcal{O}_0(\tilde{y}(t))$ as

$$\mathcal{O}_0(\tilde{y}(t)) = -\sum_{i=1}^{N} \bar{F}_i^z \tilde{y}(t-\tau_i) - \int_0^\tau H(\nu)\tilde{y}(t-\nu)d\nu. \tag{7.41}$$

We can now write the following theorem

Theorem 7.2.2 *Consider the operators $\mathcal{O}_0$ defined by equation (7.41). Consider that Assumption 7.2.2 is verified. Define the observer states $(\hat{X},\hat{u},\hat{v},\hat{Y}) = \mathcal{F}_o(0,0,\hat{\tilde{X}},\ \hat{\alpha},\hat{\beta},\hat{Y})$, where the transformation $\mathcal{F}_o$ is defined in Theorem 6.1.1, and where $(\hat{\tilde{X}},\hat{\alpha},\hat{\beta},\hat{Y})$ is the solution of the system (7.38). Then the state $(\hat{X},\hat{u},\hat{v},\hat{Y})$ exponentially converges to (X,u,v,Y) in the sense of the χ-norm.*

Proof : The proof is a direct consequence of the previous computations and of Lemma 7.1.1. ■

Again, it is possible to low-pass filter the measured output signal $y(t)$ to obtain strictly proper observer operators (see Remark 7.1.2).

7.2.3 . Output feedback controller

The proposed observer can be used to design a stabilizing output-feedback controller.

Theorem 7.2.3.

Consider system (7.1) with $B_X \equiv 0$ under Assumptions 6.1.1, 7.2.1 and 7.2.2. Consider the operator $\mathcal{O}_0$ defined by equation (7.41). Define the observer states $(\hat{X},\hat{u},\hat{v},\hat{Y}) = \mathcal{F}_o(0,0,\hat{\tilde{X}},\ \hat{\alpha},\hat{\beta},\hat{Y})$, where the transformation $\mathcal{F}_o$ is defined in Theorem 6.1.1, and where $(\hat{\tilde{X}},\hat{\alpha},\hat{\beta},\hat{Y})$ is the solution of the system (7.38). Define the state $(\bar{X}_c,\bar{\alpha}_c,\beta_c,Y_c) = \mathcal{F}_c(0,0,\hat{X},\hat{u},\hat{v},\hat{Y})$, where the transformation $\mathcal{F}_c$ is defined in Theorem 6.1.2. Denote $z_c(s) = \bar{\alpha}_c(s,0)$ and define Z using transformations (7.31)-(7.30) and (7.34). There exist a low pass filter $w_0(s)$ that satisfies equations (6.40) such that the control law

$$\begin{aligned}\hat{U}(s) = w(s)\Big(&-\sum_{i=1}^{N} F_i z_c(t-\tau_i) - \int_0^\tau H_z(\nu)z_c(t-\nu)d\nu - C_0\bar{X}_c(t)\\ &-(Q\gamma_\beta(0)-\gamma_\alpha(0))Y_c(t) + K_c Z(t)\Big)\end{aligned} \tag{7.42}$$

is strictly proper and exponentially stabilizes the system (7.1).

Proof : The proof is analogous to the one of Theorem 7.1.3. ■

7.2.4 . Simulation results

We illustrate Theorem 7.2.3 with some simulations. The parameters are chosen as $\Lambda^+ = 1.2$, $\Lambda^- = 2$, $\Sigma^{++} = \Sigma^{--} = 0$, $\Sigma^{-+} = -0.35\mathrm{e}^{-x}$, $\Sigma^{+-} = 0.7x$, $Q = 0.7$, $R = 1$, $E_1 = (-0.1, 0.2)^T$, $C_1 = (0.1, 0.2)$, $C_0 = (-0.4 - 0.75)$, $E_0 = (-0.1, 0.3)^T$, $B_u = 1$. $A_0 = A_1 = \begin{pmatrix} -0.15 & 0.1 \\ 0 & 0.1 \end{pmatrix}$. The matrix K_c in Theorem 7.2.3 is chosen such that the poles for the eigenvalues of $A_c + \bar{B}K$ are -0.2, -0.3, -0.4 and -0.5. We choose the same poles for the observer part. The coefficients Σ^{-+} and Σ^{+-} are subject to an additive sinusoidal uncertainty (amplitude 0.05). In Figure 7.5 we have pictured the time evolution of the χ-norm in four situations. The first case corresponds to the closed-loop behavior without a low-pass filter and delay. In the second case, we consider a 0.05 input delay. Finally, in the third and fourth cases, we consider a filtered control law (with a simple low-pass filter of 2nd order with a bandwidth of 40 rad.s^{-1} and 120 rad.s^{-1} as illustrated by Lemma 6.2.1) in presence of a $0.05s$

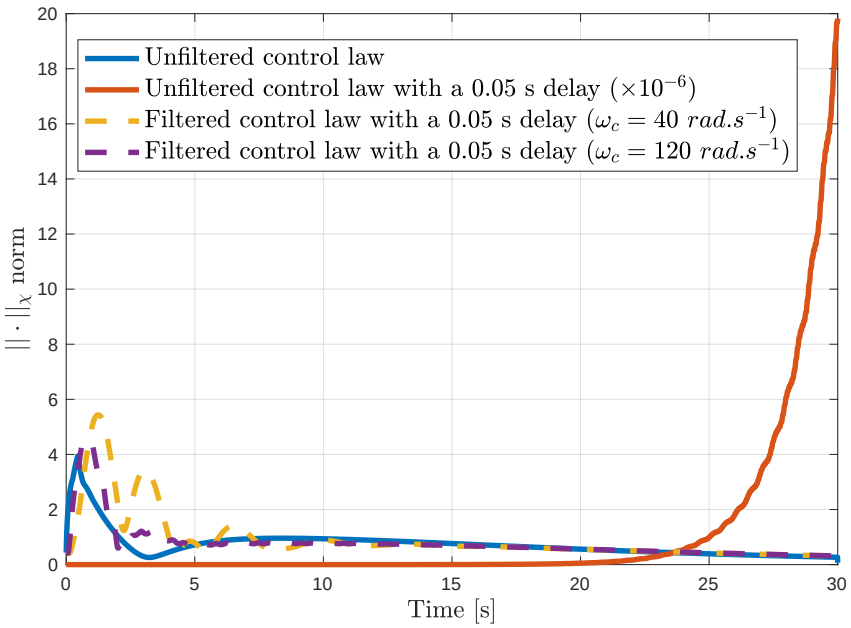

Figure 7.5: Evolution of the $||\cdot||_\chi$-norm of the state for three situations: a) Without filter and input delay (blue), b) without filter and with an input delay of (red), c) with a low-pass filter and input delay of 0.05s (yellow).

input delay. The nominal controller exponentially stabilizes the system. Note that the proposed design may be the cause of high transient values. Due to the cancellation of the reflection term $-Qv(t,0)$ in the control design, the unfiltered control law is not robust to this (small) input delay. Conversely, the filtered control law still stabilizes the system in the presence of this delay. Nevertheless, the filter slightly deteriorates the transient behavior. Increasing the bandwidth improves the performance but can deteriorate the robustness margins. Knowing the structure of the uncertainty, it is theoretically possible to increase the bandwidth (thus improving the performance) while guaranteeing that the conditions of Theorem 6.2.3 are still verified. However, due to the delay, a deeper analysis would be required to verify that the closed-loop system is still robust to delays.

7.3 . Conclusions and perspectives

In this chapter, we have introduced generic assumptions under which we could design stabilizing output-feedback controllers for the network system (7.1). We have distinguished the case of an actuated/measured ODE (Section 7.1) and the case of an actuated/measured PDE (Section 7.2). In both cases, the proposed design assumptions were essentially made on the **structure of the ODE components** and are less restrictive than those existing in the literature. The controller and observer designs are based on the time-delay methodology introduced in Chapter 6. We guaranteed the robustness of the resulting output feedback controllers using filtering techniques.

The proposed methodology avoids configurations where the PDE system is under-actuated or under-measured. More precisely, we have considered that the control input could act on all the components of one of the PDE states at the boundary (even if under Assumption 7.1.2 the X-ODE somehow filters this control input in Section 7.1), which guarantees the controllability/observability of the isolated PDE part [Li10]. Although the different assumptions we have stated throughout this chapter are verified for several industrial problems as simple drilling systems [AS18] or deepwater construction vessels [SWS10, WK22], they are not fulfilled for multiple network configurations. It is the case, for instance, of the simple interconnection of two scalar PDE systems [ADMBA19]. Therefore, we will focus on interconnected PDE systems with a chain structure in the next chapters. The interconnection will comprise several interconnected subsystems, only one being actuated through

its boundaries. In Chapter 8, the control input and measured output will be located at the end of the chain, while in Chapter 9, they will be located at one junction between two subsystems. In this last case, we will only consider the case of two subsystems. The control strategies we will design could then be coupled with the results of this chapter to deal with more general network configurations.

8 - Output-feedback stabilization of a network with a chain structure

In Chapter 7, we have designed output-feedback stabilizing controllers for a general class of ODE-PDE-ODE network under generic assumptions. Among other requirements, we imposed drastic rank conditions on the actuation matrices, B_u in the case of an actuated PDE or C_0 in the case of an actuated ODE. In many configurations, such conditions are not satisfied. It is the case, for instance, of the simple interconnection of two scalar hyperbolic systems [ADMBA19], only one of the subsystems being actuated. Although it seems for now overly ambitious to design generic control strategies for any underactuated systems or network configurations, several approaches in the literature have proposed constructive control designs for networks with **specific structures**. In particular, **chains** with a cascade structure have received particular interest. In such configurations, the graph representing the network is a straight line, and the actuator/sensor is located at one of its extremities. This class of system may appear when considering oil production systems made of connected pipes (whose principal line is known as the manifold) [MJ17]. More precisely, the lower part of the drill string is usually made up of drill collars that can significantly impact global dynamics due to their inertia. In particular, these pipes may have different lengths, densities, inertia, or Young's modulus. These spatial variations in the characteristic line impedance may cause reflections to appear in the junctions. Such simple networks with a chain structure can also model traffic systems, as described in [YK23] in the case of two cascaded freeway segments. Recently, several approaches have been developed to design stabilizing controllers for such chain structures: e.g., the multi-step approach in [DG20] or backstepping-based controllers [ADMBA19, Aur20] in the case of scalar subsystems. Although the latter approach has enabled significant advances, it only considered scalar subsystems and lacked adaptability from one chain to another. For instance, adding one additional PDE subsystem in the chain structure was not directly possible in [Aur20]. To remedy this disadvantage, we develop in this chapter a *recursive dynamics interconnection framework* to exploit the interconnection structure by recursively designing observers or controllers for each subsystem, gathering information on the nodes of the networks. Interconnection properties are used to build the desired output-feedback control law recursively. We consider an arbitrary number of non-scalar PDE subsystems interconnected through their boundaries, the actuation being located at one extremity of the chain. The proposed chapter extends the results from [ABANR21, RAN21b, ABP22] in this more generic setting.

8.1 . Problem under consideration

8.1.1 . Interconnection with a cascade structure

In this chapter, we consider a system composed of $N > 0$ PDE subsystems interconnected through their boundaries in a chain structure. Each subsystem is composed of an arbitrary number of linear hyperbolic PDEs and is modeled by the following set of equations ($i \in \{1, \dots, N\}$)

$$\partial_t u_i(t,x) + \Lambda_i^+ \partial_x u_i(t,x) = \Sigma_i^{++}(x) v_i(t,x) + \Sigma_i^{+-}(x) v_i(t,x), \tag{8.1}$$
$$\partial_t v_i(t,x) - \Lambda_i^- \partial_x v_i(t,x) = \Sigma_i^{-+}(x) u_i(t,x) + \Sigma_i^{--}(x) v_i(t,x), \tag{8.2}$$

evolving in $\{(t,x) \text{ s.t. } t > 0,\ x \in [0,1]\}$, where $u_i = (u_i^1, \dots, u_i^{n_i})^T$ and $v_i = (v_i^1, \dots, v_i^{m_i})^T$. Similarly to the general system (5.1) introduced in Chapter 6, the matrices $\Lambda_i^+ > 0$ and $\Lambda_i^- > 0$ are the constant transport velocity matrices respectively associated to equations (8.1) and (8.2). They are diagonal positive: $\Lambda_i^+ = \text{diag}(\lambda_i^j)_{1 \le j \le n_i}$ and $\Lambda_i^- = \text{diag}(\mu_i^j)_{1 \le j \le m_i}$. Moreover, we still consider that their coefficient verify

$$-\mu_i^{m_i} < \dots < -\mu_i^1 < 0 < \lambda_i^1 < \dots < \lambda_i^{n_i}.$$

We denote τ_i the maximum transport delay associated to each PDE subsystem: $\tau_i = \frac{1}{\lambda_i^1} + \frac{1}{\mu_i^1}$. The in-domain coupling terms $\Sigma_i^{\cdot\cdot}$ are regular functions, and we still consider that the diagonal entries of Σ_i^{++} and Σ_i^{--} are equal to zero. These subsystems are connected through their boundary conditions, which satisfy

$$u_i(t,0) = Q_{i,i}v_i(t,0) + Q_{i,i-1}u_{i-1}(t,1), \tag{8.3}$$
$$v_i(t,1) = R_{i,i}u_i(t,1) + R_{i,i+1}v_{i+1}(t,0) \tag{8.4}$$

where the different coupling and $R_{i,j}, Q_{i,j}$ are constant. By convention we consider that $R_{N,N+1} = 0$ and $Q_{1,0} = \mathrm{Id}$. Moreover, the function $u_0(t,1)$ corresponds to the **control input** $U(t)$. The measured output is denoted as $y(t)$ and verifies

$$y(t) = u_N(t,1). \tag{8.5}$$

System (8.1)-(8.4) is schematically pictured in Figure 5.3, and we propose in Figure 8.1 a simplified representation that underlines its chain structure. As explained in Section 5.3.3, the interconnected system (8.1)-(8.4) can be recast under the form (5.1) (without the ODEs) using a technique referred to as **folding** (see [Aur20, ABP22] for details). However, the representation (5.1) shadows the cascade structure between the different subsystems. This is why, in this chapter, we use the representation given by equations (8.1)-(8.4). The main advantage of such a representation is that it highlights that the interactions between the different subsystems only occur at the boundaries (black arrows). For instance, the output of the second subsystem entering the first subsystem could be seen as a disturbance acting on the first subsystem (even if the corresponding output of the first subsystem indirectly modifies this disturbance signal). For a subsystem i, we will call the subsystem $i+1$ the **downstream subsystem** and the subsystem $i-1$ the **upstream subsystem**.

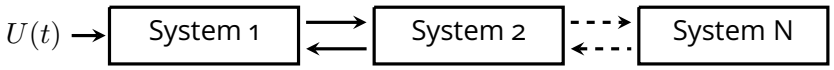

Figure 8.1: Schematic representation of system (8.1)-(8.4)

The initial conditions of each subsystem belong to $H^1([0,1],\mathbb{R}^{n_i}) \times H^1([0,1],\mathbb{R}^{m_i})$. They satisfy the appropriate compatibility conditions (as stated in Theorem 5.2.1), so that the system (8.1)-(8.4) is well-posed (Theorem 5.2.1). The objective of this chapter is to design an output-feedback control law that stabilizes the interconnected system (8.1)-(8.4) in the sense of the χ-norm (as defined in equation (5.3), with $p = q = 0$).

8.1.2 . Structural assumptions

To design an appropriate stabilizing output feedback controller, we require several assumptions. First, to guarantee the possibility of designing a delay-robust controller and avoid having an infinite number of unstable roots in the right-half plane, we still consider that Assumption 6.1.1 is verified. Then, we need the following assumption to stabilize the downstream subsystem states using actuation from the upstream subsystem.

Assumption 8.1.1 *For all $i \in \{2,\dots,N\}$, the rank of the matrix $Q_{i-1,i}$ is equal to n_i.*

This assumption implies that the matrix $Q_{i-1,i}$ admits a right inverse. A possible choice is given by the Moore–Penrose right inverse: $Q_{i-1,i}^\top (Q_{i-1,i}Q_{i-1,i}^\top)^{-1}$. This assumption will be used to design a *virtual actuation* for each subsystem. One must be aware that it is a conservative assumption. Still, to the best of our knowledge, only specific results currently exist in the literature for stabilizing underactuated systems with no specific cascade structure (see [ABABP20]). We are led to a similar assumption to designing a state observer.

Assumption 8.1.2 *For all $i \in \{2,\dots,N\}$, the rank of the matrix $Q_{i-1,i}$ is equal to n_{i-1}.*

This assumption implies that the matrix $Q_{i-1,i}$ admits a left inverse. Again, this condition is conservative, but to the best of our knowledge, only specific results currently exist in the literature for estimating under-measured systems with no specific cascade structure (see [ABABP20]). Combining Assumption 8.1.1 and Assumption 8.1.2, we obtain that all the n_i are equal and that the matrices $Q_{i-1,i}$ are invertible. This is related to the fact that we considered uncollocated measurements. In the case of collocated measurements (i.e., $y(t) = v_1(t,0)$), Assumption 8.1.2 would have been expressed as a rank condition on the matrices $R_{i,i+1}$ (as it is the case in [RAN21b]).

8.1.3 . Toward a recursive design

From Figure 8.1 and Figure 5.3, it can be seen that a subsystem i will act on the downstream subsystem $i+1$ through $u_i(t,1)$, and on the upstream subsystem $i-1$ through $v_i(t,0)$. Thus, each subsystem can only be stabilized through its upstream subsystem and estimated through its downstream subsystem. Due to the hyperbolic nature of the different subsystems, the effect of the control input $U(t)$ on the subsystem i will be delayed and modified by the different in-domain coupling terms. To stabilize the whole chain, we propose a *recursive interconnected dynamics control framework*. Roughly speaking, the control law is recursively obtained by considering stabilizing virtual inputs for each subsystem and ensuring the output of the upstream subsystem converges to this desired virtual input. The control design becomes more straightforward and is based on simple assumptions that can be independently verified for each subsystem. More precisely, we propose the following control stategy:

1. First, using recursive backstepping transformations, we simplify the structure of each subsystem to remove the in-domain coupling terms that appear in the u_i-PDEs (equation (8.1)).

2. Then, for each subsystem i, we consider the effect of the upstream subsystem $i-1$ as a delayed virtual input $U_i(t-\sum_{j=1}^{i-1}\frac{1}{\lambda_j^1})$ and the effect of the downstream subsystem $i+1$ as a disturbance term. We combine appropriate **state predictions** with a **flatness-based feedforward tracking controller** to guarantee that the right output of this subsystem converges to an appropriate function that will correspond to the delayed virtual input $U_{i+1}(t-\sum_{j=1}^{i}\frac{1}{\lambda_j^1})$ that will stabilize the downstream subsystem. Iterating such a procedure, it is possible to design a stabilizing control law $U(t)$ for the whole system.

3. The closed-loop stability is shown recursively, using **Input-to-State Stability** (ISS) properties of each subsystem.

4. A similar **recursive approach** is used to design a state observer. Going recursively from one subsystem to the next, we can estimate delayed values of the states at each subsystem boundary.

5. Finally, similarly to what has been done for finite-dimensional systems [KK17], we can adjust the state predictors used in the control design to obtain an output-feedback controller.

The proposed framework allows for a "plug-and-play"-like approach to control design since additional subsystems satisfying similar conditions can be added to the network using the same procedure. Moreover, it offers interesting perspectives as it can be applied to different classes of interconnected systems. A promising extension has, for instance, been suggested in [XLKF23] for parabolic systems.

8.2 . State-feedback controller

8.2.1 . Backstepping transformations

The first objective before applying our recursive control strategy is to simplify the structure of the interconnected system (8.1)-(8.4) in order to "clear the actuation path" of each subsystem by removing the local terms initially present in equation (8.1). Consider the i^{th} subsystem. We have shown in Chapter 6 that in the absence of the function $v_{i+1}(t,0)$ it was possible to apply classical backstepping transformations (equations (6.2) and (6.14)) to replace the local terms present in equation (8.1) by

non-local terms that depend on $v_i(t,1)$. It has been shown in [HDMVK19] that for such a simplified target system, it was possible to design a flatness-based feedforward tracking virtual control input $\hat{U}_i(t)$ that guarantees the convergence of $u_i(t,1)$ to a known reference signal (that could be chosen as a stabilizing controller for the downstream subsystem). In the presence of the signal term $v_{i+1}(t,0)$ (that can be seen as a disturbance signal), the same backstepping transformations would display additional terms (depending on $v_{i+1}(t,0)$) in the actuation path. Due to these new terms, the approach proposed in [HDMVK19] cannot directly be applied for causality reasons. This is why we present an original integral transformation to help us overcome these potential causality issues. For all $i \in \{1,\dots,N\}$, and all $t \geq \frac{1}{\lambda_i^1}$, we consider the integral transformation defined by

$$\begin{aligned}\alpha_i(t,x) = u_i(t,x) &+ \int_x^1 K_i^{uu}(x,y)u_i(t,y) + K_i^{uv}(x,y)v_i(t,y)dy \\ &+ \int_0^{\frac{x}{\lambda_i^1}} F_i(x,y)v_{i+1}(t-y,0)dy, \end{aligned} \tag{8.6}$$

$$\beta_i(t,x) = v_i(t,x) + \int_x^1 K_i^{vu}(x,y)u_i(t,y) + K_i^{vv}(x,y)v_i(t,y)dy, \tag{8.7}$$

where the kernels $K_i^{\cdot\cdot}$ are piecewise continuous functions defined on $\mathcal{T}_u$, while the kernels F_i are piecewise continuous functions defined on the triangular domain $\{(x,y) \in [0,1] \times [0, \frac{1}{\lambda_i^1}],\ y \leq \frac{x}{\lambda_i^1}\}$. By convention $F_{N+1} = 0$. The kernels $K_i^{\cdot\cdot}$ and $K_i^{\cdot\cdot}$ verify the following set of PDEs

$$\begin{cases} \Lambda_i^+\partial_x K_i^{uu}(x,y) + \partial_y K_i^{uu}(x,y)\Lambda_i^+ = -K_i^{uu}(x,y)\Sigma_i^{++}(y) - K_i^{uv}(x,y)\Sigma_i^{-+}(y) + G_i(x)K_i^{uu}(x,y), \\ \Lambda_i^+\partial_x K_i^{uv}(x,y) - \partial_y K_i^{uv}(x,y)\Lambda_i^- = -K_i^{uu}(x,y)\Sigma_i^{+-}(y) - K_i^{uv}(x,y)\Sigma_i^{--}(y) + G_i(x)K_i^{uv}(x,y), \\ \Lambda_i^-\partial_x K_i^{vu}(x,y) - \partial_y K_i^{vu}(x,y)\Lambda_i^+ = K_i^{vu}(x,y)\Sigma_i^{++}(y) + K_i^{vv}(x,y)\Sigma_i^{-+}(y), \\ \Lambda_i^-\partial_x K_i^{vv}(x,y) + \partial_y K_i^{vv}(x,y)\Lambda_i^- = K_i^{vu}(x,y)\Sigma_i^{+-}(y) + K_i^{vv}(x,y)\Sigma_i^{--}(y), \end{cases} \tag{8.8}$$

with the boundary conditions

$$\begin{cases} \Lambda_i^+ K_i^{uu}(x,x) - K_i^{uu}(x,x)\Lambda_i^+ = \Sigma_i^{++}(x) - G_i(x), \\ \Lambda_i^+ K_i^{uv}(x,x) + K_i^{uv}(x,x)\Lambda_i^- = \Sigma_i^{+-}(x), \\ \Lambda_i^- K_i^{vu}(x,x) + K_i^{vu}(x,x)\Lambda_i^+ = -\Sigma_i^{-+}(x), \\ \Lambda_i^- K_i^{vv}(x,x) - K_i^{vv}(x,x)\Lambda_i^- = -\Sigma_i^{--}(x), \\ K_i^{uu}(x,1)\Lambda_i^+ = K_i^{uv}(x,1)\Lambda_i^- R_{ii}, \end{cases} \tag{8.9}$$

where $G_i(x)$ is a piecewise continuous **strictly upper-triangular** matrix function defined on $[0,1]$ through the first boundary condition of (8.9). More precisely, for all $1 \leq k,\ell \leq n_i$, the boundary condition $\Lambda_i^+ K_i^{uu}(x,x) - K_i^{uu}(x,x)\Lambda_i^+ = \Sigma_i^{++}(x) - G_i(x)$ rewrites

$$(K_i^{uu}(x,x))_{k\ell} = \frac{(\Sigma_i^{++})_{k\ell}}{\lambda_i^k - \lambda_i^\ell}, \quad \text{if } k > \ell, \tag{8.10}$$

$$(G_i(x))_{k\ell} = (\Sigma_i^{++})_{k\ell} + (\lambda_i^\ell - \lambda_i^k)(K_i^{uu}(x,x))_{k\ell}, \quad \text{if } k \leq \ell. \tag{8.11}$$

It is important to emphasize that the matrix G_i is strictly upper-triangular since for $k = \ell$, we have $(G_i(x))_{k\ell} = 0$ due to equation (8.11) (as the diagonal entries of Σ_i^{++} are equal to zero). To these boundary conditions we add arbitrary boundary conditions for $(K_i^{vv}(0,y))_{k\ell}$ when $k < \ell$, and arbitrary conditions for $(K_i^{vv}(x,1))_{k\ell}$ when $\ell \leq k$. The set of kernel equations (8.8)-(8.11) admits a unique piecewise continuous solution [ADM16a]. The kernels F_i verify

$$\Lambda_i^+\partial_x F_i(x,y) + \partial_y F_i(x,y) = G_i(x)F_i(x,y), \tag{8.12}$$

$$F_i(x,0) = -K_i^{uv}(x,0)\Lambda_i R_{i,i+1}, \tag{8.13}$$

$$(F_i(x, \frac{x}{\lambda_i^1}))_{k\ell} = 0, \quad 1 < k \leq n_i,\ 1 \leq \ell \leq m_{i+1}. \tag{8.14}$$

Applying the method of characteristics, one can show that equations (8.12)-(8.14) admit a unique piecewise continuous solution. The transformation (8.6)-(8.7) is a Volterra transformation to which an affine term that depends on the state v_{i+1} is added. Consequently, it is invertible [Yos60] and there exist piecewise continuous functions $L_i^{\cdot\cdot}$ defined on $\mathcal{T}_u$ and piecewise continuous functions $H_i^{\cdot}$ defined on the rectangular domain $\{(x,y) \in [0,1] \times [0, \frac{1}{\lambda_i^1}]\}$ such that for all $t \geq \frac{1}{\lambda_i^1}$

$$u_i(t,x) = \alpha_i(t,x) + \int_x^1 L_i^{\alpha\alpha}(x,y)\alpha_i(t,y) + L_i^{\alpha\beta}(x,y)\beta_i(t,y)dy + \int_0^{\frac{1}{\lambda_i^1}} H_i^{\alpha}(x,y)v_{i+1}(t-y,0)dy, \tag{8.15}$$

$$v_i(t,x) = \beta_i(t,x) + \int_x^1 L_i^{\beta\alpha}(x,y)\alpha_i(t,y) + L_i^{\beta\beta}(x,y)\beta_i(t,y)dy + \int_0^{\frac{1}{\lambda_i^1}} H_i^{\beta}(x,y)v_{i+1}(t-y,0)dy. \tag{8.16}$$

For all $t \geq \frac{1}{\lambda_i^1}$, the transformation (8.6)-(8.7) maps the system (8.1)-(8.4) to the target system

$$\partial_t \alpha_i(t,x) + \Lambda_i^+ \partial_x \alpha_i(t,x) = G_i(x)\alpha_i(t,x), \tag{8.17}$$

$$\partial_t \beta_i(t,x) - \Lambda_i^- \partial_x \beta_i(t,x) = \bar{G}_i(x)\alpha_i(t,1) + \bar{f}_i(x)v_{i+1}(t,0), \tag{8.18}$$

with the boundary conditions

$$\alpha_i(t,0) = Q_{i,i}\beta_i(t,0) + Q_{i,i-1}\alpha_{i-1}(t,1) + \int_0^1 (K_i^{uu}(0,y) - Q_{i,i}K_i^{vu}(0,y))u_i(t,y)dy + \int_0^1 (K_i^{uv}(0,y) - Q_{i,i}K_i^{vv}(0,y))v_i(t,y)dy - Q_{i,i-1}\int_0^{\frac{1}{\lambda_{i-1}^1}} F_{i-1}(1,y)v_i(t-y,0)dy, \tag{8.19}$$

$$\beta_i(t,1) = R_{i,i}\alpha_i(t,1) + R_{i,i+1}v_{i+1}(t,0) - R_{i,i}\int_0^{\frac{1}{\lambda_i^1}} F_i(1,y)v_{i+1}(t-y,0)dy, \tag{8.20}$$

where $\bar{G}_i(x) = K_i^{vv}(x,1)\Lambda_i^- R_{i,i} - K_i^{vu}(x,1)\Lambda_i^+$ and $\bar{f}_i(x) = K_i^{vv}(x,1)\Lambda_i^- R_{i,i+1}$. By convention, we have $F_0 = 0$ and $Q_{1,0}\alpha_0(t,1) = U(t)$. The in-domain coupling terms appearing in equation (8.1) now have a triangular structure. In equation (8.4), all the local terms have been replaced by non-local terms that depend on $\alpha_i(t,1)$ and $v_{i+1}(t - \frac{x}{\lambda_i^1}, 0)$. This structure will simplify the design of the proposed recursive stabilizing control law. For instance, in the case of a single subsystem ($N = 1$), it becomes straightforward to design a stabilizing boundary feedback control law by canceling all the terms at the actuated boundary (8.19) [ADM16a]. To increase readability, we decided not to express some u_i and v_i terms as functions of α_i and β_i. This will not affect the proposed analysis. In the next sections, we state several elementary properties for the system (8.17)-(8.20). We will then combine these properties in Section 8.2.5 to design our recursive stabilizing controller. For $t > \max_i \frac{1}{\lambda_j^1}$ and all $1 \leq i \leq N$, all the backstepping transformations (8.6)-(8.7) are well defined.

8.2.2 . Output trajectory tracking

Consider the i^{th} subsystem composing the interconnection (8.17)-(8.20). Let us define the virtual control input acting on this subsystem as

$$\hat{U}_i(t) = Q_{i,i-1}\alpha_{i-1}(t + \sum_{j=1}^{i-1} \frac{1}{\lambda_j^1}, 1). \tag{8.21}$$

We do not choose $\hat{U}_i(t) = Q_{i,i-1}\alpha_{i-1}(t,1)$ as the virtual input to guarantee the causality of the final control law. Indeed, the delay $\sum_{j=1}^{i-1} \frac{1}{\lambda_j^1}$ corresponds to the total largest transport time between the

control input $U(t)$ and the subsystem i. It reflects the fact that the control input cannot directly act on the subsystem i, but that its effect is subject to the delay $\sum_{j=1}^{i-1}\frac{1}{\lambda_j^1}$. Equation (8.19) rewrites

$$\alpha_i(t,0) = Q_{i,i}v_i(t,0) + \hat{U}_i(t-\sum_{j=1}^{i-1}\frac{1}{\lambda_j^1}) + \int_0^1 K_i^{uu}(0,y)u_i(t,y) + K_i^{uv}(0,y)v_i(t,y)dy$$
$$- Q_{i,i-1}\int_0^{\frac{1}{\lambda_{i-1}^1}} F_{i-1}(1,y)v_i(t-y,0). \tag{8.22}$$

We have the following property that guarantees the possibility for each subsystem to track any arbitrary function as long as predictions of the different states are available

Property 8.2.1 *Consider the i^{th} subsystem* (8.17)-(8.20) *($i \in \{1,\dots,N-1\}$) and define ζ_i an arbitrary known $H^1([0,\infty),\mathbb{R}^{n_{i+1}})$ function. Assume that there exists $t_0 > 0$ such that for all $t > t_0$ and all $x \in [0,1]$, it is possible to obtain a $\sum_{j=1}^{i-1}\frac{1}{\lambda_j^1}$ units of time ahead prediction of the PDE states $u_i(t,x)$, $v_i(t,x)$, $\alpha_i(t,x)$, $\beta_i(t,x)$, i.e. there exist predictor functions P_{u_i}, P_{v_i}, P_{α_i} and P_{β_i} such that for all $t > t_0$ and all $x \in [0,1]$, $P_{u_i}(t,x) = u_i(t+\sum_{j=1}^{i-1}\frac{1}{\lambda_j^1},x)$, $P_{v_i}(t,x) = v_i(t+\sum_{j=1}^{i-1}\frac{1}{\lambda_j^1},x)$, $P_{\alpha_i}(t,x) = \alpha_i(t+\sum_{j=1}^{i-1}\frac{1}{\lambda_j^1},x)$, $P_{\beta_i}(t,x) = \beta_i(t+\sum_{j=1}^{i-1}\frac{1}{\lambda_j^1},x)$. Then, there exists a control law $\hat{U}_i(t)$ such that for any $t > t_0 + \frac{1}{\lambda_i^1}$, we have $\alpha_i(t,1) = \zeta_i(t)$. Moreover, if $\zeta_i(t) \equiv 0$, and $v_{i+1}(t) \equiv 0$, then, such a control law stabilizes the i^{th} subsystem.*

Proof : The proof is inspired by [HDMVK16]. Let us first introduce the intermediate virtual control input $\hat{U}^{tr}(t)$ such that for all $t > t_0 + \frac{1}{\lambda_i^1}$

$$\hat{U}_i(t) = \hat{U}_i^{tr}(t) - Q_{i,i}P_{v_i}(t,0) - \int_0^1 (K_i^{uu}(0,y)P_{u_i}(t,y)dy + K_i^{uv}(0,y)P_{v_i}(t,y)dy$$
$$+ Q_{i,i-1}\int_0^{\frac{1}{\lambda_{i-1}^1}} F_{i-1}(1,y)P_{v_i}(t-y,0). \tag{8.23}$$

This gives $\alpha_i(t,0) = \hat{U}_i^{tr}(t-\sum_{j=1}^{i-1}\frac{1}{\lambda_j^1})$. Applying the method of characteristics on equation (8.17), we obtain for all $1 \le j \le n_i$, for all $x \in [0,1]$, and for all $t > t_0 + \frac{1}{\lambda_i^1}$,

$$\alpha_i^j(t,x) = \alpha_i^j(t-\frac{1-x}{\lambda_i^j},0) + \sum_{k=j+1}^{n_i}\int_0^{\frac{1-x}{\lambda_i^j}} (G_i(x+\lambda_i^j\nu))_{jk}\alpha_i^k(t+\nu,x+\lambda_i^j\nu)d\nu. \tag{8.24}$$

In particular, since the matrix G_i is strictly upper-triangular, we obtain

$$\alpha_i^{n_i}(t,x) = \alpha_{n_i}^j(t+\frac{1-x}{\lambda_i^{n_i}},1).$$

Then, we can recursively show that there exist matrix functions $\check{G}_i$ such that for all $1 \le j \le n_i$, for all $x \in [0,1]$, for all $t > t_0 + \frac{1}{\lambda_i^1}$

$$\alpha_i^j(t,x) = \alpha_i^j(t+\frac{1-x}{\lambda_i^j},1) + \sum_{\ell=j+1}^{n_i}\int_0^{\frac{1-x}{\lambda_i^j}} (\check{G}_i(x,\nu))_{j\ell}\alpha_i^\ell(t+\nu,1)d\nu. \tag{8.25}$$

Therefore, for all $t \ge t_0 + \frac{1}{\lambda_i^1}$, for all $1 \le j \le n_i$, the control law

$$(\hat{U}_i^{tr}(t))_j = \alpha_i^j(t+\sum_{j=1}^{i-1}\frac{1}{\lambda_j^1},0)$$
$$= \zeta_i^j(t+\frac{1}{\lambda_i^j}+\sum_{j=1}^{i-1}\frac{1}{\lambda_j^1}) + \sum_{\ell=j+1}^{n_i}\int_0^{\frac{1}{\lambda_i^j}} (\check{G}_i(0,\nu))_{j\ell}\zeta_\ell(t+\sum_{j=1}^{i-1}\frac{1}{\lambda_j^1}+\nu)d\nu, \tag{8.26}$$

guarantees $\alpha_i(t,1) = \zeta_i(t)$. If the function ζ_i is equal to zero, then the i^{th} subsystem converges to zero in finite time. Using the method of characteristics, we can easily show that it is exponentially stable [ADM16a]. ■

The fact that we need future values of the functions u_j, v_j, α_j, β_j ($j \geq i$) is induced by the presence of the delay $\sum_{j=1}^{i-1} \frac{1}{\lambda_j^1}$ in the virtual control input $\hat{U}_i(t)$. Due to the transport delay to go from the left boundary of the α_i-PDE ($x = 0$, where is located the virtual actuation) to its right boundary ($x = 1$, where is defined the output we want to track), we also need future values of the reference signal ζ_i. However, one can verify that only $(t + \sum_{k=1}^{i} \frac{1}{\lambda_k^1})$-ahead of time values of ζ_i are required. Finally, we emphasize that Property 8.2.1 does not have to be satisfied for the last subsystem.

8.2.3 . Input-to-State stability

As explained in Section 8.1.3, the control framework we propose recursively stabilizes each subsystem, starting from the last one. For a given subsystem, the corresponding control input corresponds to the reference signal the upstream subsystem has to track. However, to guarantee closed-loop stability of the whole chain, we need the following Input-to-State Stability (ISS) property for each subsystem.

Property 8.2.2 *Consider the i^{th} subsystem ($i \in \{1, \dots, N-1\}$) and consider that Property 8.2.1 holds. Consider that $\hat{U}_i(t)$ is defined by equation (8.23). Then, there exist two constants $\kappa_i > 0$ and $\eta_i > 0$ such that for all $t > t_0 + \frac{1}{\lambda_i^1} + \frac{1}{\mu_i^1}$, we have*

$$||(\alpha_i(t,\cdot), \beta_i(t,\cdot))||_{L^2}^2 \leq \kappa_i \big(||(\zeta_i)_{[t]}||_{L^2_{\eta_i}}^2 + ||(\zeta_i)_{[t]}||_{L^2_{-\eta_i}}^2 + ||(v_{i+1}(\cdot,0))_{[t]}||_{\eta_i}^2 \big). \tag{8.27}$$

Proof : Due to Property 8.2.1, we have for all $t > t_0 + \frac{1}{\lambda_i^1}$, $\alpha_i(t,1) = \zeta_i(t)$. Applying the method of characteristics on equation (8.18), we obtain for all $j \in \{1, \dots, N\}$, for all $t > t_0 + \frac{1}{\lambda_i^1} + \frac{1}{\mu_i^1}$

$$\begin{aligned}
\beta_i^j(t,x) =& \sum_{k=1}^{n_i} (R_{i,i})_{jk} \zeta_i(t - \frac{1-x}{\mu_i^j}) + \sum_{k=1}^{m_{i+1}} (R_{i,i+1})_{jk} v_{i+1}^k(t - \frac{1-x}{\mu_i^j}, 0) - \sum_{k=1}^{n_i} \sum_{\ell=1}^{m_{i+1}} \int_0^{\frac{1}{\lambda_i^1}} (R_{i,i})_{jk} \\
& (F_i(1,y))_{k\ell} v_{i+1}^\ell(t - y - \frac{1-x}{\mu_i^j}, 0) dy + \sum_{k=1}^{n_i} \int_0^{\frac{1-x}{\mu_i^j}} (\bar{G}_i(x + \mu_i^j \nu))_{jk} \zeta_i^k(t-\nu) d\nu \\
& + \sum_{k=1}^{m_{i+1}} \int_0^{\frac{1-x}{\mu_i^j}} (\bar{f}_i(x + \mu_i^j \nu))_{jk} v_{i+1}^k(t - \nu, 0) d\nu.
\end{aligned}$$

Since the functions $\bar{f}_i$ and $\bar{G}_i$ are bounded, straightforward (but tedious), computations give the existence of a constant $K_{\beta_i} > 0$ such that

$$||\beta_i(t,\cdot)||_{L^2}^2 \leq K_{\beta_i} \big(||(\zeta_i)_{[t]}||_{L^2_{\frac{1}{\mu_i^1}}}^2 + ||(v_{i+1}(\cdot,0))_{[t]}||_{L^2_{\frac{1}{\mu_i^1} + \frac{1}{\lambda_i^1}}}^2 \big).$$

Similarly, we can show that there exists a constant $K_{\alpha_i} > 0$ such that

$$||\alpha_i(t,\cdot)||_{L^2}^2 \leq K_{\alpha_i} ||(\zeta_i)_{[t]}||_{L^2_{-\frac{1}{\lambda_i^1}}}^2.$$

This concludes the proof. ■

We emphasize that the right-hand side of equation (8.27) involves past and future values of the functions ζ_i, which is not an issue from a stability perspective. Moreover, due to Property 8.2.2, the finite-time convergence to zero of the functions ζ_i and v_{i+1} directly implies the finite-time stability of the state (α_i, β_i).

8.2.4 . State prediction

The virtual control law given in Property 8.2.1 requires the prediction of future values of the functions α_i, β_i, u_i, and v_i. The following property states that it is possible to design such predictors.

Property 8.2.3 *Consider the i^{th} subsystem (8.17)-(8.20) ($i \in \{1, \dots, N\}$) with the virtual input $\hat{U}_i(t)$ defined in equation (8.21). For $t > \max_r \tau_r + \sum_{k=1}^{i-1} \frac{1}{\lambda_k^1}$, for all $x \in [0,1]$, and all $j \in \{i, \dots, N\}$, it is possible to obtain a $\sum_{k=1}^{i-1} \frac{1}{\lambda_k^1}$-ahead of time prediction of the functions $u_j(t,x)$, $v_j(t,x)$, $\alpha_j(t,x)$, $\beta_j(t,x)$. More precisely there exist predictor functions P_{u_j}, P_{v_j}, P_{α_j}, and P_{β_j} such that for all $t > \max_r \tau_r + \sum_{k=1}^{i-1} \frac{1}{\lambda_k^1}$, for all $x \in [0,1]$, $P_{u_j}(t,x) = u_j(t + \sum_{k=1}^{i-1} \frac{1}{\lambda_k^1}, x)$, $P_{v_j}(t,x) = v_j(t + \sum_{k=1}^{i-1} \frac{1}{\lambda_k^1}, x)$, $P_{\alpha_j}(t,x) = \alpha_j(t + \sum_{k=1}^{i-1} \frac{1}{\lambda_k^1}, x)$, $P_{\beta_j}(t,x) = \beta_j(t + \sum_{k=1}^{i-1} \frac{1}{\lambda_k^1}, x)$.*

Proof : Consider the i^{th} subsystem (8.17)-(8.20) ($i \in \{1,\dots,N\}$) with the virtual input $\hat{U}_i(t)$ defined in equation (8.21). Consider $j \in \{i,\dots,N\}$. For $t > \max_r \tau_r + \sum_{k=1}^{i-1} \frac{1}{\lambda_k^1}$, we will design predictors for the functions $v_j(t,0)$, $\alpha_j(t,1)$ and $\alpha_j(t,0)$. From these predictors, it will be possible to predict the functions $u_j(t,x)$, $v_j(t,x)$, $\alpha_j(t,x)$, $\beta_j(t,x)$ ($x \in [0,1]$). Applying the method of characteristics on equation (8.17), we can recursively show that there exist matrix functions $\tilde{G}_j$ such that for all $1 \le k \le n_j$,

$$\alpha_j^k(t,1) = \alpha_j^k(t - \frac{1}{\lambda_j^k}, 0) + \sum_{\ell=k+1}^{n_j} \int_0^{\frac{1}{\lambda_j^k}} (\tilde{G}_j(\nu))_{k\ell} \alpha_j^\ell(t-\nu,0) d\nu. \tag{8.28}$$

Using the backstepping transformation (8.16) and the method of characteristics (see [ADM19, ABANR21]), we obtain, for all $1 \le k \le m_j$,

$$\begin{aligned} v_j^k(t,0) = &\sum_{\ell=1}^{n_j} (R_{j,j})_{k\ell} \alpha_j^\ell(t - \frac{1}{\mu_j^k}, 1) + \sum_{\ell=1}^{m_{j+1}} (R_{j,j+1})_{k\ell} v_{j+1}^\ell(t - \frac{1}{\mu_j^k}, 0) \\ &+ \sum_{\ell=1}^{n_j} \int_0^{\tau_j} (g_j^1)_{k\ell}(\nu) \alpha_j^\ell(t-\nu,0) d\nu + \sum_{\ell=1}^{m_{j+1}} \int_0^{\tau_j} (g_j^2)_{k\ell}(\nu) v_{j+1}^\ell(t-\nu,0) d\nu, \end{aligned} \tag{8.29}$$

where g_i^1 and g_i^2 are piecewise continuous functions. We do not give their explicit expression for the sake of concision. We recall that by convention $v_{N+1}(t,0) \equiv 0$. Consider now equation (8.22). We can substitute the terms $u_i(t,\cdot)$ and $v_i(t,\cdot)$ that appear in the right-hand side of this equation by their expressions as functions of $\alpha_i(t,\cdot)$, $\beta_i(t,\cdot)$ and $v_{i+1}(t,0)$ using the inverse transformations (8.15)-(8.16). Then, applying the method of characteristics (see [ADM19, ABANR21]), we obtain for $j > i$,

$$\begin{aligned} \alpha_j^k(t,0) = &\sum_{\ell=1}^{m_j} (Q_{j,j})_{k\ell} v_j^\ell(t,0) + \sum_{\ell=1}^{n_{j-1}} (Q_{j,j-1})_{k\ell} \alpha_{j-1}^\ell(t,1) + \sum_{\ell=1}^{n_j} \int_0^{\tau_j} (h_i^2)_{k\ell}(\nu) \alpha_j^\ell(t-\nu,0) d\nu \\ &+ \sum_{\ell=1}^{m_{j+1}} \int_0^{\tau_j} (h_j^2)_{k\ell}(\nu) v_{j+1}^\ell(t-\nu,0) d\nu + \sum_{\ell=1}^{m_j} \int_0^{\tau_{j-1}} (h_j^3)_{k\ell}(\nu) v_j^\ell(t-\nu,0) d\nu, \end{aligned} \tag{8.30}$$

where h_j^1, h_j^2, and h_j^3 are piecewise continuous functions. We do not give their explicit expression for the sake of concision. If $j = i$, the term $\sum_{\ell=1}^{n_{i-1}} (Q_{i,i-1})_{k\ell} \alpha_{i-1}^\ell(t,1)$ is replaced by $\sum_{\ell=1}^{n_{j-1}} (Q_{i,i-1})_{k\ell} (\hat{U}_i(t - \sum_{r=1}^{i-1} \frac{1}{\lambda_r^1}))_\ell$. Inspired by [BL14, BPDM16, ABABP20, ABP22], we respectively define for $t \ge \max_r \tau_r + \sum_{r=1}^{i-1} \frac{1}{\lambda_r^1}$, $k \in \{1,\dots,n_j\}$, $\ell \in \{1,\dots,m_j\}$ and $s \in [t - \max_r \tau_r - \sum_{r=1}^{i-1} \frac{1}{\lambda_r^1}, t]$, the functions $P_{\alpha_j^0}^k(t,s)$, $P_{\alpha_j^1}^k(t,s)$, and $P_{v_j^0}^\ell(t,s)$ as the respective **state predictions** of $\alpha_j^k(t,0)$, $\alpha_j^k(t,1)$, and $v_\ell^k(t,0)$ ahead a time $\sum_{r=1}^{i-1} \frac{1}{\lambda_r^1}$. They are *explicitly* defined by the following set of equations.

$$P_{\alpha_j^0}^k(t,s) = \begin{cases} \alpha_j^k(s + \sum_{r=1}^{i-1} \frac{1}{\lambda_r^1}, 0) \quad \text{if } s \in [t - \max_r \tau_r - \sum_{r=1}^{i-1} \frac{1}{\lambda_r^1}, t - \sum_{r=1}^{i-1} \frac{1}{\lambda_r^1}] \\ \sum_{q=1}^{m_j} (Q_{j,j})_{kq} P_{v_j^0}^q(t,s) + \sum_{q=1}^{n_{j-1}} (Q_{j,j-1})_{kq} P_{\alpha_{j-1}^1}^q(t,s) + \sum_{q=1}^{n_j} \int_0^{\tau_j} (h_i^1)_{kq}(\nu) P_{\alpha_j^0}^q(t,s-\nu) d\nu \\ + \sum_{q=1}^{m_{j+1}} \int_0^{\tau_j} (h_j^2)_{kq}(\nu) P_{v_{j+1}^0}^q(t,s-\nu) d\nu + \sum_{q=1}^{m_j} \int_0^{\tau_{j-1}} (h_j^3)_{kq}(\nu) P_{v_j^0}^q(t,s-\nu) d\nu, \quad \text{otherwise,} \end{cases} \tag{8.31}$$

$$P_{\alpha_j^1}^k(t,s) = \begin{cases} \alpha_j^k(s + \sum_{r=1}^{i-1} \frac{1}{\lambda_r^1}, 1) \quad \text{if } s \in [t - \max_r \tau_r - \sum_{r=1}^{i-1} \frac{1}{\lambda_r^1}, t - \sum_{r=1}^{i-1} \frac{1}{\lambda_r^1}] \\ P_{\alpha_j^0}^k(t, s - \frac{1}{\lambda_j^k}) + \sum_{q=k+1}^{n_j} \int_0^{\frac{1}{\lambda_j^k}} (\tilde{G}_j(1 - \lambda_j^k \nu))_{kq} P_{\alpha_j^0}^q(t, s-\nu) d\nu, \quad \text{otherwise,} \end{cases} \tag{8.32}$$

$$P_{v_j^0}^\ell(t,s) = \begin{cases} v_j^\ell(s + \sum_{r=1}^{i-1} \frac{1}{\lambda_r^1}, 0) \quad \text{if } s \in [t - \max_r \tau_r - \sum_{r=1}^{i-1} \frac{1}{\lambda_r^1}, t - \sum_{r=1}^{i-1} \frac{1}{\lambda_r^1}] \\ \sum_{q=1}^{n_j} (R_{j,j})_{\ell q} P_{\alpha_j^1}^q(t, s - \frac{1}{\mu_j^\ell}) + \sum_{q=1}^{m_{j+1}} (R_{j,j+1})_{\ell q} P_{v_{j+1}^0}^q(t, s - \frac{1}{\mu_j^\ell}) + \sum_{q=1}^{n_j} \int_0^{\tau_j} (g_j^1)_{\ell q}(\nu) \\ P_{\alpha_j^1}^q(t, s-\nu) d\nu + \sum_{q=1}^{m_{j+1}} \int_0^{\tau_j} (g_j^2)_{\ell q}(\nu) P_{v_{j+1}^0}^q(t, s-\nu) d\nu, \quad \text{otherwise,} \end{cases} \tag{8.33}$$

with the convention $\sum_{\ell=1}^{n_{i-1}}(Q_{i,i-1})_{kq}P^q_{\alpha^1_{i-1}}(t,s)=\hat{U}_i^q(s)$. Though the definitions (8.31)-(8.33) are implicit, through integral relations of Volterra type, the predictors are well-defined and unique. We write the predictors as functions of two arguments to emphasize that the prediction should be computed by incorporating measured delayed states available at time t to improve its robustness in practice. From these definitions, we immediately have

$$P^k_{\alpha^0_j}(t,s)=\alpha^k_j(s+\sum_{r=1}^{i-1}\frac{1}{\lambda^1_r},0),\ s\in[t-\max_r\tau_r-\sum_{r=1}^{i-1}\frac{1}{\lambda^1_r},t],$$
$$P^k_{\alpha^1_j}(t,s)=\alpha^k_j(s+\sum_{r=1}^{i-1}\frac{1}{\lambda^1_r},1),\ s\in[t-\max_r\tau_r-\sum_{r=1}^{i-1}\frac{1}{\lambda^1_r},t],$$
$$P^\ell_{v^0_j}(t,s)=v^\ell_j(s+\sum_{r=1}^{i-1}\frac{1}{\lambda^1_r},0),\ s\in[t-\max_r\tau_r-\sum_{r=1}^{i-1}\frac{1}{\lambda^1_r},t].$$

From the predictors (8.31)-(8.33), it is possible to apply the method of characteristics on the PDEs (8.17)-(8.18), to obtain the corresponding state predictions for the states $\alpha_j(t,x)$ and $\beta_j(t,x)$. Finally, using the transformations (8.15)-(8.16), we obtain the predictions of the state $u_j(t,x)$ and $v_j(t,x)$. ■

Note that the definitions of the predictors implicitly depend on the initial subsystem i we consider. Indeed, the different time horizons depend on the parameter i. We chose to omit this dependency as we believe the notations are sufficiently heavy.

8.2.5 . Recursive state-feedback stabilization

We now have all the tools to apply the proposed recursive dynamics interconnection framework

Theorem 8.2.1 *For $i\in\{1,\dots,N\}$, and for $t>\sum_{j=1}^N 2\tau_j$, define the sequences of functions ζ_i*

$$\zeta_N(t)=0, \tag{8.34}$$
$$\zeta_i(t)=Q^T_{i+1,i}(Q^T_{i+1,i}Q^T_{i+1,i})^{-1}\hat{U}_{i+1}(t-\sum_{j=1}^{i}\frac{1}{\lambda^1_j}),\ \textit{if } i<N, \tag{8.35}$$

where the functions $\hat{U}_i$ are given by equations (8.23)-(8.26)*, where the different predictors can be defined as in Property 8.2.3 (using the function $\hat{U}_i$ and equations* (8.31)-(8.33)*). Then, the interconnected system* (8.1)-(8.4) *with the control law $U(t)=\hat{U}_1(t)$ is exponentially stable in the sense of the χ-norm. Moreover, the equilibrium is reached in finite time.*

Proof : First observe that the matrices $Q^T_{i+1,i}(Q^T_{i+1,i}Q^T_{i+1,i})^{-1}$ are well defined due to Assumption 8.1.1. Moreover, observe that the quantity $\zeta_i(t+\sum_{j=1}^i\frac{1}{\lambda^j_i})$ that appears in the proof of Property 8.2.1 can be explicitly computed from $\hat{U}_{i+1}(t)$. Then, the sequences ζ_i and $\hat{U}_i$ are well defined (since equations (8.31)-(8.33) are always well defined). Consequently, the control input $U(t)$ is well-defined and causal.

Next, we briefly show that the closed-loop system (8.1)-(8.4) with the control input $U(t)$ is well-posed. This can be done either by considering the admissibility of the control operator [CHO16] (the control law is continuous in time), or by adjusting the proof of Theorem [BC16, Theorem A.1] (that is based on Lumer-Philipps theorem). Indeed, the different components of the proposed control input $U(t)$ (including the predictors) can be expressed as delayed values of the boundary states of the system (as $v_i(t,0)$) or delayed values of themselves. Such delayed values, could then be expressed using PDEs (after tedious computations).

We now need to prove that the proposed control law stabilizes the system. To ease the computations, the parameter T (that will be overloaded in the rest of the proof) denotes a finite time large enough to guarantee that the different predictors and tracking controllers are well-defined. Note that for a subsystem i, the "predictors" defined in the proof of Property 8.2.3 correspond to exact predictions of the different states only if the subsystem is subject to the virtual input $\hat{U}_i(t)$, i.e., only if $Q_{i,i+1}\alpha_{i-1}(t+\sum_{j=1}^{i-1}\frac{1}{\lambda^1_j},1)=\hat{U}_i(t)$.

Consider the first subsystem ($i=1$) with the control law $U(t)=\hat{U}_1(t)$. For $i=1$, equation (8.23) and equation (8.26) do not require any state predictions but can be computed using current values of the different functions. Then, using Property 8.2.1, we have that $\alpha_1(t,1)=\zeta_1(t)$ for $t>T$. Consequently, $Q_{2,1}\alpha_1(t,1)=\hat{U}_2(t-\frac{1}{\lambda^1_1})$. Therefore the functions defined through equations (8.31)-(8.33) corresponds to exact $\frac{1}{\lambda^1_1}$-ahead of time predictions of the real states. Thus, Property 8.2.1 implies that $\alpha_2(t,1)=\zeta_2(t)$ after a finite time T. Iterating the procedure, we obtain that after a finite time T, for all $i\in\{1,\dots,N\}$, $\alpha_i(t,1)=\zeta_i$ Consider now the last subsystem ($i=N$). Since $\alpha_N(t,1)=\zeta_N=0$, the functions $\alpha_N(t,x)$

and $\beta_N(t,x)$ converge to zero in finite time. Applying Property 8.2.2, we obtain the convergence to zero of the functions $\alpha_{N-1}(t,x)$ and $\beta_{N-1}(t,x)$ in finite time. Iterating the procedure, all the states (α_i,β_i) converge to zero in finite time. Using the inverse backstepping transformations (8.15)-(8.16), we obtain that the system (8.1)-(8.4) reaches its equilibrium in finite-time. The well-posedness of the closed-loop system implies its exponential stability. ■

One major advantage of the proposed framework and the recursive design proposed in Theorem 8.2.1 is that it can easily be extended to different classes of subsystems (as ODEs, for instance), as long as it is possible to derive analogous properties to Property 8.2.1, Property 8.2.2 and Property 8.2.3. One must be aware that Theorem 8.2.1 completely neglects the robustness aspects of the system. More precisely, the proposed control strategy consists of recursively canceling all the boundary reflection terms for each subsystem to track the virtual input of the downstream subsystem. This may lead to zero robustness margins, as shown in [ABABS+18]. The robustification procedure we proposed in Chapter 6 cannot be directly applied, as, due to the tracking part, our control law does not fit in the framework of Theorem 6.2.1. However, we believe that it should be possible to rewrite the proposed control law in a framework more suitable for the application of Theorem 6.2.1.

Remark 8.2.1 *The state-feedback controller designed in Theorem 8.2.1 can be easily extended to the case of delayed control input. Indeed, similarly to what has been done in the case of delayed ODEs [KS08], one needs to consider an additional upstream subsystem corresponding to a pure transport equation, thus inducing a delay that corresponds to the input delay.*

8.3 . State estimation and output-feedback stabilization

To design the recursive stabilizing controller we presented in Section 8.2, we need the knowledge of the states $u_i(t,x)$ and $v_i(t,x)$ all over the spatial domain $[0,1]$. Since the available measurement corresponds to $u_N(t,1)$, we must design a state observer. In this section, we show how to easily obtain estimated **delayed** values of these states. Adjusting the predictors introduced in Section 8.2.4, it is then possible to reconstruct the desired states.

8.3.1 . Delayed interconnection

Inspired by [KK17], we consider a delayed version of the interconnected system (8.1)-(8.4). Let us consider $\tau > \sum_{j=1}^{N} \frac{1}{\lambda_j^1} > 0$ a fixed, known delay. We define the *τ-delay operator* $\bar{\cdot}$, such that for all functions γ defined on $[0,+\infty)$, $\forall t > \tau, \bar{\gamma}(t) = \gamma(t-\tau)$. Using this operator, we can obtain the τ-delayed version of system (8.1)-(8.4). For all $t \geq \tau$, we have:

$$\partial_t \overline{u}_i(t,x) + \Lambda_i^+ \partial_x \overline{u}_i(t,x) = \Sigma_i^{++}(x)\overline{u}_i(t,x) + \Sigma_i^{+-}(x)\overline{v}_i(t,x), \tag{8.36}$$
$$\partial_t \overline{v}_i(t,x) - \Lambda_i^- \partial_x \overline{v}_i(t,x) = \Sigma_i^{-+}(x)\overline{u}_i(t,x) + \Sigma_i^{--}(x)\overline{v}_i(t,x), \tag{8.37}$$

with the boundary conditions:

$$\overline{u}_i(t,0) = Q_{i,i}\overline{v}_i(t,0) + Q_{i,i-1}\overline{u}_{i-1}(t,1), \tag{8.38}$$
$$\overline{v}_i(t,1) = R_{i,i}\overline{u}_i(t,1) + R_{i,i+1}\overline{v}_{i+1}(t,0), \tag{8.39}$$

where we still use the convention that $Q_{1,0}\bar{u}_0(t,0) = U(t-\tau)$ and $R_{N,N+1} = 0$. The available measurement is now given as $\bar{y}(t) = y(t-\tau)$. It implies that we know τ-ahead future values of the function $\bar{y}$(t). Using the backstepping transformations (8.6)-(8.7), we can define the states $\bar{\alpha}_i(t,x)$ and $\bar{\beta}_i(t,x)$. They are solutions of (8.17)-(8.20) with a τ-delayed control input.

8.3.2 . Estimation of the delayed states

This section shows how to estimate the delayed state $\bar{u}_i(t,x)$ and $\bar{v}_i(t,x)$ from the available measurements. We first show how to estimate the boundary functions $\bar{\alpha}_i(t,1)$ and $\bar{v}_i(t,0)$. These estimations will then be used to reconstruct the states $\bar{u}_i$ and $\bar{v}_i$. More precisely, we have the following property.

Lemma 8.3.1 *For all $i \in \{1,\dots,N\}$, we can design exact state estimators $\hat{\alpha}_i(\cdot,1)$ and $\hat{v}_{i+1}(\cdot,0)$ that causally depend on the measurement $y(t)$ such that for all $\nu \in [t, t+\sum_{j=1}^{i} \frac{1}{\lambda_j^1}]$, $\hat{\alpha}_i(t+\nu,1) = \bar{\alpha}_i(t+\nu,1)$ and $\hat{v}_{i+1}(t+\nu,0) = \bar{v}_{i+1}(t+\nu,0)$.*

Proof : The proof relies on an induction argument. Lemma 8.3.1 obviously holds for $i = N$ with $\hat{\alpha}_N(t,1) = \bar{y}(t)$ and $\hat{v}_{N+1}(t,0) = 0$. Let us now consider the i^{th} subsystem $i \in \{2,\dots,N\}$, $t > 0$ and assume that we can design exact state estimations $\hat{\alpha}_i(\nu,1)$ and $\hat{v}_{i+1}(\nu,0)$ that causally depend on the measurement $y(t)$ such that for all $\nu \in [t, t+\sum_{j=1}^{i} \frac{1}{\lambda_j^1}]$, $\hat{\alpha}_i(t+\nu,1) = \bar{\alpha}_i(t+\nu,1)$ and $\hat{v}_{i+1}(t+\nu,0) = \bar{v}_{i+1}(t+\nu,0)$. From equation (8.25), we can define the intermediate estimator $\hat{\alpha}_i(t,0)$ such that for all $1 \leq k \leq n_i$ and all $t > 0$

$$\hat{\alpha}_i^k(t,0) = \hat{\alpha}_i^k(t+\frac{1}{\lambda_i^k},1) - \sum_{\ell=k+1}^{n_i} \int_0^{\frac{1}{\lambda_i^k}} (\check{G}_i(\nu))_{k\ell} \hat{\alpha}_i^\ell(t+\nu,1) d\nu. \tag{8.40}$$

We immediately obtain that for all $\nu \in [t, t+\sum_{j=1}^{i-1} \frac{1}{\lambda_j^1}]$, $\hat{\alpha}_i(t+\nu,0) = \bar{\alpha}_i(t+\nu,0)$. We now define the function $\hat{v}_i(t,0)$, such that for all $1 \leq k \leq m_i$

$$\begin{aligned}\hat{v}_i^k(t,0) =& \sum_{\ell=1}^{n_i} (R_{i,i})_{k\ell} \hat{\alpha}_j^\ell(t-\frac{1}{\mu_i^k},1) + \sum_{\ell=1}^{m_{i+1}} (R_{i,i+1})_{k\ell} \hat{v}_{i+1}^\ell(t-\frac{1}{\mu_i^k},0) \\ &+ \sum_{\ell=1}^{n_i} \int_0^{\tau_i} (g_i^1)_{k\ell}(\nu) \hat{\alpha}_i^\ell(t-\nu,0) d\nu + \sum_{\ell=1}^{m_{i+1}} \int_0^{\tau_i} (g_i^2)_{k\ell}(\nu) \hat{v}_{i+1}^\ell(t-\nu,0) d\nu. \end{aligned} \tag{8.41}$$

We have that for all $\nu \in [t, t+\sum_{j=1}^{i-1} \frac{1}{\lambda_j^1}]$, $\hat{v}_i(t+\nu,0) = \bar{v}_i(t+\nu,0)$ due to equation (8.29). Finally, combining Assumption 8.1.2 and equation (8.30), we can obtain the desired estimations of $\bar{\alpha}_{i-1}(t,1)$. The different estimators are causal as they only require past values of the function y. This concludes the proof. ■

From Lemma 8.3.1, we obtain the following property

Property 8.3.1 *For all $i \in \{1,\dots,N\}$, we can design exact state estimators $\hat{u}(t,x)$ and $\hat{v}(t,x)$ that causally depend on the measurement $y(t)$ such that for all $t > 0$, and all $x \in [0,1]$, $\hat{u}(t,x) = \bar{u}(t,x)$ and $\hat{v}(t,x) = \bar{v}(t,x)$.*

Proof : Combining the state estimations given in Lemma 8.3.1 with the method of characteristics, it is possible to estimate the state $\bar{\alpha}_i$ and $\bar{\beta}_i$. Then, we can compute the estimators $\hat{u}(t,x)$ and $\hat{v}(t,x)$ using the inverse transformations (8.15)-(8.16). We do not give the explicit expression of these state estimators for the sake of concision. ■

8.3.3 . Stabilizing output-feedback controller

We have designed in Property 8.3.1 a state-observer that provides a real-time exact estimation of the delayed states $(\bar{u}_i, \bar{v}_i)$. This state-observer can be combined with the state-feedback controller designed in Theorem 8.2.1 to obtain an output-feedback stabilizing controller. Indeed, combining Remark 8.2.1 and Theorem 8.2.1, we can design a state-feedback controller for the delayed system (8.36)-(8.39). This state feedback controller requires the knowledge of the delayed states $(\bar{u}_i, \bar{v}_i)$, provided by Property 8.3.1. Therefore, we can obtain a stabilizing output-feedback controller for the delayed system (8.36)-(8.39). The exponential stability of the delayed system (8.36)-(8.39) implies the exponential stability of the original system (8.1)-(8.4).

8.4 . Simulation results

We now test the proposed output-feedback controller in simulations. The different predictors are implemented using a backward Euler approximation of the different integral terms. The numerical values we used are given below.

$$\Lambda_1^+ = 1,\ \Lambda_2^+ = 2,\ \Lambda_1^- = \begin{pmatrix} 1.3 & 0 \\ 0 & 1.6 \end{pmatrix},\ \Lambda_2^- = \begin{pmatrix} 0.8 & 0 \\ 0 & 1.4 \end{pmatrix},\ \Sigma_1^{++} = \Sigma_2^{++} = 0,$$

$$\Sigma_1^{+-} = \Sigma_2^{+-} = \begin{pmatrix} 0.45 & 0.23 \end{pmatrix},\ \Sigma_1^{-+} = \begin{pmatrix} 0 & 0.45 \end{pmatrix},\ \Sigma_1^{--} = \begin{pmatrix} 0 & -0.1 \\ 0.2 & 0 \end{pmatrix},$$

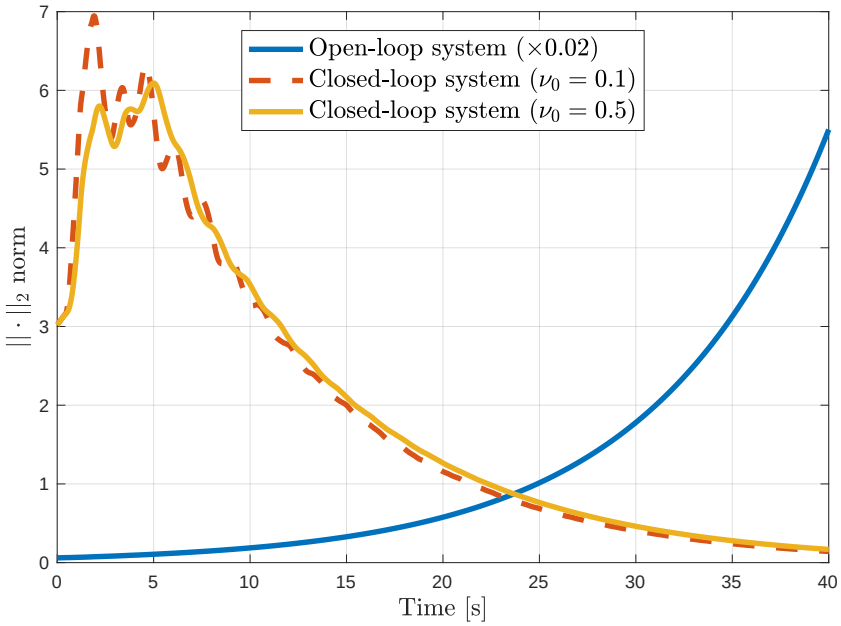

Figure 8.2: Evolution of the $||\cdot||_\chi$-norm of the open-loop system and of the closed-loop system (for two different filters) with an input delay of $0.2s$. The filters have been designed with $\nu_0 = 0.1$ and $\nu_0 = 0.5$. The norm of the open-loop system has been divided by 50 for readability reasons.

$$\Sigma_2^{-+} = \begin{pmatrix} -0.2 & 0.2 \end{pmatrix}, \ \Sigma_2^{--} = \begin{pmatrix} 0 & 0 \\ 0.45 & 0 \end{pmatrix}, \ Q_{12} = 0.3, \ Q_{11} = \begin{pmatrix} 0.3 & 0.6 \end{pmatrix},$$
$$R_{22} = \begin{pmatrix} 0.8 & 0.6 \end{pmatrix}, \ Q_{21} = \begin{pmatrix} 0.4 & 0.24 \\ 0 & 0.4 \end{pmatrix}, \ Q_{22} = \begin{pmatrix} 0.6 \\ 0.6 \end{pmatrix}, \ R_{12} = \begin{pmatrix} 0.4. \\ 0.3 \end{pmatrix}$$

These coefficients are chosen such that the two PDEs subsystems are independently unstable in open-loop and such that the resulting interconnected system remains unstable. Assumption 8.1.1 and Assumption 8.1.2 are obviously satisfied, while we can check numerically that Assumption 6.1.1 is also verified. In the simulations, we low-pass filtered the control law. We chose a low-pass filter $w(s) = \frac{1}{1+\nu_0 s}$, with $\nu_0 = 0.1$ or $\nu_0 = 0.5$. We have pictured in Figure 8.2 the evolution of the χ-norm of the open-loop system and of the closed-loop system with the filtered control law in the presence of a delay of 0.2 seconds. As it can be seen, the system exponentially converges to zero. The corresponding control effort has been plotted in Figure 8.3.

8.5 . Conclusion and perspectives

In this chapter, we have introduced a **recursive methodology** to design a stabilizing output-feedback controller for a network of N PDE subsystems with a chain structure. The different subsystems are interconnected through their boundaries, and the control input is located at one extremity of the chain. The proposed framework required several fundamental properties for each subsystem: output trajectory tracking, input-to-state stability, predictability (we can design predictors of the different states), and observability. We have shown that these properties were always satisfied for hyperbolic subsystems. The proposed approach is modular in that additional subsystems can easily be included. Moreover, we believe the proposed framework can be extended to different types of subsystems (such as ODEs and parabolic equations) as it has been done in [RAN21b] with an ODE at the end of the chain, provided similar properties can still be verified. Recent results have been developed in [XLKF23] for parabolic systems using an analogous recursive approach. One current limitation of the proposed approach is its high complexity and computational burden. We need to compute state predictions for each subsystem composing the interconnection, which may be time-consuming. This **numerical burden** may explode with the number of subsystems, thus making any implementation impossible. To

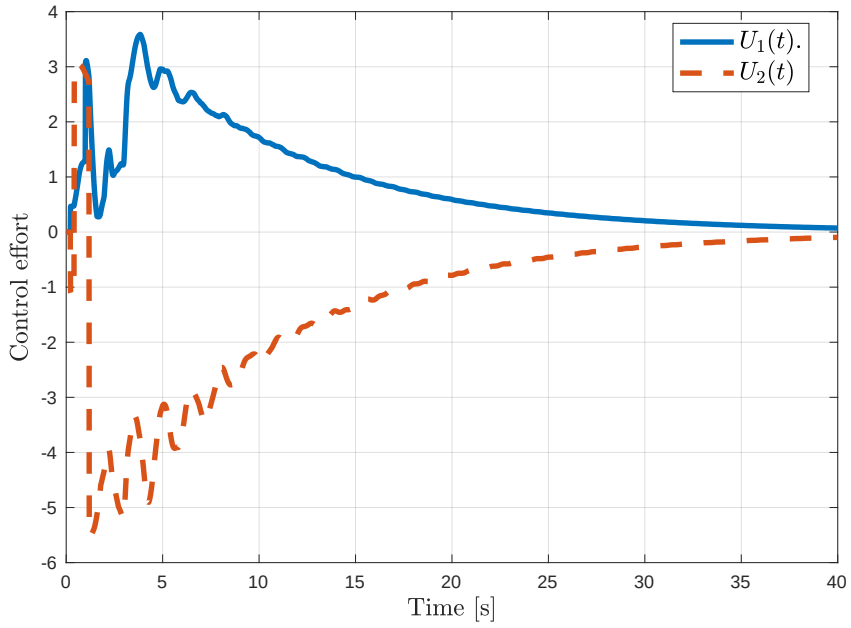

Figure 8.3: Evolution of the control effort $U_1(t)$ and $U_2(t)$ ($\nu_0 = 0.1$).

leverage the numerical effort induced by these controllers, it may be necessary to approximate them (e.g., by finite-dimensional systems). This emphasizes the necessity of investigating the questions of model reduction using late-lumping techniques [ERW17, AMDM19]. Recently, **machine-learning approximations** (based on the DeepONet algorithm) have been successfully tested in [SLY+22] on simple examples, but there is no general proof of convergence yet. Concerning implementing the proposed recursive control law, we underline that the robustness aspects have been neglected in this chapter. However, we believe Theorem 6.2.1 can be adjusted to cover the proposed control strategy.

9 - Output-feedback stabilization at the junction of two scalar interconnected systems

In Chapter 8, we have developed a recursive dynamics interconnection framework to stabilize interconnections of PDE systems with a chain structure. This approach presents the advantage of being generic and comfortable to implement as it only requires simple fundamental properties of each subsystem. However, one primary requirement is that actuators/sensors are all located at one extremity of the chain. There are several situations in which the actuator may be located at an arbitrary node of the chain. For instance, when developing traffic control strategies on vast road networks, the actuator (ramp metering) can be located at a crossroad (junction of two roads). This situation has been considered in [YK19] in a simple configuration (in particular, some boundary coupling terms were equal to zero). Having an actuator located at one of the intersection nodes of the chain raises challenging controllability questions. As we will see, such interconnected systems may not be controllable, and appropriate controllability conditions must be derived. Solving such a problem is necessary for stabilizing complex networks and underactuated systems.

The control strategy we present in this chapter is as follows: using backstepping transformation, and as suggested in Chapter 6, we rewrite the original hyperbolic network as a set of simpler Integral Delay Equations (IDEs) with pointwise and distributed control terms. Then, we can introduce a set of candidate control inputs expressed as distributed delayed feedback of the state and the input. A control law from this set will stabilize the system if an associated **Fredholm equation** admits a solution. Similar techniques will be used to design the associated state observers.

Unlike Volterra integral equations, Fredholm equations do not necessarily admit a solution [Yos60]. Consider the Fredholm integral operator $\mathcal{T} : L^2([a,b],\mathbb{R}^n) \to L^2([a,b],\mathbb{R}^n)$ defined by

$$\mathcal{T}\left(z(\cdot)\right) = Mz(\cdot) - \int_a^b K(\cdot,y)z(y)dy, \tag{9.1}$$

where $a < b$ are real, $n > 0$ is an integer, M is an invertible matrix that belongs to $\mathbb{R}^{n\times n}$, K is bounded piecewise continuous on the square $\{(x,y) \in [a,b]^2\}$. Note that the integral part of the operator has a regularizing effect, such that $\forall z \in L^2([a,b],\mathbb{R})^n$, $\int_a^b K(x,y)z(y) \in H^1([a,b],\mathbb{R}^n)$. The following lemma gives conditions under which the operator $\mathcal{T}$ is invertible.

Lemma 9.0.1 *Consider two linear operators $\mathcal{A},\mathcal{B}$, such that $D(\mathcal{A}) = D(\mathcal{B}) \subset L^2([a,b],\mathbb{R}^n)$. Consider the Fredholm integral operator $\mathcal{T} : L^2([a,b],\mathbb{R}^n) \to L^2([a,b],\mathbb{R}^n)$ as defined by equation* (9.1)*. Assume that*

(a) $\ker(\mathcal{T}) \subset D(\mathcal{A})$,

(b) $\ker(\mathcal{T}) \subset \ker(\mathcal{B})$,

(c) $\forall z \in \ker(\mathcal{T}),\ \mathcal{T}\mathcal{A}z = 0$,

(d) $\forall s \in \mathbb{C},\ \ker(sId - \mathcal{A}) \cap \ker(\mathcal{B}) = \{0\}$.

Then, the operator $\mathcal{T}$ is invertible.

Proof : The proof is analogous to the one in [CHO16, Lemma 2.2, Proposition 2.6]. Since the integral part of $\mathcal{T}$ is a compact operator, the Fredholm alternative [Bre10] implies that $\dim\ker(\mathcal{T}) < \infty$. Suppose that $\ker(\mathcal{T}) \neq \{0\}$. Due to condition (a), for all $z \in \ker(\mathcal{T})$ $\mathcal{A}z$ is well-defined, and condition (c) implies that $\ker(\mathcal{T})$ is stable by $\mathcal{A}$, that is to say, for all $z \in \ker(\mathcal{T})$, $\mathcal{A}z \in \ker(\mathcal{T})$. Since $\ker(\mathcal{T})$ is finite-dimensional and

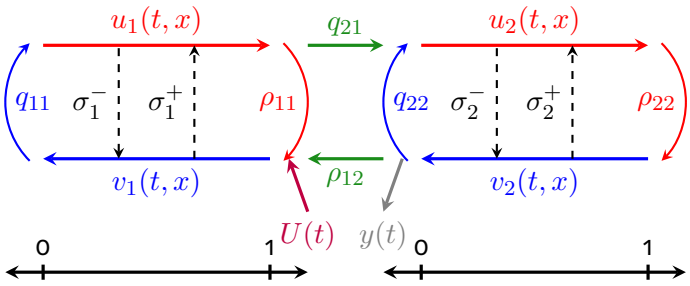

Figure 9.1: Schematic representation of the system (9.2)-(9.4).

not reduced to $\{0\}$, the restriction $\mathcal{A}_{|\ker(\mathcal{T})}$ of $\mathcal{A}$ to $\ker(\mathcal{T})$ has at least one eigenvalue $\nu \in \mathbb{C}$. Let ζ be the corresponding eigenfunction. Thus, $\zeta \in \ker(\nu - \mathcal{A})$ and $\zeta \in \ker(\mathcal{B})$ by condition (b). This is in contradiction with condition (d). Thus, $\ker(\mathcal{T}) = \{0\}$ and $\mathcal{T}$ is injective. Using the Fredholm alternative [Bre10], we obtain that $\mathcal{T}$ is invertible. ■

As it will appear through the rest of the chapter, condition (d) of Lemma 9.0.1 relates to a controllability/observability condition. The results of this chapter are inspired by [ABABP20, RAN22c, RAN21c, RAN21a, RA23] but introduce a more elegant methodology directly based on IDEs.

9.1 . Problem under consideration

In this chapter, we consider the case of a simple interconnection of two scalar hyperbolic systems. Contrary to what we have done so far, the actuator and sensor are located at the junction. More precisely, each subsystem $i \in \{1, 2\}$ is modeled by

$$\partial_t u_i(t,x) + \lambda_i \partial_x u_i(t,x) = \sigma_i^+(x) v_i(t,x), \tag{9.2}$$
$$\partial_t v_i(t,x) - \mu_i \partial_x v_i(t,x) = \sigma_i^-(x) u_i(t,x), \tag{9.3}$$

with $t > 0$, $x \in [0,1]$ and where σ_i^+, σ_i^- are two continuous in-domain coupling functions. The velocities λ_i and μ_i are constant and positive. The two subsystems are interconnected through their boundaries

$$u_1(t,0) = q_{11} v_1(t,0), \quad v_2(t,1) = \rho_{22} u_2(t,1), \tag{9.4}$$
$$v_1(t,1) = U(t) + \rho_{11} u_1(t,1) + \rho_{12} v_2(t,0), \tag{9.5}$$
$$u_2(t,0) = q_{22} v_2(t,0) + q_{21} u_1(t,1). \tag{9.6}$$

The different couplings terms q_{ij} and ρ_{ij} are assumed to be constant. The actuation $U(t)$ is located at the right boundary of the first subsystem. We assume that we measure the state at the opposite boundary of the unactuated subsystem: $y(t) = v_2(t,0)$. This system is pictured in Figure 9.1 and fits in the formalism given in Chapter 6. This can be seen by performing the change of variable "$x = 1 - x$". We denote $(u_0)_i(\cdot) = u_i(0,\cdot) \in H^1([0,1],\mathbb{R}), (v_0)_i(\cdot) = v_i(0,\cdot) \in H^1([0,1],\mathbb{R})$ the initial conditions of the system. As stated in Theorem 5.2.1, they satisfy the compatibility conditions so that the open-loop system is well-posed. We define τ_1 and τ_2 as the total transport times associated with each equation:

$$\tau_1 = \frac{1}{\lambda_1} + \frac{1}{\mu_1}, \quad \tau_2 = \frac{1}{\lambda_2} + \frac{1}{\mu_2}. \tag{9.7}$$

Since the actuator is located at the junction, the recursive methodology detailed in Chapter 8 cannot be applied. More precisely, the re-circulation induced by the couplings between the two subsystems may create some unstable loops that prevent stabilization. As it appears in the analysis, the design of stabilizing controllers will require specific controllability and observability assumptions.

9.1.1 . Operator formulation

To derive controllability and observability conditions and to design the associated controllers and observers, we need first to rewrite the system (9.2)-(9.4) in the abstract form

$$\frac{d}{dt}\begin{pmatrix} u_1 \\ v_1 \\ u_2 \\ v_2 \end{pmatrix} = A\begin{pmatrix} u_1 \\ v_1 \\ u_2 \\ v_2 \end{pmatrix} + BU, \tag{9.8}$$

where we can identify the operators A and B through their adjoints by taking formally the canonical scalar product of (9.8) with smooth test functions and comparing with the weak formulation [CHO16]. The operator A is thus defined by

$$\begin{aligned} A : D(A) \subset L^2([0,1],\mathbb{R}^4) &\to L^2([0,1],\mathbb{R}^4) \\ \begin{pmatrix} u_1 \\ v_1 \\ u_2 \\ v_2 \end{pmatrix} &\longmapsto \begin{pmatrix} -\lambda_1\partial_x u_1 + \sigma_1^+(\cdot)v_1 \\ \mu_1\partial_x v_1 + \sigma_1^-(\cdot)u_1 \\ -\lambda_2\partial_x u_2 + \sigma_2^-(\cdot)v_2 \\ \mu_2\partial_x v_2 + \sigma_2^-(\cdot)u_2 \end{pmatrix}, \end{aligned} \tag{9.9}$$

with $D(A) = \{(u_1,v_1,u_2,v_2) \in H^1([0,1],\mathbb{R}^4)|\ u_1(0) = q_{11}v_1(0),\ v_2(1) = \rho_{22}u_2(1),\ v_1(1) = \rho_{11}u_1(1) + \rho_{12}u_2(1),\ u_2(0) = q_{22}v_2(0) + q_{21}u_1(1)\}$. The operator A introduced by equation (9.9) is densely defined and closed [BC16]. Its adjoint $A^\star$ is given by

$$\begin{aligned} A^\star : D(A^\star) \subset L^2([0,1],\mathbb{R}^4) &\to L^2([0,1],\mathbb{R}^4) \\ \begin{pmatrix} u \\ v \end{pmatrix} &\longmapsto \begin{pmatrix} \lambda_1\partial_x u_1 + \sigma_1^-(\cdot)v_1 \\ -\mu_1\partial_x v_1 + \sigma_1^+(\cdot)u_1 \\ \lambda_2\partial_x u_2 + \sigma_2^-(\cdot)v_2 \\ -\mu_2\partial_x v_2 + \sigma_2^+(\cdot)u_1 \end{pmatrix}, \end{aligned} \tag{9.10}$$

with $D(A^\star) = \{(u_1,v_1,u_2,v_2) \in H^1([0,1],\mathbb{R}^4)|\ u_1(1) = \frac{\rho_{11}\mu_1}{\lambda_1}v_1(1) + \frac{q_{21}\lambda_2}{\lambda_1}u_2(0),\ u_2(1) = \frac{\rho_{22}\mu_2}{\lambda_2}v_2(1),\ v_1(0) = \frac{q_{11}\lambda_1}{\mu_1}u_1(0),\ v_2(0) = \frac{q_{22}\lambda_2}{\mu_2}u_2(0) + \frac{\rho_{12}\mu_1}{\mu_2}v_1(1)\}$. We recall that both A and $A^\star$ are quasi-dissipative [BC16] and generate C_0-semigroups. The operator $B \in \mathcal{L}(\mathbb{R}, D(A^\star)')$ is defined through its adjoint $B^\star \in \mathcal{L}(D(A^\star),\mathbb{R})$

$$B^\star(\begin{pmatrix} u_1 & v_1 & u_2 & v_2 \end{pmatrix}^\top) = \mu_1 v_1(1). \tag{9.11}$$

As mentioned in Chapter 6, one can prove that B is admissible [CHO16]. Finally, the measurement operator $C \in \mathcal{L}(D(A),\mathbb{R})$ is defined by

$$C(\begin{pmatrix} u_1 & v_1 & u_2 & v_2 \end{pmatrix}^\top) = u_2(0). \tag{9.12}$$

9.1.2 . Structural assumptions

We first consider that Assumption 6.1.1 is verified to avoid having an infinite number of unstable roots in the right-half plane. Simple computations show that when the delays are rationally independent, this assumption rewrite

$$\sup_{(\theta_1,\theta_2)\in[0,2\pi]^2} \mathrm{Sp}\left(\begin{pmatrix} \rho_{11}q_{11}\mathrm{e}^{i\theta_1} & \rho_{12}q_{11}\mathrm{e}^{i\theta_1} \\ \rho_{22}q_{21}\mathrm{e}^{i\theta_2} & \rho_{22}q_{22}\mathrm{e}^{i\theta_2} \end{pmatrix}\right) < 1, \tag{9.13}$$

which implies $|\rho_{11}q_{11}| < 1$ and $|\rho_{22}q_{22}| < 1$. We now make some structural assumptions on the boundary couplings of the interconnected system. These assumptions are natural and necessary to allow stabilization (or state estimation).

Assumption 9.1.1 *The boundary coupling coefficient q_{21} satisfies $q_{21} \neq 0$.*

This assumption is crucial for stabilizing the whole system. Indeed, if $q_{21} = 0$, it is impossible to act on subsystem "2" using the control input on subsystem "1". Thus, without this assumption, it would be impossible to stabilize the potentially unstable subsystem "2". Moreover, if $q_{21} = 0$, subsystem 1 is not observable using solely the available measurement $v_2(t, 0)$.

Assumption 9.1.2 *The coupling coefficients q_{11} and ρ_{22} satisfy*

$$q_{11} \neq 0, \text{ and } \rho_{22} \neq 0.$$

This assumption is more restrictive. If $q_{11} = 0$, the control input can act on subsystem "2" through distributed terms only. At that stage, the methodology we present in the rest of the chapter cannot be adjusted to deal with this case. Similar considerations arise in the observer design in the case $\rho_{22} = 0$. Finally, we state controllability and observability conditions.

Assumption 9.1.3 *The operators $A^\star$ and $B^\star$ defined by equation* (9.10) *and equation* (9.11) *verify*

$$\forall s \in \mathbb{C}, \ker(s - A^\star) \cap \ker(B^\star) = \{0\}. \tag{9.14}$$

Assumption 9.1.3 corresponds to a controllability condition similar to the one given in [CHO16]. It is related to the *approximate controllability* of the system and has been introduced by [Fat66] in a much larger setting. Finally, we make the dual observability assumption that reads as follows

Assumption 9.1.4 *The operators A and C defined by equation* (9.9) *and equation* (9.12) *verify*

$$\forall s \in \mathbb{C}, \ker(s - A) \cap \ker(C) = \{0\}. \tag{9.15}$$

9.2 . Time-delay representation

Following the methodology we have introduced in Chapter 6, we use backstepping transformations to rewrite the system (9.2)-(9.4) as a time-delay system. For the sake of the completeness of the chapter (and since the system is simpler than the one we considered in Chapter 6), we briefly reintroduce the backstepping transformations.

9.2.1 . Intermediate target system

Consider the two invertible integral transforms $\mathcal{L}_i$, $i \in \{1, 2\}$ acting on $H^1([0, 1], \mathbb{R}^2)$ such that $\begin{pmatrix} u_i \\ v_i \end{pmatrix} = \mathcal{L}_i \begin{pmatrix} \alpha_i \\ \beta_i \end{pmatrix}$, and defined for all $x \in [0, 1]$ by

$$\begin{cases} u_1(t,x) = \alpha_1(t,x) - \int_0^x L_1^{11}(x,y)\alpha_1(t,y) + L_1^{12}(x,y)\beta_1(t,y)\mathrm{d}y, \\ v_1(t,x) = \beta_1(t,x) - \int_0^x L_1^{21}(x,y)\alpha_1(t,y) + L_1^{22}(x,y)\beta_1(t,y)\mathrm{d}y, \end{cases} \tag{9.16}$$

$$\begin{cases} u_2(t,x) = \alpha_2(t,x) - \int_x^1 L_2^{11}(x,y)\alpha_2(t,y) + L_2^{12}(x,y)\beta_2(t,y)\mathrm{d}y, \\ v_2(t,x) = \beta_2(t,x) - \int_x^1 L_2^{21}(x,y)\alpha_2(t,y) + L_2^{22}(x,y)\beta_2(t,y)\mathrm{d}y, \end{cases} \tag{9.17}$$

where the kernels L_1^{ij} (resp. L_2^{ij}) are bounded piecewise continuous functions defined on the lower triangular part (resp. upper triangular part) of the unit square $\mathcal{T}_\ell$ (resp. $\mathcal{T}_u$) that satisfy

$$\begin{cases} \lambda_i \partial_x L_i^{11}(x,y) + \lambda_i \partial_y L_i^{11}(x,y) = \sigma_i^+(x) L_i^{21}(x,y), \\ \lambda_i \partial_x L_i^{12}(x,y) - \mu_i \partial_y L_i^{12}(x,y) = \sigma_i^+(x) L_i^{22}(x,y), \\ \mu_i \partial_x L_i^{21}(x,y) - \lambda_i \partial_y L_i^{21}(x,y) = -\sigma_i^-(x) L_i^{11}(x,y), \\ \mu_i \partial_x L_i^{22}(x,y) + \mu_i \partial_y L_i^{22}(x,y) = -\sigma_i^-(x) L_i^{12}(x,y), \end{cases} \tag{9.18}$$

with boundary conditions

$$\begin{cases} L_1^{12}(x,x) = -\frac{\sigma_1^+(x)}{\lambda_1+\mu_1}, \ L_1^{21}(x,x) = \frac{\sigma_1^-(x)}{\lambda_1+\mu_1}, \\ L_1^{11}(x,0) = \frac{\mu_1}{\lambda_1 q_{11}} L_1^{12}(x,0), \ L_1^{22}(x,0) = \frac{\lambda_1 q_{11}}{\mu_1} L_1^{21}(x,0), \\ L_2^{12}(x,x) = \frac{\sigma_2^+(x)}{\lambda_2+\mu_2}, \ L_2^{21}(x,x) = -\frac{\sigma_2^-(x)}{\mu_2+\lambda_2}, \\ L_2^{11}(x,1) = \frac{\mu_2 \rho_{22}}{\lambda_2} L_2^{12}(x,1), \ L_2^{22}(x,1) = \frac{\lambda_2}{\mu_2 \rho_{22}} L_2^{21}(x,1). \end{cases} \tag{9.19}$$

These two sets of equations admit a unique continuous solution [CVKB13]. The two Volterra transforms (9.16)-(9.17) map the original system (9.2)-(9.4) to the target system

$$\partial_t \alpha_i(t,x) + \lambda_i \partial_x \alpha_i(t,x) = 0, \tag{9.20}$$
$$\partial_t \beta_i(t,x) - \mu_i \partial_x \beta_i(t,x) = 0, \tag{9.21}$$

with the boundary conditions

$$\alpha_1(t,0) = q_{11}\beta_1(t,0),\ \beta_2(t,1) = \rho_{22}\alpha_2(t,1), \tag{9.22}$$

$$\begin{aligned}\beta_1(t,1) &= U(t) + \rho_{11}\alpha_1(t,1) + \rho_{12}v_2(t,0) + \int_0^1 (L_1^{21}(1,y) - \rho_{11}L_1^{11}(1,y))\alpha_1(t,y)dy \\ &+ \int_0^1 (L_1^{22}(1,y) - \rho_{11}L_1^{12}(1,y))\beta_1(t,y)dy - \int_0^1 \rho_{12}L_2^{21}(0,y)\alpha_2(t,y)dy \\ &- \int_0^1 \rho_{12}L_2^{22}(0,y)\beta_2(t,y)dy,\end{aligned} \tag{9.23}$$

$$\begin{aligned}\alpha_2(t,0) &= q_{22}\beta_2(t,0) + q_{21}\alpha_1(t,1) + \int_0^1 (L_2^{11}(0,y) - q_{22}L_2^{21}(0,y))\alpha_2(t,y)dy \\ &+ \int_0^1 (L_2^{12}(0,y) - q_{22}L_2^{22}(0,y))\beta_2(t,y)dy - \int_0^1 q_{21}L_1^{11}(1,y)\alpha_1(t,y)dy \\ &- \int_0^1 q_{21}L_1^{12}(1,y)\beta_1(t,y)dy.\end{aligned} \tag{9.24}$$

Again this target system can be expressed using an abstract operator formulation:

$$\frac{d}{dt}\begin{pmatrix}\alpha_1 & \beta_1 & \alpha_2 & \beta_2\end{pmatrix}^\top = A_T \begin{pmatrix}\alpha_1 & \beta_1 & \alpha_2 & \beta_2\end{pmatrix}^\top + BU, \tag{9.25}$$

where the operator A_T is defined by

$$\begin{aligned}A_T : D(A_T) \subset L^2([0,1],\mathbb{R}^2) &\to L^2([0,1],\mathbb{R}^2) \\ \begin{pmatrix}\alpha_1 & \beta_1 & \alpha_2 & \beta_2\end{pmatrix}^\top &\longmapsto \begin{pmatrix}-\lambda_1\partial_x\alpha_1 & \mu_1\partial_x\beta_1 & -\lambda_2\partial_x\alpha_2 & \mu_2\partial_x\beta_2\end{pmatrix},\end{aligned} \tag{9.26}$$

with a domain $D(A_T)$ obtained using the boundary conditions (9.23)-(9.24). Its adjoint is given by

$$\begin{aligned}A_T^\star : D(A^\star) \subset L^2([0,1],\mathbb{R}^2) &\to L^2([0,1],\mathbb{R}^2) \\ \begin{pmatrix}\alpha_1\\ \beta_1\\ \alpha_2\\ \beta_2\end{pmatrix}^\top &\longmapsto \begin{pmatrix}\lambda_1\partial_x\alpha_1 + p_1^+(\cdot)\beta_1(1) + q_1^+(\cdot)\alpha_2(0)\\ -\mu_1\partial_x\beta_1 + p_1^-(\cdot)\beta_1(1) + q_1^-(\cdot)\alpha_2(0)\\ \lambda_2\partial_x\alpha_2 + p_2^+(\cdot)\beta_1(1) + q_2^+(\cdot)\alpha_2(0)\\ -\mu_2\partial_x\beta_2 + p_2^-(\cdot)\beta_1(1) + q_2^-(\cdot)\alpha_2(0)\end{pmatrix},\end{aligned} \tag{9.27}$$

where $p_1^+(x) = L_1^{21}(1,x) - \rho_{11}L_1^{11}(1,x)$, $p_1^-(x) = L_1^{22}(1,x) - \rho_{11}L_1^{12}(1,x)$, $p_2^+(x) = -\rho_{12}L_2^{21}(0,x)$, $p_2^-(x) = -\rho_{12}L_2^{22}(0,x)$, $q_2^+(x) = L_2^{11}(0,x) - q_{22}L_1^{21}(0,x)$, $q_2^-(x) = L_2^{12}(0,x) - q_{22}L_2^{22}(0,x)$, $q_1^+(x) = -q_{21}L_1^{11}(1,x)$, $q_1^-(x) = -q_{21}L_1^{22}(1,x)$. This new operator still verifies the controllability condition. More precisely, we have the following lemma.

Lemma 9.2.1 *If Assumption 9.1.3 is verified then* $\forall s \in \mathbb{C}, \ker(s - A_T^\star) \cap \ker(B^\star) = \{0\}$.

Proof : The proof is a consequence of the invertibility of the backstepping transformations. Direct computations can show it. ■

9.2.2 . Integral Delay Equation

Let us denote $z_1(t) = \beta_1(t,1)$ and $z_2(t) = \alpha_2(t,0)$. Using the method of characteristics, we have for all $t \geq \max\{\tau_1,\tau_2\}$

$$z_1(t) = \rho_{11}q_{11}z_1(t-\tau_1) + \rho_{12}\rho_{22}z_2(t-\tau_2) + U(t)$$

$$+\int_0^{\tau_1} H_{11}(\nu)z_1(t-\nu)d\nu+\int_0^{\tau_2} H_{12}(\nu)z_2(t-\nu)d\nu, \tag{9.28}$$

$$\begin{aligned} z_2(t) =& q_{21}q_{11}z_1(t-\tau_1)+q_{22}\rho_{22}z_2(t-\tau_2)\\ &+\int_0^{\tau_1} H_{21}(\nu)z_1(t-\nu)d\nu+\int_0^{\tau_2} H_{22}(\nu)z_2(t-\nu)d\nu, \end{aligned} \tag{9.29}$$

where the functions H_{ij} are defined by

$$\begin{aligned} H_{11}(\nu) &= \mu_1(L_1^{22}(1,1-\mu_1\nu)-\rho_{11}L_1^{12}(1,1-\mu_1\nu))\mathbb{1}_{[0,\frac{1}{\mu_1}]}(\nu)+q_{11}\lambda_1(L_1^{21}(1,\lambda_1\nu-\frac{\lambda_1}{\mu_1})\\ &-\rho_{11}L_1^{11}(1,\lambda_1\nu-\frac{\lambda_1}{\mu_1}))\mathbb{1}_{]\frac{1}{\mu_1},\tau_1]}(\nu),\\ H_{12}(\nu) &= -\rho_{12}\lambda_2L_2^{21}(0,\lambda_2\nu)\mathbb{1}_{[0,\frac{1}{\lambda_2}]}(\nu)-\mu_2\rho_{12}q_{22}L_2^{22}(0,1-\mu_2\nu+\frac{\mu_2}{\lambda_2})\mathbb{1}_{]\frac{1}{\lambda_2},\tau_2]}(\nu)\\ H_{21}(\nu) &= -q_{21}\mu_1L_1^{12}(0,1-\mu_1\nu))\mathbb{1}_{[0,\frac{1}{\mu_1}]}-\lambda_1q_{11}q_{21}L_1^{11}(1,\lambda_1\nu-\frac{\lambda_1}{\mu_1}))\mathbb{1}_{]\frac{1}{\mu_1},\tau_1]}(\nu)\\ H_{22}(\nu) &= \lambda_2(L_2^{11}(0,\lambda_2\nu)-q_{22}L_2^{21}(0,\lambda_2\nu))\mathbb{1}_{[0,\frac{1}{\lambda_2}]}(\nu)-\mu_2\rho_{22}(L_2^{12}(0,1-\mu_2\nu+\frac{\mu_2}{\lambda_2})\\ &-q_{22}L_2^{22}(0,1-\mu_2\nu+\frac{\mu_2}{\lambda_2}))\mathbb{1}_{]\frac{1}{\lambda_2},\tau_2]}(\nu). \end{aligned}$$

The states z_1 and z_2 can be seen as $H^1([-\max\{\tau_1,\tau_2\},0],\mathbb{R})$ functions with the appropriate initial conditions (the compatibility conditions are still verified). Thanks to Theorem 6.1.3, the exponential stability of the time-delay system (9.28)-(9.29) in the sense of the $\chi_{\max\{\tau_1,\tau_2\}}$ norm will imply the exponential stability of the system (9.2)-(9.4) in the sense of the χ-norm. These two norms are defined in Chapter 6. Since $U(t)$ only appears in equation (9.28), we can use it to cancel the right-hand side of the equation and consider z_1 as an artificial controller acting on equation (9.29). More precisely, we can introduce the intermediate control input $\bar{U}(t)$ defined by

$$\begin{aligned} \bar{U}(t) &= \rho_{11}q_{11}z_1(t-\tau_1)+\rho_{12}\rho_{22}z_2(t-\tau_2)+U(t)\\ &+\int_0^{\tau_1} H_{11}(\nu)z_1(t-\nu)d\nu+\int_0^{\tau_2} H_{12}(\nu)z_2(t-\nu)d\nu, \end{aligned} \tag{9.30}$$

such that equation (9.29) rewrites

$$\begin{aligned} z_2(t) =& a\bar{U}(t-\tau_1)+bz_2(t-\tau_2)\\ &+\int_0^{\tau_1} H_{21}(\nu)\bar{U}(t-\nu)d\nu+\int_0^{\tau_2} H_{22}(\nu)z_2(t-\nu)d\nu, \end{aligned} \tag{9.31}$$

where $a=q_{21}q_{11}$ and $b=q_{22}\rho_{22}$. We consider that $U(t)=0$ for $t<\max\{\tau_1,\tau_2\}$. It is important to emphasize that $a\neq 0$ and $|b|<1$ due to Assumptions 9.1.1 and 9.1.2. Equation (9.31) corresponds to a *Integral Delay Equation* (IDE). The actuation in (9.31) appears through pointwise and distributed delay terms. It has been seldom studied in the literature [BLK16, Pon15], and is a major difference compared to existing results. However, we assume here that there is (at least) a pointwise delay in the actuation since $a\neq 0$. Obviously, the difficulties in stabilizing equation (9.31) are related to the simultaneous presence of a distributed-delay term for the actuation and the state. Let us formally take the Laplace transform of equation (9.31). We have $F_0(s)z_2(s)=F_1(s)U(s)$, where the holomorphic function F_0 and F_1 are defined by

$$F_0(s)=1-b\mathrm{e}^{-\tau_2 s}-\int_0^{\tau_2} H_{22}(\nu)\mathrm{e}^{-\nu s}d\nu, \tag{9.32}$$

$$F_1(s)=a\mathrm{e}^{-\tau_1 s}+\int_0^{\tau_1} H_{21}(\nu)\mathrm{e}^{-\nu s}d\nu. \tag{9.33}$$

The following lemma shows that under Assumption 9.1.3, the functions F_0 and F_1 cannot simultaneously vanish.

Lemma 9.2.2 *If Assumption 9.1.3 is verified, then for all* $s \in \mathbb{C}$, $rank[F_0(s), F_1(s)] = 1$.

Proof : Consider that Assumption 9.1.3 is verified. Then, due to Lemma 9.2.1, we have $\forall s \in \mathbb{C}, \ker(s - A_T^\star) \cap \ker(B^\star) = \{0\}$. Consider $(\alpha_1, \beta_1, \alpha_2, \beta_2)^T \in (\ker(s - A_T^\star) \cap \ker(B^\star))$. We obtain

$$
\begin{aligned}
s\alpha_1(x) &= \lambda_1 \alpha_1'(x) + q_1^+(x)\alpha_2(0) \\
s\beta_1(x) &= -\mu_1 \beta_1'(x) + q_1^-(x)\alpha_2(0) \\
s\alpha_2(x) &= \lambda_2 \alpha_2'(x) + q_2^+(x)\alpha_2(0) \\
s\beta_2(x) &= -\mu_2 \beta_2'(x) + q_2^-(x)\alpha_2(0)
\end{aligned}
$$

with the boundary conditions $\alpha_1(1) = \frac{q_{21}\lambda_2}{\lambda_1}\alpha_2(0)$, $\alpha_2(1) = \frac{\rho_{22}\mu_2}{\lambda_2}\beta_2(1)$, $\beta_1(0) = \frac{q_{11}\lambda_1}{\mu_1}\alpha_1(0)$, $\beta_2(0) = \frac{q_{22}\lambda_2}{\mu_2}\alpha_2(0)$, and $\beta_1(1) = 0$. Straightforward (but lengthy) computations show that there is a unique trivial solution only if $F_0(s)$ and $F_1(s)$ do not vanish at the same point, that is, $rank[F_0(s), F_1(s)] = 1$ ■

The fact that $rank[F_0(s), F_1(s)] = 1$ corresponds to a classical spectral controllability condition [Mou98, Pan76].

9.3 . Design of a state-feedback controller

In this section, we design a state-feedback controller $\bar{U}(t)$ that stabilizes equation (9.31). It will then be straightforward to obtain a stabilizing control law $U(t)$ for the original system (9.2)-(9.4). To simplify the computations, we will consider that

$$\tau_1 = (N+1)\tau_2, \tag{9.34}$$

where $N \in \mathbb{N}$. This assumption can be made without any loss in generality as it is always possible to artificially delay the control law $\bar{U}(t)$ in equation (9.30) by $\delta_0 > 0$ such that $\bar{\tau}_1 = \tau_1 + \delta_0$ becomes a multiple of τ_2. In the meantime, the piecewise continuous function H_{21} could be extended by 0 to be defined on $[0, \bar{\tau}_1]$.
We propose to look for the desired control law under the form

$$\bar{U}(t) = \int_0^{\tau_2} f(\nu) z_2(t-\nu) d\nu + \int_0^{\tau_1} g(\nu) \bar{U}(t-\nu) d\nu, \tag{9.35}$$

with f and g piecewise continuous matrix-valued functions to be defined. We set $\bar{U}(t) = 0$ for $t < \bar{\tau}_1$. To design f and g, we will first compute the quantity $z_2(t) - \int_0^{\tau_1} g(\nu) z_2(t-\nu) d\nu$. Using equation (9.31) and expression (9.35), we get for $t \geq \tau_1 + \tau_2$

$$
\begin{aligned}
&z_2(t) - \int_0^{\tau_1} g(\nu) z_2(t-\nu) d\nu = b z_2(t-\tau_2) + a \int_0^{\tau_2} f(\nu) z_2(t-\nu-\tau_1) \\
&- b \int_0^{\tau_1} g(\nu) z_2(t-\nu-\tau_2) + \int_0^{\tau_2} H_{22}(\nu) z_2(t-\nu) d\nu - \int_0^{\tau_1} \int_0^{\tau_2} g(\nu)(H_{22}(\eta) \\
&z_2(t-\nu-\eta) d\eta) d\nu + \int_0^{\tau_2} \int_0^{\tau_1} f(\nu)(H_{21}(\eta) z_2(t-\nu-\eta) d\eta) d\nu.
\end{aligned} \tag{9.36}
$$

Using Fubini's theorem, we can rewrite the double integrals. We have

$$
\begin{aligned}
\int_0^{\tau_2} \int_0^{\tau_1} f(\nu)(H_{21}(\eta) z_2(t-\nu-\eta) d\eta) d\nu &= \int_0^{\tau_2} (\int_0^{\nu} f(\eta) H_{21}(\nu-\eta) d\eta) z_2(t-\nu) d\nu \\
&+ \int_{\tau_2}^{\tau_1} (\int_0^{\tau_2} f(\eta) H_{21}(\nu-\eta) d\eta) z_2(t-\nu) d\nu \\
&+ \int_{\tau_1}^{\tau_2+\tau_1} (\int_{\nu-\tau_1}^{\tau_2} f(\eta) H_{21}(\nu-\eta) d\eta) z_2(t-\nu) d\nu,
\end{aligned}
$$

and

$$\int_0^{\tau_1} \int_0^{\tau_2} g(\nu)(H_{22}(\eta) z_2(t-\nu-\eta) d\eta) d\nu = \int_0^{\tau_2} (\int_0^{\nu} g(\eta) H_{22}(\nu-\eta) d\eta) z_2(t-\nu) d\nu$$

$$+\int_{\tau_2}^{\tau_1}(\int_{\nu-\tau_2}^{\nu} g(\eta)H_{22}(\nu-\eta)d\eta)z_2(t-\nu)d\nu$$
$$+\int_{\tau_1}^{\tau_2+\tau_1}(\int_{\nu-\tau_2}^{\tau_1} g(\eta)H_{22}(\nu-\eta)d\eta)z_2(t-\nu)d\nu.$$

Consequently, equation (9.36) now reads

$$z_2(t) = bz_2(t-\tau_2) + \int_0^{\tau_2} I_1(\nu)z_2(t-\nu)d\nu + \int_{\tau_2}^{\tau_1} I_2(\nu)z_2(t-\nu)d\nu + \int_{\tau_1}^{\tau_1+\tau_2} I_3(\nu)z_2(t-\nu)d\nu, \tag{9.37}$$

where I_1, I_2 and I_3 are respectively defined on $[0,\tau_2]$, $[\tau_2,\tau_1]$, and $[\tau_1,\tau_1+\tau_2]$ by

$$I_1(\nu) = g(\nu) + H_{22}(\nu) + \int_0^{\nu} f(\eta)H_{21}(\nu-\eta)d\eta - \int_0^{\nu} g(\eta)H_{22}(\nu-\eta)d\eta, \tag{9.38}$$

$$I_2(\nu) = g(\nu) - bg(\nu-\tau_2) + \int_0^{\tau_2} f(\eta)H_{21}(\nu-\eta)d\eta - \int_{\nu-\tau_2}^{\nu} g(\eta)H_{22}(\nu-\eta)d\eta, \tag{9.39}$$

$$I_3(\nu) = af(\nu-\tau_1) - bg(\nu-\tau_2) + \int_{\nu-\tau_1}^{\tau_2} f(\eta)H_{21}(\nu-\eta)d\eta - \int_{\nu-\tau_2}^{\tau_1} g(\eta)H_{22}(\nu-\eta)d\eta, \tag{9.40}$$

Provided that we can choose f and g such that $I_1 \equiv 0$, $I_2 \equiv 0$, and $I_3 \equiv 0$, we obtain $z_2(t) = bz_2(t-\tau_2)$ which implies the exponential stability of z_2 since $|b| < 1$. The following lemma states that such functions f and g can be uniquely defined.

Lemma 9.3.1 *Consider the functions I_1, I_2, and I_3 defined in equations* (9.38)-(9.40)*. There exist two unique piecewise continuous functions (f,g) such that $I_1(\nu) = 0$ for $\nu \in [0,\tau_2[$, $I_2(\nu) = 0$ for $\nu \in [\tau_2,\tau_1[$, and $I_3(\nu) = 0$ for $\nu \in [\tau_1,\tau_1+\tau_2]$.*

Proof : Let us first introduce the intermediate functions g_k defined on $[0,\tau_2]$ such that for all $\nu \in [k\tau_2,(k+1)\tau_2]$ $(0 \le k \le N)$ we have $g_k(\nu) = g(\nu+k\tau_2)$. The system $I_1(\nu) = 0, I_2(\nu) = 0, I_3(\nu) = 0$ is equivalent to

$$g_0(\nu) - \int_0^{\nu} g_0(\eta)H_{22}(\nu-\eta)d\eta + \int_0^{\nu} f(\eta)H_{21}(\nu-\eta)d\eta = -H_{22}(\nu) \tag{9.41}$$

$$g_k(\nu) - bg_{k-1}(\nu) - \int_{\nu}^{\tau_2} g_{k-1}(\eta)H_{22}(\nu-\eta+\tau_2)d\eta - \int_0^{\nu} g_k(\eta)H_{22}(\nu-\eta)d\eta + \int_0^{\tau_2} f(\eta)H_{21}(\nu+k\tau_2-\eta)d\eta = 0, \tag{9.42}$$

$$af(\nu) - bg_N(\nu) - \int_{\nu}^{\tau_2} g_N(\eta)H_{22}(\nu+\tau_2-\eta)d\eta + \int_{\nu}^{\tau_2} f(\eta)H_{21}(\nu+\tau_1-\eta)d\eta = 0, \tag{9.43}$$

where $0 < k \le N$ and $\nu \in [0,\tau_2]$. We now define the operator $\mathcal{T} : (L^2([0,\tau_2],\mathbb{R}))^{N+2} \to (L^2([0,\tau_2],\mathbb{R}))^{N+2}$ by

$$(\mathcal{T}\begin{pmatrix} f \\ g_N \\ \vdots \\ g_k \\ \\ \vdots \\ g_0 \end{pmatrix})(\nu) = \begin{pmatrix} af(\nu) - bg_N(\nu) - \int_{\nu}^{\tau_2} g_N(\eta)H_{22}(\nu+\tau_2-\eta)d\eta + \int_{\nu}^{\tau_2} f(\eta)H_{21}(\nu+\tau_1-\eta)d\eta \\ \cdots \\ \vdots \\ g_k(\nu) - bg_{k-1}(\nu) - \int_{\nu}^{\tau_2} g_{k-1}(\eta)H_{22}(\nu-\eta+\tau_2)d\eta - \int_0^{\nu} g_k(\eta)H_{22}(\nu-\eta)d\eta \\ + \int_0^{\tau_2} f(\eta)H_{21}(\nu+k\tau_2-\eta)d\eta \\ \vdots \\ g_0(\nu) - \int_0^{\nu} g_0(\eta)H_{22}(\nu-\eta)d\eta + \int_0^{\nu} f(\eta)H_{21}(\nu-\eta)d\eta \end{pmatrix}$$

We want to show that equations (9.41)-(9.43) admit a unique solution. This will result from the invertibility of the operator $\mathcal{T}$. To show this latter property, let us introduce the operators $A_{\mathcal{T}}$ defined on $D(A_{\mathcal{T}}) \subset L^2([0,\tau_2],\mathbb{R})^{N+2}$ by

$$A_{\mathcal{T}} : D(A_{\mathcal{T}}) \to L^2([0,\tau_2],\mathbb{R})^{N+2}$$

$$\begin{pmatrix} \phi \\ \psi_N \\ \vdots \\ \psi_0 \end{pmatrix} \longmapsto \begin{pmatrix} \partial_x\phi + \phi(0)H_{22}(\cdot) \\ \partial_x\psi_N + \phi(0)H_{21}(\cdot + N\tau_2) \\ \vdots \\ \partial_x\psi_0 + \phi(0)H_{21}(\cdot) \end{pmatrix}, \tag{9.44}$$

where $D(A_\mathcal{T}) = \{(\phi, \psi_N, \dots, \psi_0) \in (H^1([0,\tau_2],\mathbb{R}))^{N+2},\ \phi(\tau_2) = b\phi(0),\ \psi_N(\tau_2) = a\phi(0), \psi_k(\tau_2) = \psi_{k+1}(0),\ 0 \le k < N\}$. We define the operator $B_\mathcal{T} :\ D(A_\mathcal{T}) \to (L^2([0,\tau_2],\mathbb{R}))^{N+2}$, by

$$B_\mathcal{T}(\begin{pmatrix}\phi & \psi_N & \cdots & \psi_0\end{pmatrix}^\top) = \psi_0(0).$$

We now show that the operators $\mathcal{T}$, $A_\mathcal{T}$ and $B_\mathcal{T}$ verify the requirements of Theorem 9.0.1. Let us consider $h = (f, g_N, \cdots, g_0)$ in $\ker(\mathcal{T})$. We have for all $1 \le k \le N$

$$g_{k+1}(0) - g_k(\tau_2) = b(g_k(0) - g_{k-1}(\tau_2)).$$

Since $g_0(0) = 0$, we can recursively show that $g_k(\tau_2) = g_{k+1}(0)$. Direct computations give $af(0) = g_N(\tau_2)$ and $f(\tau_2) = bf(0)$. Consequently $h \in D(A_\mathcal{T})$. Since $g_0(0) = 0$, we also have $h \in \ker(B_\mathcal{T})$. Consider now $s \in \mathbb{C}$ and $(\phi, \psi_N, \cdots, \psi_0) \in \ker(s\mathrm{Id} - A_\mathcal{T}) \cap \ker(B_\mathcal{T})$. We have for all $0 \le k \le N$ and all $x \in [0,\tau_2]$

$$\begin{aligned} &s\phi(x) = \phi'(x) + \phi(0)H_{22}(x), \quad s\psi_k(x) = \psi_k'(x) + \phi(0)H_{21}(x + k\tau_2), \\ \Rightarrow &\phi(x) = (\mathrm{e}^{sx} - \int_0^x H_{22}(\nu)\mathrm{e}^{s(x-\nu)}d\nu)\phi(0), \quad \psi_k(x) = \mathrm{e}^{sx}\psi_k(0) - \phi(0)\int_0^x H_{21}(\nu + k\tau_2)\mathrm{e}^{s(x-\nu)}d\nu, \end{aligned}$$

The first equation gives $F_0(s)\phi(0) = 0$, where F_0 is defined in equation (9.32). In the meantime, we obtain

$$\begin{aligned} a\phi(0) = \psi_N(\tau_2) &= \mathrm{e}^{s\tau_2}\psi_N(0) - \phi(0)\int_0^{\tau_2} H_{21}(\nu + N\tau_2)\mathrm{e}^{s(\tau_2-\nu)}d\nu \\ &= \mathrm{e}^{s\tau_2}\psi_{N-1}(\tau_2) - \phi(0)\int_{N\tau_2}^{\tau_1} H_{21}(\nu)\mathrm{e}^{s((N+1)\tau_2-\nu)}d\nu. \end{aligned}$$

Iterating the procedure, we obtain $F_1(s)\phi(0)$, where F_1 is defined in equation (9.33). Applying Lemma 9.2.2, we obtain that $s = 0$ and the last requirement of Lemma 9.0.1 is verified. We now need to show the last condition of Lemma 9.0.1, i.e., $A_\mathcal{T}(h) \in \ker(\mathcal{T})$. We have for all $x \in [0,\tau_2]$

$$\begin{aligned} &af'(x) + af(0)H_{22}(x) - bg_N'(x) - bf(0)H_{21}(x + N\tau_2) - \int_x^{\tau_2}((g_N'(\eta) + f(0)H_{21}(\eta + N\tau_2))H_{22}(x+ \\ &\quad \tau_2 - \eta) - (f'(\eta) + f(0)H_{22}(\eta))H_{21}(x + \tau_1 - \eta))d\eta = af'(x) + af(0)H_{22}(x) \\ &- bg_N'(x) - bf(0)H_{21}(x + N\tau_2) + \int_x^{\tau_2}(f'(\eta)H_{21}(x + \tau_1 - \eta) - g_N'(\eta)H_{22}(x + \tau_2 - \eta))d\eta \end{aligned} \tag{9.45}$$

Since $h \in \ker(\mathcal{T})$, we also have

$$af'(x) = bg_N'(x) - g_N(x)H_{22}(\tau_2) + f(x)H_{21}(\tau_1) - \int_x^{\tau_2}(f(\eta)H_{21}'(x + \tau_1 - \eta) - g_N(\eta)H_{22}'(x + \tau_2 - \eta))d\eta.$$

Consequently, using integration by parts and injecting into (9.45), we obtain the quantity in (9.45) is equal to zero. Performing analogous computations, for all the lines of $\mathcal{T}$, we obtain that $A_\mathcal{T}(h) \in \ker(\mathcal{T})$. All the requirements of Lemma 9.0.1 are verified. Consequently, the operator $\mathcal{T}$ is invertible and the set of equations (9.41)-(9.43) admit a unique solution in $(L^2([0,\tau_2],\mathbb{R}))^{N+2}$. These solutions are piecewise continuous due to the regularity of the functions H_{21} and H_{22} and to the regularizing effect of the integral. This concludes the proof. Note that this proof can be adjusted when τ_1 is not a multiple of τ_2 at the price of technical subtleties. ■

Lemma 9.3.2 *Consider the functions I_1, I_2 and I_3 defined in* (9.38)-(9.40) *and let f and g be the unique piecewise continuous functions that lead to $I_1(\nu) = 0$ for all $\nu \in [0,\tau_2]$, $I_2(\nu) = 0$ for all $\nu \in]\tau_2,\tau_1]$, and $I_3(\nu) = 0$ for $\nu \in [\tau_1, \tau_2 + \tau_1]$ (as stated in Lemma 9.3.1). Consider the control law $\bar{U}$ defined by equation* (9.35)*, and z_2 a solution of equation* (9.31)*. Then, for all $t > \tau_1 + \tau_2$, we have $\bar{U}(t) = b\bar{U}(t - \tau_2)$. Moreover, the transfer function between z_2 and $\bar{U}$ is strictly proper.*

Proof : Consider that g and f are chosen such that $I_1 \equiv I_2 \equiv I_3 \equiv 0$ (which is always possible due to Lemma 9.3.1). We have

$$\begin{aligned} &\bar{U}(t) - b\bar{U}(t - \tau_2) - \int_0^{\tau_2} H_{22}(\nu)\bar{U}(t - \nu)d\nu = \int_0^{\tau_1} g(\nu)\bar{U}(t - \nu)d\nu \\ &- b\int_0^{\tau_1} g(\nu)\bar{U}(t - \nu - \tau_2)d\nu - \int_0^{\tau_2}(\int_0^{\tau_1} H_{22}(\nu)g(\eta)\bar{U}(t - \nu - \eta)d\eta)d\nu \end{aligned}$$

$$+a\int_0^{\tau_2} f(\nu)\bar{U}(t-\tau_1-\nu)d\nu+\int_0^{\tau_2} f(\nu)(\int_0^{\tau_1} H_{21}(\eta)\bar{U}(t-\eta-\nu)d\eta)d\nu,$$

where we have first used the expression of $\bar{U}$ given in equation (9.35) and then substituted the z_2 terms using equation (9.31). This equation is identical to equation (9.36). Since $I_1 \equiv I_2 \equiv I_3 \equiv 0$, analogous computations to the ones performed after equation (9.36) give $\bar{U}(t) = b\bar{U}(t-\tau_2)$. Taking the Laplace transform of equation (9.35), we obtain $\hat{U}(s) = \frac{\int_0^{\tau_2} f(\nu)\mathrm{e}^{-\nu s}d\nu}{1-\int_0^{\tau_1} g(\nu)\mathrm{e}^{-\nu s}d\nu}\hat{X}(s)$, which, due to Riemann-Lebesgue's lemma, defines a strictly proper transfer function. ■

Combining Lemma 9.3.1 and Lemma 9.3.2, we can now write the following theorem.

Theorem 9.3.1 *Consider the functions I_1, I_2 and I_3 defined in* (9.38)-(9.40) *and let f and g be the unique piecewise continuous functions that lead to $I_1(\nu) = 0$ for all $\nu \in [0, \tau_2]$, $I_2(\nu) = 0$ for all $\nu \in]\tau_2, \tau_1]$, and $I_3(\nu) = 0$ for $\nu \in [\tau_1, \tau_2 + \tau_1]$ (as stated in Lemma 9.3.1). Then, the closed-loop system consisting of the plant* (9.2)-(9.4) *and the control law*

$$\begin{aligned} U(t) &= -\rho_{11}q_{11}z_1(t-\tau_1) - \rho_{12}\rho_{22}z_2(t-\tau_2) + \bar{U}(t) \\ &- \int_0^{\tau_1} H_{11}(\nu)z_1(t-\nu)d\nu - \int_0^{\tau_2} H_{12}(\nu)z_2(t-\nu)d\nu, \end{aligned} \tag{9.46}$$

where $\bar{U} = \int_0^{\tau_2} f(\nu)z_2(t-\nu)d\nu + \int_0^{\tau_1} g(\nu)\bar{U}(t-\nu)d\nu$ is exponentially stable. Moreover, the control law $U(t)$ exponentially converges to zero and can be low-pass filtered such that the resulting filtered control operator is strictly proper while stabilizing the plant (9.2)-(9.4).

Proof : Lemma 9.3.1, guarantees the existence of f and g such that $I_1 \equiv I_2 \equiv I_3 \equiv 0$. Consequently, equation (9.37) rewrites $z_2(t) = bz_2(t-\tau_2)$ which implies the exponential stability of z_2 since $|b| < 1$. Due to Lemma 9.3.2, the control law $\bar{U}(t)$ also verifies $\bar{U}(t) = b\bar{U}(t-\tau_2)$ and is therefore exponentially stable. Due to the definition of $\bar{U}$ given in equation (9.35), the L^2-norm of $\bar{U}$ can be bounded by the L^2 norm of the initial condition associated to z_2. Since $z_1(t) = \bar{U}(t)$, for $t \geq \max\{\tau_1, \tau_2\}$ the state (z_1, z_2) is exponentially stable, which implies the exponential convergence of the control input $U(t)$ and of the plant (9.2)-(9.4) (using the invertibility of the backstepping transformations and Theorem 6.1.3). Finally, applying Theorem 6.2.1, we can low-pass filter the control operator to make it strictly proper. ■

9.4 . State-observer and output-feedback controller

In this section, we design a state observer for the system (9.2)-(9.6), using the available measurement $y(t) = v_2(t, 0)$.

9.4.1 . Simplification of the system

Similarly to what we have done in the previous chapters, we first transform the system (9.2)-(9.6) into a simpler target system. Consider the backstepping integral transformations $\mathcal{M}_i$, $i \in \{1, 2\}$ defined on $H^1([0,1], \mathbb{R}^2)$ such that $\begin{pmatrix} u_i \\ v_i \end{pmatrix} = \mathcal{M}_i \begin{pmatrix} a_i \\ b_i \end{pmatrix}$. More precisely, we have

$$\begin{cases} u_1 = a_1 + \int_x^1 M_1^{11}(x,y)a_1(y) + M_1^{12}(x,y)b_1(y)\mathrm{d}y, \\ v_1 = b_1 + \int_x^1 M_1^{21}(x,y)a_1(y) + M_1^{22}(x,y)b_1(y)\mathrm{d}y, \end{cases} \tag{9.47}$$

$$\begin{cases} u_2 = a_2 + \int_0^x M_2^{11}(x,y)a_2(y) + M_2^{12}(x,y)b_2(y)\mathrm{d}y, \\ v_2 = b_2 + \int_0^x M_2^{21}(x,y)a_2(y) + M_2^{22}(x,y)b_2(y)\mathrm{d}y, \end{cases} \tag{9.48}$$

where the kernels M_1^{ij} (resp. M_2^{ij}) are piecewise continuous bounded functions defined on $\mathcal{T}_u$ (resp. $\mathcal{T}_\ell$). They satisfy the same set of equations (9.18) as kernels $L_i^{\cdot\cdot}$ with the boundary conditions

$$\begin{cases} M_1^{12}(x,x) = -\frac{\sigma_1^+(x)}{\lambda_1+\mu_1},\ M_1^{21}(x,x) = \frac{\sigma_1^-(x)}{\lambda_1+\mu_1}, M_1^{22}(0,y) = \frac{1}{q_{11}}M_1^{12}(0,y), \\ M_1^{11}(0,y) = q_{11}M_1^{21}(0,y),\ M_2^{12}(x,x) = \frac{\sigma_2^+(x)}{\lambda_2+\mu_2},\ M_2^{21}(x,x) = -\frac{\sigma_2^-(x)}{\mu_2+\lambda_2}, \\ M_2^{11}(1,y) = \frac{1}{\rho_{22}}M_2^{21}(1,y),\ M_2^{22}(1,y) = \rho_{22}M_2^{12}(1,y). \end{cases}$$

These two sets of equations admit a unique piecewise continuous solution [VKC11]. Applying the transformations (9.47) -(9.48) we obtain the target system

$$\partial_t a_i(t,x) + \lambda_i \partial_x a_i(t,x) = H_i^a(x) a_1(t,1) + F_i^a(x) b_2(t,0) + K_i^a(x) U(t), \tag{9.49}$$
$$\partial_t b_i(t,x) - \mu_i \partial_x b_i(t,x) = H_i^b(x) a_1(t,1) + F_i^b(x) b_2(t,0) + K_i^b(x) U(t), \tag{9.50}$$

with the boundary conditions

$$a_1(t,0) = q_{11} b_1(t,0),\ b_1(t,1) = \rho_{11} a_1(t,1) + \rho_{12} b_2(t,0) + U(t), \tag{9.51}$$
$$a_2(t,0) = q_{22} b_2(t,0) + q_{21} a_1(t,1),\ b_2(t,1) = \rho_{22} a_2(t,1). \tag{9.52}$$

The associated initial conditions are $(a_i^0(\cdot), b_i^0(\cdot))^T = \mathcal{M}_i^{-1}((u_i^0(\cdot), v_i^0(\cdot))^T) \in H^1([0,1],\ \mathbb{R}^2)$ and satisfy the appropriate compatibility conditions The in-domain coupling terms $F_i^a, F_i^b, H_i^a,\ H_i^b$ are defined by the set of equations

$$H_1^*(x) + \int_x^1 M_1^{i1}(x,\nu) H_1^a(\nu) + M_1^{i2}(x,\nu) H_1^b(\nu) \mathrm{d}\nu = \lambda_1 M_1^{i1}(x,1) - \mu_1 \rho_{11} M_1^{i2}(x,1),$$
$$F_1^*(x) + \int_x^1 M_1^{i1}(x,\nu) F_1^a(\nu) + M_1^{i2}(x,\nu) F_1^b(\nu) \mathrm{d}\nu = -\mu_1 \rho_{12} M_1^{i2}(x,1),$$
$$H_2^*(x) + \int_0^x M_2^{i1}(x,\nu) H_2^a(\nu) + M_2^{i2}(x,\nu) H_2^b(\nu) \mathrm{d}\nu = -\lambda_2 q_{21} M_2^{i1}(x,0),$$
$$F_2^*(x) + \int_0^x M_2^{i1}(x,\nu) F_2^a(\nu) + M_2^{i2}(x,\nu) F_2^b(\nu) \mathrm{d}\nu = \mu_2 M_2^{i2}(x,0) - \lambda_2 q_{22} M_2^{i1}(x,0),$$

with $i = 1$ if $* = a$, and $i = 2$ if $* = b$. The coupling terms K are defined by

$$\begin{pmatrix} K_1^a(x) \\ K_1^b(x) \end{pmatrix} = \mathcal{M}_1^{-1}(\begin{pmatrix} -\mu_1 M_1^{12}(x,1) \\ -\mu_1 M_1^{22}(x,1) \end{pmatrix}),\ \begin{pmatrix} K_2^a(x) \\ K_2^b(x) \end{pmatrix} \equiv 0. \tag{9.53}$$

These coupling terms are well-defined since the associated equations are Volterra integral equations that admit a unique solution [Yos60]. Due to the piecewise continuity of the kernels M^{ij} and the regularizing property of the integral operator, H_i^*, F_i^*, K_1^* are piecewise continuous. We finally have $y(t) = b_2(t,0)$.

9.4.2 . Observer design

We design our observer as a copy of the target system (9.49)-(9.52) with output injection terms (Luenberger-type observer). We denote $\hat{a}_i$ and $\hat{b}_i$ the observer states. They verify the following set of equations

$$\begin{aligned} \partial_t \hat{a}_i(t,x) + \lambda_i \partial_x \hat{a}_i(t,x) &= H_i^a(x) \hat{a}_1(t,1) + F_i^a(x) y(t) + K_i^a(x) U(t) \\ &\quad + G_i^a(x)(\hat{b}_2(t,0) - y(t)), \end{aligned} \tag{9.54}$$
$$\begin{aligned} \partial_t \hat{b}_i(t,x) - \mu_i \partial_x \hat{b}_i(t,x) &= H_i^b(x) \hat{a}_1(t,1) + F_i^b(x) y(t) + K_i^b(x) U(t) \\ &\quad + G_i^b(x)(\hat{b}_2(t,0) - y(t)), \end{aligned} \tag{9.55}$$

with the boundary conditions

$$\hat{a}_1(t,0) = q_{11} \hat{b}_1(t,0),\ \hat{b}_1(t,1) = \rho_{11} \hat{a}_1(t,1) + \rho_{12} y(t) + U(t), \tag{9.56}$$
$$\hat{a}_2(t,0) = q_{22} y(t) + q_{21} a_1(t,1),\ \hat{b}_2(t,1) = \rho_{22} \hat{a}_2(t,1). \tag{9.57}$$

The piecewise-continuous functions G_i^a and G_i^b still have to be defined. The initial conditions of system (9.54)-(9.57) are arbitrary H^1-functions that satisfy the appropriate compatibility conditions. We define $\tilde{a}_i = a_i - \hat{a}_i$ and $\tilde{b}_i = b_i - \hat{b}_i$ the error states. They verify

$$\partial_t \tilde{a}_i(t,x) + \lambda_i \partial_x \tilde{a}_i(t,x) = H_i^a(x) \tilde{a}_1(t,1) + G_i^a(x) \tilde{b}_2(t,0), \tag{9.58}$$

$$\partial_t \tilde{b}_i(t,x) - \mu_i \partial_x \tilde{b}_i(t,x) = H_i^b(x)\tilde{a}_1(t,1) + G_i^b(x)\tilde{b}_2(t,0), \tag{9.59}$$

with the boundary conditions

$$\tilde{a}_1(t,0) = q_{11}\tilde{b}_1(t,0),\ \tilde{b}_1(t,1) = \rho_{11}\tilde{a}_1(t,1), \tag{9.60}$$

$$\tilde{a}_2(t,0) = q_{21}\tilde{a}_1(t,1),\ \tilde{b}_2(t,1) = \rho_{22}\tilde{a}_2(t,1). \tag{9.61}$$

This error system can be expressed using an abstract operator formulation:

$$\frac{d}{dt}\begin{pmatrix}\tilde{a}_1 & \tilde{b}_1 & \tilde{a}_2 & \tilde{b}_2\end{pmatrix}^\top = (\tilde{A} + \mathcal{G}C)\begin{pmatrix}\tilde{a}_1 & \tilde{b}_1 & \tilde{a}_2 & \tilde{b}_2\end{pmatrix}^\top, \tag{9.62}$$

where the operator $\tilde{A}$ is defined by

$$\begin{aligned}\tilde{A} : D(\tilde{A}) \subset L^2([0,1],\mathbb{R}^2) &\to L^2([0,1],\mathbb{R}^2)\\ \begin{pmatrix}\tilde{a}_1\\ \tilde{b}_1\\ \tilde{a}_2\\ \tilde{b}_2\end{pmatrix} &\longmapsto \begin{pmatrix}-\lambda_1\partial_x\tilde{a}_1(1) + H_1^a(\cdot)\tilde{a}_1(1)\\ \mu_1\partial_x\tilde{b}_1 + H_1^b(\cdot)\tilde{a}_1(1)\\ -\lambda_2\partial_x\tilde{a}_2 + H_2^a(\cdot)\tilde{a}_1(1)\\ \mu_2\partial_x\tilde{b}_2 + H_2^b(\cdot)\tilde{a}_1(1)\end{pmatrix},\end{aligned} \tag{9.63}$$

with a domain $D(\tilde{A}) = \{(\tilde{a}_1,\tilde{b}_1,\tilde{a}_2,\tilde{b}_2) \in (H^1([0,1],\mathbb{R})^4,\ \tilde{a}_1(0) = q_{11}\tilde{b}_1(0),\ \tilde{a}_2(0) = q_{21}\tilde{a}_1(1),\ \tilde{b}_1(1) = \rho_{11}\tilde{a}_1(1),\ \tilde{b}_2(1) = \rho_{22}\tilde{a}_2(1)\}$. Finally, the operator $\mathcal{G}$ is defined on $\mathbb{R}$ by $\mathcal{G}(x) = (G_1^a(x), G_1^b(x), G_2^a(x), G_2^b(x))$. We have the following lemma

Lemma 9.4.1 *If Assumption 9.1.4 is verified then* $\forall s \in \mathbb{C}, \ker(s - \tilde{A}) \cap \ker(C) = \{0\}$.

Proof : The proof is analogous to the one of Lemma 9.2.1. ■

Design of the observer gains

The objective is to design the gains G_i^a and G_i^b such that the error system (9.58)-(9.61) exponentially converges to zero. Let us denote $\tilde{w}_1 = \tilde{a}_1(t,1)$ and $\tilde{w}_2 = \tilde{b}_2(t,0)$. Using the method of characteristics, we obtain for $t \geq \max\{\tau_1,\tau_2\}$

$$\tilde{w}_1(t) = \rho_{11}q_{11}\tilde{w}_1(t-\tau_1) + \int_0^{\tau_1} H_{11}^w(\nu)\tilde{w}_1(t-\nu) + H_{12}^w(\nu)\tilde{w}_2(t-\nu)d\nu, \tag{9.64}$$

$$\tilde{w}_2(t) = \rho_{22}q_{21}\tilde{w}_1(t-\tau_2) + \int_0^{\tau_2} H_{21}^w(\nu)\tilde{w}_1(t-\nu) + H_{22}^w(\nu)\tilde{w}_2(t-\nu)d\nu, \tag{9.65}$$

where

$$\begin{aligned}H_{11}^w(\nu) &= H_1^a(1-\lambda_1\nu)\mathbb{1}_{[0,\frac{1}{\lambda_1}]}(\nu) + q_{11}H_1^b(\mu_1\nu - \frac{\mu_1}{\lambda_1})\mathbb{1}_{]\frac{1}{\lambda_1},\tau_1]}(\nu),\\ H_{12}^w(\nu) &= G_1^a(1-\lambda_1\nu)\mathbb{1}_{[0,\frac{1}{\lambda_1}]}(\nu) + q_{11}G_1^b(\mu_1\nu - \frac{\mu_1}{\lambda_1})\mathbb{1}_{]\frac{1}{\lambda_1},\tau_1]}(\nu),\\ H_{21}^w(\nu) &= H_2^b(\mu_2\nu)\mathbb{1}_{[0,\frac{1}{\mu_2}]}(\nu) + \rho_{22}H_2^a(1-\lambda_2\nu + \frac{\lambda_2}{\mu_2})\mathbb{1}_{]\frac{1}{\mu_2},\tau_2]}(\nu),\\ H_{22}^w(\nu) &= G_2^b(\mu_2\nu)\mathbb{1}_{[0,\frac{1}{\mu_2}]}(\nu) + \rho_{22}G_2^a(1-\lambda_2\nu + \frac{\lambda_2}{\mu_2})\mathbb{1}_{]\frac{1}{\mu_2},\tau_2]}(\nu).\end{aligned}$$

The observability condition given in Lemma 9.4.1 can be rewritten as a spectral observability condition.

Lemma 9.4.2 *Define the holomorphic functions* $\tilde{F}_0(s) = 1 - \rho_{11}q_{11}\mathrm{e}^{-\tau_1 s} + \int_0^{\tau_1} H_1^w 1(\nu)\ \mathrm{e}^{-\nu s}d\nu$ *and* $\tilde{F}_1(s) = 1 - \rho_{22}q_{21}\mathrm{e}^{-\tau_2 s} + \int_0^{\tau_2} H_2^w 1(\nu)\mathrm{e}^{-\nu s}d\nu$. *If Assumption 9.1.4 is verified, then for all* $s \in \mathbb{C}$, $rank[\tilde{F}_0(s), \tilde{F}_1(s)] = 1$.

Proof : The proof is analogous to the one of Lemma 9.2.2. ■

Let us compute $\tilde{w}_1(t) - \int_0^{\tau_2} H_{22}^w(\nu)\tilde{w}_1(t-\nu)d\nu$. Using equation (9.65), we obtain

$$\tilde{w}_1(t) - \int_0^{\tau_2} H_{22}^w(\nu)w_1(t-\nu) = \rho_{11}q_{11}\tilde{w}_1(t-\tau_1) + \int_0^{\tau_1} H_{11}^w(\nu)\tilde{w}_1(t-\nu)d\nu -$$
$$\int_0^{\tau_2} \rho_{11}q_{11}H_{22}^w(\nu)\tilde{w}_1(t-\nu)d\nu - \int_0^{\tau_2} H_{22}^w(\nu)(\int_0^{\tau_1} H_{11}^w(\eta)\tilde{w}_1(t-\nu-\eta)d\eta)d\nu$$
$$- \int_0^{\tau_1} H_{12}^w(\nu)\rho_{22}q_{21}\tilde{w}_1(t-\nu)d\nu - \int_0^{\tau_1} H_{12}^w(\nu)(\int_0^{\tau_2} H_{21}^w(\eta)\tilde{w}_1(t-\nu-\eta)d\eta)d\nu$$

Analogous computations to the ones done in Section 9.3 give

$$\tilde{w}_1(t) = \rho_{11}q_{11}(t-\tau_1) + \int_0^{\tau_1} \tilde{I}_1(\nu)\tilde{w}_1(t-\nu)d\nu + \int_{\tau_1}^{\tau_2} \tilde{I}_2(\nu)\tilde{w}_1(t-\nu)d\nu$$
$$+ \int_{\tau_2}^{\tau_1+\tau_2} \tilde{I}_3(\nu)\tilde{w}_1(t-\nu)d\nu, \tag{9.66}$$

where $\tilde{I}_1$, $\tilde{I}_2$ and $\tilde{I}_3$ are respectively defined on $[0,\tau_1]$, $[\tau_1,\tau_2]$, and $[\tau_2,\tau_1+\tau_2]$ by

$$\tilde{I}_1(\nu) = H_{22}^w(\nu) + H_{11}^w(\nu) - \int_0^{\nu} H_{22}^w(\eta)H_{11}^w(\nu-\eta) + H_{12}^w(\eta)H_{21}^w(\nu-\eta)d\eta \tag{9.67}$$

$$\tilde{I}_2(\nu) = H_{22}^w(\nu) - \rho_{11}q_{11}H_{22}^w(\nu-\tau_1) - \int_{\nu-\tau_1}^{\nu} H_{22}^w(\eta)H_{11}^w(\nu-\eta)d\eta$$
$$- \int_0^{\tau_1} H_{12}^w(\eta)H_{21}^w(\nu-\eta)d\eta, \tag{9.68}$$

$$\tilde{I}_3(\nu) = -\rho_{11}q_{11}H_{22}^w(\nu-\tau_1) - \rho_{22}q_{21}H_{12}^w(\nu-\tau_2) - \int_{\nu-\tau_1}^{\tau_2} H_{22}^w(\eta)H_{11}^w(\nu-\eta)d\eta$$
$$- \int_{\nu-\tau_2}^{\tau_1} H_{12}^w(\eta)H_{21}^w(\nu-\eta)d\eta, \tag{9.69}$$

The following lemma states that we can find G_i^a, G_i^b such that the integral terms $\tilde{I}_i$ vanish.

Lemma 9.4.3 *Consider the functions $\tilde{I}_1$, $\tilde{I}_2$, and $\tilde{I}_3$ defined by equations* (9.67)-(9.69)*. There exist four unique piecewise continuous functions $(G_1^a, G_2^a, G_1^b, G_2^b)$ such that $I_1(\nu) = 0$ for $\nu \in [0,\tau_1[$, $I_2(\nu) = 0$ for $\nu \in [\tau_1,\tau_2[$, and $I_3(\nu) = 0$ for $\nu \in [\tau_2,\tau_1+\tau_2]$.*

Proof : Define $\tilde{g} = H_{22}^w$ and $\tilde{f} = \rho_{22}q_{21}H_{12}^w$. This change of coordinates is invertible since $\rho_{22}q_{21} \neq 0$ due to Assumption 9.1.1 and Assumption 9.1.2. We can then adjust the proof of Lemma 9.3.1 using Assumption 9.1.4 (expressing it for the target system (9.58)-(9.61)). It is then straightforward to compute the functions G_i^a and G_i^b. ■

Theorem 9.4.1 *Consider the functions $\tilde{I}_1$, $\tilde{I}_2$ and $\tilde{I}_3$ defined by equations* (9.67)-(9.69) *and let G_i^a and G_i^b be the unique piecewise continuous functions that lead to $I_1(\nu) = 0$ for all $\nu \in [0,\tau_2]$, $I_2(\nu) = 0$ for all $\nu \in]\tau_2,\tau_1]$, and $I_3(\nu) = 0$ for $\nu \in [\tau_1,\tau_2+\tau_1]$ (as stated in Lemma 9.3.1). Define the functions $(\hat{u}_i,\hat{v}_i) = \mathcal{M}_i(\hat{a}_i,\hat{b}_i)$, where $(\hat{\alpha}_i,\hat{\beta}_i)$ are solutions of the system* (9.54)-(9.57) *and where the transformations $\mathcal{M}_i$ are defined by equations* (9.47)-(9.48)*. Then, the states $(\hat{u}_i,\hat{v}_i)$ exponentially converge to the original states (u_i,v_i).*

Proof : Let us choose G_i^a and G_i^b such that $I_1(\nu) = 0$ for all $\nu \in [0,\tau_2]$, $I_2(\nu) = 0$ for all $\nu \in]\tau_2,\tau_1]$, and $I_3(\nu) = 0$ for $\nu \in [\tau_1,\tau_2+\tau_1]$. Then $\tilde{w}_1(t) = \rho_{11}q_{11}\tilde{w}_1(t-\tau_1)$ and consequently $\tilde{w}_1$ exponentially converges to zero. Computing $\tilde{w}_2(t) - \rho_{11}q_{11}\tilde{w}_2(t-\tau_1) - \int_0^{\tau_1} H_{11}(\nu)\tilde{w}_2(t-\nu)$, we can show that $\tilde{w}_2(t) = \rho_{11}q_{11}\tilde{w}_2(t-\tau_1)$ and that consequently w_2 is exponentially stable. It is then straightforward to conclude the proof using Theorem 6.1.3. ■

Since the boundary condition of the observer system contains non-strictly proper terms corresponding to the measurement, it may lead to some robustness issues. To avoid such a problem, it is possible to low-pass filter the output $y(t)$, as done for the control input. However, this step is not mandatory if the objective is the design of output-feedback controllers since the controllers are already low-pass filtered.

9.4.3 . Output-feedback controller

We can now combine the state observer designed in Section 9.4.2 with the full state feedback control law $U(t)$ designed in Section 9.3, to obtain an output feedback controller.

Theorem 9.4.2 *Consider the observer system* (9.54)-(9.57)*, with the appropriate observer gains defined as in Theorem 9.4.1. Define the functions* $(\hat{\alpha}_i, \hat{\beta}_i) = \mathcal{L}_i^{-1}(\mathcal{M}_i(\hat{a}_i, \hat{b}_i))$*, where the transformations* $\mathcal{L}_i$ *(resp.* $\mathcal{M}_i$*) are defined by equations* (9.16)-(9.17) *(resp.* (9.47)-(9.48)*). Consider the functions* f*,* g *defined as in Theorem 9.3.1. Then, the closed-loop system consisting of the plant* (9.2)-(9.4) *and the control law*

$$\begin{aligned} U(t) = &-\rho_{11} q_{11} \hat{\beta}_1(t-\tau_1, 1) - \rho_{12}\rho_{22}\hat{\alpha}_2(t-\tau_2, 0) + \bar{U}(t) \\ &- \int_0^{\tau_1} H_{11}(\nu)\hat{\beta}_1(t-\nu)d\nu - \int_0^{\tau_2} H_{12}(\nu)\hat{\alpha}_2(t-\nu, 0)d\nu, \end{aligned} \tag{9.70}$$

where $\bar{U} = \int_0^{\tau_2} f(\nu)\hat{\alpha}_2(t-\nu, 0)d\nu + \int_0^{\tau_1} g(\nu)\bar{U}(t-\nu)d\nu$ *is exponentially stable. Moreover, the control law* $U(t)$ *exponentially converges to zero and can be low-pass filtered such that the resulting filtered control operator is strictly proper while stabilizing the plant* (9.2)-(9.4)*.*

Proof : The control law $U(t)$ can be rewritten as the sum of the nominal control law designed in Theorem 9.3.1 to which is added an error term that is exponentially stable. Using the input-to-state stability of the system and the boundedness/invertibility of the different integral operators [LADMA18], we can show the simultaneous exponential convergence of the original system (9.2)-(9.4) and of the error system (9.58)-(9.61). ■

9.5 . Simulation results

In this section, we illustrate the performance of the proposed output-feedback controller with some simulation results. The numerical values of the parameters are $\begin{pmatrix}\lambda_1 \\ \lambda_2\end{pmatrix} = \begin{pmatrix}1 \\ 2\end{pmatrix}$, $\begin{pmatrix}\mu_1 \\ \mu_2\end{pmatrix} = \begin{pmatrix}1.3 \\ 1.8\end{pmatrix}$, $\begin{pmatrix}\sigma_1^+ \\ \sigma_2^+\end{pmatrix} = \begin{pmatrix}-0.5 \\ -0.3\end{pmatrix}$, $\begin{pmatrix}\sigma_1^- \\ \sigma_2^-\end{pmatrix} = \begin{pmatrix}0.8 \\ 0.7\end{pmatrix}$, $\begin{pmatrix}q_{11} & * \\ q_{21} & q_{22}\end{pmatrix} = \begin{pmatrix}1 & * \\ 0.6 & 0.9\end{pmatrix}$, $\begin{pmatrix}\rho_{11} & \rho_{12} \\ * & \rho_{22}\end{pmatrix} = \begin{pmatrix}0.3 & 0.8 \\ * & 0.9\end{pmatrix}$. The observer values are initialized to 0. We simulated our system on a time scale of 50s. As illustrated in Figure 9.2 (blue curve), the parameters are chosen such that the whole interconnected system remains unstable in open-loop. However, the closed-loop system with the control law (9.70) is exponentially stable, as expected. We have pictured in Figure 9.3a the corresponding control effort. Finally, we illustrate the performance of our observer on Figure 9.3b. The L^2-norm of the error state $(\tilde{u}_1, \tilde{v}_1, \tilde{u}_2, \tilde{v}_2)$ converges to zero, so the estimated states converge towards the real ones.

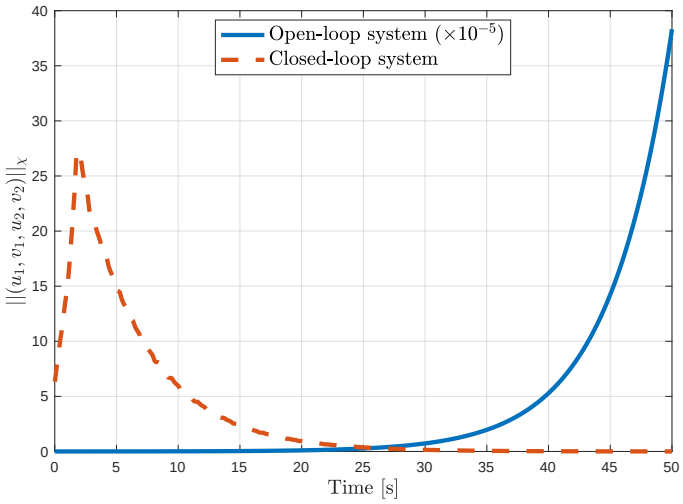

Figure 9.2: Time evolution of the χ-norm of the system (9.2)-(9.6) in open-loop (blue) and in closed-loop (red).

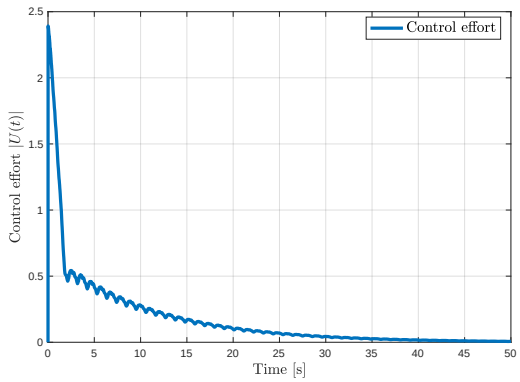

(a) Time evolution of the control effort $U(t)$.

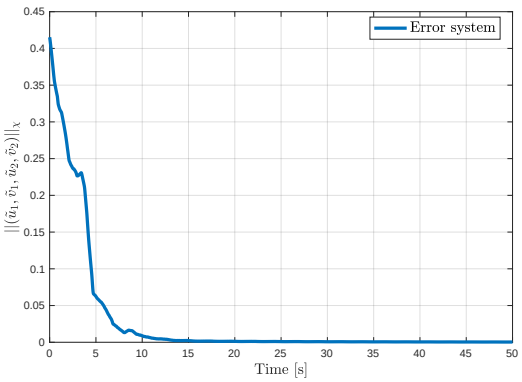

(b) Time evolution of the χ-norm of the error.

Figure 9.3: Time evolution of the control effort and of the χ-norm of the error state.

9.6 . Conclusions and perspectives

This chapter introduces a new methodology to stabilize a chain of two interconnected hyperbolic PDE subsystems for which the actuator and the measurement are located at the junction. Using a backstepping transformation, we have rewritten the original hyperbolic network as a set of simpler IDEs with pointwise and distributed control terms. Then, we introduced a set of candidate control inputs expressed as distributed delayed feedback of the state and the input. We have shown that a control law from this set stabilizes the system if an associated set of Fredholm equations admits a solution. Interestingly, spectral controllability conditions implied the existence of solutions for these integral equations. Following a similar path, we could design state observers and obtain an output-feedback controller. We believe that our constructive approach can be extended to a larger number of non-scalar subsystems. It could also be combined with the results of Chapter 8 to tackle a wider diversity of physical systems with an arbitrary number of PDEs or ODEs.

Interestingly, the proposed methodology could be a milestone for the control of underactuated systems. Consider, for instance, the following underactuated 1+2 hyperbolic system, in which only one of the two leftward-convecting equations is actuated

$$\partial_t w(t,x) + \Lambda \partial_x w(t,x) = \Sigma(x) w(t,x), \tag{9.71}$$

where $w(t,x) = (u(t,x), v_1(t,x), v_2(t,x))^T$, $\{(t,x) \text{ s.t. } t > 0, x \in [0,1]\}$, and with the following boundary conditions

$$u(t,0) = q_1 v_1(t,0) + q_2 v_2(t,0), \tag{9.72}$$

$$v_1(t,1) = \rho_1 u(t,1) + U(t), \; v_2(t,1) = \rho_2 u(t,1). \tag{9.73}$$

The diagonal matrix Λ is given by $\Lambda = \text{diag}(\lambda, -\mu_1, -\mu_2)$, where the different velocities λ, μ_1, μ_2 are assumed to be constant and positive. The components of the matrix Σ are continuous functions. Such a system was stabilized in [ABABP20] under restrictive assumptions since the authors assumed exponentially stable actuation dynamics. Rewriting the system as an IDE with distributed actuation, it is possible to adjust the techniques proposed in this chapter to obtain a stabilizing controller under appropriate controllability conditions.

10 - Application to the estimation of the drill bit source signature in a drilling device

In this chapter, we apply the theoretical findings of the previous chapters to an application case. More precisely, we propose a **sensing and computational framework** to estimate the drill bit source signature during drilling operations. The proposed methodology is adjusted from the approach proposed in Chapter 8.

A drilling device comprises three components: the surface drill rig, which includes a rotating mechanism (usually a rotary table or a top drive suspended over the drill floor by the traveling block), the drill string, and the Bottom Hole Assembly (BHA). The torsional and axial motions generated at the surface are transferred to the drill string and the BHA. The drill string is an interconnection of pipes that are steel tubes with a length of typically 10 m. These pipes are usually run in tension to avoid the effect of fatigue due to a potential helical buckling. They are hollow so that a mud pump can inject a drilling fluid to clean, cool, and lubricate the bit to evacuate the rock cuttings. The BHA comprises the bit (a rock-cutting device), a series of relatively heavy pipe sections known as drill collars (much thicker pipes that provide the necessary weight to perform the perforation), stabilizers (at least two spaced apart), which prevent the drill string from unbalancing, and "shock subs" that absorb vibrations between the bit and the drill-collars. While the BHA length remains constant, the drill pipes total length may increase as the borehole depth does. The weight exerted on the bit impacts the cutting process performance, measured by the Rate-Of-Penetration (ROP). The nature of the boundary conditions at the bit–rock interface is a critical aspect of the model and is discussed in detail below. This mechanical part is combined with a hydraulic system to maintain the Bottom-Hole Circulating Pressure (BHCP) between pre-specified constraints. Such a drilling system is schematically pictured in Figure 10.1.

While drilling, the interaction with the rock can generate significant vibrations, resulting in an inefficient ROP. It may also raise safety issues. These vibrations have been extensively studied in the literature [DA98, Jan93, SMLR11]. Among them, torsional oscillations, known as **stick-slip**, are characterized by a series of stopping – "sticking" – and releasing – "slipping" – events of the bit. These oscillations can reduce the Rate of Penetration, damage the well by causing fatigue on the equipment, and eventually lead to premature failure of the bit [KKD+99]. Such oscillations are caused by Coulomb friction-induced side forces [AS18] and non-linear frictional force actuating at the bit by contact with the rock [LvCK02, NW13]. Indeed, numerous models consider those stick-slip oscillations are related to the velocity-weakening of the frictional force at the bit (Stribeck-like effect) associated with typical dry friction profiles (static friction and dynamic friction) [Bre92, KHC+15]. However, the stick-slip phenomenon can also occur off-bottom and does not require a velocity weakening in the bit-rock interaction [BBHS89, ATK86, ZHS16]. In this context, to reduce the harmful effects of such vibrations and improve the performance of the drilling device, it appears necessary to clearly understand the dynamics of the drill string. A class of distributed models has been extensively analyzed in [AvdW19, GDD09]: the axial and torsional dynamics are described by a set of hyperbolic PDEs. A validation against field data for the corresponding torsional model has been proposed in [AS18]. Based on these distributed models, control mechanisms have been proposed to reduce the effects of undesirable vibrations in the system [vdWVvH+18, ADMS18a, ADMS18b]. However, such control mechanisms often depend on the properties of the drilled rock (which is a priori unknown). The dependence of the drill string dynamic response to the bit-rock interaction and rock properties is verified in [SDHC15]. Accordingly, estimating the drilled rock's characteristics (such as seismic velocity or intrinsic specific energy) appears necessary to improve drilling devices' performance. Estimating

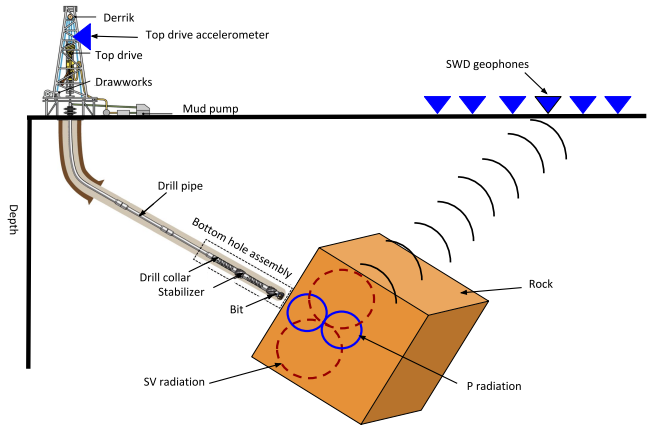

Figure 10.1: Schematic representation of the drilling and sensing system (Figure modified from [CCH+19]).

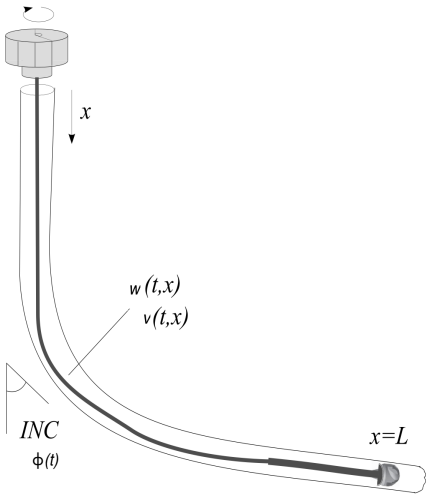

Figure 10.2: Schematic indicating the distributed drill string lying in deviated bore-hole.

rocks' seismic velocities while drilling is difficult as downhole sensors are expensive and may raise potential technical risks. **This chapter aims to design three algorithms that provide a near-real-time estimation of the rock's nature for a directional multi-sectional well**.

Drill bit-rock interactions generate compressional (P) and vertical components of shear (SV) waves. These waves propagate through the sub-surface and reach sensing devices (geophones or hydrophones). In onshore environments, geophones record the particle velocity, and hydrophones, in offshore environments, measure the pressure component. The drill bit-rock interaction wavefields recorded by the sensors near the surface are known as **Seismic While Drilling** (SWD) data surface [PM04]. Drill bit-rock interactions can also generate reflected wavefields that travel through the drill string. These wavefields can be recorded by accelerometers mounted on top-drive. The accelerometers provide hook-load and hook-speed measurements. The sensing tools give vital information about the sub-surface, which helps us efficiently model the drill string dynamics. SWD measurements can provide the drill bit position through check shots or sonic calibrations through reflectivity characterization [PM04] or provide subsurface structure around and ahead of the drill bit [KSI18, NKC+20b]. In drilling environments where recording the SWD data is not feasible or lacks quality, we need to explore alternative options. Here, we use the approach proposed in Chapter 8 to obtain expressions of the downhole force and velocity as functions of top-drive measurements. Then, we can use SWD data or classical parameter estimation techniques [BA77] on the downhole boundary condition to estimate the rock properties. These estimations can then improve state estimations and control strategies [AKIS20, NKC+20b]. We also propose an alternative approach based on machine learning [CBG90, GBC16].

The results of this chapter are inspired from [AKS+19, AKN21].

10.1 . Drill string model

In this section, we present a model that describes the mechanical dynamics of the drill string. This model is similar to the one presented in [AKS+19] and is inspired by [AvdW19, GDD09].

10.1.1 . Distributed Axial dynamics of the drill string

We model the dynamics of a directional drilling system of length L (Figure 10.2). In this model, x denotes the curvilinear abscissa, $x = 0$ is the top-drive position, and $x = L$ is the position of the drill bit. We denote $\phi(x)$ the well's inclination at the position x. Let us denote $\xi(t, x)$ the axial displacement of the drill string. It is a function of (t, x) evolving in $\{(t, x) \mid 0 < t < T,\ x \in$

$[0, L]\}$ (where T is a positive time). The axial force associated to ξ can be found from the strain, given as the local relative compression: $w(t,x) = AE\frac{(\xi(t,x)-\xi(t,x+dx))}{dx}$, A being the cross-sectional area of the drill string, E being its Young's modulus and $dx \to 0$ the infinitesimal axial position increment. The axial velocity satisfies $v(t,x) = \frac{\partial \xi(t,x)}{\partial t}$. These states are pictured in Figure 10.2. The drill string ratio diameter/length, typically less than 10^{-4}, implies that the drill string can be modeled using an Euler–Bernoulli beam model. More precisely, using the distributed model given in [DMA15, GvdWNS09], we can derive the dynamics of interest by assuming elastic deformations and using equations of continuity and state. The axial motion satisfies the following wave Partial Differential Equation

$$\frac{\partial^2 \xi}{\partial t^2}(t,x) - c_\xi^2 \frac{\partial^2 \xi}{\partial x^2}(t,x) = -k_\xi \frac{\partial \xi}{\partial t}(t,x) + \frac{\bar{\rho}}{\rho} g \sin(\phi(x)), \tag{10.1}$$

where $c_\xi = \sqrt{\frac{E}{\rho}}$, ρ being the pipe mass density and k_ξ is a damping coefficient representing the viscous shear stresses acting on the pipe. The term $h(x) = \frac{\bar{\rho}}{\rho} g \sin(\phi(x))$ accounts for the acceleration of gravity acting on the submerged weight $\bar{\rho}$. It is a simple (but still realistic and consistent) model for the gravitational force. From (10.1), we have that the axial force and velocity satisfy the following set of PDEs

$$\frac{\partial w(t,x)}{\partial t} + AE\frac{\partial v(t,x)}{\partial x} = 0, \tag{10.2}$$

$$\frac{\partial v(t,x)}{\partial t} + \frac{1}{A\rho}\frac{\partial w(t,x)}{\partial x} = -k_\xi v(t,x) + h(x). \tag{10.3}$$

The topside weight on the drill string, $w(t,0)$, corresponds to the system actuation. The downhole boundary condition at $x = L$ is obtained from a force balance on the lumped Bottom-Hole Assembly (BHA). These two boundary conditions will be introduced below. Model (10.2)-(10.3) does not consider the Coulomb friction between the drill string and the borehole, also known as the side force. It has been shown in [AS18] that for torsional oscillations, the normal component of this Coulomb friction term (usually modeled using a differential inclusion) can have significant effects on stability, even when the bit is off-bottom since it can be a source of stick-slip. Consequently, the axial components of such Coulomb non-linear friction terms may also have a non-negligible effect on the dynamics (even if this has not been broadly studied in the literature) [BVDWN11]. We choose not to include this differential inclusion in our model to simplify the design of our different algorithms. The proposed model (10.2)-(10.3) has been extensively analyzed in [AvdW19, GDD09]. All the trends the models predict are supported by field measurements [RGD07]. Moreover, validation against field data (at least for the torsional part of the model) has been proposed in [AS18].

10.1.2 . Discontinuities of a multiple sectioned drill string

The lower part of the drill string is usually made up of drill collars that may greatly impact the global dynamics due to their inertia [AA16]. In particular, these pipes may have different lengths, densities, inertia, or Young's modulus. This change in the characteristic line impedance may cause reflections in the traveling waves. Let us assume we have N different sections ($N \in \mathbb{N}$), and let us denote x_i the spatial coordinate of the junction point between the $(i-1)^{\text{th}}$-section and the i^{th}-section. Let us denote $x_1 = 0$, $x_{N+1} = L$ and $(w^i(t,x), v^i(t,x))$ the force and velocity along the i^{th} section of the drill string. The corresponding physical parameters will also be expressed using the superscript i (for instance, ρ^i will be the density of the i^{th} section). The boundary conditions at the transition are given by the following continuity constraints

$$v^i(t,x_{i+1}) = v^{i+1}(t,x_{i+1}), \quad w^i(t,x_{i+1}) = w^{i+1}(t,x_{i+1}). \tag{10.4}$$

When there is no ambiguity, this superscript will be omitted to ease the notations.

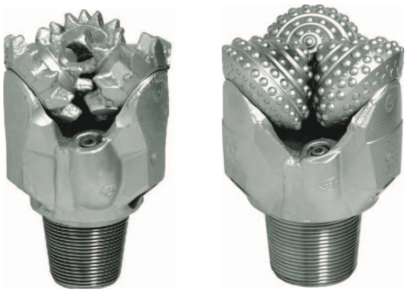

Figure 10.3: Roller-cone bits used in softer and shallower formations (a); roller-cone bits used in deeper and harder formations (b) (Source: Adapted from [Fra10]).

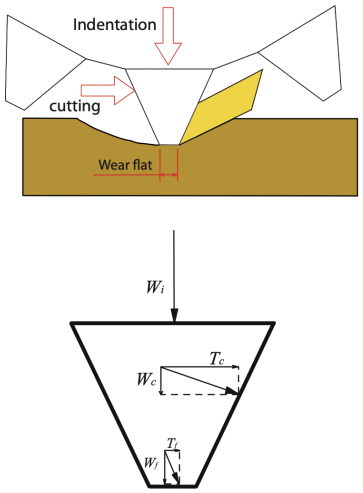

Figure 10.4: Forces acting on an inverted V shape tooth (Source: Adapted from [Fra10]).

10.1.3 . Topside boundary condition

The drill string is connected at the top to the *top-drive* suspended over the drill floor by the *traveling block*. Several drill lines connect this block, one attached to the deadline anchor and the other spooled on a drum controlled by AC induction motors [Cay18]. Thus, we can consider that the operator controls the weight on the drill string $w_0(t) = w(t, 0)$. This yields

$$-EA\frac{\partial \xi(t,x)}{\partial x}|_{x=0} = w_0(t), \tag{10.5}$$

where w_0 is considered as a (known) input.

10.1.4 . Downhole boundary condition: bit-rock interaction

In this section, we compute the downhole boundary condition. As the length of the BHA (≈ 200m) is much smaller than the one of the drill string (≈ 2000m), its effect can be lumped into an ODE coupled with the drill string [AAK19, DMA15]. Thus, the downhole boundary condition at $x = L$ can be obtained from a force balance on the lumped BHA. This yields

$$M_b\frac{\partial v}{\partial t}(t, L) = -w_b(v(t, L), w(t, L)) + w(t, L) + \frac{\bar{\rho}}{\rho}M_b g, \tag{10.6}$$

where M_b is the mass of the lumped BHA and $w_b(\cdot, \cdot)$ the force acting from the rock on the BHA through the drilling bit, known as the ***weight on bit*** (WOB). To express the bit-rock interface laws, we follow the approach developed in [RGD07] for drag bits (consistent with laboratory results). As suggested in [Fra10], the tool's action is decomposed into three independent processes: a pure cutting process taking place ahead of the cutting face, a pure indentation process, and a frictional contact process mobilized along with the interface between the wear flat and the rock. Integrating the effects of all the individual cutters, the weight-on-bit w_b can be decomposed into a contribution associated with the forces transmitted by the cutting face of each cutter (w_c), a contribution corresponding to the indentation process (w_i) and another corresponding to the forces acting on the cutter wear flats (w_f). In what follows, we choose to include the contribution w_i into w_f since both are constant. These two forces are pictured in Figure 10.4. Following the approach elaborated within the context of PDC bits [DRS08, AAK19], the cutting process is split into three successive regimes. A frictional contact process dominates the first phase (*Phase I*) due to bit dullness. During the second phase (*Phase II*), contact forces are fully mobilized, and additional forces contribute to cutting. Finally, during the

last phase (*Phase III*), the frictional contact forces increase due to insufficient hole cleaning. Ideally, drilling should be performed to the foundering point (Phase II/III transition). As shown in [AAK19], the expression of the WOB depends on the phase. We will assume that we are in Phase II (cutting phase) and that the depth of cut is greater than the combined depth of cut at Phase II/III transition. Consequently, the WOB is expressed as

$$w_b(v(t,L),w(t,L)) = w_f + w_c = w_f + Kd(t) = w_f + a\zeta\epsilon d(t), \tag{10.7}$$

where w_f is a friction weight independent of the bit velocity (and therefore constant) while $K = a\zeta\epsilon$, with a being the bit radius, ζ a characterization of the cutting angle and ϵ the intrinsic specific energy of the rock [DD92, RGD07]. The function $d(t)$ is the *combined depth of cut per revolution* [Cay18, GvdWNS09, RGD07]. It satisfies the following equation, $d(t) = \frac{v(t,L)}{\omega_{\text{bit}}(t)}$, where the bit angular velocity ω_{bit} is assumed known here. We have previously presented a fully validated torsional model to estimate ω_{bit}, which may be integrated into the present here through a coupling at the drill bit [AAS20]. Experimental evidence for the proposed expression of the weight-on-bit (equation (10.7)) for drag bits has been obtained with a small drilling machine in [DRS08]. For a roller-cone bit, such an expression has been validated in [Fra10] with a series of laboratory tests at atmospheric pressure conducted with an in-house designed drilling rig together with published experimental data. Thus, the boundary condition (10.6) rewrites as

$$M_b\frac{\partial^2\xi}{\partial t^2}(t,L) = -\frac{a\zeta\epsilon}{\omega_{\text{bit}}}\frac{\partial\xi(t,L)}{\partial t} - w_f - EA\frac{\partial\xi(t,L)}{\partial x} + \frac{\bar{\rho}}{\rho}M_b g. \tag{10.8}$$

10.1.5 . Problem under consideration

Our objective is to provide a near real-time **estimation of the nature of the drilled rock**, i.e., intrinsic energy ϵ or seismic velocity, to improve drill string dynamics estimation. To properly model the drill string dynamics, we need to know the seismic velocity of the drilled rocks. However, the seismic velocities provided by surface seismic processing may be inaccurate before drilling. The methodology we proposed to estimate the seismic velocities of rocks relies on the recursive framework designed in Chapter 8. As shown in Section 9.4.2, we can estimate the (delayed) downhole force and velocity. Then, we can apply one of the following estimation procedures:

1. The first algorithm uses **seismic-while-drilling** measurements. We first express the force exerted on the bit as a function of the (measured) top-drive force and velocity without depending on the downhole boundary condition or the subsurface. We estimate the rock's seismic velocity by combining this expression with the knowledge of far-field radial and angular displacements (obtained using seismic sensors).

2. The second algorithm directly uses the boundary condition (10.8). We express the force exerted on the bit and the corresponding velocity as functions of the (measured) top-drive force and velocity. Then, we apply signal filtering and parameters estimation techniques to equation (10.8) to obtain the intrinsic specific energy of the rock.

3. The last algorithm is based on a **machine learning approach**. Applying a Fast Fourier Transform (FFT) to the measured outputs (top-drive force and velocity) and choosing relevant attributes such as the dominant frequencies and their corresponding gains. Then, by pairing the relevant attributes to their corresponding ϵ, we run a neural network learning algorithm to train the model. The training is done with a set of thousand of simulations for which the parameters of interest are modified between each run.

10.2 . Expression of the drill bit axial force and velocity

Two of the three algorithms we introduce in this chapter require knowledge of the axial force and velocity exerted at the drill bit. Once the system has been rewritten in the Riemann coordinates [LeV02], we can obtain such estimations using the recursive methodology presented in Chapter 8.

10.2.1 . Derivation of Riemann invariants

On the set $\{(t,x)|\ 0<t<T,\ x\in[x_i,x_{i+1}]\}$, we define the Riemann invariants as

$$u^i(t,x)=(\frac{\partial}{\partial t}\xi^i(t,x)-c_\xi^i\frac{\partial}{\partial x}\xi^i(t,x))\mathrm{e}^{\frac{k_\xi^i}{2c_\xi^i}x}, \tag{10.9}$$

$$z^i(t,x)=(\frac{\partial}{\partial t}\xi^i(t,x)+c_\xi^i\frac{\partial}{\partial x}\xi^i(t,x))\mathrm{e}^{-\frac{k_\xi^i}{2c_\xi^i}x}. \tag{10.10}$$

Consequently, on each section, equation (10.1) rewrites

$$\frac{\partial}{\partial t}u^i(t,x)+c_\xi^i\frac{\partial}{\partial x}u^i(t,x)=-\frac{k_\xi^i}{2}\mathrm{e}^{\frac{k_\xi^i}{c_\xi^i}x}z^i(t,x)+h_1^i(x), \tag{10.11}$$

$$\frac{\partial}{\partial t}z^i(t,x)-c_\xi^i\frac{\partial}{\partial x}z^i(t,x)=-\frac{k_\xi^i}{2}\mathrm{e}^{-\frac{k_\xi^i}{c_\xi^i}x}u^i(t,x)+h_2^i(x), \tag{10.12}$$

where $h_1^i(x)=h(x)\mathrm{e}^{\frac{k_\xi^i}{2c_\xi^i}x}$ and $h_2^i(x)=h(x)\mathrm{e}^{-\frac{k_\xi^i}{2c_\xi^i}x}$. In the Riemann coordinates, the boundary conditions at the junctions (10.4) rewrite for $i<N+1$

$$z^i(t,x_{i+1})=a_1^iu^i(t,x_{i+1})+a_2^iz^{i+1}(t,x_{i+1}), \tag{10.13}$$

$$u^{i+1}(t,x_{i+1})=a_3^iu^i(t,x_{i+1})+a_4^iz^{i+1}(t,x_{i+1}), \tag{10.14}$$

where

$$a_1^i=\frac{1-Z^i}{1+Z^i}\mathrm{e}^{-\frac{k_\xi^i}{c_\xi^i}x_{i+1}},\ a_2^i=\frac{2Z^i}{1+Z^i}\mathrm{e}^{(\frac{k_\xi^{i+1}}{2c_\xi^{i+1}}-\frac{k_\xi^i}{2c_\xi^i})x_{i+1}},\ a_3^i=\frac{1}{Z^i}a_2^i,\ a_4^i=\frac{Z^i-1}{1+Z^i}\mathrm{e}^{\frac{k_\xi^{i+1}}{c_\xi^{i+1}}x_{i+1}},$$

where we have denoted the relative magnitude of the impedance as $Z^i=\frac{c_\xi^i}{E^iA^i}/\frac{c_\xi^{i+1}}{E^{i+1}A^{i+1}}$. The boundary condition (10.5) remains unchanged

$$u^1(t,0)=z^1(t,0)+\frac{2c_\xi^1}{E^1A^1}w_0(t), \tag{10.15}$$

while the boundary condition (10.8) rewrites

$$z(t,L)=-\mathrm{e}^{-\frac{k_\xi}{c_\xi}L}u(t,L)+2\mathrm{e}^{-\frac{k_\xi}{2c_\xi}L}X(t), \tag{10.16}$$

$$\dot{X}(t)=-\frac{a\zeta\epsilon}{M_b\omega_{\mathsf{bit}}}X(t)-\frac{w_f}{M_b}+\frac{\bar{\rho}}{\rho}g-\frac{EA_s}{2c_\xi M_b}(z(t,L)\mathrm{e}^{\frac{k_\xi}{2c_\xi}L}-u(t,L)\mathrm{e}^{-\frac{k_\xi}{2c_\xi}L}). \tag{10.17}$$

The system (10.11)-(10.17) corresponds to a chain of N scalar PDE systems with an ODE at the end of the chain. Thus, it does not exactly fit the framework we considered in Chapter 8. However, the ODE subsystem satisfies similar properties to those required for the different PDE subsystems, and the methodology introduced in Chapter 8 can easily be extended here. Its application becomes even more straightforward as the different PDE subsystems are scalar.

10.2.2 . Expression of the downhole velocity and force

As in Chapter 8, the objective is first to express our PDEs as time-delay equations before applying a recursive procedure to obtain a (delayed) estimation of the downhole states. Consider the backstepping transformations

$$\alpha^i(t,x)=u^i(t,x)+\int_{x_i}^x(K_i^{uu}(x,y)u^i(t,y)+K_i^{uz}(x,y)z^i(t,y))dy, \tag{10.18}$$

$$\beta^i(t,x) = z^i(t,x) + \int_{x_i}^{x} (K_i^{zu}(x,y)u^i(t,y) + K_i^{zz}(x,y)z^i(t,y))dy, \tag{10.19}$$

where the kernels $K_i^{uu}, K_i^{zu}, K_i^{uz}$ and K_i^{zz} are continuous functions defined on the domain $\mathcal{T}_i = \{(x,y) \in [x_i, x_{i+1}]^2,\ y \leq x\}$. They satisfy a set of PDEs given in [AKS+19] (replacing 0 by x_i). These kernels can be explicitly computed following the approach given in [AKS+19]. The states α^i and β^i satisfy the following set of transport PDEs

$$\frac{\partial}{\partial t}\alpha^i(t,x) + c_\xi^i \frac{\partial}{\partial x}\alpha^i(t,x) = -c_\xi^i K_i^{uz}(x,x_i)\beta^i(t,x_i) + h_3^i(x), \tag{10.20}$$

$$\frac{\partial}{\partial t}\beta^i(t,x) - c_\xi^i \frac{\partial}{\partial x}\beta^i(t,x) = c_\xi^i K_i^{zu}(x,x_i)\alpha^i(t,x_i) + h_4^i(x). \tag{10.21}$$

where

$$h_3^i(x) = h_1^i(x) + \int_{x_i}^{x} K_i^{uu}(x,y)h_1(y) + K_i^{uv}(x,y)h_2(y)dy,$$

$$h_4^i(x) = h_2^i(x) + \int_{x_i}^{x} K_i^{vu}(x,y)h_1(y) + K_i^{vv}(x,y)h_2(y)dy.$$

Applying the method of characteristics, we obtain

$$\begin{aligned} w^i(t,x_{i+1}) &= \frac{E^iA^i}{2c_\xi^i}(\mathrm{e}^{-\frac{k_\xi^i\Delta_i}{2c_\xi}} v^i(t-\frac{\Delta_i}{c_\xi^i},x_i) - \mathrm{e}^{\frac{k_\xi^i\Delta_i}{2c_\xi^i}} v^i(t+\frac{\Delta_i}{c_\xi^i},x_i)) + \frac{1}{2}(\mathrm{e}^{-\frac{k_\xi^i\Delta_i}{2c_\xi^i}} w^i(t-\frac{\Delta_i}{c_\xi^i},x_i) \\ &+ \mathrm{e}^{\frac{k_\xi^i\Delta_i}{2c_\xi^i}} w^i(t+\frac{\Delta_i}{c_\xi^i},x_i)) + \int_{-\frac{\Delta_i}{c_\xi^i}}^{\frac{\Delta_i}{c_\xi^i}} (\mathrm{e}^{\frac{k_\xi^i}{2c_\xi^i}x_i} f_u^i(s) + \mathrm{e}^{-\frac{k_\xi^i}{2c_\xi^i}x_i} f_z^i(s))v^i(t-s,x_i)ds \\ &+ \int_{-\frac{\Delta_i}{c_\xi^i}}^{\frac{\Delta_i}{c_\xi^i}} \frac{c_\xi^i}{EA}(\mathrm{e}^{\frac{k_\xi^i}{2c_\xi^i}x_i} f_u^i(s) - \mathrm{e}^{-\frac{k_\xi^i}{2c_\xi^i}x_i} f_z^i(s))w^i(t-s,x_i)ds + G_w^i, \end{aligned} \tag{10.22}$$

and

$$\begin{aligned} v^i(t,x_{i+1}) &= \frac{1}{2}(\mathrm{e}^{-\frac{k_\xi^i\Delta_i}{2c_\xi}} v^i(t-\frac{\Delta_i}{c_\xi^i},x_i) + \mathrm{e}^{\frac{k_\xi^i\Delta_i}{2c_\xi^i}} v^i(t+\frac{\Delta_i}{c_\xi^i},x_i)) + \frac{c_\xi^i}{2E^iA^i}(\mathrm{e}^{-\frac{k_\xi^i\Delta_i}{2c_\xi^i}} w^i(t-\frac{\Delta_i}{c_\xi^i},x_i) \\ &- \mathrm{e}^{\frac{k_\xi^i\Delta_i}{2c_\xi^i}} w^i(t+\frac{\Delta_i}{c_\xi^i},x_i)) + \int_{-\frac{\Delta_i}{c_\xi^i}}^{\frac{\Delta_i}{c_\xi^i}} (g_u^i(s)\mathrm{e}^{\frac{k_\xi^i}{2c_\xi^i}x_i} + g_z^i(s)\mathrm{e}^{-\frac{k_\xi^i}{2c_\xi^i}x_i})v^i(t-s,x_i)ds \\ &+ \int_{-\frac{\Delta_i}{c_\xi^i}}^{\frac{\Delta_i}{c_\xi^i}} \frac{c_\xi^i}{EA}(g_u^i(s)\mathrm{e}^{\frac{k_\xi^i}{2c_\xi^i}x_i} - g_z^i(s)\mathrm{e}^{-\frac{k_\xi^i}{2c_\xi^i}x_i})w^i(t-s,x_i)ds + G_z^i, \end{aligned} \tag{10.23}$$

where $\Delta_i = x_{i+1} - x_i$, where f_u^i, f_z^i , g_u^i and g_z^i are defined by

$$\begin{aligned} f_u^i(s) &= \frac{E^iA^i}{2}(\mathrm{e}^{-\frac{k_\xi^i x_{i+1}}{2c_\xi}} (f_1)_i^u(s) - \mathrm{e}^{\frac{k_\xi^i x_{i+1}}{2c_\xi^i}} (f_1)_i^z(s)), \\ f_z^i(s) &= \frac{E^iA^i}{2}(\mathrm{e}^{-\frac{k_\xi^i x_{i+1}}{2c_\xi^i}} (f_2)_i^u(s) - \mathrm{e}^{\frac{k_\xi^i x_{i+1}}{2c_\xi^i}} (f_2)_i^z(s)), \\ g_u^i(s) &= \frac{c_\xi^i}{2}(\mathrm{e}^{-\frac{k_\xi^i x_{i+1}}{2c_\xi}} (f_1)_i^u(s) + \mathrm{e}^{\frac{k_\xi^i x_{i+1}}{2c_\xi^i}} (f_1)_i^z(s)), \\ g_z^i(s) &= \frac{c_\xi^i}{2}(\mathrm{e}^{-\frac{k_\xi^i x_{i+1}}{2c_\xi^i}} (f_2)_i^u(s) + \mathrm{e}^{\frac{k_\xi^i x_{i+1}}{2c_\xi^i}} (f_2)_i^z(s)). \end{aligned}$$

and where

$$G_w^i = \frac{E^i A^i}{2c_\xi^i}(\mathrm{e}^{-\frac{k_\xi^i}{2c_\xi^i}x_{i+1}} H_u^i - \mathrm{e}^{\frac{k_\xi^i}{2c_\xi^i}x_{i+1}} H_z^i), \quad G_z^i = \frac{1}{2}(\mathrm{e}^{-\frac{k_\xi^i}{2c_\xi^i}x_{i+1}} H_u^i + \mathrm{e}^{\frac{k_\xi^i}{2c_\xi^i}x_{i+1}} H_z^i),$$

the functions H_u^i and H_z^i being defined by

$$\begin{aligned} H_u^i = &\int_0^{\frac{\Delta_i}{c_\xi^i}} h_3^i(x_{i+1} - c_\xi^i y)dy + \int_{x_i}^{x_{i+1}} \int_0^{\frac{y-x_i}{c_\xi^i}} (L_i^{\alpha\alpha}(x_{i+1}, y)h_3^i(y - c_\xi^i \nu) \\ &- L_i^{\alpha\beta}(x_{i+1}, y)h_4^i(y - c_\xi^i \nu))d\nu dy. \\ H_z^i = &- \int_0^{\frac{\Delta_i}{c_\xi^i}} h_4^i(x_{i+1} - c_\xi^i y)dy + \int_{x_i}^{x_{i+1}} \int_0^{\frac{y-x_i}{c_\xi^i}} (L_i^{\beta\alpha}(x_{i+1}, y)h_3^i(y - c_\xi^i \nu) \\ &- L_i^{\beta\beta}(x_{i+1}, y)h_4^i(y - c_\xi^i \nu))d\nu dy, \end{aligned}$$

the kernels $L_i^{\cdot\cdot}$ being the inverse kernels associated to the kernels $K_i^{\cdot\cdot}$ (see [AKN21] for details). Equations (10.22) and (10.23) allow us to compute the velocity and the force at the point $x = x_{i+1}$ simply knowing past and futures values of these states at the point $x = x_i$. Using the continuity of the force and velocity at each junction, we can iterate the procedure and consequently express the downhole velocity and force as functions of past and futures values of the topside states (the total time-delay window being $[-\sum_{i=1}^N \frac{\Delta_i}{c_\xi^i}, \sum_{i=1}^N \frac{\Delta_i}{c_\xi^i}]$). Interestingly, such an expression does not directly depend on the downhole boundary condition. It is now possible to use the **drill bit source signature** to estimate the nature of the drilled rock.

10.3 . Estimation of the specific intrinsic energy

The **intrinsic specific energy** refers to the energy required to cut a unit volume of rock. This value depends on cutter geometry, depth of cut, and rock. However, similar to scratch test studies in rock mechanics, we assume that the specific intrinsic energy is a constant quantity characterizing a particular combination of cutter geometry and rock. This section presents three different algorithms to estimate the parameter ϵ and discusses their advantages and drawbacks.

10.3.1 . Wavelet-based approaches

The two first algorithms we present are based on the drill bit source signature knowledge. The first one combines the drill bit force and velocity estimation with Seismic While Drilling (SWD) techniques, while the second one estimates the parameter ϵ directly from the model.

Seismic While Drilling estimation (Algo. 1)

We now estimate intrinsic specific energy for different rocks using SWD data. Richard and Dagrain [RDPD12], by using different rock types, have studied the relationship between the parameter ϵ and the Uniaxial Compressive Strength (UCS). They have shown that by expressing the ϵ as stress rather than energy, the parameter ϵ is correlated with UCS

$$\epsilon(MPa) = UCS(MPa). \tag{10.24}$$

Several recent works aimed to relate the rock strength to the seismic velocity of primary wave [SS08]. For example, by comprehensive analysis of different rock types, ranging from sedimentary to metamorphic, it was shown that the seismic velocity of the primary wave and UCS are linearly correlated [SS08]. The relationship is as follows

$$UCS = 0.0642V_p - 117.99, \tag{10.25}$$

where $V_p(m/s)$ is the seismic velocity of the primary wave. This relationship was derived from linear regression, and a strong correlation of $R^2 = 0.9022$ was reported. By plugging equation (10.25) into equation (10.24), we get

$$\epsilon \approx 0.0642 V_p - 117.99. \tag{10.26}$$

Hence, by knowing the rock's seismic velocity that the system is drilling into, the estimation of ϵ is possible. Next, we show how to estimate the velocities of rocks while drilling. SWD measurements record the radiated elastic energy from the drill bit rock interaction that travels through the earth's structure. For example, variations in the amplitude of P-waves and S-waves direct arrivals in the processed SWD measurements, after removing the source signature, reflect the changes in the rock properties near the drill bit. In other words, changes in the energy of P-waves and S-waves direct arrivals can imply that the bit is turning right and that the trajectory of the well is modified. The direct arrivals can be used in a relative sense to infer the relative changes in the rock properties, such as their seismic velocities or unconstrained rock strengths [AKIS20]. However, the radiation patterns of the direct arrivals depend on the V_p and V_s velocities of the rock interacting with the drill bit [RIH92]. For a deviated well with an inclination angle of γ, the radiation pattern for the primary wave is as follows

$$U_{r_j}(r_j, \phi_j, t) = \frac{A_1 \cos(\phi_j + \gamma)}{\rho_f V_p^2 r_j} \hat{w}(t - \frac{r_j}{V_p}, L), \tag{10.27}$$

where r_j is the distance from the drill bit to the j^{th} receiver near the surface, ϕ_j is the opening angle between the drill bit and j^{th} receiver, measured relative to z axis, γ is the inclination angle of the drill string, which is measured as a deviation angle with respect to z axis, t is time, L is the length of the drill string, ρ_f is the density of the interacting rock with the drill bit, $\hat{w} = w \odot w$ is the auto-correlation of drill bit source signature, A_1 is a constant, and U_{r_j} is the far field radial component of the primary wave radiation pattern recorded by the j^{th} receiver. In most rocks we have $\rho_f = 1.74 V_p^{0.25}$, hence equation (10.25) simplifies to

$$U_{r_j}(r_j, \phi_j, t) = \frac{A_1 \cos(\phi_j + \gamma)}{1.74 V_p^{2.25} r_j} \hat{w}(t - \frac{r_j}{V_p}, L). \tag{10.28}$$

Similarly, the far-field radiation pattern for secondary wave reads

$$U_{\phi_j}(r_j, \phi_j, t) = \frac{A_1 \sin(\phi_j + \gamma)}{1.74 V_p^{0.25} V_s^2 r_j} \hat{w}(t - \frac{r_j}{V_s}, L). \tag{10.29}$$

By matching the direct arrivals of the primary wave in the source compensated SWD data to the radiation pattern in equation (10.28), we can estimate the primary velocity of rock interacting with the drill bit. However, there are three unknowns in equation (10.28), i.e., V_p, A_1, and w. Hence, first, we need to estimate the drill bit source signature. Using the previously described recursive estimation procedure, we can consider as available the (delayed) values of the downhole force, i.e., drill bit source signature. Thus, the only unknowns in equation (10.28) are the scaling factor A_1 and the primary velocity of rock V_p. The cross-correlation of the estimated source signature with the SWD data gives the primary and secondary direct arrivals. By least-squares matching of the primary direct arrivals in the source compensated SWD data, $U_{r_j}^{obs}(r_j, \phi_j, t)$, with the radiation pattern represented in equation (10.28) and after plugging the auto-correlation of the estimated source signature, we estimate the primary wave velocity of the rock by minimizing the following cost function

$$\{\hat{A}_1, \hat{V}_p\} = \underset{A_1, V_p}{\operatorname{argmin}} \sum_{i=1}^{N} \sum_{j=1}^{M} (U_{r_j}^{obs}(r_j, \phi_j, t_i) - U_{r_j}^{cal}(r_j, \phi_j, t_i))^2, \tag{10.30}$$

where $U_{r_j}^{cal}$ is the radiation pattern of primary wave estimated by using equation (10.28), N is the number of time samples in the data, and M is the number of receivers or channels that are recoding the SWD data. Equation (10.30) is solved by the least-squares matching method. Finally, after

estimating the primary wave velocity of rock, we estimate ϵ using (10.26). After solving for V_p, we can also apply the same procedure to estimate the secondary velocity of rocks V_s. To do so, we minimize

$$\hat{V_s} = \underset{V_s}{\operatorname{argmin}} \quad \sum_{i=1}^{N}\sum_{j=1}^{M}(U_{\phi_j}^{obs}(r_j,\phi_j,t_i) - U_{\phi_j}^{cal}(r_j,\phi_j,t_i))^2. \tag{10.31}$$

Equation (10.31) is solved by the least-squares matching method, as well. Note that, after solving equation (10.30), the values of V_p, and A_1 are known. So, by plugging the estimates of V_p, A_1, and the auto-correlation of drill bit source signature into the cost function of equation (10.31), the only unknown is V_s. By having the estimates of V_p, and V_s, the $\frac{V_p}{V_s}$ ratio can be further used to identify reservoir fluids [GCD97]. Although this algorithm requires several seismic sensors, the corresponding advantage is increased robustness.

Direct estimation from equation (10.8) **(Algo. 2)**

Again, applying our recursive methodology, we can consider the (delayed) values of the downhole force and velocity as available. The specific intrinsic energy of the rock naturally appears in equation (10.8). Regarding the term $\frac{\partial^2 \xi}{\partial t^2}(t,L)$ (that corresponds to $\frac{\partial v}{\partial t}(t,L)$) that appears in equation (10.8), we can obtain it by differentiating the estimated downhole velocity $v(t,L)$. Of course, the corresponding signals should be low-pass filtered to minimize the negative effects of the boosted high-frequency noise. Equation (10.8) rewrites as $\psi(t) = \epsilon\phi(t) + C$, where ϕ and ψ are *known* functions defined by

$$\psi(t) = M_b\frac{\partial v}{\partial t}(t,L) - w(t,L), \quad \phi(t) = \frac{a\zeta}{\omega_{\text{bit}}(t)}v(t), \tag{10.32}$$

and where C is a constant that is defined by

$$C = -w_f + \frac{\bar{\rho}}{\rho}M_b g. \tag{10.33}$$

Note that the term C is potentially unknown (due to the term w_f). Then, it becomes possible to use **parameter estimation techniques** (such as Recursive Least Squares) to estimate the unknown parameters ϵ and B. More precisely, these parameters are estimated by minimizing the following cost function

$$\{\hat{\epsilon},\hat{C}\} = \underset{\epsilon,C}{\operatorname{argmin}} \quad \sum_{i=1}^{N}(\hat{\psi}(t_i) - \epsilon\hat{\phi}(t_i) - C)^2, \tag{10.34}$$

where $\hat{\phi}$ and $\hat{\psi}$ are the estimations of the functions ϕ and ψ obtained using the recursive methodology. It is worth mentioning that with this procedure, the gravitational forces (i.e., the functions G_w^i and G_z^i that appear in equations (10.22) and (10.23)) do not need to be estimated since these constant terms could be embedded into the term C. The main advantage of this approach is that it is easy to implement and only requires top-drive measurements and knowledge of the different physical parameters of the well. However, such a procedure may be sensitive to noise or sensor defaults. To reduce the noise negative effects, we can **filter** the measured signals with a low-pass filter (Butterworth filter, for instance). Finally, this procedure strongly depends on the accuracy of our model to describe the bit-rock interaction.

10.3.2 . Machine Learning estimation (Algo. 3)

The last procedure we present in this paper is based on Machine Learning [GBC16]. It does not require any specific knowledge of the system (no model is needed). Using adaptive neural networks, machine learning algorithms have already been used in control applications in [FWYL20] or in [YSLL20]. Since the measured outputs (top-drive force and velocity) somehow depend on the rock's intrinsic specific energy, their spectrum should contain sufficient information to distinguish the drilled rock's nature. We can obtain these signals spectra by applying a Fast Fourier Transform (FFT) to the measured outputs (top-drive force and velocity). Let us denote $y(t)$ as the continuous output. In

practice, this signal is not continuous but sampled (with a sampling rate that depends on our sensors quality). Let us denote Y, the vector obtained by concatenating all our measurements. Let us assume Y has N components (i.e., we have N measurements). Its discrete Fourier transform $\hat{Y}$ is a vector with N components defined by

$$\hat{Y}(k) = \sum_{n=1}^{N} y(k) \mathrm{e}^{-2\pi i * \frac{(k-1)(n-1)}{N}}. \tag{10.35}$$

The vector $\hat{Y}$ is a complex function with several attributes. Among them, we can cite the dominant peak (highest value of the modulus of $\hat{Y}$), the number of peaks, and the corresponding frequencies. The values of these attributes are somehow related to the value of ϵ. For a set of known physical parameters that characterize the well (including its geometry), we can run thousands of simulations, only modifying the unknown parameters (i.e., ϵ but also the potentially unknown friction weight) between each simulation. From this data set, for which the correct values of ϵ are known (since these data are simulated), similar to what is done by the human brain (*experience*), the machine learning algorithm will learn and find the suitable correlations between the previously defined attributes and the unknown parameter ϵ. Once adequately trained, the machine learning algorithm can be applied to predict new data sets (for which the parameter ϵ is unknown).

To solve this regression problem and correctly predict the parameter ϵ, we use a **neural network algorithm**. This kind of Machine Learning algorithm is efficient and easy to implement [GBC16]. Such a network consists of different connected nodes (that model the neurons of an actual brain) called artificial neurons. Each neuron receives different inputs and produces a single output that can be sent to other neurons. The output of each neuron is obtained by applying an *activation function* to a weighted sum of the inputs. This activation function is usually non-linear. Among the most commonly used activation functions, we can cite the *Sigmoid function* or the *tanh* function. More details on how to choose the activation function or the weight can be found in [GBC16, NIGM18]. A neural network can have several layers. The input of the first layers corresponds to the attributes we have chosen (in our case, the attributes that characterize the spectrum of the top-drive force and velocity), while the inputs for the next layers correspond to the neurons outputs in the previous layer. The global output of the neural network is the predicted value of ϵ. To train the network, we first simulate thousands of test points for which we know the correct output and measure the corresponding top-drive velocity. We generate the spectrum of the top-drive velocity signal for each simulation and choose a set of relevant features (such as the dominant peak and the corresponding frequency) that will constitute our dataset. While training our neural network, it appeared that the relevant attributes for learning are the two dominant gains (and their corresponding frequencies) of the top-drive velocity spectrum. This dataset is divided into two sets: the *training set* and the *testing set*. We first construct the network (i.e., we choose the number of neurons, layers, and weights) and train it on the training set. We then test its performance on the testing set by computing the mean squared error between the real values of ϵ and the predicted ones. We repeat the procedure, changing the parameters of the network and mixing the training and testing set (*cross-validation*). Finally, we choose the best network (i.e., the one for which the error is minimal) and train the algorithm with the available data. Our algorithm can then be used on unknown datasets.

Such a neural network algorithm is fast, reliable, and easy to implement. However, the main drawback is that it requires many data (i.e., the number of simulations) to train the algorithm. Moreover, changing the physical parameters or the well's geometry implies training the algorithm again with a new data set. The algorithm may also depend on the initial condition of the system and on the input (although this is not a real problem since we can always consider a rest state and the same input to estimate ϵ). A solution to increase the robustness could be to include these parameters in the neural network at the cost of producing more training points. Another approach to improving the generalizability of our approach is to use transfer learning concepts [YCBL14, THDS15, Kaz20] or transformers [VSP+17a] as their attention-based architecture allows them to capture complex patterns and dependencies while enabling better parallelization while outperforming recurrent networks in all domains.

Table 10.1: Numerical values of the parameters for the drill string model in Figure 10.5.

Param.	Value	Param.	Value	Param.	Value
E^1	2.25×10^{11} Pa	ρ^1	9000 kg/m^3	w_f	71280 N
c_ξ^1	5000 m/s	k_ξ^1	$0.23/s$	ζ	0.6
A^1	3.5×10^{-3} m^2	L	2000 m	a	0.1m
E^2	2.5×10^{11} Pa	ρ^2	8500 kg/m^3	ω_{bit}	5 rad/s
c_ξ^2	5423 m/s	k_ξ^2	$0.3/s$	M_b	27000 kg
A^2	5×10^{-2} m^2	x_1	1750 m		

10.4 . Simulation results

In this section, we test the performance of our different algorithms against simulated data. First, we evaluate the quality of the weight-on-bit estimations and the bit velocity provided by equations (10.22) and (10.23) in the presence of noisy measurements. Then, we will compare the efficiency of our three algorithms in estimating the nature of the rock interacting with the drill bit.

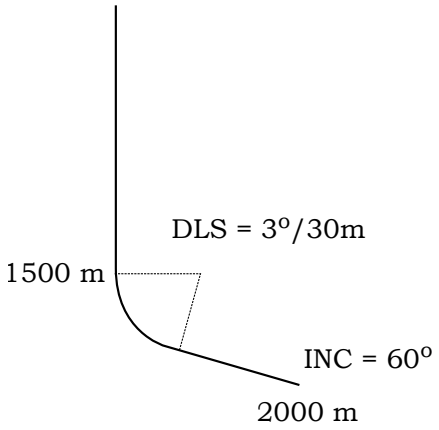

Figure 10.5: Wellbore survey of the well. The length of the drill string is 1750m.

The axial dynamics is simulated by adjusting the model of [AvdW19]. We consider the wellbore survey described in Figure 10.5. The control input w_0 is chosen as a constant to which is added a sinusoidal function. In the model's numerical implementation, the wave equation is transformed into transport equations discretized using a first-order upwind scheme. To guarantee numerical accuracy, we choose a sufficiently fine spatial grid. This is an amenable approach since the simulation speed is not critical for the present analysis (only the computational efforts of the estimation algorithms matter). All simulations use a spatial grid of 500 cells for the drill string. We choose the time-step such that the Courant-Friedrichs-Lewy (CFL) condition [CFL67] is satisfied. All the simulations use Matlab except the neural network algorithm, which uses Python.

10.4.1 . Estimation of the drill bit source signature

In this section, we evaluate the quality of our estimations in the case of a drill bit interacting with metamorphic rocks for which $\epsilon = 165$ Jcm^{-3}. The corresponding force-on-bit and bit velocity are denoted $w_{\text{bit}}^{\text{real}}$ and $v_{\text{bit}}^{\text{real}}$ while their estimations denoted $w_{\text{bit}}^{\text{est}}$ and $v_{\text{bit}}^{\text{rest}}$. These estimations are obtained using equations (10.22) and (10.23). The kernels $K^{\cdot\cdot}$ are computed using the method of characteristics and a fixed point algorithm (see [Aur18] for details). The different integrals are computed using a trapezoidal method with adjustable precision. We consider the case of a constant signal input with a periodic (sinusoidal) modulation. We have noisy measurements. We model the noise by a white Gaussian noise characterized by its **Signal-to-Noise Ratio** (SNR). As it is done in [KBS16], the SNR is defined as $SNR = \frac{a_{rms}^2}{\sigma_n^2}$, where a_{rms} is the root-mean-square amplitude of the noise-free

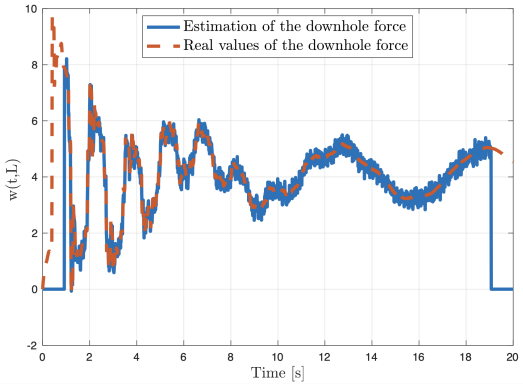

Figure 10.6: Comparison of the simulated normalized force-on-bit and of the estimated one using noisy top-drive measurements in the case of unconsolidated sands (SNR=10).

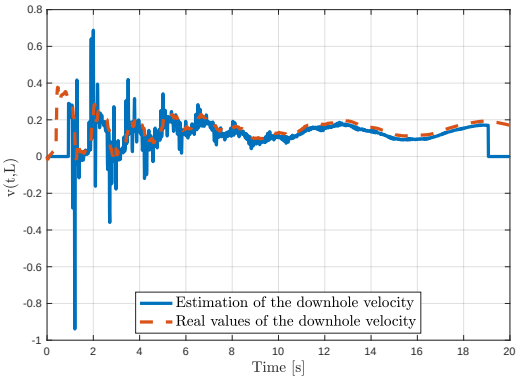

Figure 10.7: Comparison of the simulated normalized bit velocity and of the estimated one using noisy top-drive measurements in the case of unconsolidated sands (SNR=10).

signal, and σ_n^2 is the variance of the noise. Choosing a value for the SNR gives the corresponding amplitude for the white Gaussian noise. Note that the SNR value may differ for the velocity and force measurements. We compare the real force-on-bit with our estimation in Figure 10.6. The comparison between the real axial bit velocity and the estimated one is done in Figure 10.7. The SNR is equal to 10. The estimation is only performed for $\frac{x_1}{c_\xi^1} + \frac{L-x_1}{c_\xi^2} < t < T_f - (\frac{x_1}{c_\xi^1} + \frac{L-x_1}{c_\xi^2})$ since we cannot compute all the terms present in equations (10.22) and (10.23) out of this time interval (we recall that x_1 corresponds to the length of the pipe-section). To reduce the effect of the noise we use a second-order Butterworth low-pass filter on the noisy measurements. The functions $w_{\text{bit}}^{\text{real}}$ and $w_{\text{bit}}^{\text{est}}$ are plotted in Figure 10.6, while the functions $v_{\text{bit}}^{\text{est}}$ and $v_{\text{bit}}^{\text{est}}$ are plotted in Figure 10.7. We notice that despite the presence of noise, the estimations are comparable to the real states. For a space grid of 500 cells, our algorithm needs 90 seconds to compute $v_{\text{bit}}^{\text{est}}$ and $v_{\text{bit}}^{\text{est}}$. This computational time is directly related to the space step (and consequently to the time step, with the CFL condition). However, most of the computations can be done offline (computation of the backstepping kernels for instance), and the real computational time is around 20s to estimate on a 20s time window. This makes the current code amenable for real implementation, although in that case complexity of the algorithm should also be considered. Note that the computational burden can be reduced by using a less time-consuming algorithm to compute the different integral terms or by decreasing the space step (at the cost of a lower accuracy).

As is done in [AKS+19, KBS16] we introduce the quality of the reconstruction metric for the estimated force-on-bit. This will help us to examine the performance of the proposed method. A similar verification is done for the bit velocity. Let us denote y_0 as true generic signal (in our case $y_0 = w_{bit}^{real}$) and y its estimation (in our case $y = w_{bit}^{est}$). We define the quality of the reconstruction Q as follows

$$Q = 10 \log \frac{\|y_0\|_2^2}{\|y_0 - y\|_2^2}, \tag{10.36}$$

where $\|\cdot\|_2$ is the ℓ_2 norm. We have plotted in Figure 10.8 and Figure 10.9 the variations of Q_F and Q_v (reconstruction for the downhole force and downhole velocity) for different values of the SNR of top-drive velocity and the top-drive force (the SNR being chosen between 1 and 15). We used Monte Carlo simulations with 75 realizations for each noise level pair and reported the average value of the quality of the reconstruction Q. We have also plotted a dashed line that corresponds to the limit value of $Q = 10$, which is used as the **success limit** for the drill bit source estimation. We can observe a symmetrical effect between the SNR of top-drive velocity and the SNR of top-drive force. The critical value of $Q = 10$ is not reached for low SNR values ($SNR < 2$). In our simulations, we

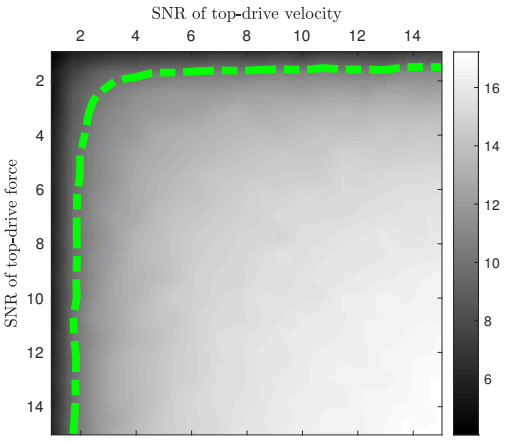

Figure 10.8: Noise sensitivity analysis of the drill bit force estimation. The dashed line corresponds to $Q = 10$ contour. Figure adjusted from [AKS+19].

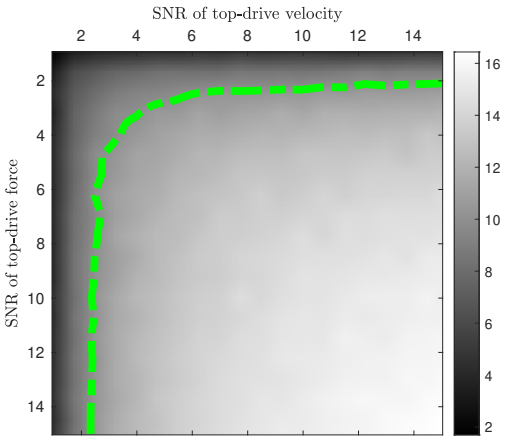

Figure 10.9: Noise sensitivity analysis of the drill bit velocity estimation. The dashed line corresponds to $Q = 10$ contour. Figure adjusted from [AKS+19].

find that when the quality factor is larger than 10, the rock intrinsic energy estimation algorithms result in satisfactory performances.

10.4.2 . Estimation of the rock interacting with the drill bit

We now use our three algorithms to estimate the nature of the rock interacting with the drill bit. The efficiency of the different algorithms is compared for three different types of rocks that have different hardness (i.e., different compressional and shear velocities)

- Unconsolidated sands (i.e. water saturated) for which $V_p = 1990$ m$/s$, $V_s = 1150$ m$/s$, $\rho_f = 2$ g$/cm^3$ and $\epsilon = 10$ J$/cm^3$.
- Sedimentary rocks (e.g. sandstone) for which $V_p = 2600$ m$/s$, $V_s = 1500$ m$/s$, $\rho_f = 2.2$ g$/cm^3$ and $\epsilon = 50$ J$/cm^3$.
- Igneous or metamorphic rocks (e.g. granite) for which $V_p = 4500$ m$/s$ $V_s = 2700$ m$/s$, $\rho_f = 2.7$ g$/cm^3$and $\epsilon = 170$ J$/cm^3$.

Seismic While Drilling Algorithm (Algo. 1)

We use our first algorithm (SWD Algorithm) to estimate the rock's velocity interacting with the drill bit. We consider that 100 seismic sensors are available (50 on each side of the drill string). The distance between each receiver is equal to 25 meters. Note that this distribution may not be optimal due to the bit's final orientation (which is equal to 60 degrees according to Figure 10.5). Using the simulated weight-on-bit and the (known) value of V_p, we compute the radiation patterns for each sensor to which we add noise with SNR equal to 5. Moreover, using the top-drive force and velocity measurements given by the PDE simulation, we estimate the weight-on-bit using our recursive procedure. For the three different rocks, we have performed 75 simulations and computed the corresponding ϵ using such a procedure. Table 10.2 gives our estimations' mean and standard deviation values. One can notice that the estimations are almost equal to the real values, even in the presence of significant noise. Moreover, the standard deviation remains extremely low. This underlines the robustness of the proposed approach that uses many sensors. For one testing point, Algo. 1 runs in 0.06s.

Table 10.2: Mean and standard deviation of the intrinsic specific energy of the rock ϵ using SWD estimation (100 sensors), direct estimation, and Machine Learning estimation. Seventy-five simulations and estimations have been performed for each rock. The SNR for all the signals is equal to 5.

Rock	Real ϵ		Algo. 1	Algo. 2	Algo. 3
Unconsolidated sands	10	Mean	10.1	9.6	9.1
		Stand. Dev.	0.3	1.05	1.8
Sedimentary Rocks	50	Mean	50.2	47.8	55.9
		Stand. Dev.	0.32	2.1	3.1
Metamorphic Rocks	170	Mean	170.28	181	178
		Stand. Dev.	0.5	21	15.6

Direct Estimation Algorithm (Algo. 2)

We now estimate ϵ using the second algorithm. The results are shown in Table 10.2. We have assumed that the constant C in (10.33) is unknown. One can notice that the estimations are close to the real data (even if, due to the important noise (SNR equal to 5), the standard deviation may be substantial). However, one must remember that such an approach hugely depends on our model for the downhole boundary condition. The computational time to run Algo. 2 on one testing point is 0.01s.

Machine Learning Algorithm (Algo. 3)

We now design our machine learning algorithm. As explained in Section 10.3.2, we first train our algorithm on a set of data made of 10000 simulations for which only the values of ϵ and w_f change between each simulation. We have used Python's algorithm *sklearn.neural_network to run our neural network.MLPRegressor* with 50 hidden layers, a BFGS solver for weight optimization, and an adaptive learning rate. Again, the results are shown in Table 10.2. One can notice that these predictions are close to the actual values (at least for low to medium ϵ). The prediction is more accurate for large values of ϵ (metamorphic rocks) than the one we obtained using the two other algorithms. The computational time to train the network is 140s, while the time required to run the algorithm on one testing point is 0.01s.

Comparison between the different algorithms

The three different algorithms provide satisfying and reliable estimations for the rock's intrinsic specific energy in the presence of important noises. However, the SWD algorithm presents an impressively high accuracy with a low standard deviation. This is related to its inherent robustness properties due to the use of a large number of sensors. Moreover, the estimation procedure is simple and can be easily adjusted for new constant physical parameters. The second algorithm also gives reliable estimates (at least for low values of ϵ). However, one must be aware that this algorithm requires a reliable model for the downhole condition (bit rock interaction). Finally, even if the Machine Learning algorithm shows satisfactory performance, it requires important datasets to be run, which can be time-consuming. Another drawback of our ML procedure is that the available data currently comes from simulations, which implies a model dependency (although it is less crucial than in the second procedure). However, such a Machine Learning algorithm is easy to implement and fast to run once adequately trained. Moreover, it is not sensitive to the discretization step since it only uses top-drive measurements.

We now compare the robustness properties of the different algorithms concerning uncertainties on the different physical parameters. More precisely, we address the effects of mismatch between the physical and mathematically modeled drill string dynamics (especially errors in downhole boundary condition: bit-rock interaction modeling) on the three algorithms' performances. Adding discrepancies

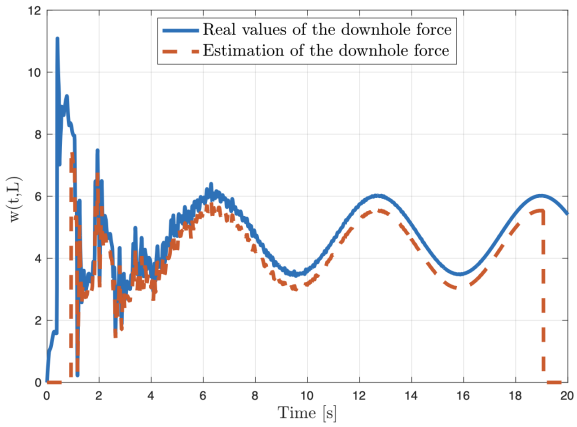

Figure 10.10: Comparison of the normalized simulated force-on bit and the estimated one in the presence of a discrepancy of 10% between the physical parameters used for the simulation and those used for the simulation (no noise). Figure adjusted from [AKS+19].

to the modeling will introduce errors in estimating the force-on-bit but not the measured hook load, hook speed, and SWD measurements. Hence, an incorrect source will be correlated with the data in the SWD algorithm. In the direct estimation algorithm, the effect of incorrect bit-rock interaction coefficients will be added to a wrong estimation of the force-on-bit. Finally, the machine learning algorithm will be trained with the wrong model. The proposed analysis is the first step towards a complete *sensitivity analysis* (that would be outside the scope of this paper). In what follows, we consider that all the physical parameters used to simulate the drilling system (e.g., inertia, inclination, length, mass) are subject to a random uncertainty (bounded by a maximum percentage d). In Figure 10.10, we have pictured the comparison between the simulated force-on bit and the estimated one in the absence of noise but in the presence of a discrepancy of 10% between the physical parameters used for the simulation and those used for the simulation. Note that all the uncertainties have been set to the maximum bound of 10% for this simulation. As expected, there is a mismatch between the estimated and simulated force (around 15 $\%$). Note that the phase of the function is barely changed. We now compare our three algorithms' performance in the presence of uncertainties on the different parameters. We consider the case of sedimentary rock for which $\epsilon = 57$. We have performed 75 simulations for which there is a discrepancy up to $d\%$ between the parameters used for the estimation (and for the training of the latest algorithm) and the real ones. We have given in Table 10.3 the values of the mean and the standard deviation of our estimations for different maximal bound d ($10\%, 20\%$ and 30%). We have used an SNR of 10 for all the measured signals. All three algorithms provide relevant estimations even in the presence of important uncertainties. The machine learning algorithm seems to be the most accurate but suffers from an important standard deviation. A similar dispersion of the estimations can be observed for the direct estimation algorithm. This is unsurprising since these two algorithms are trained on a false model. Conversely, the SWD algorithm accurately estimates with a relatively low standard deviation. We can explain these good performances because the uncertainties barely affect the phase of the estimated force-on-bit. As the phase is the most important attribute when correlating the estimated force with SWD measurements, this results in better estimation and a lower standard deviation. This emphasizes the robustness of such an approach, even if this is done at the cost of an important number of sensors. That said, the SWD method is an alternating minimization method, which requires proper initial estimation of the formation velocity. In Algorithm 1, we use the time delay between the recorded data near the surface and the calculated force-on-bit (source signature) at the bit location to provide an initial estimation of formation velocity, i.e., V_p^0. This method may not always give a proper initial estimation of formation velocity. Accordingly, we can use the direct estimation and machine learning methods in providing V_p^0 necessary in the SWD algorithm. Moreover, in the SWD algorithm, having access to a proper V_p^0 value will also improve the robustness and convergence rate of the SWD algorithm.

Table 10.3: Influence of a parameter mismatch on the estimation of the intrinsic specific energy of a sedimentary rock ϵ (real value: 57) for each algorithm (SWD estimation (100 sensors), direct estimation, and Machine Learning estimation). Seventy-five simulations and estimations have been performed for each level of disturbance. The SNR for all the signals is equal to 5.

Disturbance		Algo. 1	Algo. 2	Algo. 3
10%	Mean	54.7	51.6	57.5
	Stand. Dev.	2.47	6	7.6
20%	Mean	53.7	50	57.5
	Stand. Dev.	10.7	12.5	17
30%	Mean	48.9	46.1	58.4
	Stand. Dev.	11	18	21

10.5 . Conclusions and Perspectives

In this chapter, we have developed three algorithms for a near-real-time estimation of the intrinsic specific energy of the rock interacting with the drill bit. The proposed algorithms only require surface measurements and do not depend on any explicit knowledge about the subsurface properties. The algorithms were based on seismic-while-drilling, direct parameter estimation techniques, and machine learning. They provided an efficient and reliable framework for estimating the nature of rocks interacting with the drill bit, enabling a subsurface's practical characterization. We needed to estimate the drill bit source signature to derive the two first algorithms. This estimation was obtained by introducing a *sensing and computational framework* inspired by the recursive methodology introduced in Chapter 8. More precisely, in Riemann's coordinates, we could model the considered multi-sectional directional drilling device as an interconnection of scalar hyperbolic PDE systems and adjust the results of Chapter 8 in this new setting. We have then discussed the advantages and drawbacks of each approach.

The three algorithms we design in this chapter provide an efficient and reliable estimation of the nature of the rock that interacts with the drill bit, enabling a more precise characterization of the subsurface. Even though the proposed approach is a necessary and significant step in incorporating formation information and sensing in drill string dynamics estimation, the axial dynamics given by equations (10.2)-(10.3) neglect several crucial aspects to envision real implementation. First, we did not consider the Coulomb friction between the drill string and the borehole. The main reason behind this choice of an (over)-simplistic model was to facilitate the design of our different procedures. It has been shown in [AS18] that this Coulomb friction term may have a non-negligible impact on the dynamics of torsional oscillations. More precisely, it has a velocity-weakening effect that may generate stick-slip oscillations. As far as we know, the side force effect on the axial motion of the drill string has not been studied in the literature. However, it seems reasonable to assume that this force can be expressed using a similar model as the one used for torsional oscillations, namely a differential inclusion. More precisely, inspired by [AS18], we may add the term $\mathcal{F}(t,x)$ to equation (10.3) that is a differential inclusion modelling the Coulomb friction between the drill-string and the borehole. The model we propose uses the following inclusion

$$\begin{cases} \mathcal{F}(t,x) = \mu_k^a F_A(x), & v(t) > v_c, \\ \mathcal{F}(t,x) \in \pm\mu_s^a F_A(x), & |v(t)| < v_c, \\ \mathcal{F}(t,x) = -\mu_k^a F_A(x), & v(t) < -v_c, \end{cases} \tag{10.37}$$

where μ_s^a is the static friction coefficient (i.e., the friction between two or more solid objects that are not moving relative to each other) and μ_k^a kinetic friction coefficient (also known as dynamic friction or sliding friction, which occurs when two objects are moving relative to each other and rub together), v_c is the threshold on the axial velocity where the Coulomb friction transits from static to dynamic. The function F_A is the normalized axial force between the drill string and the borehole wall. The

function $\mathcal{F}(t,x) \in \pm\mu_s^a F_A(x)$ denotes the inclusion where

$$\mathcal{F}(t,x) = -\frac{1}{A\rho}\frac{\partial}{\partial x}w(t,x) - k_\xi v(t,x) \in [-\mu_s^a F_A(x), \mu_s^a F_A(x)], \tag{10.38}$$

and takes the boundary values $\pm\mu_s^a F_A(x)$ if this relationship does not hold. Adaptive observers [AADMS19] can be designed to estimate the coefficients μ_s^a, μ_k^a, and v_c and the function F_A. When all the points of the drill string reach the kinematic mode, then the function $\mathcal{F}(t,x)$ does not (directly) depend on time anymore since we have $\mathcal{F}(t,x) = \pm\mu_k^a F_A(x)$. Thus, this term can be added to the function h in (10.3), and the previous computations can still be applied to compute the downhole force and velocity as functions of past and future values of the top-drive states. These estimations only hold if we have $|v| > v_c$ for all drill-string points. Consequently, we need to apply our formula to all points (in practice, to a sufficiently large number of points) of the drill string to verify that the condition is not violated. Among all the drill-bit source signature estimations, only the ones for which this condition is fulfilled can be used to estimate the nature of the rock using Algorithms 1 and 2. Note that using adequate control laws may force the system to remain in a steady state for which this condition is always verified. The machine learning algorithm can straightforwardly be adjusted to deal with this Coulomb friction term.

Finally, we focused in this chapter on the drill bit axial motion and assumed that the bit angular velocity ω_{bit} was a known positive function. However, the proposed axial dynamics must be coupled with a torsional model to obtain an axial-torsional drill-string model. Such a torsional model has been proposed in [AS18] in the case of an off-bottom bit. The equations have the same structure as (10.2)-(10.3), including a non-linear Coulomb friction term similar to (10.37). Nevertheless, for non-vertical wells, in the presence of angular and axial movements, the Coulomb friction term couples the angular and axial dynamics, and equation (10.37) has to be modified accordingly. Regarding the downhole boundary conditions (equation (10.8) and the analogous equation for torque as given in [AAS20]), as suggested in [DD92], the term $\frac{1}{\omega_{\text{bit}}}$ has to replaced by an inclusion (non-linearity) to deal with small axial and angular velocities. Such a term can be the source of stick-slip oscillations for torsional oscillations. The derivation of a complete and validated axial-torsional model is a challenging ongoing scientific challenge [FTY+23].

11 - Application to the stabilization of two cascaded freeway segments

In this chapter, we show how the techniques introduced in the previous chapters can be used to develop boundary output feedback control laws for traffic flow on two cascaded freeway segments connected by a junction. **Freeway traffic modeling and management** have been intensively investigated due to the increasing demand for traffic mobility over the past decades. Among the different models, macroscopic models represent the traffic dynamics at an aggregate level and are widely used for freeway traffic control. The macroscopic models use hyperbolic PDEs that govern traffic density and velocity dynamics evolution. The most widely-used macroscopic traffic PDE models include the classical first-order Lighthill-Whitham-Richards (LWR) model [LW55, Ric56] and the state-of-art second-order Aw-Rascle-Zhang (ARZ) model [AR00, Zha02]. The LWR model corresponds to the conservation law of traffic density. It predicts the formation and propagation of traffic shockwaves on the freeway but fails to describe the stop-and-go oscillatory phenomenon [FKN+09], which causes unsafe driving conditions, increased fuel consumption, and delays in travel time. Subsequently, the second-order ARZ traffic model was conceived to address this stop-and-go traffic pattern, introducing a velocity PDE to augment the LWR model. The ARZ traffic model is characterized by non-linear, second-order hyperbolic PDEs. This category of models underwent extension in works such as [GP06] and [HR06], which endeavored to describe freeway traffic within intricate road network configurations. Consequently, we embrace this second-order macroscopic traffic network model as posited in [HR06]. Specifically, we posit the conservation of mass and driver attributes at the junction interconnecting the diverse roadways.

To regulate freeway traffic and avoid the **stop-and-go oscillatory phenomenon**, different traffic control strategies have been developed and successfully implemented for the traffic management infrastructures, namely, ramp metering and varying speed limits (VSL). Ramp metering controls the traffic lights on a ramp such that the inflow traffic is regulated for the mainline traffic. The VSL regulates traffic velocity by displaying driving velocities that are time-varying and dependent on real-time traffic. A complete survey on freeway traffic control can be found in [SPSF21]. Boundary controllers have been developed for traffic control of a single freeway segment in [BC16] [KP19] [YK19] [ZPQ19]. However, these control laws are restricted to control traffic problems on one freeway segment which necessitates certain road homogeneity. Only a few contributions considered road junctions. In [ZLLP21], the authors designed PI boundary control of a cascaded freeway network modeled by the linearized homogeneous AR model. Finally, backstepping boundary control laws for ramp metering were designed to suppress the stop-and-go traffic oscillations on the freeway either upstream or downstream of the ramp in [YK23, YK19]. The associated observers were validated on freeway data in [YGBK21]. Nonetheless, it is imperative to note that despite these control design efforts, the simultaneous stabilization of both freeway segments was not achieved, and the model failed to address diverse traffic scenarios manifesting within the interconnected segments.

Here, we focus on the oscillations generated by the in-domain traffic that can only be modeled by the inhomogeneous ARZ model. We will consider two connected roads. Contrary to [ZPQ19, ZLLP21], we will consider that only one boundary of the network is actuated. As shown in Fig 11.1, the traffic flow rate is actuated through on-ramp traffic lights. We will consider different actuators and sensors configurations.

The results of this chapter are adjusted from [YAK22, YAK20b, YAK20a, EAYK22b].

11.1 . Problem description

11.1.1 . The ARZ model

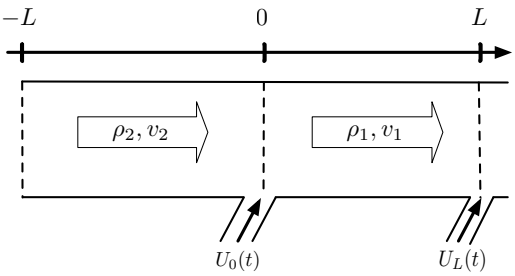

Figure 11.1: Traffic flow on upstream and downstream roads of a junction with actuation either from the junction or the outlet (Figure from [YAK22]).

We consider a road network that consists of two connected road segments with unidirectional traffic flow and different road conditions, as shown in Figure 11.1. The two segments are assumed to have the same length L. The spatial scaling can be easily made for equations that describe traffic states on segments with different lengths. The first segment (downstream segment) is defined on $[0, L]$ while the second segment (upstream segment) is defined on $[-L, 0]$. These two segments are connected at the junction through the boundary $x = 0$. The traffic dynamics are described with the **ARZ PDE model**, and the junction between the two segments is represented with the boundary conditions of the PDE model. The evolution of **traffic density** $\rho_1(t, x)$ and **velocity** $v_1(t, x)$ (with $(t, x) \in [0, \infty) \times [0, L]$) on the downstream road segment and traffic density $\rho_2(t, x)$ and velocity $v_2(t, x)$ ($(t, x) \in [0, \infty) \times [-L, 0]$) on the upstream road segment are modeled by the following ARZ model

$$\partial_t \rho_i + \partial_x (\rho_i v_i) = 0, \tag{11.1}$$

$$\partial_t (\rho_i (v_i + p_i)) + \partial_x (\rho_i v_i (v_i + p_i)) = -\frac{\rho_i (v_i - \mathcal{V}_i(\rho_i))}{\tau_i}, \tag{11.2}$$

where $i \in \{1, 2\}$ represents downstream and upstream road respectively. The labeling of freeway segments is chosen as the reverse direction of traffic flow but corresponds to the propagation direction of the control signal, which will be explained later. The **traffic pressure** $p_i(\rho_i)$ is defined as an increasing function of the density $p_i(\rho_i) = v_m \rho_i^{\gamma_i} / \rho_{m,i}^{\gamma_i}$. The coefficient γ_i represents the overall **drivers' property**, reflecting their change of driving behavior to the increase of density. The positive constant v_m represents the maximum velocity, and the positive constant $\rho_{m,i}$ is the maximum density defined as the number of vehicles per unit length. The equilibrium density-velocity relation $\mathcal{V}_i(\rho_i)$ is given by $\mathcal{V}_i(\rho_i) = v_m - p_i(\rho_i)$ for both segments, which assumes the same maximum velocity for the two segments when there are no vehicles on the road, $\rho_i = 0$. We define the following variable

$$w_i = v_i + p_i(\rho_i), \tag{11.3}$$

which is interpreted as **traffic "friction"** or drivers' property [FS13]. This property transports in the traffic flow with vehicle velocity, representing the heterogeneity of individual drivers with respect to the **equilibrium density-velocity relation** $\mathcal{V}_i(\rho_i)$. The maximum velocity v_m is assumed to be the same for the two road segments while the maximum density $\rho_{m,i}$ and coefficient γ_i are allowed to vary. The positive constant τ_i is the relaxation time that represents the time scale for traffic velocity v_i adapting to the equilibrium density velocity relation $\mathcal{V}_i(\rho_i)$. We denote the traffic flow rate on each road as $q_i = \rho_i v_i$. The equilibrium flow and density relation, also known as the fundamental diagram, is then given by $Q_i(\rho_i) = \rho_i \mathcal{V}_i(\rho_i) = \rho_i v_m (1 - (\rho_i/\rho_{m,i})^{\gamma_i})$. We assume the equilibrium traffic relation differs for the two segments due to the change in road situations and access to road junctions. The illustration is given in Figure 11.2. The **critical density** ρ_c splits the free and congested regimes of traffic states. The critical density is given by $\rho_{c,i} = \rho_{m,i} / (1 + \gamma_i)^{1/\gamma_i}$ such that $Q_i'(\rho_i)|_{\rho_i = \rho_{c,i}} = 0$. For a section i, the traffic is **free** when the density satisfies $\rho_i < \rho_{c,i}$. The traffic is defined as **congested** when the density satisfies $\rho_i > \rho_{c,i}$. For the free traffic, oscillations around the steady states will be damped out fast. For congested traffic, there are two directional waves on the road,

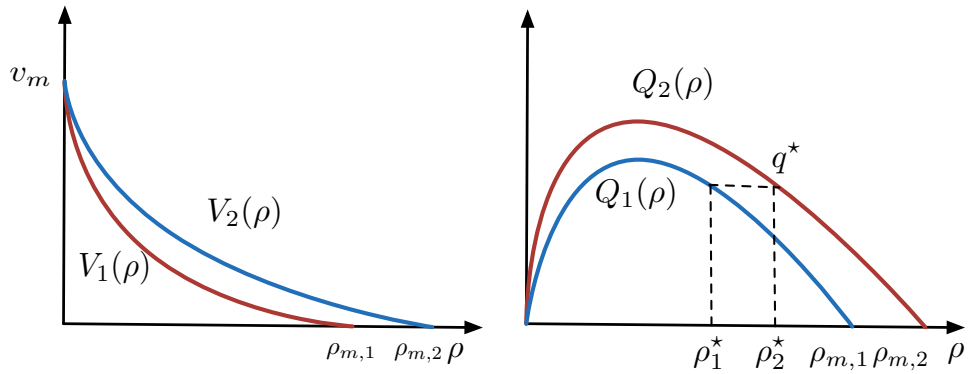

Figure 11.2: The equilibrium density and velocity relation $V_i(\rho)$ on the left, the equilibrium density and flux relation $Q_i(\rho)$ on the right (Figure from [YAK22]).

one being the velocity oscillation propagating upstream and the other being the density oscillation propagating downstream with the traffic. The congested traffic can become unstable [YK18].

We consider the situation that the upstream road segment 2 for $s \in [-L, 0]$ has more lanes than the downstream road segment for $x \in [0, L]$, in which congested traffic is usually formed up from downstream to upstream. Therefore, the maximum density $\rho_{m,2} > \rho_{m,1}$. The maximum driving speed v_m is assumed to be the same for the two segments. The maximum flow rate of the upstream road $Q_2(\rho_c)$ is reduced in the downstream to $Q_1(\rho_c)$, due to the change of road conditions from segment 2 to segment 1.

Boundary conditions

We now focus on the boundary conditions connecting the two PDE systems. The Rankine-Hugoniot condition is satisfied at the junction such that the weak solution exists for the network (11.1)-(11.2). This condition implies piecewise smooth solutions and corresponds to the conservation of the mass and drivers' properties defined in (11.3) at the junction. Thus the flux and drivers' properties are assumed to be continuous across the boundary conditions at $x = 0$, that is

$$\rho_1(t,0)v_1(t,0) = \rho_2(t,0)v_2(t,0), \quad w_1(t,0) = w_2(t,0). \tag{11.4}$$

For the open-loop system, we assume a constant inflow $q^\star$ entering the inlet boundary $x = -L$ and a constant outflow $q^\star$ at the outlet boundary for $x = L$:

$$q_2(t,-L) = q^\star, \quad q_1(t,L) = q^\star \tag{11.5}$$

The control problem we solve consists of stabilizing the traffic flow in upstream and downstream road segments with a single actuator. Three possible locations for implementing a ramp metering control input are either at the inlet $x = -L$, at the middle junction $x = 0$ or the outlet $x = L$. Actuation at the inlet $x = -L$ is a less challenging control problem that can be solved following [YK19] by reducing the traffic inflow.

Ramp metering control $U_0(t)$ from the junction $x = 0$. The traffic flow entering from the junction to the mainline road is controlled by $U_0(t)$. Given the flux continuity condition, the boundary condition at the junction is

$$q_1(t,0) = q_2(t,0) + U_0(t), \tag{11.6}$$

where the downstream segment flow consists of the inflow from the mainline upstream segment and the actuated traffic flow from the on-ramp.

Ramp metering control $U_L(t)$ from the outlet $x = L$. The downstream outflow at $x = L$ is actuated by $U_L(t)$,

$$q_1(t,L) = q^\star + U_L(t), \tag{11.7}$$

where the outflow rate equals the summation of the on-ramp metering flow and the constant mainline flow. In what follows, when we implement one choice of control input, the other control input equals zero. It should be noted that since we will stabilize the system (11.1)-(11.2) using its linearization around a given steady state, the corresponding controllers U_0 in (35) and U_L in (49) will correspond to the flow rate perturbations around a nominal flow rate. We assume that the steady-state flow rate consists of a nominal onramp flow rate $q_r \geq 0$, a component of the steady-state flow rate $q^\star$. Then the actual ramp flow input at an onramp is given by $q_{\text{ramp}}(t) = q_r + U_0(t) \geq 0$. In practice, we only need to guarantee that $q_{\text{ramp}}(t)$ is non-negative so that $U_0(t) \geq -q_r$. The value of q_r depends on the road configuration and real-time traffic conditions.

Congested steady states $(\rho_1^\star, v_1^\star, \rho_2^\star, v_2^\star)$

We are concerned with the congested traffic and assume that the equilibrium of both segments $(\rho_1^\star, v_1^\star), (\rho_2^\star, v_2^\star)$ are in the congested regime, which is the only one of theoretical control interest among all four traffic scenarios including free and free, free and congested, congested and free, congested and congested. If the traffic of both segments is free, there is no need for ramp metering control. If the upstream segment 2 is in the free regime and the downstream segment 1 is congested, then we only need to control the congested downstream traffic as presented in [YK19]. The oscillations propagated from the congested segment to the free regime segment will be damped out soon. The same applies to the scenario of free traffic in downstream segment 1 and congested traffic in upstream segment 2. The control objective is stabilizing the traffic flow in the two segments around the steady states. In practice, the steady states represent the equilibrium state values of the traffic flow when oscillations are successfully suppressed by our control design. The steady states $(\rho_1^\star, v_1^\star), (\rho_2^\star, v_2^\star)$ are considered to be in the congested regime and the boundary conditions (11.4) are satisfied, i.e.,

$$\rho_1^\star v_1^\star \quad = \rho_2^\star v_2^\star = q^\star, \quad w_1^\star = w_2^\star = v_m, \tag{11.8}$$

where the steady state velocities satisfy the equilibrium density-velocity relation $v_i^\star = \mathcal{V}_i(\rho_i^\star)$, as shown in Figure 11.2. According to (11.3), the constant driver's property in (11.8) implies that we have the same maximum velocity v_m for the two segments (which corresponds to our initial assumption):

$$v_1^\star + p_1^\star = v_2^\star + p_2^\star = v_m, \tag{11.9}$$

where $p_i^\star = p_i(\rho_i^\star)$. The steady states can be solved from the above nonlinear equations (11.8)-(11.9) however, there are no explicit solutions. Therefore we show the derivation process for obtaining the steady state values when $\rho_1^\star$ and the model parameters $v_m, \rho_{m,i}$ and γ_i are given. The functions $\mathcal{V}_i(\rho)$ $Q_i(\rho)$ and $p_i(\rho)$ are also known. The steady-state flow rate is obtained as $q^\star = Q_1(\rho_1^\star)$, and the constant flux $Q_1(\rho_1^\star) = Q_2(\rho_2^\star)$, yields a relation for the steady state densities of the two segments $\frac{\rho_1^\star \rho_{m,1}^{\gamma_1} - (\rho_1^\star)^{\gamma_1+1}}{\rho_2^\star \rho_{m,2}^{\gamma_2} - (\rho_2^\star)^{\gamma_2+1}} = \frac{\rho_{m,1}^{\gamma_1}}{\rho_{m,2}^{\gamma_2}}$. Knowing $\rho_1^\star, \rho_2^\star$ and $q^\star$, the steady states velocities are obtained as $v_i^\star = q^\star / \rho_i^\star$.

11.1.2 . Linearized equations in the Riemann coordinates

We linearize the ARZ based traffic network model (ρ_i, v_i) in (11.1)-(11.2) with the boundary conditions (11.4)-(11.5) around the steady states $(\rho_i^\star, v_i^\star)$ defined in the previous section. In order to simplify the control design, the linearized model is then rewritten into the Riemann variables to which we apply an invertible spatial transformation

$$\bar{w}_i \quad = \quad \exp\left(\frac{x}{\tau_i v_i^\star}\right)\left(\frac{\gamma_i p_i^\star}{q^\star}\left(\rho_i v_i - \rho_i^\star v_i^\star\right) + \frac{1}{r_i}\left(v_i - v_i^\star\right)\right), \tag{11.10}$$

$$\bar{v}_i \quad = \quad v_i - v_i^\star, \quad \bar{q}_i = \rho_i v_i - \rho_i^\star v_i^\star, \tag{11.11}$$

where $p_i^\star = p_i(\rho_i^\star)$ and the constant coefficients r_i are defined as $r_i = -\frac{v_i^\star}{\gamma_i p_i^\star - v_i^\star}$. For the congested regime we have $\rho_i^\star > \frac{\rho_{m,i}}{(1+\gamma_i)^{1/\gamma_i}}$ so that the characteristic speed $\gamma_i p_i^\star - v_i^\star > 0$. The velocity variations $\bar{v}_1(t,x)$, $\bar{v}_2(t,x)$ transport upstream, which means the action of velocity acceleration or deceleration

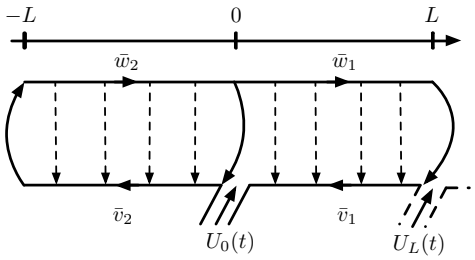

Figure 11.3: Control diagram for the closed-loop system with either the actuation from the middle junction $x = 0$ or from the outlet $x = L$ (Figure from [YAK22]).

is repeated from the leading vehicle to the following vehicle. More precisely, since $v_i^\star = v_m - p_i^\star$, we obtain $\gamma_i p_i^\star - v_i^\star = (1+\gamma_i)p_i^\star - v_m$. We also have $p_i^\star = v_m - \mathcal{V}_i(\rho_i^\star) = v_m \left(\frac{\rho_i^\star}{\rho_{m,i}}\right)^{\gamma_{v_m}} > \frac{v_m}{1+\gamma_i}$, since $\rho_i^\star > \frac{\rho_{m,i}}{(1+\gamma_i)^{1/\gamma_i}}$. Consequently, we obtain $\gamma_i p_i^\star - v_i^\star > 0$. The linearized system is written as

$$\begin{cases} \partial_t \bar{w}_1(t,x) + v_1^\star \partial_x \bar{w}_1(t,x) = 0, \\ \partial_t \bar{v}_1(t,x) - (\gamma_1 p_1^\star - v_1^\star)\partial_x \bar{v}_1(t,x) = \bar{c}_1(x)\bar{w}_1(t,x), \\ \partial_t \bar{w}_2(t,x) + v_2^\star \partial_x \bar{w}_2(t,x) = 0, \\ \partial_t \bar{v}_2(t,x) - (\gamma_i p_2^\star - v_2^\star)\partial_x \bar{v}_2(t,x) = \bar{c}_2(s)\bar{w}_2(t,x), \end{cases} \tag{11.12}$$

with boundary conditions,

$$\begin{cases} \bar{w}_1(t,0) = \bar{w}_2(t,0), \\ \bar{v}_1(t,L) = r_1 \exp\left(\frac{-L}{\tau_1 v_1^\star}\right)\bar{w}_1(t,L) + \frac{1-r_1}{\rho_1^\star} U_L(t), \\ \bar{w}_2(t,-L) = \frac{1}{r_2}\exp\left(\frac{-L}{\tau_2 v_2^\star}\right)\bar{v}_2(t,-L), \\ \bar{v}_2(t,0) = \delta\frac{r_2}{r_1}\bar{v}_1(t,0) + (1-\delta)r_2\bar{w}_2(t,0) + \frac{1-r_2}{\rho_2^\star}U_0(t), \end{cases} \tag{11.13}$$

where the spatially varying coefficient $\bar{c}_1(x)$, $\bar{c}_2(x)$ are defined, respectively, by

$$\bar{c}_1(x) = -\frac{1}{\tau_1}\exp\left(-\frac{x}{\tau_1 v_1^\star}\right), \quad \bar{c}_2(x) = -\frac{1}{\tau_2}\exp\left(\frac{x}{\tau_2 v_2^\star}\right). \tag{11.14}$$

The constant coefficient δ (ratio related to the traffic pressure of the segments) is defined by $\delta = \frac{\gamma_2 p_2^\star}{\gamma_1 p_1^\star} > 0$ We assume that the **available measurements** correspond to the values of $\bar{q}_i$ and $\bar{v}_i$ at the left side of the outlet $x = L$ or at the right side of the junction $x = 0$. Since we have $\bar{w}_1(t,L) = \exp\left(\frac{L}{\tau_1 v_1^\star}\right)\left(\frac{\gamma_1 p_1^\star}{q^\star}\bar{q}_1(t,L) - \frac{1}{r_1}\bar{v}_1(t,L)\right)$, and $\bar{w}_2(t,0) = \frac{\gamma_2 p_2^\star}{q^\star}\bar{q}_2(t,0) - \frac{1}{r_2}\bar{v}_2(t,0)$, we can consider that the boundary measurement corresponds to

$$Y_L(t) = \bar{w}_1(t,L) \quad \text{or} \quad Y_0(t) = \bar{w}_2(t,0). \tag{11.15}$$

The cascade structure of the network given Figure 11.3 fits in the general framework given in Chapter 6. This can be seen using the *folding transformation* $\bar{x} = -x$ on the second subsystem (the variable $\bar{x}$ belongs to $[0, L]$). Similarly to what has been done in Chapter 6, we will consider initial conditions that belong to $H^1([0,1],\mathbb{R})$ and satisfy the appropriate compatibility conditions. Our objective is to design the control law $U_0(t)$ or $U_L(t)$ to stabilize the system (11.12)-(11.13) in the sense of the L^2-norm. Depending on the actuators and sensors locations, we can either use the results of Chapter 8 or Chapter 9 to design stabilizing output-feedback controllers. In what follows we denote $\tau_1 = \frac{1}{v_1^\star} + \frac{1}{\gamma_1 p_1^\star - v_1^\star}$ and $\tau_2 = \frac{1}{v_2^\star} + \frac{1}{\gamma_2 p_2^\star - v_2^\star}$. Moreover, we still consider the exponential convergence of the system in the sense of the χ-norm (even if there is no ODE here). Obviously, we still consider that Assumption 6.1.1 holds. However, in this case, it can be rewritten more simply. More precisely, we have the following lemma

Lemma 11.1.1 *Assumption 6.1.1 is verified if*

$$\delta < \frac{1+\exp(\frac{L}{\tau_2 v_2^\star})}{1+\exp(\frac{-L}{\tau_1 v_1^\star})}. \tag{11.16}$$

Proof : Assumption 6.1.1 corresponds to the exponential stability of the open-loop system (11.12)-(11.13) in the absence of in-domain couplings. We have

$$\bar{w}_2(t,-L) = (1-\delta)\exp\left(\tfrac{-L}{\tau_2 v_2^\star}\right)\bar{w}_2(t-\tau_2,L) + \delta\exp\left(\tfrac{-L}{\tau_2 v_2^\star}\right)\exp\left(\tfrac{-L}{\tau_1 v_1^\star}\right)\bar{w}_2(t-\tau_2-\tau_1,-L).$$

Applying [HVL93], we have that condition (11.16) implies the exponential stability of $\bar{w}_2(t,-L)$ and consequently of the open-loop system (11.12)-(11.13). ■

11.2 . State feedback Control Designs

In this section, we design full-state feedback laws that guarantee the stabilization of the system (11.12)-(11.13) for the different actuation locations. In each case, we adjust the results of Chapter 8 and Chapter 9 to write these systems in a more amenable form.

11.2.1 . Feedback law with flow rate control from x=0

We consider first the case of an actuator located at the junction $x = 0$. Adjusting the methodology detailed in Chapter 9, the control input $U_0(t)$ is given by

$$\begin{aligned} U_0(t) = \frac{\rho_2^\star}{1-r_2}\Bigg(&\int_{-L}^{0} K_2^{vw}(0,y)\bar{w}_2(t,y) + K_2^{vv}(0,y)\bar{v}_2(t,y)dy \\ &- \delta\frac{r_2}{r_1}\int_0^L K_1^{vw}(0,y)\bar{w}_1(t,y) + K_1^{vv}(0,y)\bar{v}_1(t,y)dy\Bigg) \end{aligned} \tag{11.17}$$

where the kernels K_1^{vw} and K_1^{vv} are continuous functions defined on the set $\{(x,y) \in [0,L]^2, y \geq x\}$, while the kernels K_2^{vw} and K_2^{vv} are continuous functions defined on the set $\mathcal{T}_2 = \{(x,y) \in [-L,0]^2$, $y \leq x\}$. On their corresponding domains of definition, they satisfy the following set of PDEs:

$$(\gamma_i p_i^\star - v_i^\star)\partial_x K_i^{vw}(x,y) - v_i^\star \partial_y K_i^{vw}(x,y) = c_i(y)K_i^{vv}(x,y), \tag{11.18}$$

$$\partial_x K_i^{vv}(x,y) + \partial_y K_i^{vv}(x,y) = 0, \tag{11.19}$$

along with the boundary conditions

$$K_1^{vv}(x,L) = -\exp\left(\frac{L}{\tau_1 v_1^\star}\right)K_1^{vw}(x,L), \quad K_1^{vw}(x,x) = \frac{c_1(x)}{\gamma_1 p_1^\star}, \tag{11.20}$$

$$K_2^{vv}(x,-L) = -\exp\left(\frac{-L}{\tau_2 v_2^\star}\right)K_2^{vw}(x,-L), \quad K_2^{vw}(x,x) = -\frac{c_2(x)}{\gamma_2 p_2^\star}. \tag{11.21}$$

Note that the control law (11.17) is simpler than the one proposed in Chapter 9 since some in-domain coupling terms are equal to zero, thus preventing the apparition of integral coupling terms at the unactuated boundary when performing the backstepping transformation.

Theorem 11.2.1.

The PDE system (11.12)-(11.13) with the feedback law U_0 defined in (11.17) is exponentially stable.

Proof : Consider the following backstepping transformations

$$\alpha_i(t,x) = \bar{w}_i(t,x), \tag{11.22}$$

$$\beta_1(t,x) = \bar{v}_1(t,x) - \int_x^L K_1^{vw}(x,y)\bar{w}_1(t,y)dy - \int_x^L K_1^{vv}(x,y)\bar{v}_1(t,y)dy, \tag{11.23}$$

$$\beta_2(t,x) = \bar{v}_2(t,x) - \int_{-L}^{x} K_2^{vw}(x,y)\bar{w}_2(t,y)dy - \int_{-L}^{x} K_2^{vv}(x,y)\bar{v}_2(t,y)dy. \tag{11.24}$$

The transformation (11.23)-(11.24) maps the original system (11.12)-(11.13) to the following decoupled target system

$$\begin{cases} \partial_t\alpha_i(t,x) + v_i^\star\partial_x\alpha_i(t,x) = 0 \quad \partial_t\beta_i(t,x) - (\gamma_i p_i^\star - v_i^\star)\partial_x\beta_i(t,x) = 0, \\ \beta_1(t,L) = r_1 \exp\left(-\frac{L}{\tau_1 v_1^\star}\right)\alpha_1(t,L), \quad \alpha_1(t,0) = \alpha_2(t,0), \\ \alpha_2(t,-L) = \exp\left(\frac{-L}{\tau_2 v_2^\star}\right)\frac{1}{r_2}\beta_2(t,-L), \quad \beta_2(t,0) = \delta\frac{r_2}{r_1}\beta_1(t,0) + r_2(1-\delta)\alpha_2(t,0), \end{cases}$$

which is exponentially stable due to Assumption 6.1.1. ■

11.2.2 . Feedback law with flow rate control from x=L

We now consider that the available actuation is located at the outlet $x = L$. Our approach is adjusted from Chapter 8. The control input $U_L(t)$ is defined as

$$U_L(t) = \frac{\rho_1^\star}{1-r_1}\left(\int_0^L \bar{K}_1^{vw}(L,y)w_1(t,y) + \bar{K}_1^{vv}(L,y)v_1(t,y)dy \right. \\ \left. + \int_{-L}^{0} M^w(L,y)w_2(t,y) + M^v(L,y)v_2(t,y)dy\right), \tag{11.25}$$

where the kernels $\bar{K}_1^{vw}$ and $\bar{K}_1^{vv}$ are defined on the set $\{(x,y) \in [0,L]^2,\ y \geq x\}$, the kernels $\bar{K}_2^{vw}$ and $\bar{K}_2^{vv}$ are defined on the set $\{(x,y) \in [-L,0]^2,\ y \geq x\}$. The kernels M^w and M^v are bounded functions defined on $\{(x,y) \in [-L,0] \times [0,L]\}$. On their corresponding domains of definition, they satisfy the following set of PDEs

$$\begin{cases} (\gamma_i p_i^\star - v_i^\star)\partial_x\bar{K}_i^{vw}(x,y) - v_i^\star\partial_y\bar{K}_i^{vw}(x,y) = c_i(y)\bar{K}_i^{vv}(x,y), \\ \partial_x\bar{K}_i^{vv}(x,y) + \partial_y\bar{K}_i^{vv}(x,y) = 0, \\ (\gamma_1 p_1^\star - v_1^\star)\partial_x M^v(x,y) + (\gamma_2 p_2^\star - v_2^\star)\partial_y M^v(x,y) = 0, \\ (\gamma_1 p_1^\star - v_1^\star)\partial_x M^w(x,y) - v_2^\star\partial_y M^w(x,y) = c_2(y)M^v(x,y), \end{cases} \tag{11.26}$$

with the boundary conditions

$$\begin{cases} \bar{K}_i^{vw}(x,x) = -\frac{c_i(x)}{\gamma_i p_i^\star}, \quad \bar{K}_1^{vv}(x,0) = \frac{v_2^\star}{v_1^\star}\delta M^v(x,0), \\ \bar{K}_2^{vv}(x,-L) = -\exp\left(\frac{-L}{\tau_2 v_2^\star}\right)\bar{K}_2^{vw}(x,-L), \\ M^w(0,y) = \frac{r_1}{\delta r_2}\bar{K}_2^{vw}(0,y), \quad M^v(0,y) = \frac{r_1}{\delta r_2}\bar{K}_2^{vv} \\ M^w(x,0) = (1-\delta)M^v(x,0) + \frac{v_1^\star}{v_2^\star}\bar{K}_1^{vw}(x,0), \\ M^v(x,-L) = -\exp\left(\frac{-L}{\tau_2 v_2^\star}\right)M^w(x,-L). \end{cases} \tag{11.27}$$

The following lemma assesses the existence of the kernels

Lemma 11.2.1 *System* (11.26)-(11.27) *admits a unique solution piecewise continuous solution* $\bar{K}_1^{vw}$, $\bar{K}_1^{vv}$, $\bar{K}_2^{vw}$, $\bar{K}_2^{vv}$, M^v, M^w .

Proof : We start by assessing the existence of $\bar{K}_2^{vw}$ and $\bar{K}_2^{vv}$ using [CVKB13]. The rest of the proof is based on an induction argument and is adjusted from the one given in Chapter 8. Let us define $\chi = \frac{\gamma_2 p_2^\star - v_2^\star}{v_2^\star}$ and let us define the sequence x_k by $x_k = \min(\chi \times k, 1)$. Let us now define the following triangular domains defined for $k \geq 1$.

$$\mathcal{R}_k = \{(x,y) \in [0,1] \times [-1,0],\ y \leq -\frac{1}{\chi}(x - x_{k-1})\},$$
$$\bar{\mathcal{R}}_k = \{(x,y) \in [0,1] \times [-1,0],\ y \geq -\frac{1}{\chi}(x - x_{k-1})\},\ \mathcal{S}_k = \{(x,y) \in [0,x_k]^2,\ x \geq y\}$$

Applying [DMBAHK18, Theorem 3.2], we can prove the existence of the kernels M^v and M^w on the triangular domain $\mathcal{R}_1$. Consequently, these kernels are defined on the line $x = -\chi y$. Let us now perform the change of variables $\bar{y} = -\frac{1}{\chi}y$ to map the domain $\mathcal{S}_1$ to $\bar{\mathcal{R}}_1$. Consequently, we can express the kernels $\bar{K}_1^{\cdot\cdot}$ on the domain $\bar{\mathcal{R}}_1$ (when $x \leq \chi$). We denote by $\hat{K}_1$ the corresponding kernels after this change of variables. Again, we can apply [DMBAHK18, Theorem 3.2] to prove the existence of the kernels M^w, M^v and $\hat{K}_1^{\cdot\cdot}$ on $\bar{\mathcal{R}}_1$. This implies the existence of $\bar{K}_1^{\cdot\cdot}$ on $\mathcal{S}_1$. We then iterate the procedure on the intervals $[x_{k-1}, x_k]$ to conclude the proof. ■

We have the following theorem.

Theorem 11.2.2.

The PDE system (11.12)-(11.13) with the feedback law U_L defined in (11.25) is exponentially stable.

Proof : Consider the backstepping transformation

$$\bar{\alpha}_1(t,x) = \bar{w}_1(t,x), \quad \bar{\alpha}_2(t,x) = \bar{w}_2(t,x), \tag{11.28}$$

$$\begin{aligned}\bar{\beta}_1(t,x) =& \bar{v}_1(t,x) - \int_0^x \bar{K}_1^{vw}(x,y)\bar{w}_1(t,y)dy - \int_0^x \bar{K}_1^{vv}(x,y)\bar{v}_1(t,y)dy \\ &- \int_{-L}^0 M^w(x,y)\bar{w}_2(t,y)dy - \int_{-L}^0 M^v(x,y)\bar{v}_2(t,y)dy,\end{aligned} \tag{11.29}$$

$$\bar{\beta}_2(t,x) = \bar{v}_2(t,x) - \int_{-L}^x \bar{K}_2^{vw}(x,y)\bar{w}_2(t,y)dy - \int_{-L}^x \bar{K}_2^{vv}(x,y)\bar{v}_2(t,y)dy, \tag{11.30}$$

Note that the transformation (11.28)-(11.30) is invertible (as it is a Volterra transformation [Yos60, Chapter 4]). Thus, the first transformation (11.28)-(11.29) is invertible as it combines a Volterra transformation with an affine transformation. It maps the original system (11.12)-(11.13) to the following decoupled target system

$$\begin{cases} \partial_t\alpha_i(t,x) + v_i^\star\partial_x\alpha_i(t,x) = 0, \ \partial_t\beta_i(t,x) - (\gamma_i p_i^\star - v_i^\star)\partial_x\beta_i(t,x) = 0, \\ \alpha_1(t,0) = \alpha_2(t,0), \quad \beta_1(t,L) = r_1\exp\left(-\frac{L}{\tau_1 v_1^\star}\right)\alpha_1(t,L), \\ \alpha_2(t,-L) = \exp\left(\frac{-L}{\tau_2 v_2^\star}\right)\frac{1}{r_2}\beta_2(t,-L), \quad \beta_2(t,0) = \delta\frac{r_2}{r_1}\beta_1(t,0) + r_2(1-\delta)\alpha_2(t,0), \end{cases}$$

which is exponentially stable due to Assumption 6.1.1. ■

11.3 . Boundary Observer Designs

The control laws designed in the previous section require the value of the state all over the spatial domain. Therefore we design boundary observers which rely either on the measurement of traffic states from the junction or from the outlet. Again, the proposed approach is adjusted from Chapter 8 and Chapter 9

11.3.1 . Observer with measurement at x=0

We consider here that the measurement $Y_0(t) = \bar{w}_2(t,0)$ is available. The observer equations are a copy of the original dynamics with output injection gains, which read as follows

$$\begin{cases} \partial_t\hat{w}_i(t,x) + v_i^\star\partial_x\hat{w}_i(t,x) = -\phi_i(x)(\bar{w}_2(t,0) - \hat{w}_i(t,0)), \\ \partial_t\hat{v}_i(t,x) - (\gamma_i p_i^\star - v_i^\star)\partial_x\hat{v}_i(t,x) = c_i(x)\hat{w}_i - \chi_i(x)(\bar{w}_2(t,0) - \hat{w}_i(t,0)), \\ \hat{w}_1(t,0) = \hat{w}_2(t,0), \ \hat{v}_1(t,L) = r_1\exp\left(\frac{-L}{\tau_1 v_1^\star}\right)\hat{w}_1(t,L) + \frac{1-r_1}{\rho_1^\star}U_L(t), \\ \hat{w}_2(t,-L) = \exp\left(\frac{-L}{\tau_2 v_2^\star}\right)\frac{1}{r_2}\hat{v}_2(t,-L), \\ \hat{v}_2(t,0) = \delta\frac{r_2}{r_1}\hat{v}_1(t,0) + (1-\delta)r_2\hat{w}_2(t,0) + \frac{1-r_2}{\rho_2^\star}U_0(t), \end{cases} \tag{11.31}$$

where $\hat{w}_i(t,x), \hat{v}_i(t,x)$ are the estimates of the state variables $\bar{w}_i(t,x)$ and $\bar{v}_i(t,x)$. The terms ϕ_i and χ_i are output injection gains, defined as

$$\phi_1(x) = -v_1^\star N_1^{ww}(x,0), \quad \chi_1(x) = -v_1^\star N_1^{vw}(x,0), \tag{11.32}$$

$$\phi_2(x) = v_2^\star N_2^{ww}(x,0), \quad \chi_2(x) = v_2^\star N_2^{vw}(x,0), \tag{11.33}$$

where the kernels kernels N_1^{ww} and N_1^{wv} are continuous functions defined on $\{(x,y) \in [0,L]^2, \ y \leq x\}$, while the kernels N_2^{ww} and N_2^{wv} are piecewise continuous functions defined on the set $\{(x,y), \in [-L,0]^2, \ y \geq x\}$. They satisfy the following set of equations

$$\partial_x N_i^{ww}(x,y) + \partial_y N_i^{ww}(x,y) = 0, \tag{11.34}$$

$$(\gamma_i p_i^\star - v_i^\star)\partial_x N_i^{vw} - v_i^\star\partial_y N_1^{vw}(x,y) = -c_i(x)N_i^{ww}(x,y), \tag{11.35}$$

along with the boundary conditions

$$N_1^{vw}(x,x) = \frac{c_1(x)}{\gamma_1 p_1^\star},\ N_1^{ww}(L,x) = \frac{1}{r_1}\exp\left(\frac{L}{\tau_1 v_1^\star}\right) N_1^{vw}(L,x), \tag{11.36}$$

$$N_2^{ww}(-L,x) = \exp\left(\frac{-L}{\tau_2 v_2^\star}\right)\frac{1}{r_2} N_2^{vw}(-L,x),\ N_2^{vw}(x,x) = \frac{-c_2(x)}{\gamma_2 p_2^\star}. \tag{11.37}$$

We then have the following theorem

Theorem 11.3.1.

Consider the PDE system (11.31) with the output injections gains defined in (11.32)-(11.33). Then, for any initial condition $(\hat{w}_i(\cdot,0), \hat{v}_i(\cdot,0))$, the states $(\hat{w}_i, \hat{v}_i)$ exponentially converge to the states $(\bar{w}_i, \bar{v}_i)$.

Proof : The proof is straightforward using the backstepping transformation of Chapter 9. It can be found in [YAK20a]. ■

11.3.2 . Observer with measurement at x=L

We now assume the available measurements correspond to $Y_L(t) = \bar{w}_1(t,L)$. Following the dual approach proposed in Chapter 8, the observer system is now given by

$$\begin{cases} \partial_t \hat{w}_i(t,x) + v_i^\star \partial_x \hat{w}_i(t,x) = -\mu_i(x)(\bar{w}_1(t,L) - \hat{w}_1(t,L)), \\ \partial_t \hat{v}_i(t,x) - (\gamma_i p_i^\star - v_i^\star)\partial_x \hat{v}_i(t,x) = c_i(x)\hat{w}_i - \nu_i(x)(\bar{w}_1(t,L) - \hat{w}_1(t,L)), \\ \hat{w}_1(t,0) = \hat{w}_2(t,0),\ \hat{v}_1(t,L) = r_1 \exp\left(-\frac{L}{\tau_1 v_1^\star}\right)\hat{w}_1(t,L) + \frac{1-r_1}{\rho_1^\star} U_L(t), \\ \hat{w}_2(t,-L) = \exp\left(\frac{-L}{\tau_2 v_2^\star}\right)\frac{1}{r_2}\hat{v}_2(t,-L), \\ \hat{v}_2(t,0) = \delta\frac{r_2}{r_1}\hat{v}_1(t,0) + (1-\delta) r_2 \hat{w}_2(t,0) + \frac{1-r_2}{\rho_2^\star} U_0(t), \end{cases} \tag{11.38}$$

where $\hat{w}_i(t,x), \hat{v}_i(t,x)$ are the estimates of the state variables $\bar{w}_i(t,x)$ and $\bar{v}_i(t,x)$. The terms μ_i and ν_i are output injection gains. They are defined by

$$\mu_1(x) = -v_1^\star \bar{N}_1^{ww}(x,L) + \int_x^L \mu_1(y)\bar{N}_1^{ww}(x,y)dy, \tag{11.39}$$

$$\nu_1(x) = -v_1^\star \bar{N}_1^{vw}(x,L) + \int_x^L \mu_1(y)\bar{N}_1^{vw}(x,y)dy, \tag{11.40}$$

$$\mu_2(x) = -v_1^\star F^w(x,L) + \int_x^0 \mu_2(y)\bar{N}_2^{ww}(x,y)dy + \int_0^L \mu_1(y) F^w(x,y)dy, \tag{11.41}$$

$$\nu_2(x) = -v_1^\star F^v(x,L) + \int_x^0 \mu_2(y)\bar{N}_2^{vw}(x,y)dy + \int_0^L \mu_1(y) F^v(x,y)dy. \tag{11.42}$$

These output injection gains are perfectly defined. Since (11.39) is a Volterra equation of the second kind, it is invertible, and we can obtain μ_1. Once μ_1 is obtained, then equation (11.41) becomes a Volterra equation, and we can compute μ_2. Once μ_1 and μ_2 are obtained, the expressions of ν_1 and ν_2 are explicit. The functions $\bar{N}_1^{ww}$ and $\bar{N}_1^{vw}$ are piecewise continuous functions defined on $\{(x,y) \in [0,L]^2,\ y \le x\}$. The functions $\bar{N}_2^{ww}$ and $\bar{N}_2^{vw}$ are piecewise continuous functions defined on $\{(x,y) \in [-L,0]^2,\ y \ge x\}$. The functions F^w and F^v are piecewise continuous functions defined on $\{(x,y) \in [-L,0]\times[0,L]\}$. They verify the following set of equations

$$(\gamma_i p_i^\star - v_i^\star)\partial_x \bar{N}_i^{vw}(x,y) - v_i^\star \partial_y \bar{N}_i^{vw}(x,y) = 0,\ \partial_x \bar{N}_i^{ww}(x,y) + \partial_y \bar{N}_i^{ww}(x,y) = 0,$$
$$v_2^\star \partial_x F^w(x,y) + v_1^\star \partial_y F^w(x,y) = 0,\quad (\gamma_2 p_2^\star - v_2^\star)\partial_x F^v(x,y) - v_1^\star \partial_y F^v(x,y) = 0,$$

with the boundary conditions

$$\bar{N}_2^{vw}(x,x) = \frac{c_2(x)}{\gamma_2 p_2^\star},\ \bar{N}_1^{vw}(x,x) = \frac{c_1(x)}{\gamma_1 p_1^\star},\ \bar{N}_2^{ww}(-L,y) = \exp(-\frac{L}{\tau_2 v_2^\star})\frac{1}{r_2}\bar{N}_2^{vw}(-L,y),$$

$$F^v(x,0)=\frac{v_2^\star}{v_1^\star}\bar{N}_2^{vw}(x,0),\ F^w(x,0)=\frac{v_2^\star}{v_1^\star}\bar{N}_2^{ww}(x,0),\ \bar{N}_1^{ww}(0,y)=F^w(0,y),$$
$$F^v(0,y)=\delta\frac{r_2}{r_1}\bar{N}_1^{vw}(0,y)+(1-\delta)r_2F^w(0,y),\ F^w(-L,y)=\exp(\frac{-L}{\tau_2 v_2^\star})\frac{1}{r_2}F^v(-L,y),$$

The well-posedness of this kernel PDE-system can be shown using [ADMBA19, Lemma 2]. We have the following theorem.

Theorem 11.3.2.

Consider the PDE system (11.38) with the output injections gains defined in (11.39)-(11.40). Then, for any initial condition $(\hat{w}_i(\cdot,0),\hat{v}_i(\cdot,0))$, the states $(\hat{w}_i,\hat{v}_i)$ exponentially converge to the states $(\bar{w}_i,\bar{v}_i)$.

Proof : Let us define the error estimates $\tilde{w}_i=\tilde{w}_i-\hat{w}_i$ and $\tilde{v}_i=\tilde{v}_i-\hat{v}_i$. The error system is obtained by subtracting the observer equations in (11.38) from (11.12)-(11.13). The rest of the proof is straightforward, using the invertible backstepping transformation

$$\tilde{\alpha}_1(t,x)=\tilde{w}_1(t,x)-\int_x^L\bar{N}_1^{ww}(x,y)\tilde{w}_1(t,y),\ \tilde{\beta}_1(t,x)=\tilde{v}_1(t,x)-\int_x^L\bar{N}_1^{vw}(x,y)\tilde{w}_1(t,y)dy, \tag{11.43}$$
$$\tilde{\alpha}_2(t,x)=\tilde{w}_2(t,x)-\int_x^0\bar{N}_2^{ww}(x,y)\tilde{w}_2(t,y)dy-\int_0^L F^w(x,y)\tilde{w}_1(t,y)dy, \tag{11.44}$$
$$\tilde{\beta}_2(t,x)=\tilde{v}_2(t,x)-\int_x^0\bar{N}_2^{vw}(x,y)\tilde{w}_2(t,y)dy-\int_0^L F^v(x,y)\tilde{w}_1(t,y)dy. \tag{11.45}$$

■

11.4 . Output Feedback Laws

The previously designed state feedback laws and the two observers can be employed to construct four possible output feedback laws, which consist of two collocated and two anti-collocated ones, as shown in Table 11.1.

Table 11.1: Possible configuraitons for the output feedback law

actuator/sensor location	sensor $x=0$	sensor $x=L$
actuator at $x=0$	collocated	anti-collocated
actuator at $x=L$	anti-collocated	collocated

We are now able to design the corresponding output-feedback controllers.

Theorem 11.4.1.

Consider the two possible control laws at $x=0$ or at $x=L$

$$U_0(t)=\frac{\rho_2^\star}{1-r_2}\left(\int_{-L}^0 K_2^{vw}(0,y)\hat{w}_2(t,x)+K_2^{vv}(0,y)\hat{v}_2(t,x)dy\right.$$
$$\left.-\frac{r_2}{r_1}\int_0^L K_1^{vw}(0,y)\hat{w}_1(t,x)+K_1^{vv}(0,y)\hat{v}_1(t,x)dy\right), \tag{11.46}$$
$$U_L(t)=\frac{\rho_1^\star}{1-r_1}\left(\int_0^L\bar{K}_1^{vw}(L,y)\hat{w}_1(t,x)dy+\bar{K}_1^{vv}(L,y)\hat{v}_1(t,x)dy\right.$$
$$\left.+\int_{-L}^0 M^w(L,y)\hat{w}_2(t,x)dy+M^v(L,y)\hat{v}_2(t,x)dy\right), \tag{11.47}$$

where the estimated states are either given by equations (11.31) or (11.38), depending on the

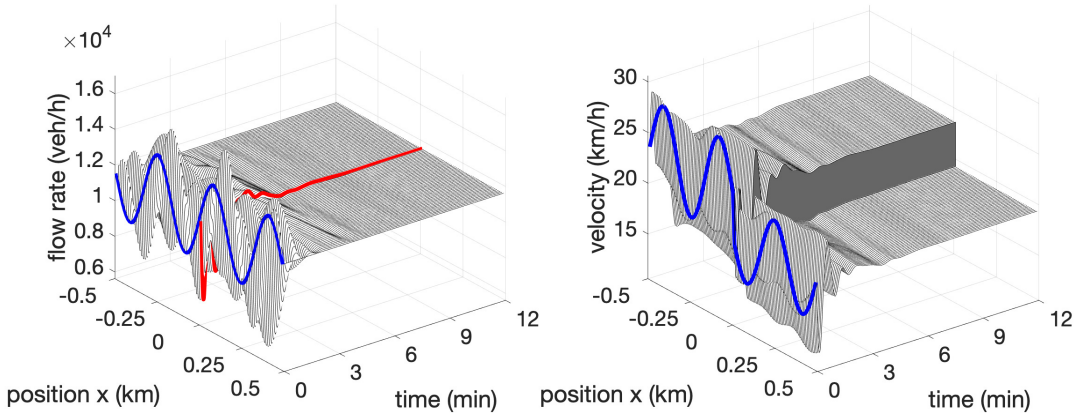

Figure 11.4: Closed-loop simulation of traffic flow rate and velocity, with the ramp metering control input $U_0(t)$ and measurement $Y_0(t)$ from the middle junction $x = 0$. The controlled flow rate evolution at $x = 0$ is highlighted in red.

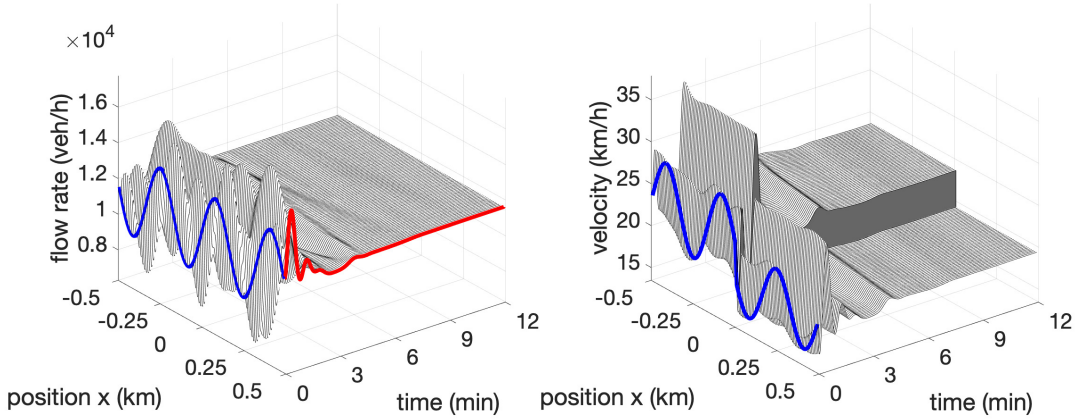

Figure 11.5: Closed-loop simulation of traffic flow rate and velocity, with the ramp metering control input $U_L(t)$ and measurement $Y_L(t)$ from the outlet boundary $x = L$. The controlled flow rate evolution at $x = L$ is highlighted in red.

available measurements. Then, the closed-loop system (11.12)-(11.13) with the controller (11.46) or (11.47) is exponentially stable at the origin. This implies the local convergence of the initial states of ρ_i and v_i to the steady states $\rho_i^\star$ and $v_i^\star$.

Proof : The proof is analogous to the ones proposed in Chapter 8 and Chapter 9. ■

11.5 . Simulation results

In this section, we first validate the control design with numerical simulations and compare the two collocated output feedback laws. Then we demonstrate the robustness of the proposed controllers to delays in the actuation path. Ultimately, our control design is compared with PI boundary controllers, which fully actuate the interconnected system. As stated in Table 11.1, there are four proposed output feedback controllers, but we only present the simulation results of the two collocated configurations. The collocated controllers are the most relevant in practice since the anti-collocated sensor and actuator in the distance will have delays and errors caused by long-distance communication.

The length of each freeway segment is chosen to be $L = 0.5$ km, so the total length of the two connected segments is 1 km. The simulation time is $T = 12$ min. The maximum speed limit is $v_m = 35$ m/s $= 126$ km/h. We consider six lanes for the downstream freeway segment 1. Assuming the av-

erage vehicle length is 5 m plus the minimum safety distance of 50% vehicle length, the maximum density of the road is obtained as $\rho_{m,1} = 6/7.5$ vehicles/m $= 800$ vehicles/km. The upstream segment has fewer functional lanes. Thus, its maximum density is $\rho_{m,2} = 700$ vehicles/km. We take $\gamma_i = 0.5$. The steady states $(\rho_1^\star, v_1^\star)$ and $(\rho_2^\star, v_2^\star)$ are chosen respectively as $(600$ vehicles/km$, 19.4$ km/h$)$ and $(488.6$ vehicles/km$, 23.8$ km/h$)$, both of which are in the congested regime. The constant flow rate is $q^\star = \rho_1^\star v_1^\star = \rho_2^\star v_2^\star = 11640$ vehicles/h, same for the two segments. If we consider segment 1 with six lanes, then the average flow rate of each lane is 1940 vehicles/h/lane. The equilibrium steady state of the downstream road has higher density and lower velocity and thus is more congested than the upstream road. The relaxation time is $\tau_1 = 80$ s and $\tau_2 = 60$ s. We use sinusoidal initial conditions for flow rate and velocity field, which represent the stop-and-go oscillations on the connected freeway and are highlighted in the figures in blue. The two-step Lax-Wendroff numerical scheme [LeV02] is applied.

11.5.1 . Output feedback stabilization

We consider in this traffic scenario that the downstream traffic in segment 1 is denser with slower velocity compared with the upstream traffic in segment 2, as illustrated by the steady states. The closed-loop simulation with the collocated output feedback control input from the middle junction shows that the exponential convergence to the steady states is achieved simultaneously for the upstream and downstream segments in Fig. 11.4, where the actuated junction flow rate by the on-ramp metering is highlighted in red. The output feedback stabilization with the control input and measurement of velocity and flow rate from the outlet boundary is shown in Fig. 11.5. Comparing the two closed-loop simulations in Fig. 11.4 and Fig. 11.5, we find out that the outlet controller takes around the same convergence time.The controlled flow rate at the middle junction with ramp metering input $U_0(t)$, highlighted in red in Fig. 11.4, first decreases such that less traffic is allowed into the downstream where traffic is denser. The controlled flow rate at the outlet with $U_L(t)$, highlighted in red in Fig. 11.5, increases initially such that more traffic is discharged from the segment.

To further compare the two collocated output feedback stabilization results, the closed-loop performance is demonstrated with the temporal evolution of the state variables in the spatial averaged L^2-norm, defined as

$$S_{q_i}(t) = \left| \frac{1}{L} \int_X \left(\frac{q_i(t,x) - q^\star}{q^\star} \right)^2 dx \right|^{1/2}, \tag{11.48}$$

$$S_{v_i}(t) = \left| \frac{1}{L} \int_X \left(\frac{v_i(t,x) - v_i^\star}{v_i^\star} \right)^2 dx \right|^{1/2}, \tag{11.49}$$

where $X = [-L, 0] \cup [0, L]$ represents the spatial domain of the two segments. As shown in Fig. 11.6, the closed-loop convergence time of both output controllers is around $t = 9\,\mathrm{min}$, whereas the output feedback controller at the outlet has a larger transient for all the state variables than the output feedback at the middle junction. At around $t = 2\,\mathrm{min}$, the blue highlighted line has a bigger overshoot than the red one. The ramp metering control input located at the downstream outlet is carried upstream by the propagation of velocity variations to mitigate traffic oscillations in both segments. In contrast, the ramp metering control input located at the middle junction works so that the actuated velocity variation at the junction travels upstream, and the actuated flow rate variations travel downstream with the traffic. Therefore, it takes longer for the control input to take effect on the upstream segment 2 when the output feedback is applied at the downstream outlet. The output feedback at the middle junction instantly starts stabilizing both the upstream segment 2 and downstream segment 1. The proposed output feedback controllers are robust to external boundary disturbances and delays in the actuation path as they are strictly proper (see Theorem 6.2.3). Here we conduct a simulation for the closed-loop system with constant input delays D_0 and D_L that are respectively 0 s$, 30$ s$, 60$ s$, 120$ s, where 0 s represents no delay and 120 s is the time length for the control input signal to traverse the two segments. Based on the definition in (11.48)-(11.49), we define an overall

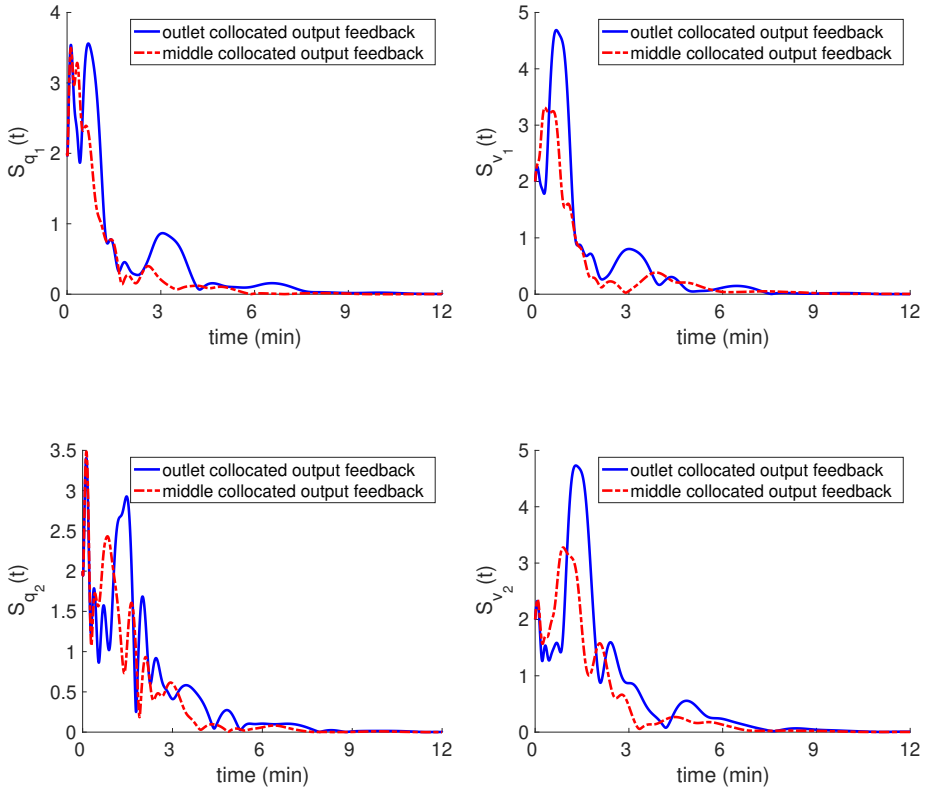

Figure 11.6: Comparison of the closed-loop performance of the two collocated output feedback controllers at $x = 0$ or $x = L$.

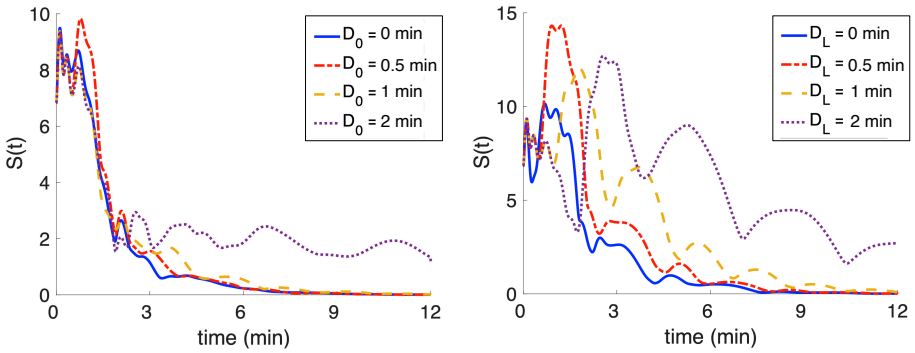

Figure 11.7: The temporal evolution of $S(t)$ of the closed-loop with delayed control inputs with delay time to be 0 min, 0.5 min, 1 min, and 2 min.

closed-loop performance index

$$S(t) = S_{q_i}(t) + S_{v_i}(t), \tag{11.50}$$

where $i = 1, 2$. Then the temporal evolution of $S(t)$ is plotted for the closed-loop system with the delayed collocated output feedback in Fig. 11.7.

11.5.2 . Comparison with PI controllers

PI control has been applied for traffic control by ramp metering [PHSB91]. For the macroscopic second-order PDE model, [ZLLP21] and [ZPQ19] developed PI boundary feedback controllers for the linearized ARZ model. For control of traffic on two cascaded freeway segments, boundary controllers are employed by [ZW19] including one ramp metering at inlet $x = -L$, one ramp metering and one

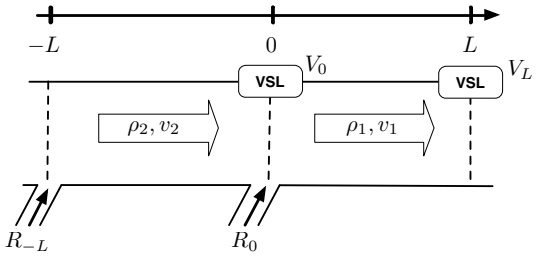

Figure 11.8: The fully-actuated traffic system with two ramp metering R_{-L}, R_0 and two VSL PI controllers V_0 and V_L (Figure from [YAK22]).

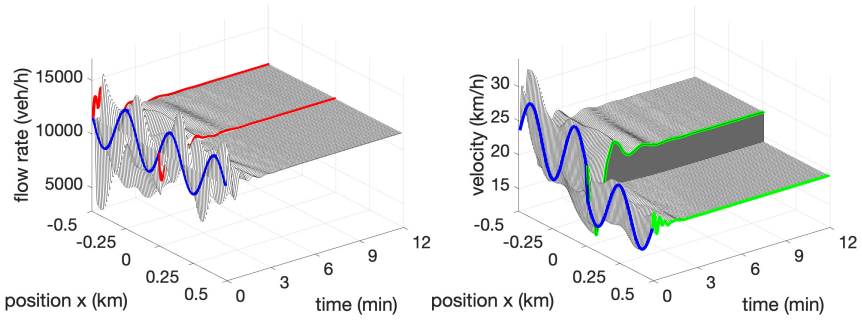

Figure 11.9: The closed-loop simulation with two PI boundary feedback ramp metering controllers $R_{-L}(t)$, $R_0(t)$, highlighted in red, and two VSL PI controllers $V_0(t)$ and $V_L(t)$, highlighted with green.

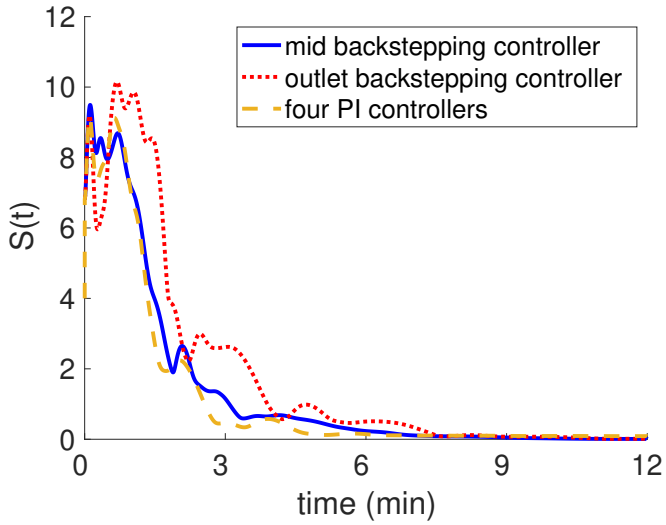

Figure 11.10: The closed-loop performance with ramp metering backstepping controller $U_0(t)$, ramp metering backstepping controller $U_L(t)$ and with four PI controllers including two ramp metering $R_{-L}(t)$, $R_0(t)$, and two VSLs $V_0(t)$ and $V_L(t)$.

VSL at middle junction $x = 0$, and one VSL at outlet $x = L$, as illustrated in Fig. 11.8. The controlled system is fully actuated since there are four boundary conditions, all of which are being actuated. In our design, only one boundary is actuated by ramp metering, either at the middle junction or at the outlet.

The four PI boundary controllers R_{-L}, R_0, V_0, V_L are defined respectively for the controlled flow rate at inlet $x = -L$, the controlled flow rate at middle junction $x = 0$, the controlled velocity at middle junction $x = 0$ and the controlled velocity at outlet $x = L$. The fully actuated boundaries are

defined as

$$q_2(-L,t) = R_{-L}(t), \quad v_2(0,t) = V_0(t), \tag{11.51}$$
$$q_1(0,t) = R_0(t), \quad v_1(L,t) = V_L(t), \tag{11.52}$$

where the boundary feedback controllers are given by

$$R_{-L}(t) = q^\star + k_P^r \tilde{\rho}_2(0,t) + k_I^r \int_0^t \tilde{\rho}_2(0,t)ds, \tag{11.53}$$
$$V_0(t) = v_2^\star + k_P^v \tilde{v}_2(-L,t) + k_I^v \int_0^t \tilde{v}_2(-L,t)ds, \tag{11.54}$$
$$R_0(t) = q^\star + l_P^r \tilde{\rho}_1(L,t) + l_I^r \int_0^t \tilde{\rho}_1(L,t)ds, \tag{11.55}$$
$$V_L(t) = v_1^\star + l_P^v \tilde{v}_1(0,t) + l_I^v \int_0^t \tilde{v}_1(0,t)ds. \tag{11.56}$$

where $k_P^r, k_I^r, k_P^v, k_I^v$ are tuning gains for the upstream segment 2, $l_P^r, l_I^r, l_P^v, l_I^v$ are tuning gains for the downstream segment 1 and $q^\star, v_i^\star$ are the steady states. We use the previous model parameters and conduct the simulation under the same initial conditions such that the PI controllers can be directly compared with the control design in this paper. The tuning gains are chosen to be $k_P^r = -55, k_I^r = -0.035, k_P^v = -0.6, k_I^v = -0.025$ and $l_P^r = -10, l_I^r = -0.035, l_P^v = -0.5, l_I^v = -0.005$. The closed-loop system behavior is shown in Fig. 11.9 where the temporal evolution of the four PI control inputs are highlighted, including two ramp metering in red and two VSLs in green. We then compare the closed-loop performance of the PDE backstepping controller and the PI controllers with the evolution of state variables in the spatial averaged L^2-norm, defined with $S(t)$ in (11.50). In Fig. 11.10, the closed-loop performance with the ramp metering backstepping controller at middle junction $U_0(t)$ is plotted with the blue line, the one with the ramp metering backstepping controller at outlet $U_L(t)$ is plotted in red dotted line, and the one with the four PI controllers is plotted with the yellow dashed line. We can see that the convergence time and the transient are about the same for $U_0(t)$ and four PI controllers. The outlet backstepping controller $U_L(t)$ takes a relatively more significant time to stabilize the system.

11.6 . Conclusions and perspectives

In this chapter, we have shown how the theoretical results developed in Chapters 8-9 could be used to design continuous boundary control and estimation strategies for traffic problems. We considered the output-feedback stabilization of two cascaded freeway segments with various actuator/sensor configurations. With numerous simulations, we have shown that the proposed advanced control techniques based on the backstepping methodology allow similar performance to those obtained using simpler PI controllers but with considerably fewer actuators and sensors. This emphasizes the possible advantages of the methods and techniques presented in this manuscript. However, these strategies need to be implemented into digital platforms. More precisely, the rate inflow is controlled through traffic light modulation that cannot be carried out continuously. Typically, periodic strategies are used to modulate the frequency of light changes. It has to be done either periodically or at events. The drawback with periodic implementations is that one may produce unnecessary updates of the controllers, which may cause overutilization of computational/communication resources, actuator changes that are more frequent than necessary, and unsafe driving conditions. Therefore, for the arising continuous time boundary controllers, the issue of sampling has to be carefully studied. Indeed, if sampling is not appropriately addressed, the stability and estimation properties may be lost. Therefore, sampled data and event-triggered control can offer suitable approaches for digital realizations. For hyperbolic PDEs, sampled-data control has been studied in [DBPPDM18] and event-triggered control in [EGMP16, EGMP17, Esp20] and in [LLLL21, WK21] for coupled hyperbolic PDE-ODEs. It is worth saying that the event-triggered strategies in the infinite-dimensional setting have been inspired by some

of those already well-established for finite-dimensional systems, e.g., [Tab07, Lem10, Gir15, PTNA15, LZJ19] and the references therein. Moreover, event-triggered control strategies applied to traffic flow have been proposed for freeway discrete-time models (e.g., those coming from the Cell Transmission Model (CTM), where subdivision of the freeway into cells and the discretization of the time horizon are typically done). They are suitable for implementation-oriented control design: e.g., using Model Predictive Control (MPC) combined with event-triggered control to determine the ramp metering actions, as is proposed in [FSS15] and later in [FSS16]. Overall, event-triggered model predictive control is more efficient than solely MPC strategies, especially when reducing the frequency of solving the optimization problem and updating the control laws only when needed.

Consequently, designing an event-triggered output-feedback law to stabilize the traffic on the two cascaded road segments is a relevant extension to the results presented in this chapter. Such an event-triggered algorithm, based on emulating the proposed output-feedback laws, has been designed in [EAYK22b, EAYK22a]. The control signal was updated according to a suitable dynamic triggering condition. We proved that under this strategy, there exists a uniform minimal dwell time (independent of initial conditions), thus avoiding the Zeno phenomenon. We also guaranteed the exponential convergence of the closed-loop system under the proposed event-triggered boundary control. The resulting suitably sampled control law avoids useless actuation solicitations. Possible extensions would include the design of a periodic event-triggered control strategy to monitor the triggering condition periodically, hence, saving computational resources. Moreover, the questions related to quantized implementations of event-triggered controllers should also be considered.

Part III

Perspectives and Concluding Remarks

12 - Perspectives

This chapter presents perspectives and ongoing work that build upon the results presented in Part II. This part aims to highlight the potential of the results developed in the manuscript, mainly regarding the study of general networks of hyperbolic systems. It also highlights challenging problems and promising advances. Some ideas and claims introduced in this chapter will be presented without proof since they are still preliminary.

P1 . Designing explicit output-feedback control laws for arbitrary networks

The constructive methods proposed in this manuscript for controlling networks of hyperbolic systems require **specific structural assumptions**. In Chapter 7, we considered configurations where the PDE system is not under-actuated or under-measured (even if an ODE can filter the actuation). Although the corresponding design assumptions are less restrictive than those existing in the literature, there are many configurations for which they are not satisfied. In Chapter 8, we focused on a network with a **chain** structure (i.e., the graph representing the network is a straight line, and the actuator is located at one of its extremities) and generalized the recursive interconnected framework introduced in [RAN21b]. In Chapter 9, we considered a simple chain with two subsystems but actuated at the junction. We have shown that the design of stabilizing controllers was only possible under specific controllability conditions. This emphasizes that depending on the actuator/sensor locations, networks with a chain structure may not be controllable/observable.

A network of hyperbolic systems can be described as a **graph**. For instance, each elementary hyperbolic subsystem can be identified with an edge of a given graph. At the same time, interactions between the PDEs occur at the graph's vertices. This **graph representation** has been used in [DZ06] to describe networks of wave equations. We believe such a representation will be a cornerstone to designing control strategies for complex networks of hyperbolic systems. Examples of possible network configurations are given in Figure 12.1. Then, two **theoretical challenges** naturally arise

1. Given a configuration of actuators/sensors, we want to verify that this configuration makes the system controllable/observable before designing an appropriate modular, scalable, and numerically implementable control law. This will require enhancing the **qualitative analysis** to understand the links between the structure of the network (e.g., number of cycles, incidence matrix) and its **controllability/observability** properties.

2. Considering a given number of actuators, we aim to find admissible locations to guarantee controllability/observability. We aim to characterize the **possible actuator/sensor configurations** for a given graph structure that guarantee controllability/observability. For each location, we will then design properly tuned output-feedback controllers.

To solve these challenging open questions, we aim to develop an innovative methodology that

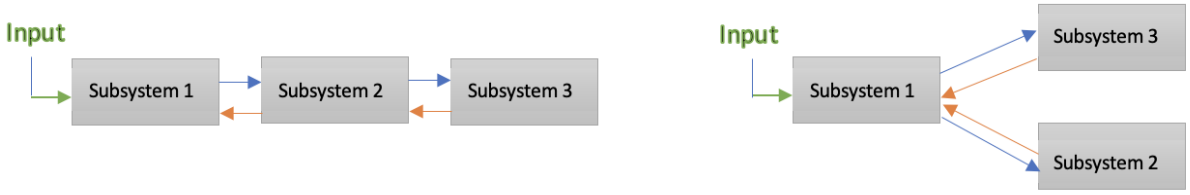

Figure 12.1: Examples of possible network configurations: chain structure (left), junction/tree (right). The arrows picture possible boundary couplings between the subsystems.

extends the approach developed in Chapter 9 in the case of two interconnected scalar hyperbolic systems. It relies on the **theory of integral equations**. As shown in Chapter 6, in the absence of the ODEs systems, the original hyperbolic network can be rewritten as a set of simpler **Integral Delay Equations** (IDEs)

$$z(t) = \sum_{k=1}^{N} A_k z(t-\tau_k) + \int_0^{\tau_N} f(\nu) z(t-\nu) d\nu + \sum_{k=1}^{N} B_k U(t), \tag{12.1}$$

where we still denote z the state and U the control input. The parameters τ_k are positive delays, the matrices A_k and B_k are constant, and f is a piecewise continuous function. We have shown in Chapter 9 that by performing adequate changes of variables, this equation can be rewritten as

$$z(t) = \sum_{k=1}^{N} A_k z(t-\tau_k) + \int_0^{\tau_N} f(\nu) z(t-\nu) d\nu + \sum_{k=1}^{N} B_k U(t) + \int_0^{\tau_N} g(\nu) U(t-\nu) d\nu, \tag{12.2}$$

where we have overloaded the different variables and where g is a piecewise continuous function. Equation (12.2) is an IDE with pointwise and distributed control terms. The advantage of equation (12.2) compared to equation (12.1) is that the **dimension of the state is smaller**. As seen in Chapter 9 spectral controllability conditions can easily be obtained for such systems [Mou98]. These conditions have been shown to be sufficient to design exponentially stabilizing controllers for the test case considered in Chapter 9.

The future work of I. Balogoun (postdoctoral fellow co-supervised with I. Boussaada and G. Mazanti) will fit a part of this research axis. I also plan to hire Ph.D. students and interns using the funding obtained from the PANOPLY ANR JCJC project and funding from Université Paris-Saclay.

P1.1 . Controllability, observability and control design

We believe the approaches developed in Chapter 9 can be extended to stabilize equation (12.2), thus generalizing the backstepping approach to IDEs. More precisely, we introduce a set of **candidate control inputs** expressed as distributed delayed feedback of the state and the input (namely $VUt) = \int_0^{\tau_N} M(\nu)X(t-\nu) + N(\nu)U(t-\nu)d\nu$). A control law from this set will stabilize the system if the functions M and N are solutions to Fredholm equations. It appeared in Chapter 9 that the spectral controllability conditions implied the existence of solutions for these integral equations. Although the analysis of Fredholm integral equations is a difficult problem [KMK89], we believe the constructive approach presented in Chapter 9 can be first extended to a chain with a larger number of non-scalar subsystems. Then, to deal with *more involved network structures*, we will use **graph theory** to simplify the description of the network and subdivide it into simpler sub-networks. Indeed, the structure of the matrices A_k and B_k are related to the graph properties (e.g., number of cycles, incidence matrix). In that sense, our approach relates to the spectral methodology proposed in [DZ06] for wave-equations networks. We could also take advantage of the analysis performed [CMS20] to obtain controllability conditions. Moreover, using the concept of structural controllability [Lin74], we will identify reflections of graph-theoretic notions on the system properties and relate the graph structure of the network with the proposed IDE representation (particularly regarding the sparsity of the different coupling matrices appearing in equation (12.2)). We believe we can take advantage of these properties to show that the corresponding set of Fredholm equations admits a solution. This should simplify the controllability conditions and, therefore, the design of the corresponding controllers. Moreover, this could help to identify configurations for which the network is always controllable. The results from Chapter 8 and Chapter 9 suggest possible controllability conditions depending on the minimal number of paths required to browse the entire network starting from the actuator nodes. In this context, the **recursive framework** developed in Chapter 8 could be a promising path to simplify the design by subdividing the graph into sub-graphs. Note that this approach can be leveraged to obtain numerical solutions to the problem. State observers will be designed following a similar path.

P1.2 . Admissible actuator and sensor locations

The second objective consists of finding the minimum number of actuators/sensors (and their respective position in the network) to guarantee the possibility of controlling/observing a given network of hyperbolic systems. Then, assuming we now have a fixed number of actuators/sensors greater than this value, we want to know all the **admissible configurations** under which it is possible to design output-feedback controllers. Even if there is a *paradigm change* compared to Section P1.1 as the actuators/sensors can now be arbitrarily placed in the network, there are also strong connections between the two objectives. Thus, we will use similar tools (structural controllability [Lin74], spectral controllability conditions, integral approach) to establish the links between the structure of the graph describing the network and admissible locations for actuators/sensors (i.e., the ones for which the system is controllable/observable). We expect to connect the minimal number of actuators/sensors with some of the network graph properties (e.g., number of cycles, branches). Similarly, admissible locations should be expressed in terms of **graph properties**.

To simplify the analysis, we may first consider that all the network subsystems have the same dimensions. We may also start by considering a gradation in the complexity of the network by focusing on **specific network configurations**: chain, divergence, star, simple trees, one cycle. We believe the proposed methodologies can be adjusted to deal with the presence of ODEs in the network. Interestingly, the results we will obtain for stabilizing general networks will directly affect the design of stabilizing controllers for underactuated systems, as shown in [ABABP20].

P2 . Performance specifications and robustness analysis

In the whole manuscript, we mostly focused on stabilizing system (6.1) and did not directly consider the closed-loop performance of the designed output-feedback controllers. To guarantee the existence of robustness margins, we have derived simple sufficient conditions under which appropriate low-pass filters can be combined with the proposed control law to obtain a strictly proper controller, as stated in Theorem 6.2.3. However, considering practical applications, we believe a deeper quantitative analysis of the performance and robustness properties of the closed-loop system is necessary.

I plan to hire a postdoctoral fellow to work with me on this research axis, using the funding obtained from the PANOPLY JCJC ANR project.

P2.1 . Analytical tools to quantify closed-loop performance

We believe it is crucial to assess and **quantify the performance** of the output-feedback controllers we design with respect to a set of performance criteria. This set of performance criteria should be defined in terms of **practical relevant properties** for industrial applications [ÅM21]. So far, such a complete performance analysis has yet to be developed. A thorough literature review and classification of existing criteria (such as disturbance rejection, robustness margins, sensitivity functions, or convergence rate) for finite-dimensional systems is needed to separate candidates for distributed parameter systems. Furthermore, these concepts must be tailored to the specific requirements of infinite-dimensional systems: the concept of phase margin is, for instance, an insufficient metric for infinite-dimensional systems since significant dynamics can be spread over a wide frequency range and with more esoteric behavior of systems that are not strictly proper [CM09, LRW96]. Consequently, one of our first objectives is defining a set of **relevant performance criteria**.

Then, we aim to develop **analytical techniques** to quantify the performance of our output-feedback laws regarding this set of specifications. Using the time delay representation (6.23)-(6.25), we wish to apply **frequency-domain methods** developed for time-delay systems to analyze the qualitative and quantitative properties of our closed-loop systems [MN07, LNC+16]. The main difficulties lie in the performance limitations of the neutral asymptotic chains and in treating the distributed delay terms. Finally, the Port-Hamiltonina Systems (PHS) methodology can provide a framework with clear energy interpretations [JZ12] to quantify the closed-loop performance. This will require establishing clear links between the representation (6.23)-(6.25) of our *controlled* network and a possible PHS rewriting. These analytical techniques should be benchmarked on examples and test case studies, such as in Chapter 11 when designing stabilizing controllers for freeway segments. We will

define simple and realistic scenarios to test the proposed control strategies. This would allow us to quantitatively compare our control strategies with conventional controllers (namely PI controllers) with respect to a given set of specifications.

P2.2 . Robustness with respect to stochastic uncertainties

Although the robustness guarantees given in Theorem 6.2.3 provide admissible bounds for constant uncertainties, we want to investigate the robustness properties of the controllers designed in this manuscript with respect to time-varying uncertainties or even stochastic ones. Only a few results in the literature focus on hyperbolic systems with time-varying coefficients [CN21b, MAK22]. However, when considering applications as freeway transportation systems, some parameters may be subject to abrupt changes due to external causes, e.g., the random flux at the entrance of the freeway [Col03] or changes in drivers' behavior. This has motivated the stability analysis of switching hyperbolic systems [AHB11] or Markov jump linear hyperbolic conservation laws [ZP17]. In this latter contribution, the authors considered stochastic velocities and showed mean-square exponential stability under appropriate conditions (balance between the dissipativity of the hyperbolic and the transition probability of the Markov process). Below are some recent preliminary results that guarantee the mean-square exponential stabilization of coupled hyperbolic systems with random parameters. More precisely, consider the scalar hyperbolic system (simplified version of (5.1))

$$\partial_t u(t,x) + \lambda(t)\partial_x u(t,x) = \sigma^+(t)v(t,x), \tag{12.3}$$
$$\partial_t v(t,x) - \mu(t)\partial_x v(t,x) = \sigma^-(t)u(t,x), \tag{12.4}$$

with the boundary conditions

$$u(t,0) = q(t)v(t,0),\ \ v(t,1) = \rho(t)u(t,1) + U(t), \tag{12.5}$$

with the nominal backstepping control law

$$U(t) = \int_0^1 K(y)u(t,y) + L(y)v(t,y)dy, \tag{12.6}$$

where the functions K and L are designed using the backstepping approach for nominal values of the parameters $(\lambda(t), \mu(t), \sigma^+(t), \sigma^-(t), q(t), \rho(t)) = (\lambda_0, \mu_0, \sigma_0^+, \sigma_0^-, q_0, \rho_0)$ [CVKB13]. However, we consider here that the parameters are stochastic. More precisely, they are modeled by independent Markov processes with a finite number of states [KM01]. We denote $\mathfrak{S} = \{\lambda, \mu, \sigma^+, \sigma^-, q, \rho\}$ the set of random variables. Each random element X of the set $\mathfrak{S}$ is a Markov process with the following properties.

- (P1) $X(t) \in \{X_i, i \in \{1, \dots, r_X\}\}$, $r_X \in \mathbb{N}$ with $\underline{X} \leq X_1 < \dots < X_{r_X} \leq \bar{X}$.
- (P2) The transition probabilities $P_{ij}^X(t_1, t_2)$ qualify the probability to switch from X_i at time t_1 to X_j at time t_2 ($(i,j) \in \{1, \dots, r_X\}^2,\ 0 \leq t_1 \leq t_2$). They satisfy
  1. $P_{ij}^X : \mathbb{R}^2 \to [0,1]$ with $\sum_{j=1}^{r_X} P_{ij}^X(t_1, t_2) = 1$.
  2. P_{ij}^X is a differentiable function which, for $s < t$ follows the Kolmogorov equation

$$\partial_t P_{ij}^X(s,t) = -c_j^X(t)P_{ij}^X(s,t) + \sum_{k=1}^{r_X} P_{ik}^X(s,t)\tau_{kj}^X(t),$$
$$P_{ii}^X(s,s) = 1, \text{ and } P_{ij}^X(s,s) = 0 \text{ for } i \neq j, \tag{12.7}$$

  where τ_{ij} and $c_j^X = \sum_{k=1}^{r_X} \tau_{jk}^X$ are nonnegative-valued functions such that for any t, $\tau_{ii}^X(t) = 0$. Moreover, the functions τ_{ik}^X are upper bounded by a constant $\tau_X^\star$.
- (P3) The realizations of X are right-continuous.

Moreover, we assume that for all $X \in \mathfrak{S}$, we have $\underline{X} \leq X_0 \leq \bar{X}$ (where X_0 is the nominal value, e.g. $X_0 = \lambda_0$ if $X = \lambda$). We also assume that $\underline{\lambda} > 0$, $\underline{\mu} > 0$ and $|\bar{\rho}\bar{q}| < 1$. It is common to assume only a finite number of values in (P1) [KM01, SBO19]. Similarly, it is standard to assume Property (P3) for the modeling of continuous-time Markov chains. It is important to mention that the properties (P1) and (P3), along with the Markov property, guarantee that P_{ij}^X satisfies the Kolmogorov Equation (12.7) for certain positive-valued functions τ_{ij}^X, c_j^X [RH03, Ros14]. Thus Property (P2) only implies that the functions τ_{ij}^X are bounded, which is a mild modeling assumption. We emphasize that the parameter $\tau_{ij}^X \Delta t$ is approximately the probability of transition from X_i to X_j on the interval $[t, t + \Delta t)$. Moreover, $1 - c_j^X(t)\Delta t$ is the probability of staying at X_j during this time interval. The stochastic system under consideration is well-posed.

Lemma P2.1 *For any initial condition $(u^0, v^0) \in L^2[0,1]$ and for any initial states $\delta(0)$ for the stochastic parameters, the closed-loop system* (12.3)-(12.4) *with the nominal control law* (12.6) *admits a unique solution (u, v) such that for any t,*

$$\mathbb{E}_{[0,(u^0,v^0,\delta(0))]}\{||(u(t,\cdot), v(t,\cdot)||_{L^2[0,1]}\} < \infty.$$

Proof : The proof can be easily adjusted from [ZP17]. Almost every sample path of our stochastic processes is a right-continuous step function with a finite number of jumps in any finite time interval. We can then define a sequence $\{t_k;\ k = 0, 1, \dots\}$ of stopping time such that $t_0, \lim_{k\to\infty} t_k = \infty$ and every $X \in \mathfrak{S}$ is constant on $t_k \leq t < t_{k+1}$. We can then iteratively build the solution on each interval $[t_k, t_{k+1}]$ by applying [BC16, Theorem A.4]. The rest of the proof is analogous to [ZP17, Proof of Proposition 1]. ■

Then, we can generalize the deterministic robustness results stated in [ADM20] to the case of stochastic parameters.

Theorem P2.1.

Consider the closed-loop system (12.3)-(12.5) with the control law (12.6). There exists a positive constant $\epsilon^\star$, such that if, for all time $t \geq 0$ and all $X \in \mathfrak{S}$,

$$\sum_{X\in\mathfrak{S}} \mathbb{E}_{[0,X(0)]}(|X_0 - X(t)|) \leq \epsilon^\star, \tag{12.8}$$

then the closed loop system is *mean-square exponentially stable*, that is, there exists $\kappa > 0$ and $\gamma > 0$ such that

$$\mathbb{E}_{[0,(w(0),\delta(0))]}(w(t)) \leq \kappa \mathrm{e}^{-\gamma t} w(0), \tag{12.9}$$

where $w(t) = \int_0^1 u^2(t,x) + v^2(t,x)dx$.

Proof : The proof of Theorem P2.1 is inspired by [KBP22b]. It can be found in [APK23]. First, the system is simplified using a backstepping transformation, and then, the stability is shown using a Lyapunov analysis. The exponential stability is shown using the so-called technique of probabilistic delay averaging [KM01]. Applying the nominal backstepping transformation, we can map the system (12.3)-(12.5) to the target system

$$\begin{aligned}\partial_t\alpha(t,x) + \lambda(t)\partial_x\alpha(t,x) &= f_1(\delta(t))v(t,x) + f_2(\delta(t))\beta(t,0)\\ &\quad + \int_0^x f_3(\delta(t),x,y)u(t,y) + f_4(\delta(t),x,y)v(t,y)dy \qquad (12.10)\\ \partial_t\beta(t,x) - \mu(t)\partial_x\beta(t,x) &= g_1(\delta(t))u(t,x) + g_2(\delta(t))\beta(t,0)\\ &\quad + \int_0^x g_3(\delta(t),x,y)u(t,y) + g_4(\delta(t),x,y)v(t,y)dy, \qquad (12.11)\end{aligned}$$

with the boundary conditions

$$\alpha(t,0) = q(t)\beta(t,0), \tag{12.12}$$

$$\beta(t,1) = \rho(t)\alpha(t,1) + (\rho(t) - \rho_0)\int_0^1 K^{vu}(1,y)u(t,y)dy + (\rho(t) - \rho_0)\int_0^1 K^{vv}(1,y)v(t,y)dy, \tag{12.13}$$

where the functions f_i and g_i are such that exists a constant $M_0 > 0$ such that for any realization $\delta(t) = \delta_j$ ($j \in \mathfrak{R}$) of the stochastic variable δ and for any $(x, y) \in \mathcal{T}$, for all $i \in \{1, 2, 3, 4\}$, we have

$$|f_i(\delta_j)| < M_0 \sum_{X \in \mathfrak{S}} |X_0 - X_j|, \ |g_i(\delta_j)| < M_0 \sum_{X \in \mathfrak{S}} |X_0 - X_j|. \tag{12.14}$$

Consider the following Lyapunov functional candidate

$$V(z, \delta) = \int_0^1 \frac{\mathrm{e}^{-\frac{\nu}{\lambda(t)}x}}{\lambda(t)} \alpha^2(t, x) + a \frac{\mathrm{e}^{\frac{\nu}{\mu(t)}x}}{\mu(t)} \beta^2(t, x) dx, \tag{12.15}$$

with $a, \nu > 0$. This functional explicitly depend on δ through the velocities λ and μ. Since the velocities $\lambda(t)$ and $\mu(t)$ are upper and lower bounded, the functional V is equivalent to the L^2-norm of the state (α, β). We define the infinitesimal generator L [KM13, Ros14] acting on the functional $V : (L^2([0, 1], \mathbb{R}))^2 \times \mathfrak{T} \to \mathbb{R}$ as

$$LV(z, \delta) = \limsup_{\Delta t \to 0^+} \frac{1}{\Delta t} \mathbb{E}_{[t,(z,\delta)]}(V(z(t + \Delta t), \delta(t + \Delta t)) - V(z, \delta)). \tag{12.16}$$

We define L_j, the infinitesimal generator of the Markov process (z, δ) (where $z(t, \cdot) = (\alpha(t, \cdot), \beta(t, \cdot))$ obtained from the system (12.10)-(12.13) by fixing $\delta(t) = \delta_j$ ($j \in \mathfrak{R}$) as

$$L_j V(z) = \frac{dV}{dz}(z, \delta_j) h_j(z) + \sum_{\ell \in \mathfrak{R}} (V_\ell(z) - V_j(z)) \tau_{j\ell}(t), \tag{12.17}$$

where $V_\ell(z) = V(z, \delta_\ell)$, and h_j is the operator corresponding to the dynamics of the target system (12.10)-(12.13) with the fixed value $\delta(t) = \delta_j$. From now, we consider that $\delta(t = 0) = \delta_i$ for some $i \in \mathfrak{R}$. Performing a classical Lyapunov analysis and using (12.14) and Young's inequality, we can show there exists $\eta > 0$ and $M_1 > 0$ such that

$$\frac{dV_j}{dz}(z) h_j(z) \leq -\eta V(t) + M_1 \sum_{X \in \mathfrak{S}} |X_0 - X_j| V(t). \tag{12.18}$$

In the meantime, we have

$$\sum_{\ell=1}^{r} (V_\ell(z) - V_j(z)) \tau_{j\ell} = \sum_{\ell=1}^{r} \tau_{j\ell} \int_0^1 \left(\frac{\mathrm{e}^{-\frac{\nu}{\lambda_{\ell_\lambda}}x}}{\lambda_{\ell_\lambda}} - \frac{\mathrm{e}^{-\frac{\nu}{\lambda_{j_\lambda}}x}}{\lambda_{j_\lambda}} \right) \alpha^2(t, x) + a \left(\frac{\mathrm{e}^{\frac{\nu}{\mu_{\ell_\mu}}x}}{\mu_{\ell_\mu}} - \frac{\mathrm{e}^{\frac{\nu}{\mu_{j_\mu}}x}}{\mu_{j_\mu}} \right) \beta^2(t, x) dx.$$

Using the mean value theorem, on the functions $\lambda \mapsto \frac{\mathrm{e}^{-\frac{\nu}{\lambda}x}}{\lambda}$ and $\mu \mapsto \frac{\mathrm{e}^{\frac{\nu}{\mu}x}}{\mu}$, we obtain

$$\sum_{\ell=1}^{r} (V_\ell(z) - V_j(z)) \tau_{j\ell} \leq M_2 \sum_{\ell=1}^{r} \sum_{X \in \mathfrak{S}} \tau_{j\ell} |X_\ell - X_j| V(t),$$

where $M_2 > 0$. Combining this inequality with equation (12.18), we get

$$L_j V(t) \leq -\eta V(t) + M_1 \sum_{X \in \mathfrak{S}} |X_0 - X_j| V(t) + M_2 \sum_{\ell=1}^{r} \sum_{X \in \mathfrak{S}} \tau_{j\ell} |X_\ell - X_j| V(t). \tag{12.19}$$

We now compute the quantity $\bar{L} = \sum_{j=1}^{r} P_{ij}(0, t) L_j V(t)$. Notice first that $\sum_{j=1}^{r} P_{ij}(0, t) \sum_{X \in \mathfrak{S}} |X_0 - X_j|$ $= \mathbb{E}_{[0,\delta(0)]} \left(\sum_{X \in \mathfrak{S}} |X_0 - X(t)| \right) = \sum_{X \in \mathfrak{S}} \mathbb{E}_{[0,X(0)]}(|X_0 - X(t)|)$, since all the variables are independent. Thus, applying the triangular inequality, the following inequality holds

$$\begin{aligned}
\bar{L} &\leq [-(\eta - M_1 \sum_{X \in \mathfrak{S}} \mathbb{E}_{[0,X(0)]}(|X_0 - X(t)|)) + M_2 \sum_{j=1}^{r} \sum_{\ell=1}^{r} P_{ij}(0, t) \sum_{X \in \mathfrak{S}} \tau_{j\ell}(|X_\ell - X_0| + |X_j - X_0|)] V(t) \\
&\leq -(\eta - (M_1 + M_2 r \tau^\star) \sum_{X \in \mathfrak{S}} \mathbb{E}_{[0,X(0)]}(|X_0 - X(t)|)) V(t) + M_2 \sum_{j=1}^{r} \sum_{\ell=1}^{r} P_{ij}(0, t) \sum_{X \in \mathfrak{S}} \tau_{j\ell} |X_\ell - X_0| V(t)
\end{aligned}$$

Applying (12.7), we obtain

$$\sum_{j=1}^{r} P_{ij}(0, t) L_j V(t) \leq -V(t) \big(\eta - M_2 k(t) - (M_1 + M_2 r \tau^\star) \sum_{X \in \mathfrak{S}} \mathbb{E}_{[0,X(0)]}(|X_0 - X(t)|) \big), \tag{12.20}$$

where the function k is defined by

$$k(t) = \sum_{X \in \mathfrak{S}} \sum_{j=1}^{r} |X_j - X_0| (\partial_t P_{ij}(0, t) + c_j P_{ij}(0, t)).$$

Let us denote $k_0(t) = \eta - (M_1 + M_2 r\tau^\star)\sum_{X\in\mathfrak{S}} \mathbb{E}_{[0,X(0)]}(|X_0 - X(t)|) - M_2 k(t))$ and define the functional $Z(t)$ as $Z(t) = \exp(\int_0^t k_0(s)ds)V(t)$. We have

$$\int_0^t k(s)ds \leq \sum_{X\in\mathfrak{S}} (\mathbb{E}_{[0,X(0)]}(|X_0 - X(t)|) + c^\star \int_0^t \mathbb{E}_{[0,X(0)]}(|X_0 - X(s)|)ds),$$

where $c^\star = r\tau^\star$. Consequently, defining $\epsilon^\star = \frac{\eta}{2(2M_2c^\star)+M_1}$, if $\sum_{X\in\mathfrak{S}} \mathbb{E}_{[0,X(0)]}(|X_0 - X(t)|) \leq \epsilon^\star$, we obtain

$$\mathbb{E}_{[0,(z,\delta)(0))]}(Z(t)) \geq \mathbb{E}_{[0,(z,\delta)(0))]}(\mathrm{e}^{-M_2\epsilon^\star + \frac{\eta}{2}t}V(t)). \tag{12.21}$$

In the meantime, we have

$$\mathbb{E}_{[0,(z(0),\delta(0))]}(LZ(t)) = \mathrm{e}^{\int_0^t k_0(s)ds}\mathbb{E}_{[0,(z(0),\delta(0))]}(LV(t)).$$

Since $\mathbb{E}_{[0,(z(0),\delta(0))]}(LV(t)) = \mathbb{E}_{[0,(z(0),\delta(0))]}(\sum_{j=1}^r P_{ij}(0,t)\ L_jV(t))$, we obtain using equation (12.20)

$$\mathbb{E}_{[0,(z(0),\delta(0))]}(LZ(t)) \leq \exp(\int_0^t k_0(s)ds)\mathbb{E}_{[0,(z(0),\delta(0))]}(k_0(t)V(t) + \sum_{j=1}^r P_{ij}(0,t)L_jV(t)) \leq 0.$$

Therefore, according to Dynkin's formula [Dyn12, Theorem 5.1, p. 132], we obtain

$$\mathbb{E}_{[0,(z(0),\delta(0))]}(Z(t)) - Z(0) = \mathbb{E}_{[0,(z(0),\delta(0))]}(\int_0^t LZ(s)ds) \leq 0. \tag{12.22}$$

Consequently, defining $\gamma = \frac{\eta}{2}$, and combining equations (12.21) and (12.22), we obtain

$$\mathbb{E}_{[0,(z(0),\delta(0))]}(V(t)) \leq V(0)\mathrm{e}^{M_2\epsilon^\star}\mathrm{e}^{-\gamma t}. \tag{12.23}$$

This concludes the proof. ■

Although Theorem P2.1 is only shown in the case of the elementary scalar hyperbolic system (12.3)-(12.5), we believe the ingredients of the proofs would remain identical when dealing with complex networks, provided an appropriate Lyapunov functional is available. This motivates the research on explicit Lyapunov functionals for networks of hyperbolic systems. We should also focus on the generalization of our approach to non-independent stochastic parameters and to a larger class of random variables (that may not be described by Markov processes) and random fields.

P3 . Lyapunov functional for hyperbolic systems

Consider the general hyperbolic system

$$\begin{cases} \partial_t u(t,x) + \Lambda^+\partial_x u(t,x) = \Sigma^{++}(x)u(t,x) + \Sigma^{+-}(x)v(t,x), \\ \partial_t v(t,x) - \Lambda^-\partial_x v(t,x) = \Sigma^{-+}(x)u(t,x) + \Sigma^{--}(x)v(t,x), \\ v(t,1) = Ru(t,1),\ u(t,0) = Qv(t,0) + f(t), \end{cases} \tag{12.24}$$

where $f(t)$ is an exogenous signal that may correspond to the control input. As we have seen in Chapter 5, equations (12.24) can model a wide variety of networks. We have omitted the ODE part for the sake of simplicity. Even if we may know how to design a stabilizing controller for system (12.24) (for instance, using the techniques developed in Section P1), it may be interesting to obtain an explicit Lyapunov functional. First, it can help us characterize the open-loop stability of the system (using simpler conditions than the one proposed in [HVL93]). Then, several control strategies (as event-triggered controllers) require Lyapunov functionals (see, e.g., [EGMP16, EAYK22b]). Consequently, having an appropriate Lyapunov functional is crucial to improve our controllers by adding an event-trigger mechanism (as mentioned in Chapter 11), thus avoiding useless actuator solicitations. Moreover, having a Lyapunov function also opens some interesting perspectives regarding robustness analysis as seen in Section P2.2 (see also [AKBP22] for a discussion on the interest of having such a general functional to deal with robustness with respect to stochastic delays in the actuation).

In the absence of the exogenous signal $f(t)$, some sufficient conditions based on Linear Matrices Inequalities have been proposed in [BC16]. In the case of conservation laws (i.e., the matrices $\Sigma^{\cdot\cdot}$ all equal zero), the functionals given in [CBdN08, BC16] require dissipative boundary conditions, i.e.

$$\inf\{||\Delta \begin{pmatrix} 0 & Q \\ R & 0 \end{pmatrix} \Delta^{-1}||,\ \Delta \in \mathcal{D}^+_{n+m}\} < 1, \tag{12.25}$$

where $\mathcal{D}^+_{n+m}$ is the set of diagonal matrices of dimension $n+m$ whose elements on the diagonal are positive. However, exponentially stable systems exist for which dissipative boundary conditions are not verified [BSBAA+19], thus limiting the applicability of the corresponding Lyapunov functionals.

To characterize the Input-to-State Stability (ISS) of networks of PDEs, we may consider the equivalent IDE representation (as given in Chapter 6) and rely on Lyapunov ISS functionals already developed for such time-delay systems (see [PK13, Pep14]). Nevertheless, while the Input-to-State Stability of a large number of PDEs with bounded control operator or admissible boundary control is now well-grounded (see [MP20] for a complete review of this field) and its characterization with a coercive ISS Lyapunov function clearly investigated, it is not the case for IDEs and even for difference equations. Indeed, to our best knowledge, some of the only works investigating this question are [HVL93] and [KK14]. On the one hand, [HVL93] proved that the asymptotic stability of the homogeneous difference equation is equivalent to the ISS of the non-homogeneous one (via Duhamel's principle) but did not consider Lyapunov characterization. On the other hand, [KK14] proposed Lyapunov ISS conditions of general nonlinear difference equations, but they are only sufficient. Note that ISS Lyapunov characterizations for nonlinear continuous-time difference equations are provided in [Pep14] in terms of Lyapunov functional continuous-time difference operator.

In this section, we detail some recent advances in the characterization with a Lyapunov functional of ISS of **linear difference equations** (that can represent systems of conservation laws). We believe analogous results can be obtained for IDEs, thus resulting in the characterization of Input-to-State stability for system (12.24). The proposed approach grounds on the recent work of [RCMDL18]. More precisely, we focus on the difference equation

$$X(t) = \sum_{k=1}^{M} A_k X(t-\tau_k) + f(t), \quad t \geq 0 \tag{12.26}$$

where $A_k \in \mathbb{R}^{n\times n}$ and the positive time-delays $\tau_k > 0$ $(1 \leq k \leq M)$ are ordered as $0 < \tau_1 < \tau_2 < ... < \tau_M$. The function f is an exogenous signal which belongs to $C^{pw}([0,\infty),\mathbb{R}^n)$. The function $X : [-\tau_M, \infty) \to \mathbb{R}^n$ is considered to be piecewise continuous. In the following, we assume that in the absence of f, the system (12.26) is exponentially stable in the sense of the $L^2_{\tau_M}$-norm. The reader is referred to [ABP23] for the proofs.

This research axis could strengthen the collaborations with Ecole des Mines and with N. Espitia from Cristal-Lab in Lille. It could open interesting perspectives for a possible thesis subject.

P3.1 . Preliminary definitions and properties

In this section, we define the fundamental and Lyapunov matrix associated with the homogenous system (12.26) (i.e., $f \equiv 0$)

$$X(t) = \sum_{k=1}^{M} A_k X(t-\tau_k), \quad t \geq 0. \tag{12.27}$$

We also recall some properties that have been shown in [RMDL17].

Lemma P3.1 ([RMDL17]) *Assume that* $\det(Id - \sum_{k=1}^{M} A_k) \neq 0$. *The* $n \times n$ *matrix function* $K(t)$ *defined for all* $t \geq 0$ *by*

$$K(t) = \sum_{k=1}^{M} K(t-\tau_k)A_k = \sum_{k=1}^{M} A_k K(t-\tau_k), \quad t \geq 0, \tag{12.28}$$

with the initial condition $K(\theta) = K_0 = (\sum_{k=1}^{M} A_k - Id)^{-1}$ *for* $\theta \in [-\tau_M, 0)$ *is called the fundamental matrix of system* (12.27). *For any initial condition* $X^0 \in C^{pw}_{\tau_M}$, *the response of system* (12.27) *is given by*

$$X(t) = \sum_{k=1}^{M} D^+ \int_{-\tau_k}^{0} K(t-\theta-\tau_k)A_k X^0(\theta)d\theta. \tag{12.29}$$

Obviously, the matrix K is perfectly defined when the system (12.27) is exponentially stable. Formula (12.29) is known as the **Cauchy formula**. The fundamental matrix $K(t)$ is a piecewise constant function, with discontinuity points defined by

$$t_k = \min_{p_k^1,\dots p_k^m} \{\sum_{j=1}^{M} p_k^j \tau_j \mid \sum_{j=1}^{M} p_k^j \tau_j > t_{k-1},\ p_k^j \in \mathbb{N}\}. \tag{12.30}$$

We denote the set of discontinuity instants of K as $\mathcal{I}_\mathcal{K} = \{t_k\}_{k\in\mathbb{N}}$. For all $t \geq 0$, we define ΔK as $\Delta K(t) = K(t^+) - K(t^-)$. It can be easily verified that $\Delta K(0) = \mathrm{Id}$. Moreover, if the homogeneous system (12.27) is exponentially stable, then the matrix ΔK exponentially converges to zero. We now define the Lyapunov matrix associated with system (12.27).

Definition P3.1 ([RCMDL18]) *Let* (12.27) *be exponentially stable. For every $n \times n$ symmetric positive definite matrix W, the Lyapunov matrix*

$$V(\tau) = \int_0^\infty (K(t) - K_0)^T W K(t+\tau) dt, \tag{12.31}$$

is well defined for all $\tau \geq -\tau_M$.

The matrix V plays a crucial role in the design of the Lyapunov-Krasovskii functional introduced in [RCMDL18]. Unlike the matrix K, the definition of this functional is only needed on the interval $[-\tau_M, \tau_M]$. Its derivative can be expressed as $V'(\tau) = \sum_{k\geq 0}(K^T(t_k - \tau) - K_0^T)W\Delta K(t_k)$. Due to the discontinuities of K, V' is also discontinuous. We define the derivative's jump discontinuities as $\Delta V'(\tau) = V'(\tau^+) - V'(\tau^-),\ \tau \in [-\tau_M, \tau_M]$. and it holds for $\tau \in [-\tau_M, \tau_M]$

$$\Delta V'(\tau) = -\sum_{k\geq 0} \Delta K^T(t_k - \tau) W \Delta K(t_k). \tag{12.32}$$

It is important to emphasize that when the delays τ_i are not rationally independent, the matrix V' may have an infinite number of discontinuities on the interval $[0, \tau_M]$. In what follows, for any $-\tau_M < t_0 < t_1 < \tau_M$, we denote $\mathcal{I}((t_0, t_1))$ the set of discontinuity points of the function V' that belong to (t_0, t_1). We establish the following lemma [ABP23].

Lemma P3.2 *The set $\mathcal{I}((-\tau_M, \tau_M))$ is countable and $\Delta V'$ is thus equal almost everywhere to the zero function. Moreover, if the homogeneous system* (12.27) *is exponentially stable then the quantity $\sum_{\tau_c \in \mathcal{I}((-\tau_M,\tau_M))} ||\Delta V'(\tau_c)||$ is finite.*

P3.2 . Lyapunov-Krasovskii functional

Let us first introduce the functional $v_0(\varphi)$ defined for all $\varphi \in C^{pw}_{\tau_M}$ by

$$v_0(\varphi) = \sum_{i=1}^{M}\sum_{j=1}^{M} \int_{-\tau_i}^{0}\int_{-\tau_j}^{0} \varphi^T(\xi) A_i^T D_\xi^+ D_\theta^+ \Big(\int_0^\infty K^T(\nu - \xi - \tau_i) W K(\nu - \theta - \tau_j) d\nu\Big) A_j \varphi(\theta) d\theta d\xi,$$

where we have denoted D_ξ^+ and D_θ^+ the Dini derivative with respect to ξ and θ. The integral term $\int_0^\infty K^T(\nu - \xi - \tau_i) W K(\nu - \theta - \tau_j) d\nu$ is well-defined since the fundamental matrix verifies equation (12.28), which is assumed to be exponentially stable. The functional v_0 corresponds to the one given in [RCMDL18]. From the definition of V in equation (12.31), we obtain $D_\xi^+ D_\theta^+ \int_0^\infty K^T(\nu - \xi - \tau_i) W K(\nu - \theta - \tau_j) d\nu = D_\theta^+ D_\xi^+ V(-\theta - \tau_j + \xi + \tau_i)$. We emphasize that the definition of the functional v_0 requires system (12.27) to be exponentially stable. We have the following lemma.

Lemma P3.3 *If system* (12.27) *is exponentially stable, then there exists $\alpha_1 > 0$, such that for all $\varphi \in C^{pw}_{\tau_M}$*

$$0 \leq v_0(\varphi) \leq \alpha_1 ||\varphi||^2_{L^2_{\tau_M}}. \tag{12.33}$$

The next lemma gives the expression of the time-derivative of $v_0(X_{[t]})$, when $X_{[t]}$ is the solution of equation (12.26).

Lemma P3.4 *Consider the functional v_0 and $X_{[t]}$ the solution of equation* (12.26)*. Assume that system* (12.27) *is exponentially stable. Then, for all $t \geq 0$ we have*

$$D^+v_0(X_{[t]}) = -X^T(t)WX(t) - 2X^T(t)\Delta V'(0)f(t) + f^T(t)\Delta V'(0)f(t) \\ - 2\sum_{i=1}^{M}\sum_{\tau_c\in\mathcal{I}((0,\tau_i))} X^T(t+\tau_k-\tau_i)A_i^T\Delta V'(\tau_c)f(t). \qquad (12.34)$$

Note that the expression given by equation (12.34) is well defined due to Lemma P3.2. In the absence of the exogenous signal f, we have the negativity of the time-derivative of $v_0(X_{[t]})$. However, the functional v_0 is not equivalent to the L^2 norm. Moreover, we wish to obtain a strict Lyapunov functional, that is, with an exponential decay in the absence of the exogenous signal f. Inspired by [DBC12], we introduce two intermediate functionals defined for $\varphi \in C^{pw}_{\tau_M}$ by

$$\bar{v}_0(\varphi) = \sum_{i=1}^{M}\sum_{j=1}^{M}\int_{-\tau_i}^{0}\int_{-\tau_j}^{0}\varphi^T(\xi)A_i^TD_\xi^+D_\theta^+\Big(\int_0^\infty K^T(\nu-\xi-\tau_i)WK(\nu-\theta-\tau_j)d\nu\Big)A_j\varphi(\theta)\mathrm{e}^{\frac{\rho}{2}(\theta+\xi)}d\theta d\xi,$$
$$\tilde{v}_0(\varphi) = \bar{v}_0(\varphi) - v_0(\varphi),$$

where $\rho > 0$ is a tuning parameter that will be defined later. Since $\bar{v}_0(\varphi) = v_0(\mathrm{e}^{\frac{\rho}{2}\cdot}\varphi)$, we have $\bar{v}_0(\varphi) \geq 0$ for all $\varphi \in C^{pw}_{\tau_M}$. The functional $\bar{v}_0$ is introduced to obtain an exponential decay rate.

Lemma P3.5 *Consider $X_{[t]}$ the solution of equation* (12.26) *and assume that system* (12.27) *is exponentially stable. Then, there exist real parameters $K_1 > 0, K_2 > 0, a > 0, \bar{a} > 0$, a sequence of positive coefficients $\bar{d}_q$ such that the series $\sum_{q\geq 0}\bar{d}_q$ converges and a sequence of increasing scalar numbers $\bar{\tau}_q$ with $\bar{\tau}_0 = 0$ (all independent on ρ) which are such that, for all $t \geq 0$ and all $\epsilon > 0$, we have*

$$D^+\bar{v}_0(X_{[t]}) \leq -\rho\bar{v}_0(X_{[t]}) - X^T(t)WX(t) + (\frac{a}{\epsilon}+\bar{a})||f(t)||^2 \\ + (K_1(1-\mathrm{e}^{-\rho\tau_M}) + K_2\epsilon)\sum_q \bar{d}_q||X(t-\bar{\tau}_q)||^2. \qquad (12.35)$$

Consider a sequence of positive coefficients b_q such that the series $\sum_{q\geq 1} b_q$ converges and define, for all $\varphi \in C^{pw}_{\tau_M}$, the functional v_1 as

$$v_1(\varphi) = \bar{v}_0(\varphi) + \sum_{q\geq 1} b_q\int_{-\bar{\tau}_q}^0 \varphi(\nu)^T\varphi(\nu)\mathrm{e}^{\rho\nu}d\nu + b\int_{-\tau_M}^0\varphi(\nu)^T\varphi(\nu)\mathrm{e}^{\rho\nu}d\nu, \qquad (12.36)$$

where $b > 0$. We have the following lemma.

Lemma P3.6 *For all $\varphi \in C^{pw}_{\tau_M}$, $v_1(\varphi) \geq 0$. Consider $X_{[t]}$ the solution of equation* (12.26) *and assume that system* (12.27) *is exponentially stable. Then, the parameters $\rho > 0$, $b > 0$, $b_q > 0$ and $\epsilon > 0$ can be chosen such that*

$$D^+v_1(X_{[t]}) \leq -\rho v_1(X_{[t]}) + (\frac{a}{\epsilon}+\bar{a})||f(t)||^2 - be^{-\rho\tau_M}||X(t-\tau_M)||^2, \qquad (12.37)$$

the coefficients $\bar{a}$ and a being defined in the statement of Lemma P3.5.

We now establish the existence of quadratic bounds for v_1.

Lemma P3.7 *If system* (12.27) *is exponentially stable, then there exist $\alpha_\ell > 0, \alpha_u > 0$ such that for all $\varphi \in C^{pw}_{\tau_M}$*

$$\alpha_\ell||\varphi||^2_{L^2_{\tau_M}} \leq v_1(\varphi) \leq \alpha_u||\varphi||^2_{L^2_{\tau_M}}. \qquad (12.38)$$

We can now state the main result of this section, which characterizes the Input-to-State Stability of System (12.26) with a Lyapunov functional.

Theorem P3.1 *Consider system* (12.26) *with the initial data* $X^0 \in C^{pw}_{\tau_M}$. *Assume that* f *belongs to* $C^{pw}([0,\infty),\mathbb{R}^n)$. *The two following statements are equivalent:*

1. *the solution to* (12.26) *is* L^2*-ISS;*
2. *there exists a quadratic function* $v_1 : C^{pw}_{\tau_M} \to \mathbb{R}_+$ *such that*
   - *(a)* $\exists\, \rho, \sigma > 0 \quad D^+ v_1(X_{[t]}) \leq -\rho v_1(X_{[t]}) + \sigma \|f(t)\|^2$
   - *(b)* $\exists\, \alpha_l, \alpha_u > 0 \quad \forall \varphi \in C^{pw}_{\tau_M} \ \alpha_\ell ||\varphi||^2_{L^2_{\tau_M}} \leq v_1(\varphi) \leq \alpha_u ||\varphi||^2_{L^2_{\tau_M}}$.

This result constitutes somehow an extension of [HVL93, Chapter 9, Theorem 6.1], which proved that the asymptotic stability of (12.27) is equivalent to the ISS of (12.26) with respect to the exogenous signal f. However, Theorem P3.1 proposes a Lyapunov characterization of this property, along with an explicit form of the corresponding Lyapunov functional. Besides, it is worth underlining that this result complements the ISS Lyapunov characterizations for nonlinear continuous-time difference equations provided in [Pep14], in terms of Lyapunov functional continuous-time difference operator in lieu of the differential operator proposed here. The numerical evaluation of the ISS gain γ is an important practical question, which requires exploring the numerical implementation of the Lyapunov functional v_1. The main related difficulty is due to the series $\sum_{q\geq 1} b_q \int_{-\bar{\tau}_q}^0 \varphi(\nu)^T \varphi(\nu) \mathrm{e}^{\rho\nu} d\nu$. Moreover, the term v_0 requires computing the function $V''(\tau)$, which is not easy in the case of rationally independent delays. Interestingly, the computations become much simpler when the delays are rationally dependent (as the $\Delta V'$ only has a finite number of discontinuities in this case). Thus, for practical use of the Lyapunov v_1 (to design stabilizing control laws, for instance), one could consider a sufficiently good approximation of the Lyapunov matrix V using rationally dependent delays (see [RMDL17] for more details).

P3.3 . Extensions and applications

In the near future, a promising research axis would be to extend the proposed analysis to IDEs grounding on the recent necessary Lyapunov stability conditions obtained in [OEM22]. This would help characterize the stability properties of hyperbolic systems [BSGB18, SBS17, BSBAA+19]. We believe analogous strategies would still hold. Such developments resulting in explicit Lyapunov functions would have major consequences in terms of control perspectives for networks of PDEs, as these systems can be rewritten as IDEs. In particular, combining classical backstepping controllers with event-triggered control mechanisms would be possible, extending the results of [EGMP16, EGMP17]. Such generic Lyapunov functions could also be used to assess the existence of robustness margins. For instance, in light of what has already been done for time delay systems, a Lyapunov functional can be adequately used to show robustness with respect to stochastic uncertainties or stochastic delays [KBP22a, KBP22b, AKBP22].

P4 . Easily parametrizable target systems and performance tuning

One of the main difficulties with the backstepping method is finding a **suitable target system**. It should be simple enough to allow the design of the control law. Still, in the meantime, we must prove the existence of a transformation mapping the original system to this target system. The choice of the target system directly impacts the **closed-loop performance**. The general question of reachable target systems is still an open problem. For elementary hyperbolic equations, they were usually chosen as finite-time stable [CN21a], thereby shadowing the robustness properties of the corresponding closed-loop systems [LRW96, MVZ+09]. In this manuscript, we considered backstepping transformations that remove as many coupling terms as possible to simplify the control design. Similarly, the objective of the integral transformation defined in Chapter 9 when designing the control law (9.35) was to remove

all the integral coupling terms. Such transformations are ideally suited to fulfill the desired stabilization objectives. However, there may be an interest in considering alternative, more complex target systems. For instance, in [ADM20], we introduced tuning parameters in the design, thus guaranteeing potential trade-offs between different specifications (namely delay-robustness and convergence rate). However, these tuning parameters had a limited range of action since they only affected the boundary conditions of the systems.

General target systems (and thus additional degrees of freedom) could be obtained by preserving dissipative in-domain couplings. This would require precise knowledge of their influence in terms of stability. In this context, the **Port-Hamiltonian approach** [LGZM05] could be a path to follow as it corresponds to a multi-physical and modular energy-based representation that considers the system's natural physical properties (e.g., passivity, dissipativity, reversibility). The PHS framework was initially developed for finite-dimensional systems [DMSB09] and was then extended to PDEs [vdSM02, Vil07, LGZM05, JZ12, HP17]. This formalism is highly advantageous for depicting the dynamics of extensive-scale multiphysics systems, exemplified in fields such as fluid mechanics [SvdSB11], heat transfer [vdSGM02], and structural mechanics [WS17]. The Port-Hamiltonian approach offers a structured methodology to highlight and capitalize on the intrinsic physical properties of the considered systems. Its application has yielded successes across various engineering domains, encompassing performance optimization [DvdSBF16], systems stability analysis [BMP15], and the design of controllers for complex systems [OvdSCA08, MLGRZ17]. Therefore, the PHS framework is particularly relevant for control design using damping assignment or energy shaping methods. It has been used to design boundary controllers that effectively leverage the physical attributes of the system. This is the case of energy-shaping methods [MLGRZ17] that modify the closed-loop energy function of the system.

We believe the natural physical properties of the system can be advantageously used to define well-posed, exponentially stable target system candidates. Such a strategy was successfully applied on simple test cases (wave equation and Timoshenko beam) to design state-feedback controllers that assign the distributed damping of the closed-loop system, thus determining the decay rate of the solutions while reducing the associated control effort cases [RZLGM17, RALG22b, RALG22a]. In this section, we give some insights into developing easily parametrizable target systems and how to use the newly available degrees of freedom.

I plan to hire a postdoctoral fellow to work with me on this research axis, using the funding obtained from the PANOPLY JCJC ANR project, funding from the INS2I AURA project, and funding for Université Paris-Saclay. Collaborations with AS2M in Besançon will be considered.

P4.1 . Development of easily parametrizable target systems

Our first objective will be to introduce degrees of freedom in the design to obtain a class of easily parametrizable closed-loop systems. To develop this class of attainable (exp. stable) systems, we will take advantage of the PHS framework, which can help identify naturally dissipative terms. This property has been successfully used in [RALG22b, RALG24] to perform damping assignment using the backstepping approach and design modulable controllers guaranteeing satisfying closed-loop behavior (namely a given exponential rate of convergence) while reducing the control effort. Therefore, the PHS framework will help us to introduce **degrees of freedom** in the design and obtain a class of easily parametrizable (exponentially stable) closed-loop target systems. Other tuning parameters could also be added by following the robustness approach proposed in [ADM20]. We will then need to adjust the control methods presented in the manuscript or in Section P1 to design the associated controllers.

To illustrate the proposed methodology, let us consider the following Port-Hamiltonian systems [JZ12] defined by

$$\frac{\partial w}{\partial t} = P_1 \frac{\partial}{\partial x}(\mathcal{H}(x)w(t,x)) + (P_0 - \Pi_0)\mathcal{H}(x)w(t,x), \tag{12.39}$$

where $w(t,x)$ is the vector of energy variables defined on $[0,+\infty)\times[0,1]$. It has $2n$ components. The matrix $\mathcal{H}$ is a symmetric and Lipschitz continuous coercive matrix-valued function defined on $[0,1]$, P_1 is a full rank matrix such that $P_1 = P_1^\top \in \mathbb{R}^{2n\times 2n}$, the matrix P_0 verifies $P_0 = -P_0^\top \in \mathbb{R}^{2n\times 2n}$

and $\Pi_0 \in \mathbb{R}^{2n\times 2n}$ verifies $\Pi_0 = \Pi_0^\top \in \mathbb{R}^{2n\times 2n}$. The boundary inputs/outputs are defined by

$$u_\partial(t) = W_B \begin{pmatrix} \mathcal{H}(1)w(t,1) \\ \mathcal{H}(0)w(t,0) \end{pmatrix}, \; y_\partial(t) = W_C \begin{pmatrix} \mathcal{H}(1)w(t,1) \\ \mathcal{H}(0)w(t,0) \end{pmatrix}, \tag{12.40}$$

where $W_B, W_C \in \mathbb{R}^{2n\times 4n}$ are defined by

$$W_B = \begin{pmatrix} \frac{1}{\sqrt{2}}\left(\Xi^- + \Xi^+ P_1\right) & \frac{1}{\sqrt{2}}\left(\Xi^- - \Xi^+ P_1\right) \end{pmatrix}, \tag{12.41}$$

$$W_C = \begin{pmatrix} \frac{1}{\sqrt{2}}\left(\Xi^+ + \Xi^- P_1\right) & \frac{1}{\sqrt{2}}\left(\Xi^+ - \Xi^- P_1\right) \end{pmatrix}, \tag{12.42}$$

where Ξ^+ and Ξ^- in $\mathbb{R}^{2n\times 2n}$ satisfy

$$\Xi^{-\top}\Xi^+ + \Xi^{+\top}\Xi^- = 0, \text{ and } \Xi^{-\top}\Xi^- + \Xi^{+\top}\Xi^+ = \mathrm{Id}_{2n}. \tag{12.43}$$

For all $t \geq 0$, we can define the total energy of the system $\mathcal{E}(w(t))$ as

$$\mathcal{E}(w(t)) = \frac{1}{2}\int_0^1 \left(w^\top(t,x)\mathcal{H}(x)w(t,x)\right) dx.$$

We have [JZ12]

$$\frac{\partial \mathcal{E}(w(t))}{\partial t} = y_\partial^\top(t)u_\partial(t) - \int_0^1 w^\top(t,x)\Pi_0 w(t,x)dx.$$

It has been shown in [LGZM04] that if Π_0 is semi-definite positive, the system (12.39)-(12.40) defines a boundary control system [CZ12]. Under simple assumptions, the system (12.39) can be rewritten in the framework (6.1). For instance, we can consider that one boundary is fully actuated while the other is set to zero, i.e.,

$$u_\partial(t) = \begin{pmatrix} U(t) \\ 0 \end{pmatrix},$$

where U is the control input, and the matrix W_B is bloc diagonal or bloc anti-diagonal, the different blocks being of dimension $n \times 2n$. Since the matrix P_1 is full rank and $\mathcal{H}(x)$ coercive, $P_1\mathcal{H}(x)$ is diagonalizable, i.e., there exist a matrix-valued function $Q_1(x) \in \mathbb{R}^{2n\times 2n}$, a diagonal matrix-valued function $\Lambda(x)$ defined on $[0,1]$, such that

$$\forall\, x \in [0,1],\; P_1\mathcal{H}(x) = Q_1(x)\Lambda(x)Q_1^{-1}(x).$$

Consequently, we can define $\begin{pmatrix} u(t,x) \\ v(t,x) \end{pmatrix} = Q_1^{-1}(x)w(t,x)$ to rewrite the system (12.39) as an elementary hyperbolic system actuated at one boundary

$$\begin{cases} \partial_t u(t,x) + \Lambda^+\partial_x u(t,x) = \Sigma^{++}(x)u(t,x) + \Sigma^{+-}(x)v(t,x), \\ \partial_t v(t,x) - \Lambda^-\partial_x v(t,x) = \Sigma^{-+}(x)u(t,x) + \Sigma^{--}(x)v(t,x), \\ v(t,1) = Ru(t,1),\; u(t,0) = Qv(t,0) + BU(t), \end{cases} \tag{12.44}$$

where B is an invertible matrix. Note that the matrices Σ^{++} and Σ^{--} may not have zero diagonal components after this transformation but this can be obtained, performing a simple exponential change of variables [VKC11].

We aim to obtain a class of easily parametrizable closed-loop systems with tuning parameters (degrees of freedom). The desired target systems correspond to the original system (12.39) but with modified *in-domain damping* terms. More precisely, we want to obtain the following closed-loop behavior

$$\frac{\partial \bar{w}}{\partial t} = P_1\frac{\partial}{\partial x}\left(\mathcal{H}\bar{w}(t,x)\right) + \left(P_0 - \bar{\Pi}_0\right)\left(\mathcal{H}\bar{w}(t,x)\right), \tag{12.45}$$

where $\bar{\Pi}_0 \in \mathbb{R}^{2n\times 2n}$ satisfies $\bar{\Pi}_0 + \bar{\Pi}_0^T \leq 0$. The boundary conditions are given by

$$W_{\bar{B}} \begin{pmatrix} \mathcal{H}(1)x(t,1) \\ \mathcal{H}(0)x(t,0) \end{pmatrix} = 0_{2n}, \text{ with } W_{\bar{B}} \begin{pmatrix} 0 & I_{2n} \\ I_{2n} & 0 \end{pmatrix} W_{\bar{B}}^T \geq 0. \tag{12.46}$$

where $W_{\bar{B}} \in \mathbb{R}^{2n\times 4n}$ has a structure analogous to the one of W_B. Note that for the sake of simplicity, the matrix $\bar{\Pi}_0$ has been chosen constant but it could have been chosen as a function of x, i.e. $\bar{\Pi}_0(x)$ is a real matrix-valued function satisfying $\bar{\Pi}_0(x) + \bar{\Pi}_0^T(x) \leq 0, \quad \forall x \in [0,1]$. This target system defines an exponentially stable Boundary Control System (BCS) that satisfies

$$\frac{d\mathcal{E}(\bar{w}(t))}{dt} = \int_0^1 \bar{w}^\top(t,x)\bar{\Pi}_0\bar{w}(t,x)dx \leq 0. \tag{12.47}$$

Therefore, in closed-loop, the energy decay is determined by the matrix $\bar{\Pi}_0$. This matrix parametrizes the target system. The only requirement is that the associated energy of the system should be decreasing. Again, performing appropriate change of coordinates, the target system (12.45) can be rewritten as

$$\begin{cases} \partial_t\bar{u}(t,x) + \bar{\Lambda}^+\partial_x\bar{u}(t,x) = \bar{\Sigma}^{++}(x)\bar{u}(t,x) + \bar{\Sigma}^{+-}(x)\bar{v}(t,x), \\ \partial_t\bar{v}(t,x) - \bar{\Lambda}^-\partial_x\bar{v}(t,x) = \bar{\Sigma}^{-+}(x)\bar{u}(t,x) + \bar{\Sigma}^{--}(x)\bar{v}(t,x), \\ \bar{v}(t,1) = \bar{R}\bar{u}(t,1), \ \bar{u}(t,0) = Q\bar{v}(t,0). \end{cases} \tag{12.48}$$

Note that the matrix Q remains unchanged.

P4.2 . From the original system to the target system

Now that we have defined a possible target system candidate, we need to show that it is possible to map the original system (12.44) to the target system (12.48). Performing backstepping transformations [CHO17, Aur18], the system (12.44) can be mapped to

$$\frac{\partial\alpha}{\partial t}(t,x) + \Lambda^+\frac{\partial\alpha}{\partial x}(t,x) = G_1(x)\beta(t,0), \tag{12.49}$$

$$\frac{\partial\beta}{\partial t}(t,x) - \Lambda^-\frac{\partial\beta}{\partial x}(t,x) = G_2(x)\beta(t,0), \tag{12.50}$$

with the boundary conditions

$$\alpha(t,0) = Q\beta(t,0), \tag{12.51}$$

$$\beta(t,1) = R\alpha(t,1) + u(t) + \int_0^1 K(y)\alpha(t,y) + L(y)\beta(t,y)dy, \tag{12.52}$$

where the matrix G_1 and G_2 are piecewise continuous. The matrix G_2 is strictly upper-diagonal. Similarly, the system the system (12.48) can be mapped to

$$\frac{\partial\bar{\alpha}}{\partial t}(t,x) + \bar{\Lambda}^+\frac{\partial\bar{\alpha}}{\partial x}(t,x) = \bar{G}_1(x)\bar{\beta}(t,0), \tag{12.53}$$

$$\frac{\partial\bar{\beta}}{\partial t}(t,x) - \bar{\Lambda}^-\frac{\partial\bar{\beta}}{\partial x}(t,x) = \bar{G}_2(x)\bar{\beta}(t,0), \tag{12.54}$$

with the boundary conditions

$$\bar{\alpha}(t,0) = Q\beta(t,0), \tag{12.55}$$

$$\bar{\beta}(t,1) = \bar{R}\alpha(t,1) + \int_0^1 \bar{K}(y)\bar{\alpha}(t,y) + \bar{L}(y)\bar{\beta}(t,y)dy, \tag{12.56}$$

where the matrix $\bar{G}_1$ and $\bar{G}_2$ are piecewise continuous. The matrix $\bar{G}_2$ is strictly upper-diagonal. Therefore, we now need to find a transformation that maps the system (12.49)-(12.52) to the system (12.53)-(12.56). Consider the time-affine transformation defined by

$$\bar{\beta}_i(t,z) = \beta_i(t,z) + \int_0^{\frac{1-x}{\mu_i}} \sum_{j=1}^{i-1} F_{ij}^-(x,y)\beta_j^-(t-y,0) + \sum_{j=2}^{i-1} H_{ij}^-(x,y)\bar{\beta}_j(t-y,0)\mathrm{d}y, \ 1 \leq i \leq m, \tag{12.57}$$

$$\bar{\alpha}_i(t,x) = \alpha_i(t,x) + \int_0^{\frac{x}{\lambda_i}} \sum_{j=1}^{m} F_{ij}^+(x,y)\beta_j(t-y,0) + \sum_{j=2}^{m} H_{ij}^+(x,y)\bar{\beta}_j(t-y,0)\mathrm{d}y$$
$$+ \int_{\frac{x}{\lambda_i}}^{\frac{1}{\mu_1}+\frac{x}{\lambda_i}} \sum_{j=1}^{m-1} M_{ij}^+(x,y)\beta_j(t-y,0) + \sum_{j=2}^{m-1} N_{ij}^+(x,y)\bar{\beta}_j(t-y,0)\mathrm{d}y.\ 1 \leq i \leq n, \tag{12.58}$$

where the different kernels are piecewise continuous functions defined on their respective domains by

$$H_{ij}^-(x,y) = (\bar{G}_2(x+\mu_i y))_{ij},\ H_{ij}^+(x,y) = (\bar{G}_1(x-\lambda_i y))_{ij},$$
$$F_{im}^-(x,y) = -(G_2(x+\mu_i y))_{im} + (\bar{G}_2(x+\mu_i y))_{im},$$
$$F_{in}^+(x,y) = -(G_1(x-\lambda_i y))_{in} + (\bar{G}_1(x-\lambda_i y))_{in}$$
$$F_{ij}^-(x,y) = -(G_2(x+\mu_i y))_{ij}\ j<m,\ F_{ij}^+(x,y) = -(G_1(x-\lambda_i y))_{ij}\ j<n,$$
$$M_{ij}^+(x,y) = \sum_{k=1}^{j-1} \mathbb{1}_{[\frac{x}{\lambda_i}, \frac{1}{\mu_k}+\frac{x}{\lambda_i}]}(y) Q_{ik} F^-(0, y-\frac{x}{\lambda_i}),$$
$$N_{ij}^+(x,y) = \sum_{k=1}^{j-1} \mathbb{1}_{[\frac{x}{\lambda_i}, \frac{1}{\mu_k}+\frac{x}{\lambda_i}]}(y) Q_{ik} H^-(0, y-\frac{x}{\lambda_i}).$$

Notice that the transformation (12.57)-(12.58) requires past values of the boundary state $\bar{\gamma}(.,0)$. Therefore, it is only defined for t large enough. Also note that the last component of the leftward convecting state is not modified: $\forall x \in [0,1],\ \bar{\gamma}_m^-(t,z) = \gamma_m^-(t,z)$. Differentiating (12.57)-(12.58) with respect to time and space and integrating by parts, we can easily verify that, for $t \geq t^*$, the transformation (12.57)-(12.58) maps the solution of (12.49)-(12.52) to the solution of (12.53)-(12.56). We can then define the control input as

$$U(t) = \bar{R}\bar{u}(t,1) - Ru(t,1) - \int_0^1 K(y)\alpha(t,y) + L(y)\beta(t,y)\beta(t,y)dy$$
$$+ \int_0^1 \bar{K}(y)\bar{\alpha}(t,y) + \bar{L}(y)\bar{\beta}(t,y)dy, \tag{12.59}$$

where the variables $\bar{\alpha}$ and $\bar{\beta}$ are defined through (12.57)-(12.58). Adjusting the proof of Theorem 6.1.3, we can show that the systems (12.49)-(12.52) and (12.53)-(12.56) have identical stability properties. Consequently, using appropriate time-integral transformations, we can map the original system (12.44) to any system with the same structure but with arbitrary in-domain couplings. These degrees of freedom can be adequately chosen using the PHS approach. We believe such a control strategy can be extended to any network of hyperbolic systems, although the transformations (12.57)-(12.58) may have to be adjusted. In this context, working with the IDEs representation (6.23)-(6.25) may be more convenient. This will require establishing clear links between the IDE representation of our network and a possible PHS rewriting. Then, we will have to introduce an appropriate transformation (analogous to (12.57)-(12.58)) whose structure will be related to the graph structure of the network.

P4.3 . Development of tuning methods

In Section P2.1, we mention as a possible perspective the development of analytical techniques to quantify the performance of our output-feedback laws regarding a given set of specifications. Then, we aim to derive **tuning methods** to use best the available degrees of freedom previously introduced in the design with respect to this set of performance specifications. To define an adequate and general optimal cost function (e.g., a quadratic function of the state), we will adjust existing results for in-domain actuator placement [Mor20]. The different specifications (e.g., robustness margins) will be considered as constraints. In this context, sensitivity analysis methods [BS13] could be of specific interest. Note that our approach optimizes the tuning of the available degrees of freedom and consequently differs from direct optimal control design [Lio71] that would require solving infinite-dimensional Riccati equations and may not be constructive. These developments could allow the implementation of a control toolbox analogous to what already exists for finite-dimensional systems.

P5 . Integration, model reduction, and benchmarking

Simplicity and low computational burden have always been two crucial reasons for the success of **classical control design algorithms** (such as P, PI, and PID controllers) in industrial engineering applications. For instance, the current industry standard in handling torsional vibrations in drilling devices are the two products SoftSpeed and Soft-Torque [Dwa15], which are both based on PI regulators. Infinite-dimensional observer controllers require know-how and some computing power to be implemented. Rather than relying on finite-dimensional controllers, the incentive to do so is a performance criterion: explicitly taking into account the delays and high-frequency content in the model should lead to overall increased performance for the chosen specifications. Moreover, there are some configurations for which PI controllers cannot stabilize the system [RAN22a]. Although the development of electronic technology has allowed the implementation of **high computational demanding techniques** such as nonlinear model predictive control [SABA21], or reinforcement learning, and supervised learning algorithms [SB18], one must assess whether the overall trade-off can be favorable than industry standards by applying these methods to an industrial problem. As shown in [ADMS18b], sophisticated torque control laws can effectively remove stick-slip oscillations at the cost of delivering high instantaneous torque, which may not be admissible. Again, this legitimates the need for generic analytical techniques to quantify closed-loop performances with respect to industry-inspired performance indices.

This research axis should be embedded in the other ones, and different Ph.D. students and interns will collaborate on these implementation-related aspects.

P5.1 . Integration and model reduction

Performing real-time state estimation for hyperbolic systems using rapidly converging observers, such as those based on backstepping, is computationally expensive and, in many cases, prohibitive. For instance, the method presented in Chapter 8 must compute state predictions for each subsystem composing the interconnection, which is time-consuming. This **numerical burden** may explode with the complexity of the network. Moreover, the implementation of output-feedback laws on microcontrollers requires numerical approximations whose effects in terms of stability and convergence should be verified. Consequently, evaluating the computational costs of our design control methods appears crucial. To leverage the numerical effort induced by these controllers, it may be necessary to approximate them (e.g., by finite-dimensional systems). The approximation scheme should nonetheless guarantee satisfying closed-loop properties (and, in particular, closed-loop stability). Different late-lumping approximation methods have been suggested in [ERW17] or [AMDM19] to leverage the computational burden of the proposed controllers while guaranteeing comparable closed-loop performance. Recently, **machine-learning approximations** of backstepping controllers (based on the DeepONet algorithm) have been successfully tested in [SLY+22] on simple examples. Indeed, recent advances have shown that deep neural networks can be used to learn distributed dynamics from measurements [LJK21, BHKS21, LKA+20]. Physics-informed neural networks have improved the generalization capacity of the different solutions [WWP21, LZK+21]. Such methods could, therefore, be used to solve the kernel equations inherent to the backstepping approach or to emulate the backstepping observers (that require solving a set of PDEs analogous to the original PDEs in real-time). When approximating simple backstepping state-feedback controllers, some convergence guarantees for the closed-loop system were given in [BSK23] using Lyapunov approaches. We believe that the Lyapunov analysis initiated in [AMDM19] on simple examples could be extended to guarantee the convergence of approximation schemes under generic conditions. In this context, the Lyapunov functionals designed in Section P3 could be of specific interest. Such strategies could also be applied to derive parameter estimation strategies [ASNK22]. In the near future, we plan to investigate such machine-learning reduction strategies to propose fast emulation of infinite-dimensional observers.

P5.2 . Test-case implementation

Several contributions provided a complete and thorough theoretical analysis of some of the previously presented control strategies on test case studies. It is the case, for instance, in [BC16],

where the authors emphasize the main technological features that may occur in the control of navigable rivers. Similarly, an analysis of the controllers for pneumatic systems was proposed in [GK18]. However, only a few contributions have considered a **real implementation** of such output-feedback controllers. Test-field validations have been proposed in [AADMS19] for backstepping-based adaptive observers for mechanical vibrations on drilling devices. Similarly, backstepping observers for a single freeway lane have been validated on real freeway data in [YK23]. Concerning the control of vibrations in thin mechanical structures equipped with piezoelectric components, robust controllers of reduced order have been designed from dynamical models [TAK05]. Such controllers have been successfully experimented in [TAKP05], focusing on the real-time computational burden to avoid introducing a destabilizing delay in the feedback loop. To **deploy, demonstrate, and validate** the techniques developed in this manuscript, it appears necessary to benchmark them on an experimental setup. Results will be analyzed based on the industrial performance indices. The proposed output-feedback controllers will be experimentally compared with state-of-the-art controllers. This study is key to enabling efficient and possible industrial deployment of our control strategies on industrial test cases in the near future. Among the possible test-case studies, we can cite **traffic estimation** on interconnected freeway segments [YK23] or the **active control of vibrations in mechanical structures**. The latter class of systems can model micro-endoscopes actuated with electro-active polymers. A schematic representation is given in Figure 12.2. Such tools are used in the medical sector to allow visual exploration of the interior of a cavity inaccessible to the eye while avoiding invasive surgery. The endoscope can be modeled by a flexible tube (Timoshenko beam) surrounded by a sheath formed of electro-active polymers. Such polymers can be stimulated locally by an electric field to allow the deformation of the endoscope and ensure its progression in the conduit to be explored. A finite number of electric actuators are punctually located along the tube. The questions of digital implementation, settle time, robustness, and precision are crucial for these systems [MWR+20].

A first, simple experimental test case will be the **active control of vibrations in mechanical structures** (see Figure 12.3). This test case corresponds to a thin mechanical beam with one clamped edge and is equipped with piezoelectric sensors and piezoelectric actuators as addressed in [BTN+18].The application purpose is similar to industrial issues, such as active damping of onboard optical and/or electronic equipment or the control of micro-endoscopes actuated with electro-active polymers. Moreover, a **test bench** has been developed in L2S and will serve as a starting point for the implementations. Various experiments will be defined and done to demonstrate and validate our control solutions for several actuator and sensor locations. We will then compare the effects in terms of closed-loop performance with the previously obtained theoretical results. The proposed output-feedback controllers will be experimentally compared with state-of-the-art controllers. This study is key to enabling efficient and possible industrial deployment of our control strategies on industrial test cases in the near future.

P6 . In-domain stabilization of hyperbolic systems

Beyond developing general methods for stabilizing networks of hyperbolic systems, and generally speaking, of underactuated hyperbolic systems, we believe the approaches we presented in this manuscript can be extended to stabilize hyperbolic systems with a distributed control input. More precisely, consider the scalar system

$$\partial_t u(t,x) + \lambda \partial_x u(t,x) = \sigma^+(x) v(t,x) + h_u(x) U(t), \tag{12.60}$$

$$\partial_t v(t,x) - \mu \partial_x v(t,x) = \sigma^-(x) v(t,x) + h_v(x) U(t), \tag{12.61}$$

with the boundary conditions

$$u(t,0) = q v(t,0), \quad v(t,1) = \rho u(t,1), \tag{12.62}$$

where U is the control input and h_u and h_v are continuous functions. Such a distributed control input can, for instance, appear when modeling vibrating structures (namely wave equations) with distributed

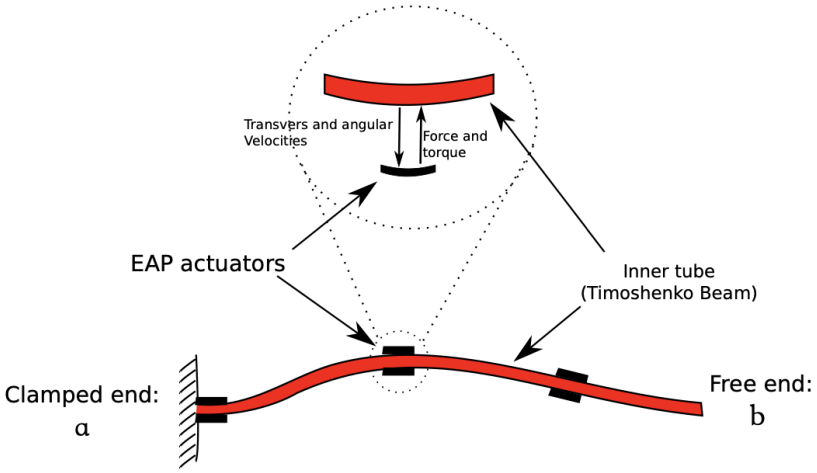

Figure 12.2: Example of a micro-endoscope (picture obtained by courtesy of Y. Le Gorrec)

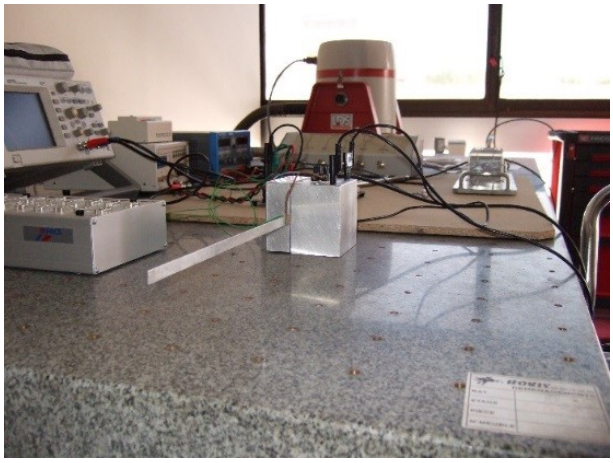

Figure 12.3: Experimental test-bench for the active control of vibrations in mechanical structures.

piezoelectric actuators [MWR+20, TAKP05], or tubular reactors [DVP05]. Only a few results exist in the literature and sometimes assume that the control input depends on space [PTDS16]. Interestingly, after performing classical backstepping transformations [ABABS+18], the system can be rewritten as the following IDE

$$z(t) = \rho q z(t-\tau) + \int_0^\tau N_z(\nu) z(t-\nu) d\nu \int_0^\tau + N_U(\nu) U(t-\nu) d\nu, \tag{12.63}$$

where the functions N_z and N_U are piecewise continous. Equation (12.63) is identical to equation (9.31), except that the pointwise-delayed actuation term is now set to zero. This corresponds to the critical case $a = 0$ in equation (9.31). The analysis proposed in Chapter 9 cannot directly be applied since having $a = 0$ means we have to show the invertibility of a Hilbert-Schmidt operator of the form

$$\mathcal{T}(z(\cdot)) = \int_0^1 K(\cdot, y) z(y) dy, \tag{12.64}$$

instead of the Fredholm operator (9.1). Therefore, Lemma 9.0.1, a key ingredient to prove Lemma 9.3.1, cannot be applied anymore. Although we believe the invertibility of the operator is still related to the spectral controllability of the system, a deeper analysis of the properties of the Hilbert-Schmidt operator (12.64) is required. In particular, we should take advantage of the properties of the kernels K, as it was done in the proof of Lemma 9.3.1. Such a result would open wide perspectives for stabilizing PDE systems with distributed actuators/sensors.

P7 . Control of coupled Stochastic and Partial differential Equations

Although the class of system (5.1) can model a wide variety of complex networks of interconnected PDEs and ODEs systems, we plan to consider new types of interconnections in the future. For instance, Stochastic Differential Equations (SDEs), coupled with (possibly non-linear) PDEs, are systems that naturally arise when modeling processes whose dominant probabilistic dynamics are affected by destabilizing second-order convection-diffusion-reaction effects. We refer to such control systems as SDE+PDE systems. A relevant example of an SDE+PDE system is provided by District Heating and Cooling Systems (DHCSs) [LRB17, vdZP20]. DHCSs deliver thermal energy to a network of buildings from an outside source. They offer numerous advantages over individual building apparatus, including greater safety and reliability, reduced emissions, and reliance on alternative fuels such as biomass or waste. However, due to low operating temperatures and limited flow capacity, customer demand can be met only if: 1) non-linear SDE-based dynamical models are leveraged to capture as many uncertain weather fluctuations as possible, and 2) the aforementioned stochastic models are coupled with sophisticated (possibly non-linear) PDEs to accurately capture energy losses which often occur along pipelines and hinder performance. Unfortunately, too few and specific works on SDE+PDE systems exist in the literature, hence calling for the design of novel tools for the efficient modelization and control of such systems. Therefore, we plan to design methods for efficient and theoretically guaranteed control of a broad class of SDE+PDE systems. The proposed approaches will have to be constructive to obtain a semi-explicit design of the corresponding control laws, enabling performance-efficient numerical paradigms. In this context, we have already obtained promising results when considering SDEs with delays in the actuation. The proposed approach combines Artstein's transformations [Art82] with covariance steering and optimal control methods [BLP22, OT19]. These results could pave the path toward more complex configurations as cascade interconnections from a PDE system to an SDE before considering more complex interconnections. In the future, we plan to combine the methods proposed in this manuscript for networks of deterministic systems with stochastic approaches as statistical linearization [BJ20]. The objective will be to develop techniques as independent as possible from any inherent regularizing property of the system (e.g., optimization methods). Moreover, although the objective consists of developing control methods that work in very general settings, we plan to showcase the efficiency of the proposed approaches through numerical simulations on specific examples (for instance, on DHCSs).

The research works of G. Velho (Ph.D. student co-supervised with R. Bonalli and I. Boussaada) fit this research axis. Collaborations with the Chalmers University will also be considered.

P8 . Application test cases

The different research axis we have presented above may have important consequences for the two test cases we considered in this manuscript.

P8.1 . Parameters estimation and stick-slip mitigation for drilling devices

Regarding the drilling test case, we would like first to focus on coupled axial-torsional dynamics. A complete analysis will include model validation against field data, as it has already been done for torsional models [AS18]. We also envision tests of the proposed techniques on real drilling devices (at least for the observers) in collaboration with the University of Calgary. In the meantime, estimating parameters (such as the friction or the nature of the drilled rock) during the drilling processes is a crucial problem since knowing such parameters is necessary to design state observers.

To tackle these issues, deep neural networks can be used. They can learn the system dynamics from the available surface measurements and estimate the evolution of the physical parameters in the model, particularly the static and kinetic friction parameters. For instance, a possible architecture would consist of two interconnected neural networks. Both are fed with temporal sequences of surface measurements and known physical parameters (mechanical properties of the drill string, depth of the drill bit, inclination, etc.). The first neural network could be a transformer [VSP+17b] trained to estimate the unknown physical parameters. In the meantime, the second neural network could be a physics-inspired transformer-based neural network used to predict the whole distributed state using the physical parameters estimated by the first network. Inspired by [LKA+20], it outputs the intensity, frequency, and phase of the Fourier decomposition of each state on its spatiotemporal domain. The physical laws could be incorporated during the training phase [SIH21]. Collaborations with UQAM could also be considered.

P8.2 . Traffic congestion control

Regarding the traffic network test case, we could first consider more complex networks than the simple junction presented in Chapter 11. Such configurations could, for instance, have a star-shaped structure. A future avenue of exploration entails the development of a periodic event-triggered control strategy, which periodically evaluates the activation condition, thus conserving computational resources. Furthermore, inquiries into the viability of quantized implementations for event-triggered controllers are on the horizon [BL20]. These endeavors will serve as the bedrock for realizing digitally implemented boundary-backstepping-based controllers. We also aim to extend our results to the case of multi-lane roads or roads with different types of vehicles [BYK21].

An additional captivating perspective revolves around analyzing vehicular platoons, approached from a macroscopic and microscopic point of view. This entails investigating and quantifying the interrelations between the two modeling paradigms. To achieve this goal, a coupled hyperbolic-ODEs model emerges as a pertinent choice. The linkage is established through the integration of macroscopic variables into the control laws governing the microscopic model of the vehicles. Consequently, the hyperbolic component becomes dependent on the average speed value derived from the finite-dimensional dynamics of the vehicle ensemble. Such an amalgamated model could potentially yield more precise evaluations of the overarching state of the system, encompassing both macroscopic and microscopic facets. These robust estimations could lay the foundation for the development of more efficient control algorithms aimed at ameliorating stop-and-go oscillations. In particular, it would allow taking into account the string stability [PSVDWN13] into the stabilization of macroscopic variables.

Bibliography

[AA16] U. J. F. Aarsnes and O. M. Aamo. Linear stability analysis of self-excited vibrations in drilling using an infinite dimensional model. *Journal of Sound and Vibration*, 360:239–259, 2016.

[AA19] J. Auriol and F. Bribiesca Argomedo. Delay-robust stabilization of an $n+m$ hyperbolic PDE-ODE system. In *Conference on Decision and Control*, pages 4964–4970. IEEE, 2019.

[AA22] H. Anfinsen and O. M. Aamo. Leak detection, size estimation and localization in branched pipe flows. *Automatica*, 140:110213, 2022.

[AADMS19] U. J. F. Aarsnes, J. Auriol, F. Di Meglio, and R. Shor. Estimating friction factors while drilling. *Journal of Petroleum Science and Engineering*, 179:80–91, 2019.

[AADMS20] J. Auriol, U. J. F. Aarsnes, F. Di Meglio, and R. Shor. Robust control design of underactuated 2$\times$ 2 PDE-ODE-PDE systems. *IEEE control systems letters*, 5(2):469–474, 2020.

[AAK19] U. J. F Aarsnes, O. M. Aamo, and M. Krstic. Extremum seeking for real-time optimal drilling control. In *2019 American Control Conference (ACC)*, pages 5222–5227. IEEE, 2019.

[Aam12] O. M. Aamo. Disturbance rejection in 2 x 2 linear hyperbolic systems. *IEEE transactions on automatic control*, 58(5):1095–1106, 2012.

[Aam16] O. M. Aamo. Leak detection, size estimation and localization in pipe flows. *IEEE Transactions on Automatic Control*, 61(1):246–251, 2016.

[AAMDM18] J. Auriol, U. J. F. Aarsnes, P. Martin, and F. Di Meglio. Delay-robust control design for heterodirectional linear coupled hyperbolic PDEs. *IEEE Transactions on Automatic Control*, 63(10):3551–3557, 2018.

[AAS20] J. Auriol, U. J. F. Aarsnes, and R. Shor. Self-tuning torsional drilling model for real-time applications. In *2020 American Control Conference (ACC)*, pages 3091–3096. IEEE, 2020.

[ABA19] J. Auriol and F. Bribiesca-Argomedo. Delay-robust stabilization of a $n+m$ hyperbolic PDE-ODE system. In *IEEE Conference on Decision and Control*, pages 4996–5001. IEEE, 2019.

[ABA22] J. Auriol and F. Bribiesca-Argomedo. Observer design for $n+m$ linear hyperbolic ODE-PDE-ODE systems. *IEEE Control Systems Letters*, 7:283–288, 2022.

[ABABP20] J. Auriol, F. Bribiesca-Argomedo, and D. Bresch-Pietri. Stabilization of an underactuated 1+2 linear hyperbolic system with a proper control. *Conference on Decision and Control*, 2020.

[ABABS$^+$18] J. Auriol, F. Bribiesca Argomedo, D. Bou Saba, M. Di Loreto, and F. Di Meglio. Delay-robust stabilization of a hyperbolic PDE–ODE system. *Automatica*, 95:494–502, 2018.

[ABADM23] J. Auriol, F. Bribiesca Argomedo, and F. Di Meglio. Robustification of stabilizing controllers for ODE-PDE-ODE systems: a filtering approach. *Automatica*, 147:110724, 2023.

[ABANR21] J. Auriol, F. Bribiesca-Argomedo, S.-I. Niculescu, and J. Redaud. Stabilization of a hyperbolic PDEs-ODE network using a recursive dynamics interconnection framework. In *2021 European control conference (ECC)*, pages 2493–2499. IEEE, 2021.

[ABMN21] J. Auriol, I. Boussaada, H. Mounier, and S.-I. Niculescu. Torsional-vibrations damping in drilling systems: Multiplicity-induced-dominancy based design. *IFAC-PapersOnLine*, 54:428–433, 2021.

[ABP22] J. Auriol and D. Bresch-Pietri. Robust state-feedback stabilization of an underactuated network of interconnected $n+m$ hyperbolic PDE systems. *Automatica*, 136:110040, 2022.

[ABP23] J. Auriol and D. Bresch-Pietri. On input-to-state stability of linear difference equations and its characterization with a Lyapunov functional. In *IFAC World Congress 2023*, 2023.

[ABS+22] J. Auriol, I. Boussaada, R. J. S., H. Mounier, and S.-I. Niculescu. Comparing advanced control strategies to eliminate stick-slip oscillations in drillstrings. *IEEE Access*, 10:10949–10969, 2022.

[AdAV20] J. Auriol, G. de Andrade, and R. Vazquez. A differential-delay estimator for thermoacoustic oscillations in a Rijke tube using in-domain pressure measurements. In *2020 59th IEEE Conference on Decision and Control (CDC)*, pages 4417–4422. IEEE, 2020.

[ADM16a] J. Auriol and F. Di Meglio. Minimum time control of heterodirectional linear coupled hyperbolic PDEs. *Automatica*, 71:300–307, 2016.

[ADM16b] J. Auriol and F. Di Meglio. Two-sided boundary stabilization of two linear hyperbolic PDEs in minimum time. In *Decision and Control (CDC), 2016 IEEE 55th Conference on*, pages 3118–3124. IEEE, 2016.

[ADM17] J. Auriol and F. Di Meglio. Trajectory tracking for a system of two linear hyperbolic pdes with uncertainties. *IFAC-PapersOnLine*, 50(1):7089–7095, 2017.

[ADM18] J. Auriol and F. Di Meglio. Two-sided boundary stabilization of heterodirectional linear coupled hyperbolic pdes. *IEEE Transactions on Automatic Control*, 63(8):2421–2436, 2018.

[ADM19] J. Auriol and F. Di Meglio. An explicit mapping from linear first order hyperbolic PDEs to difference systems. *Systems & Control Letters*, 123:144–150, 2019.

[ADM20] J. Auriol and F. Di Meglio. Robust output feedback stabilization for two heterodirectional linear coupled hyperbolic PDEs. *Automatica*, 115:108896, 2020.

[ADMBA19] J. Auriol, F. Di Meglio, and F. Bribiesca-Argomedo. Delay robust state feedback stabilization of an underactuated network of two interconnected PDE systems. In *2019 American Control Conference (ACC)*, pages 593–599. IEEE, 2019.

[ADMS18a] U. J. F Aarsnes, F. Di Meglio, and R. J. Shor. Avoiding stick slip vibrations in drilling through startup trajectory design. *Journal of Process Control*, 70:24–35, 2018.

[ADMS18b] U. J. F. Aarsnes, F. Di Meglio, and R. J. Shor. Benchmarking of industrial stick-slip mitigation controllers. *IFAC-PapersOnLine*, 51(8):233–238, 2018.

[ADMV22] J. Auriol, J. Deutscher, G. Mazanti, and G. Valmorbida. *Advances in Distributed Parameter Systems*. Springer, 2022.

[AH80] C. Avellar and J. Hale. On the zeros of exponential polynomials. *Journal of Mathematical Analysis and Applications*, 73(2):434–452, 1980.

[AHB08] S. Amin, F. M. Hante, and A. M. Bayen. On stability of switched linear hyperbolic conservation laws with reflecting boundaries. In *Hybrid Systems: Computation and Control*, pages 602–605. Springer, 2008.

[AHB11] S. Amin, F. Hante, and A. Bayen. Exponential stability of switched linear hyperbolic initial-boundary value problems. *IEEE Transactions on Automatic Control*, 57(2):291–301, 2011.

[AKBP22] J. Auriol, S. Kong, and D. Bresch-Pietri. Explicit prediction-based control for linear difference equations with distributed delays. *IEEE Control Systems Letters*, 6:2864–2869, 2022.

[AKIS20] J. Auriol, N. Kazemi, K. Innanen, and R. J. Shor. Combining formation seismic velocities while drilling and a pde-ode observer to improve the drill-string dynamics estimation. In *2020 American Control Conference (ACC)*, pages 3120–3125. IEEE, 2020.

[AKN21] J. Auriol, N. Kazemi, and S.-I. Niculescu. Sensing and computational frameworks for improving drill-string dynamics estimation. *Mechanical Systems and Signal Processing*, 160:107836, 2021.

[AKS+19] J. Auriol, N. Kazemi, R. J. Shor, K. A. Innanen, and I. D. Gates. A sensing and computational framework for estimating the seismic velocities of rocks interacting with the drill bit. *IEEE Transactions on Geoscience and Remote Sensing*, 58(5):3178–3189, 2019.

[ÅM21] K. J. Åström and R. Murray. *Feedback systems: an introduction for scientists and engineers*. Princeton Univ. press, 2021.

[AMDM19] J. Auriol, K. Morris, and F. Di Meglio. Late-lumping backstepping control of Partial Differential Equations. *Automatica*, 100:247–259, 2019.

[APK23] J. Auriol, M. Pereira, and B. Kulcsar. Mean-square exponential stabilization of coupled hyperbolic systems with random parameters. In *IFAC World Congress 2023*, 2023.

[AR00] A. Aw and M. Rascle. Resurrection of "second order" models of traffic flow. *SIAM Journal on Applied Mathematics*, 60(3):916–938, 2000.

[Art82] Z. Artstein. Linear systems with delayed controls: a reduction. *IEEE Transactions on Automatic Control*, 27(4):869–879, 1982.

[AS18] U. J. F. Aarsnes and R. J. Shor. Torsional vibrations with bit off bottom: Modeling, characterization and field data validation. *Journal of Petroleum Science and Engineering*, 163:712–721, 2018.

[ASADM20] J. Auriol, R. J. Shor, U. J. F. Aarsnes, and F. Di Meglio. Closed-loop tool face control with the bit off-bottom. *Journal of Process Control*, 90:35–45, 2020.

[ASNK22] J. Auriol, R. Shor, S.-I. Niculescu, and N. Kazemi. Estimating drill string friction with model-based and data-driven methods. In *2022 American Control Conference (ACC)*, pages 3464–3469. IEEE, 2022.

[ATK86] T. Aarrestad, H. Tonnesen, and A. Kyllingstad. Drillstring vibrations: Comparison between theory and experiments on a full-scale research drilling rig. In *IADC/SPE Drilling Conference*. OnePetro, 1986.

[Aur18] J. Auriol. *Robust design of backstepping controllers for systems of linear hyperbolic PDEs*. PhD thesis, PSL Research University, 2018.

[Aur20] J. Auriol. Output feedback stabilization of an underactuated cascade network of interconnected linear PDE systems using a backstepping approach. *Automatica*, 117:108964, 2020.

[AvdW19] U. J. F. Aarsnes and N. van de Wouw. Axial and torsional self-excited vibrations of a distributed drill-string. *Journal of Sound and Vibration*, 444:127–151, 2019.

[AW92] W. A. Adkins and S. H. Weintraub. *Algebra: An approach via module theory*, volume 136 of *Graduate Texts in Mathematics*. Springer-Verlag, 1992.

[BA77] J. V. Beck and K. J. Arnold. *Parameter estimation in engineering and science*. James Beck, 1977.

[BBHS89] J. F. Brett, A. D. Beckett, C. A. Holt, and D. L. Smith. Uses and Limitations of Drillstring Tension and Torque Models for Monitoring Hole Conditions. *SPE Drilling Engineering*, 4(03):223–229, sep 1989.

[BC63] R. E. Bellman and K. L. Cooke. *Differential-difference equations*. Rand Corporation, 1963.

[BC16] G. Bastin and J.-M. Coron. *Stability and boundary stabilization of 1-D hyperbolic systems*, volume 88. Springer, 2016.

[BCA22] L. Brivadis, A. Chaillet, and J. Auriol. Online estimation of Hilbert-Schmidt operators and application to kernel reconstruction of neural fields. In *2022 IEEE 61st Conference on Decision and Control (CDC)*, pages 597–602. IEEE, 2022.

[BCG+14] A. Bressan, S. Canic, M. Garavello, M. Herty, and B. Piccoli. Flows on networks: recent results and perspectives. *EMS Surveys in Mathematical Sciences*, 1(1):47–111, 2014.

[BCT15] G. Bastin, J.-M. Coron, and S. O. Tamasoiu. Stability of linear density-flow hyperbolic systems under PI boundary control. *Automatica*, 53:37–42, 2015.

[BHKS21] K. Bhattacharya, B. Hosseini, N. Kovachki, and A. Stuart. Model reduction and neural networks for parametric PDEs. *The SMAI journal of computational mathematics*, 7:121–157, 2021.

[BJ20] B. Berret and F. Jean. Efficient computation of optimal open-loop controls for stochastic systems. *Automatica*, 115:108874, 2020.

[BL14] N. Bekiaris-Liberis. Simultaneous compensation of input and state delays for nonlinear systems. *Systems and Control Letters*, 73:96–102, 2014.

[BL20] N. Bekiaris-Liberis. Hybrid boundary stabilization of linear first-order hyperbolic pdes despite almost quantized measurements and control input. *Systems & Control Letters*, 146:104809, 2020.

[BLK10] N. Bekiaris-Liberis and M. Krstic. Stabilization of linear strict-feedback systems with delayed integrators. *Automatica*, 46(11):1902–1910, 2010.

[BLK16] N. Bekiaris-Liberis and M. Krstic. Stability of predictor-based feedback for nonlinear systems with distributed input delay. *Automatica*, 70:195–203, 2016.

[BLP22] R. Bonalli, T. Lew, and M. Pavone. Sequential convex programming for non-linear stochastic optimal control. *ESAIM: Control, Optimisation and Calculus of Variations*, 28:64, 2022.

[BMP15] R. Bagherpour, S. Moheimani, and I. Petersen. Stability and energy-preserving boundary control of flexible mechanical systems with distributed parameters using the port-Hamiltonian approach. *IEEE Transactions on Control Systems Technology*, 23(5):1981–1993, 2015.

[Boi13] S. Boisgérault. Growth bound of delay-differential algebraic equations. *Comptes Rendus Mathematique*, 351(15):645–648, 2013.

[BPDM16] D. Bresch-Pietri and F. Di Meglio. Prediction-based control of linear input-delay system subject to state-dependent state delay-application to suppression of mechanical vibrations in drilling. *IFAC-PapersOnLine*, 49(8):111–117, 2016.

[Bra68] R. Brayton. Small-signal stability criterion for electrical networks containing lossless transmission lines. *IBM Journal of Research and Development*, 12(6):431–440, 1968.

[Bre92] J. F. Brett. The Genesis of Bit-Induced Torsional Drillstring Vibrations. *SPE Drilling Engineering*, 7(03):168–174, 1992.

[Bre10] H. Brezis. *Functional analysis, Sobolev spaces and partial differential equations*. Springer Science & Business Media, 2010.

[BS13] F. Bonnans and A. Shapiro. *Perturbation analysis of optimization problems*. Springer Science & Business Media, 2013.

[BSBAA+19] D. Bou Saba, F. Bribiesca Argomedo, J. Auriol, M. Di Loreto, and F. Di Meglio. Stability analysis of linear 2×2 hyperbolic PDEs. *IEEE Transactions on Automatic Control*, 65(7):2941–2956, 2019.

[BSBADLE17] D. Bou Saba, F. Bribiesca-Argomedo, M. Di Loreto, and D. Eberard. Backstepping stabilization of $2\times$ 2 linear hyperbolic pdes coupled with potentially unstable actuator and load dynamics. In *2017 IEEE 56th Annual Conference on Decision and Control (CDC)*, pages 2498–2503. IEEE, 2017.

[BSBADLE19] D. Bou Saba, F. Bribiesca-Argomedo, M. Di Loreto, and D. Eberard. Strictly proper control design for the stabilization of 2×2 linear hyperbolic ODE-PDE-ODE systems. In *2019 IEEE 58th Conference on Decision and Control (CDC)*, pages 4996–5001. IEEE, 2019.

[BSGB18] M. Barreau, A. Seuret, F. Gouaisbaut, and L. Baudouin. Lyapunov stability analysis of a string equation coupled with an ordinary differential system. *IEEE Transactions on Automatic Control*, 63(11):3850–3857, 2018.

[BSK23] L. Bhan, Y. Shi, and M. Krstic. Neural operators for bypassing gain and control computations in PDE backstepping. *arXiv preprint arXiv:2302.14265*, 2023.

[BTA22] L. Brivadis, C. Tamekue, and J. Auriol. A comment on "robust stabilization of delayed neural fields with partial measurement and actuation"[automatica 83 (2017) 262-274]. *Automatica*, 2022.

[BTN+18] I. Boussaada, S. Tliba, S.-I. Niculescu, H. U. Ünal, and T. Vyhlídal. Further remarks on the effect of multiple spectral values on the dynamics of time-delay systems. application to the control of a mechanical system. *Linear Algebra and its Applications*, 542:589–604, 2018.

[BVDWN11] B. Besselink, N. Van De Wouw, and H. Nijmeijer. A semi-analytical study of stick-slip oscillations in drilling systems. *Journal of Computational and Nonlinear Dynamics*, 2011.

[BY15] L. Baudouin and M. Yamamoto. Inverse problem on a tree-shaped network: unified approach for uniqueness. *Applicable Analysis*, 94(11):2370–2395, 2015.

[BYK21] M. Burkhardt, H. Yu, and M. Krstic. Stop-and-go suppression in two-class congested traffic. *Automatica*, 125:109381, 2021.

[CANB99] J.-M. Coron, B. Andréa-Novel, and G. Bastin. A Lyapunov approach to control irrigation canals modeled by saint-venant equations. In *Proc. European Control Conference, Karlsruhe*, 1999.

[Car96] L. Carvalho. On quadratic Liapunov functionals for linear difference equations. *Linear Algebra and its applications*, 240:41–64, 1996.

[Cay18] E. Cayeux. On the Importance of Boundary Conditions for Real-Time Transient Drill-String Mechanical Estimations. In *IADC/SPE Drilling Conference and Exhibition*. Society of Petroleum Engineers, 2018.

[CBdN08] J-M. Coron, G. Bastin, and B. d'Andréa Novel. Dissipative boundary conditions for one-dimensional nonlinear hyperbolic systems. *SIAM Journal on Control and Optimization*, 47(3):1460–1498, 2008.

[CBG90] S. Chen, S. A. Billings, and P. M. Grant. Non-linear system identification using neural networks. *International journal of control*, 51(6):1191–1214, 1990.

[CCH+19] K.-D. Chen, J.-Q. Chen, D.-F. Hong, X.-Y. Zhong, Z.-B. Cheng, Q.-H. Lu, J.-P. Liu, Z.-H. Zhao, and G.-X. Ren. Efficient and high-fidelity steering ability prediction of a slender drilling assembly. *Acta Mechanica*, 230(11):3963–3988, 2019.

[CFL67] R. Courant, K. Friedrichs, and H. Lewy. On the partial difference equations of mathematical physics. *IBM journal of Research and Development*, 11(2):215–234, 1967.

[CHO16] J.-M. Coron, L. Hu, and G. Olive. Stabilization and controllability of first-order integro-differential hyperbolic equations. *Journal of Functional Analysis*, 271(12):3554–3587, 2016.

[CHO17] J.-M. Coron, L. Hu, and G. Olive. Finite-time boundary stabilization of general linear hyperbolic balance laws via Fredholm backstepping transformation. *Automatica*, 84:95–100, 2017.

[CK68] K. Cooke and D. Krumme. Differential-difference equations and nonlinear initial-boundary value problems for linear hyperbolic partial differential equations. *Journal of Mathematical Analysis and Applications*, 24(2):372–387, 1968.

[CK76] K. Cooke and J. Kaplan. A periodicity threshold theorem for epidemics and population growth. *Mathematical Biosciences*, 31(1):87–104, 1976.

[CKG96] M. Courtemanche, J. P. Keener, and L. Glass. A delay equation representation of pulse circulation on a ring in excitable media. *SIAM Journal on Applied Mathematics*, 56(1):119–142, 1996.

[CM09] R. Curtain and K. Morris. Transfer functions of distributed parameter systems: A tutorial. *Automatica*, 45(5):1101–1116, 2009.

[CMS16] Y. Chitour, G. Mazanti, and M. Sigalotti. Stability of non-autonomous difference equations with applications to transport and wave propagation on networks. *Networks and Heterogeneous Media*, 11(4):563–601, 2016.

[CMS20] Y. Chitour, G. Mazanti, and M. Sigalotti. Approximate and exact controllability of linear difference equations. *Journal de l'École polytechnique—Mathématiques*, 7:93–142, 2020.

[CN20] J.-M. Coron and H.-M. Nguyen. Finite-time stabilization in optimal time of homogeneous quasilinear hyperbolic systems in one dimensional space. *ESAIM: Control, Optimisation and Calculus of Variations*, 26:119, 2020.

[CN21a] J.-M. Coron and H.-M. Nguyen. Null-controllability of linear hyperbolic systems in one dimensional space. *Systems & Control Letters*, 148:104851, 2021.

[CN21b] J.-M. Coron and H.-M. Nguyen. On the optimal controllability time for linear hyperbolic systems with time-dependent coefficients. *arXiv preprint arXiv:2103.02653*, 2021.

[Col03] R. Colombo. Hyperbolic phase transitions in traffic flow. *SIAM Journal on Applied Mathematics*, 63(2):708–721, 2003.

[Cor09] J.-M. Coron. *Control and nonlinearity*. American Mathematical Soc., 2009.

[CVKB13] J.-M. Coron, R. Vazquez, M. Krstic, and G. Bastin. Local exponential H^2 stabilization of a $2\times$ 2 quasilinear hyperbolic system using backstepping. *SIAM Journal on Control and Optimization*, 51(3):2005–2035, 2013.

[CZ12] R. F. Curtain and H. Zwart. *An introduction to infinite-dimensional linear systems theory*, volume 21. Springer Science & Business Media, 2012.

[D'A49] J. D'Alembert. Suite des recherches sur la courbe que forme une corde tendue, mise en vibration. *Histoire de l'Académie Royale des Sciences et des Belles Lettres de Berlin*, pages 220–249, 1749.

[DA98] V. A. Dunayevsky and F. Abbassian. Application of Stability Approach to Bit Dynamics. *SPE Drilling & Completion*, 13(2):22–25, 1998.

[dAVP18] G. A. de Andrade, R. Vazquez, and D. J. Pagano. Backstepping stabilization of a linearized ODE–PDE Rijke tube model. *Automatica*, 96:98–109, 2018.

[DBAR12] S. Dudret, K. Beauchard, F. Ammouri, and P. Rouchon. Stability and asymptotic observers of binary distillation processes described by nonlinear convection/diffusion models. In *American Control Conference (ACC), 2012*, pages 3352–3358. IEEE, 2012.

[DBC12] A. Diagne, G. Bastin, and J.-M. Coron. Lyapunov exponential stability of 1-D linear hyperbolic systems of balance laws. *Automatica*, 48(1):109–114, 2012.

[DBPPDM18] M. Davo, D. Bresch-Pietri, C Prieur, and F. Di Meglio. Stability analysis of a 2×2 linear hyperbolic system with a sampled-data controller via backstepping method and looped-functionals. *IEEE Transactions on Automatic Control*, 2018.

[DBVdHJ10] S. Djordjevic, O.H. Bosgra, P.M.J. Van den Hof, and D. Jeltsema. Boundary actuation structure of linearized two-phase flow. In *American Control Conference (ACC), 2010*, pages 3759–3764. IEEE, 2010.

[DD92] E. Detournay and P. Defourny. A phenomenological model for the drilling action of drag bits. *International Journal of Rock Mechanics and Mining Sciences & Geomechanics Abstracts*, 29(1):13–23, 1992.

[DDLM15] S. Damak, M. Di Loreto, and S. Mondié. Stability of linear continuous-time difference equations with distributed delay: Constructive exponential estimates. *International Journal of Robust and Nonlinear Control*, 25(17):3195–3209, 2015.

[DG19] J. Deutscher and J. Gabriel. Periodic output regulation for general linear heterodirectional hyperbolic systems. *Automatica*, 103:208–216, 2019.

[DG20] J. Deutscher and N. Gehring. Output feedback control of coupled linear parabolic ODE–PDE–ODE systems. *IEEE Transactions on Automatic Control*, 66(10):4668–4683, 2020.

[DG21] J. Deutscher and J. Gabriel. A backstepping approach to output regulation for coupled linear wave–ODE systems. *Automatica*, 123:109338, 2021.

[DGK18] J. Deutscher, N. Gehring, and R. Kern. Output feedback control of general linear heterodirectional hyperbolic ODE–PDE–ODE systems. *Automatica*, 95:472–480, 2018.

[dHPC+03] J. de Halleux, C. Prieur, J.-M. Coron, B. d'Andréa Novel, and G. Bastin. Boundary feedback control in networks of open channels. *Automatica*, 39(8):1365–1376, 2003.

[DLP86] R. Datko, J. Lagnese, and M.P. Polis. An example on the effect of time delays in boundary feedback stabilization of wave equations. *SIAM Journal on Control and Optimization*, 24(1):152–156, 1986.

[DM11] F. Di Meglio. *Dynamics and control of slugging in oil production*. PhD thesis, École Nationale Supérieure des Mines de Paris, Centre Automatique et Systèmes (CAS), 2011.

[DMA15] F. Di Meglio and U. J. F. Aarsnes. A distributed parameter systems view of control problems in drilling. *IFAC-PapersOnLine*, 48(6):272–278, 2015.

[DMBAHK18] F. Di Meglio, F. Bribiesca-Argomedo, L. Hu, and M. Krstic. Stabilization of coupled linear heterodirectional hyperbolic PDE–ODE systems. *Automatica*, 87:281–289, 2018.

[DMLA20] F. Di Meglio, P.-O. Lamare, and U. J. F. Aarsnes. Robust output feedback stabilization of an ODE–PDE–ODE interconnection. *Automatica*, 119:109059, 2020.

[DMSB09] V. Duindam, A. Macchelli, S. Stramigioli, and H. Bruyninckx. *Modeling and control of complex physical systems: the port-Hamiltonian approach*. Springer Science & Business Media, 2009.

[DRS08] E. Detournay, T. Richard, and M. Shepherd. Drilling response of drag bits: theory and experiment. *International Journal of Rock Mechanics and Mining Sciences*, 45(8):1347–1360, 2008.

[DvdSBF16] J. P Dunn, A. J van der Schaft, P. Bauer, and H. J. Ferreau. Optimization-based design of a high-performance hybrid vehicle powertrain using the port-Hamiltonian framework. *IEEE Transactions on Control Systems Technology*, 25(2):706–715, 2016.

[DVP05] D. Del Vecchio and N. Petit. Boundary control for an industrial under-actuated tubular chemical reactor. *Journal of Process Control*, 15(7):771–784, 2005.

[Dwa15] S. Dwars. Recent advances in soft torque rotary systems. In *SPE drilling conference and exhibition*. OnePetro, 2015.

[Dyn12] E. B. Dynkin. *Theory of Markov processes*. Courier Corporation, 2012.

[DZ06] R. Dager and E. Zuazua. *Wave propagation, observation and control in 1-d flexible multi-structures*, volume 50. Springer Science & Business Media, 2006.

[EAYK22a] N. Espitia, J. Auriol, H. Yu, and M. Krstic. Event-triggered output feedback control of traffic flow on cascaded roads. In *Advances in Distributed Parameter Systems*, pages 243–267. Springer, 2022.

[EAYK22b] N. Espitia, J. Auriol, H. Yu, and M. Krstic. Traffic flow control on cascaded roads by event-triggered output feedback. *International Journal of Robust and Nonlinear Control*, 32(10):5919–5949, 2022.

[EGMP16] N. Espitia, A. Girard, N. Marchand, and C. Prieur. Event-based control of linear hyperbolic systems of conservation laws. *Automatica*, 70:275–287, 2016.

[EGMP17] N. Espitia, A. Girard, N. Marchand, and C. Prieur. Event-based boundary control of a linear 2×2 hyperbolic system via backstepping approach. *IEEE Transactions on Automatic Control*, 63(8):2686–2693, 2017.

[EM14] A. Egorov and S. Mondié. Necessary stability conditions for linear delay systems. *Automatica*, 50(12):3204–3208, 2014.

[ERW17] S. Ecklebe, M. Riesmeier, and F. Woittennek. Approximation and implementation of transformation based feedback laws for distributed parameter systems. *PAMM*, 17(1):785–786, 2017.

[Esp20] N. Espitia. Observer-based event-triggered boundary control of a linear 2 x 2 hyperbolic systems. *Systems & Control Letters*, 138:104668, 2020.

[Fat66] H. Fattorini. Some remarks on complete controllability. *SIAM Journal on Control*, 4(4):686–694, 1966.

[FKA+22] A. Fathalian, N. Kazemi, J. Auriol, D. Trad, K. Innanen, and R. Shor. Forward modeling of seismic-while-drilling data in anisotropic viscoelastic media with anisotropic attenuation. In *83rd EAGE Annual Conference & Exhibition*, pages 1–5. European Association of Geoscientists & Engineers, 2022.

[FKN+09] M. Flynn, A. Kasimov, J. Nave, R. Rosales, and B. Seibold. Self-sustained nonlinear waves in traffic flow. *Physical Review E*, 79(5)(1):56–113, 2009.

[Fra10] L. Franca. Drilling action of roller-cone bits: modeling and experimental validation. *Journal of Energy Resources Technology*, 132(4), 2010.

[Fri02] E. Fridman. Stability of linear descriptor systems with delay: a Lyapunov-based approach. *Journal of Mathematical Analysis and Applications*, 273(1):24–44, 2002.

[FS13] S. Fan and B. Seibold. Data-fitted first-order traffic models and their second-order generalizations: Comparison by trajectory and sensor data. *Transportation Research Record 2391*, 1:32–43, 2013.

[FSS15] A. Ferrara, S. Sacone, and S. Siri. Event-triggered model predictive schemes for freeway traffic control. *Transportation Research Part C*, 59(554-567), 2015.

[FSS16] A. Ferrara, S. Sacone, and S. Siri. Design of networked freeway traffic controllers based on event-triggered control concepts. *International Journal of Robust and Nonlinear Control*, 26:1162–1183, 2016.

[FTY+23] M. Faghihi, S. Tashakori, E. A. Yazdi, H. Mohammadi, M. Eghtesad, and N. van de Wouw. Control of axial–torsional dynamics of a distributed drilling system. *IEEE Transactions on Control Systems Technology*, 2023.

[FW75] B. Francis and W. Wonham. The internal model principle for linear multivariable regulators. *Applied mathematics and optimization*, 2(2):170–194, 1975.

[FWYL20] C. Fu, Q.-G. Wang, J. Yu, and C. Lin. Neural network-based finite-time command filtering control for switched nonlinear systems with backlash-like hysteresis. *IEEE Transactions on Neural Networks and Learning Systems*, 2020.

[GBC16] I. Goodfellow, Y. Bengio, and A. Courville. *Deep learning*. MIT press, 2016.

[GCD97] B. Goodway, T. Chen, and J. Downton. Improved AVO fluid detection and lithology discrimination using lamé petrophysical parameters;"$\lambda\rho$","$\mu\rho$", & "λ/μ fluid stack", from p and s inversions. In *SEG Technical Program Expanded Abstracts 1997*, pages 183–186. Society of Exploration Geophysicists, 1997.

[GD11] M. Gugat and M. Dick. Time-delayed boundary feedback stabilization of the isothermal euler equations with friction. *Math. Control Relat. Fields*, 1(4):469–491, 2011.

[GDD09] C. Germay, V. Denoël, and E. Detournay. Multiple mode analysis of the self-excited vibrations of rotary drilling systems. *Journal of Sound and Vibration*, 325(1-2):362–381, aug 2009.

[Geh22] N. Gehring. A systematic backstepping design of tracking controllers for ODE-PDE-ODE systems with nonlinear actuator dynamics. In *Advances in Distributed Parameter Systems*, pages 171–196. Springer, 2022.

[Gir15] A. Girard. Dynamic triggering mechanisms for event-triggered control. *IEEE Transactions on Automatic Control*, 60(7):1992–1997, 2015.

[GK18] N. Gehring and R. Kern. Flatness-based tracking control for a pneumatic system with distributed parameters. *IFAC-PapersOnLine*, 51(2):487–492, 2018.

[GL11] Q. Gu and T. Li. Exact boundary controllability of nodal profile for quasilinear hyperbolic systems in a tree-like network. *Mathematical Methods in the Applied Sciences*, 34(8):911–928, 2011.

[GP06] M. Garavello and B. Piccoli. Traffic flow on a road network using the Aw–Rascle model. *Communications in Partial Differential Equations*, 31(2):243–275, 2006.

[GS10] M. Gugat and M. Sigalotti. Stars of vibrating strings: switching boundary feedback stabilization. *Networks and Heterogeneous Media*, 5(2):299–314, 2010.

[GvdWNS09] C. Germay, N. van de Wouw, H. Nijmeijer, and R. Sepulchre. Nonlinear Drillstring Dynamics Analysis. *SIAM Journal on Applied Dynamical Systems*, 8(2):527–553, jan 2009.

[HAK16] A. Hasan, O. M. Aamo, and M. Krstic. Boundary observer design for hyperbolic PDE–ODE cascade systems. *Automatica*, 68:75–86, 2016.

[HDMVK16] L. Hu, F. Di Meglio, R. Vazquez, and M. Krstic. Control of homodirectional and general heterodirectional linear coupled hyperbolic PDEs. *IEEE Transactions on Automatic Control*, 61(11):3301–3314, 2016.

[HDMVK19] L. Hu, F. Di Meglio, R. Vazquez, and M. Krstic. Boundary exponential stabilization of 1-dimensional inhomogeneous quasi-linear hyperbolic systems. *SIAM Journal on Control and Optimization*, 57(2):963–998, 2019.

[Hen74] D. Henry. Linear autonomous neutral functional differential equations. *Journal of Differential Equations*, 15(1):106–128, 1974.

[Hen87] D. Henry. Topics in analysis. *Publicacions de la Secció de Matemàtiques*, 31(1):29–84, 1987.

[HL02] J. Hale and S.M. Verduyn Lunel. Strong stabilization of neutral functional differential equations. *IMA Journal of Mathematical Control and Information*, 19(1 and 2):5–23, 2002.

[HP17] J.-P. Humaloja and L. Paunonen. Robust regulation of infinite-dimensional port-hamiltonian systems. *IEEE Transactions on Automatic Control*, 63(5):1480–1486, 2017.

[HR06] M. Herty and M. Rascle. Coupling conditions for a class of second-order models for traffic flow. *SIAM Journal on mathematical analysis*, 38(2):595–616, 2006.

[HV12] D. Henrion and T. Vyhlídal. Positive trigonometric polynomials for strong stability of difference equations. *Automatica*, 48(9):2207–2212, 2012.

[HVL93] J. K. Hale and S. M. Verduyn Lunel. *Introduction to functional differential equations*. Springer-Verlag, 1993.

[IGDR21] A. Irscheid, N. Gehring, J. Deutscher, and J. Rudolph. Observer design for 2×2 linear hyperbolic PDEs that are bidirectionally coupled with nonlinear ODEs. In *2021 European Control Conference (ECC)*, pages 2506–2511. IEEE, 2021.

[Jan93] J. D. Jansen. *Nonlinear dynamics of oilwell drillstrings*. PhD thesis, Delft University of Technology, 1993.

[JZ12] B. Jacob and H. Zwart. *Linear port-Hamiltonian systems on infinite-dimensional spaces*. Springer, 2012.

[KAI+21] N. Kazemi, J. Auriol, K. Innanen, R. Shor, and I. Gates. Successive full-waveform inversion of surface seismic and seismic-while-drilling datasets without low frequencies. In *82nd EAGE Annual Conference & Exhibition*, pages 1–5. European Association of Geoscientists & Engineers, 2021.

[Kaz20] N. Kazemi. Across-domains transferability of deep-red in de-noising and compressive sensing recovery of seismic data. *arXiv preprint arXiv:2007.10250*, 2020.

[KBP22a] S. Kong and D. Bresch-Pietri. Prediction-based controller for linear systems with stochastic input delay. *Automatica*, 138:110149, 2022.

[KBP22b] S. Kong and D. Bresch-Pietri. Probabilistic sufficient conditions for prediction-based stabilization of linear systems with random input delay. *IEEE Control Systems Letters*, 6:2270–2275, 2022.

[KBS16] N. Kazemi, E. Bongajum, and M. Sacchi. Surface-consistent sparse multichannel blind deconvolution of seismic signals. *IEEE Transactions on geoscience and remote sensing*, 54(6):3200–3207, 2016.

[KGBS08] M. Krstic, B.-Z. Guo, A. Balogh, and A. Smyshlyaev. Output-feedback stabilization of an unstable wave equation. *Automatica*, 44(1):63–74, 2008.

[KHC+15] M. Kapitaniak, V. V. Hamaneh, J. P. Chávez, K. Nandakumar, and M. Wiercigroch. Unveiling complexity of drill–string vibrations: Experiments and modelling. *International Journal of Mechanical Sciences*, 101:324–337, 2015.

[KK14] I. Karafyllis and M. Krstic. On the relation of delay equations to first-order hyperbolic partial differential equations. *ESAIM: Control, Optimisation and Calculus of Variations*, 20(3):894–923, 2014.

[KK17] I. Karafyllis and M. Krstić. *Predictor feedback for delay systems: Implementations and approximations*, volume 715. Springer, 2017.

[KKD+99] P. C. Kriesels, W . J. G. Keultjes, P. Dumont, I. Huneidi, O.O. Owoeye, R. A. Hartmann, et al. Cost savings through an integrated approach to drillstring vibration control. In *SPE/IADC Middle East Drilling Technology Conference*. Society of Petroleum Engineers, 1999.

[KM01] I. Kolmanovsky and T. Maizenberg. Mean-square stability of nonlinear systems with time-varying, random delay. *Stochastic analysis and Applications*, 19(2):279–293, 2001.

[KM13] V. Kolmanovskii and A. Myshkis. *Introduction to the theory and applications of functional differential equations*, volume 463. Springer Science & Business Media, 2013.

[KMK89] R. Kress, V. Mazya, and V. Kozlov. *Linear integral equations*, volume 82. Springer, 1989.

[KN09] A. Kyllingstad and P.J. Nessjøen. A new stick-slip prevention system. In *SPE/IADC Drilling Conference and Exhibition*. Society of Petroleum Engineers, 2009.

[KNA+20] Nasser Kazemi, Siavash Nejadi, Jean Auriol, Jordan Curkan, Roman J Shor, Kristopher A Innanen, Stephen M Hubbard, and Ian D Gates. Advanced sensing and imaging for efficient energy exploration in complex reservoirs. *Energy Reports*, 6:3104–3118, 2020.

[KP19] I. Karafyllis and M. Papageorgiou. Feedback control of scalar conservation laws with application to density control in freeways by means of variable speed limits. *Automatica*, 105:228–236, 2019.

[KS08] M. Krstic and A. Smyshlyaev. *Boundary control of PDEs: A course on backstepping designs*, volume 16. Siam, 2008.

[KSI18] N Kazemi, R Shor, and K Innanen. Illumination compensation with seismic-while-drilling plus surface seismic imaging. In *80th EAGE Conference and Exhibition 2018*, volume 2018, pages 1–5. European Association of Geoscientists & Engineers, 2018.

[KZ03] V. Kharitonov and A. Zhabko. Lyapunov–Krasovskii approach to the robust stability analysis of time-delay systems. *Automatica*, 39(1):15–20, 2003.

[LADMA18] P.-O Lamare, J. Auriol, F. Di Meglio, and U.J.F Aarsnes. Robust output regulation of 2 x 2 hyperbolic systems: Control law and input-to-state stability. In *2018 Annual American Control Conference (ACC)*, pages 1732–1739. IEEE, 2018.

[Lem10] M. Lemmon. Event-triggered feedback in control, estimation, and optimization. In *Networked Control Systems*, pages 293–358. Springer, 2010.

[Lev40] N. Levinson. *Gap and density theorems*, volume 26. American mathematical society New York, 1940.

[LeV02] R. J. LeVeque. *Finite volume methods for hyperbolic problems*. Cambridge university press, 2002.

[LGM99] Z.-H. Luo, B.-Z. Guo, and O. Morgül. *Stability and stabilization of infinite dimensional systems with applications*. Springer Science & Business Media, 1999.

[LGZM04] Y Le Gorrec, H Zwart, and B Maschke. A semigroup approach to port Hamiltonian systems associated with linear skew symmetric operator. In *Proceedings 16th International symposium on Mathematical Theory of Networks and Systems*. Katholieke Universiteit Leuven, 2004.

[LGZM05] Y. Le Gorrec, H. Zwart, and B. Maschke. Dirac structures and boundary control systems associated with skew-symmetric differential operators. *SIAM journal on control and optimization*, 44(5):1864–1892, 2005.

[Li10] D. Li. *Controllability and observability for quasilinear hyperbolic systems*. American Institute of Mathematical Sciences Springfield, Ill, USA, 2010.

[Lin74] C.-T. Lin. Structural controllability. *IEEE Transactions on Automatic Control*, 19(3):201–208, 1974.

[Lio71] J. L. Lions. *Optimal control of systems governed by partial differential equations*. Springer, 1971.

[LJK21] L. Lu, P. Jin, and G. E. Karniadakis. DeepONet: Learning nonlinear operators for identifying differential equations based on the universal approximation theorem of operators. *Nature Machine Intelligence*, 3(3):218–229, March 2021. arXiv:1910.03193 [cs, stat].

[LKA+20] Z. Li, N. Kovachki, K. Azizzadenesheli, B. Liu, K. Bhattacharya, and A. Stuart. Fourier neural operators for parametric partial differential equations. *arXiv preprint arXiv:2010.08895*, 2020.

[LLLL21] X. Li, Y. Liu, Jian. Li, and Fengzhong. Li. Adaptive event-triggered control for a class of uncertain hyperbolic PDE-ODE cascade systems. *International Journal of Robust and Nonlinear Control*, 2021.

[LLM+16] T. Li, G. Ledwich, Y. Mishra, J. Chow, and A. Vahidnia. Wave aspect of power system transient stability—part ii: Control implications. *IEEE Transactions on Power Systems*, 32(4):2501–2508, 2016.

[LNC+16] X. Li, S.-I. Niculescu, A. Cela, L. Zhang, and X. Li. A frequency-sweeping framework for stability analysis of time-delay systems. *IEEE Transactions on Automatic Control*, 62(8):3701–3716, 2016.

[LP61] G. Lumer and R.S. Phillips. Dissipative operators in a banach space. *Pacific Journal of Mathematics*, 11(2):679–698, 1961.

[LRB17] A. Lake, B. Rezaie, and S. Beyerlein. Review of district heating and cooling systems for a sustainable future. *Renewable and Sustainable Energy Reviews*, 67:417–425, 2017.

[LRW96] H. Logemann, R. Rebarber, and G. Weiss. Conditions for robustness and nonrobustness of the stability of feedback systems with respect to small delays in the feedback loop. *SIAM Journal on Control and Optimization*, 34(2):572–600, 1996.

[LvCK02] R. Leine, D. van Campen, and W. Keultjes. Stick-slip Whirl Interaction in Drillstring Dynamics. *Journal of Vibration and Acoustics*, 124(2):209, 2002.

[LW55] M. Lighthill and G. Whitham. On kinematic waves ii. a theory of traffic flow on long crowded roads. *Proceedings of the Royal Society of London. Series A. Mathematical and Physical Sciences*, 229(1178):317–345, 1955.

[LZJ19] T. Liu, P. Zhang, and Z.-P. Jiang. Event-triggered input-to-state stabilization of nonlinear systems subject to disturbances and dynamic uncertainties. *Automatica*, 108:108488, 2019.

[LZK+21] Z. Li, H. Zheng, N. Kovachki, D. Jin, H. Chen, B. Liu, K. Azizzadenesheli, and A. Anandkumar. Physics-informed neural operator for learning partial differential equations. *arXiv preprint arXiv:2111.03794*, 2021.

[MAK22] Y. Mokhtari and F. Ammar Khodja. Boundary controllability of two coupled wave equations with space-time first-order coupling in 1-D. *Journal of Evolution Equations*, 22(2):1–52, 2022.

[MJ17] K. Mokhtari Jadid. Performance evaluation of virtual flow metering models and its application to metering backup and production allocation. *PhD thesis, Louisiana State University*, 2017.

[MLGRZ17] A. Macchelli, Y. Le Gorrec, H. Ramirez, and H. Zwart. On the synthesis of boundary control laws for distributed port-Hamiltonian systems. *IEEE transactions on automatic control*, 62(4):1700–1713, 2017.

[MN07] W. Michiels and S.-I. Niculescu. *Stability and stabilization of time-delay systems: an eigenvalue-based approach*. SIAM, 2007.

[Mor94] O. Morgul. Robust stabilization of the wave equation against small delays. In *Proceedings of 1994 33rd IEEE Conference on Decision and Control*, volume 2, pages 1751–1756. IEEE, 1994.

[Mor95] O. Morgul. On the stabilization and stability robustness against small delays of some damped wave equations. *IEEE Transactions on Automatic Control*, 40(9):1626–1630, 1995.

[Mor20] K. Morris. *Controller Design for Distributed Parameter Systems*. Springer, 2020.

[Mou98] H. Mounier. Algebraic interpretations of the spectral controllability of a linear delay system. In *Forum Mathematicum*, volume 10, pages 39–58. De Gruyter, 1998.

[Moy77] P. Moylan. Stable inversion of linear systems. *IEEE Transactions on Automatic Control*, 22(1):74–78, 1977.

[MP20] A. Mironchenko and C. Prieur. Input-to-state stability of infinite-dimensional systems: recent results and open questions. *SIAM Review*, 62(3):529–614, 2020.

[MVZ+09] W. Michiels, T. Vyhlídal, P. Zítek, H. Nijmeijer, and D. Henrion. Strong stability of neutral equations with an arbitrary delay dependency structure. *SIAM Journal on Control and Optimization*, 48(2):763–786, 2009.

[MWR+20] A. Mattioni, Y. Wu, H. Ramirez, Y. Le Gorrec, and A. Macchelli. Modelling and control of an IPMC actuated flexible structure: A lumped port Hamiltonian approach. *Control Engineering Practice*, 101:104498, 2020.

[MWTA00] P. C. Magnusson, A. Weisshaar, V. K. Tripathi, and G. C. Alexander. *Transmission lines and wave propagation*. CRC Press, 2000.

[MZ04] T. Meurer and M. Zeitz. Flatness-based feedback control of diffusion-convection-reaction systems via k-summable power series. *IFAC Proceedings Volumes*, 37(13):177–182, 2004.

[Nic01] S.-I. Niculescu. *Delay effects on stability: a robust control approach*, volume 269. Springer Science & Business Media, 2001.

[NIGM18] C. Nwankpa, W. Ijomah, A. Gachagan, and S. Marshall. Activation functions: Comparison of trends in practice and research for deep learning. *arXiv preprint arXiv:1811.03378*, 2018.

[NKC+20a] S. Nejadi, N. Kazemi, J. Curkan, J. Auriol, P. Durkin, S. M Hubbard, K. Innanen, R. Shor, and I. Gates. Look ahead of the bit while drilling: Potential impacts and challenges in the mcmurray formation. In *SPE Canada Heavy Oil Conference*, 2020.

[NKC+20b] S. Nejadi, N. Kazemi, J. Curkan, J. Auriol, P. Durkin, S. M Hubbard, K. Innanen, R. Shor, and I. Gates. Look ahead of the bit while drilling: Potential impacts and challenges of acoustic seismic while drilling in the McMurray formation. *SPE Journal*, 25(05):2194–2205, 2020.

[NW13] K. Nandakumar and M. Wiercigroch. Stability analysis of a state dependent delayed, coupled two DOF model of drill-string vibration. *Journal of Sound and Vibration*, 332(10):2575–2592, 2013.

[OEM22] R. Ortiz, A. Egorov, and S. Mondié. Necessary and sufficient stability conditions for integral delay systems. *International Journal of Robust and Nonlinear Control*, 32(6):3152–3174, 2022.

[OT19] K. Okamoto and P. Tsiotras. Optimal stochastic vehicle path planning using covariance steering. *IEEE Robotics and Automation Letters*, 4(3):2276–2281, 2019.

[OvdSCA08] R Ortega, A van der Schaft, F Castanos, and A Astolfi. Control by interconnection and standard passivity-based control of port-Hamiltonian systems. *IEEE transactions on automatic control*, 53(11):2527–2542, 2008.

[Pan76] L. Pandolfi. Stabilization of neutral functional differential equations. *Journal of Optimization Theory and Applications*, 20(2):191–204, 1976.

[Paz12] A. Pazy. *Semigroups of linear operators and applications to partial differential equations*, volume 44. Springer Science & Business Media, 2012.

[Pep05] P. Pepe. On the asymptotic stability of coupled delay differential and continuous time difference equations. *Automatica*, 41(1):107–112, 2005.

[Pep14] P. Pepe. Direct and converse Lyapunov theorems for functional difference systems. *Automatica*, 50(12):3054–3066, 2014.

[PGW12] C. Prieur, A. Girard, and E. Witrant. Lyapunov functions for switched linear hyperbolic systems. *IFAC Proceedings Volumes*, 45(9):382–387, 2012.

[PH22] L. Paunonen and J.-P. Humaloja. On robust regulation of pdes: from abstract methods to pde controllers. In *2022 IEEE 61st Conference on Decision and Control (CDC)*, pages 7362–7357. IEEE, 2022.

[PHSB91] M. Papageorgiou, H. Hadj-Salem, and J.-M. Blosseville. ALINEA: A local feedback control law for on-ramp metering. *Transportation research record*, 1320(1):58–67, 1991.

[PK13] P. Pepe and I. Karafyllis. Converse Lyapunov–Krasovskii theorems for systems described by neutral functional differential equations in Hale's form. *International Journal of Control*, 86(2):232–243, 2013.

[PM04] F. Poletto and F. Miranda. *Seismic while drilling: Fundamentals of drill-bit seismic for exploration*, volume 35. Elsevier, 2004.

[Pon15] A. Ponomarev. Reduction-based robustness analysis of linear predictor feedback for distributed input delays. *IEEE Transactions on Automatic Control*, 61(2):468–472, 2015.

[PR14] V. Perrollaz and L. Rosier. Finite-time stabilization of 2×2 hyperbolic systems on tree-shaped networks. *SIAM Journal on Control and Optimization*, 52(1):143–163, 2014.

[PSVDWN13] J. Ploeg, D. Shukla, N. Van De Wouw, and H. Nijmeijer. Controller synthesis for string stability of vehicle platoons. *IEEE Transactions on Intelligent Transportation Systems*, 15(2):854–865, 2013.

[PTDS16] C. Prieur, S. Tarbouriech, and J. G. Da Silva. Wave equation with cone-bounded control laws. *IEEE Transactions on Automatic Control*, 61(11):3452–3463, 2016.

[PTNA15] R. Postoyan, P. Tabuada, D. Nesic, and A. Anta. A framework for the event-triggered stabilization of nonlinear systems. *IEEE Transactions on Automatic Control*, 60(4):982–996, 2015.

[Qid09] U. Qidwai. Autonomous corrosion detection in gas pipelines: a hybrid-fuzzy classifier approach using ultrasonic nondestructive evaluation protocols. *IEEE transactions on ultrasonics, ferroelectrics, and frequency control*, 56(12):2650–2665, 2009.

[RA23] J. Redaud and J. Auriol. Backstepping stabilization of a clamped string with actuation inside the domain. *IFAC-PapersOnLine*, 56(2):9936–9941, 2023.

[RALG22a] J. Redaud, J. Auriol, and Y. Le Gorrec. Distributed damping assignment for a wave equation in the port-Hamiltonian framework. *IFAC-PapersOnLine*, 55(26):155–161, 2022.

[RALG22b] J. Redaud, J. Auriol, and Y. Le Gorrec. In-domain damping assignment of a Timoshenko-beam using state feedback boundary control. In *2022 IEEE 61st Conference on Decision and Control (CDC)*, pages 5405–5410. IEEE, 2022.

[RALG24] J. Redaud, J. Auriol, and Y. Le Gorrec. In domain dissipation assignment of boundary controlled Port-Hamiltonian systems using backstepping. *Systems and Control letters*, 2024.

[RAN21a] J. Redaud, J. Auriol, and S.-I. Niculescu. Observer design for a class of delay systems using a Fredholm transform. *IFAC-PapersOnLine*, 54(18):84–89, 2021.

[RAN21b] J. Redaud, J. Auriol, and S.-I. Niculescu. Output-feedback control of an underactuated network of interconnected hyperbolic PDE-ODE systems. *Systems & control letters*, 154:104984, 2021.

[RAN21c] J. Redaud, J. Auriol, and S.-I. Niculescu. Stabilizing integral delay dynamics and hyperbolic systems using a Fredholm transformation. In *2021 60th IEEE Conference on Decision and Control (CDC)*, pages 2595–2600. IEEE, 2021.

[RAN22a] J. Redaud, J. Auriol, and S.-I. Niculescu. Characterization of PI feedback controller gains for interconnected ode-hyperbolic pde systems. *IFAC-PapersOnLine*, 55(34):102–107, 2022.

[RAN22b] J. Redaud, J. Auriol, and S.-I. Niculescu. Recursive dynamics interconnection framework applied to angular velocity control of drilling systems. In *2022 American Control Conference (ACC)*, pages 5308–5313. IEEE, 2022.

[RAN22c] J. Redaud, J. Auriol, and S.-I. Niculescu. Stabilizing output-feedback control law for hyperbolic systems using a Fredholm transformation. *IEEE Transactions on Automatic Control*, 67(12):6651–6666, 2022.

[Ras74] V. Rasvan. Some results concerning the theory of electrical networks containing lossless transmission lines. *Revue Roumaine des Sciences Techniques*, 1974.

[RBAA22] J. Redaud, F. Bribiesca-Argomedo, and J. Auriol. Practical output regulation and tracking for linear ODE-hyperbolic PDE-ODE systems. In *Advances in distributed parameter systems*, pages 143–169. Springer, 2022.

[RBAA24] J. Redaud, F. Bribiesca-Argomedo, and J. Auriol. Output regulation and tracking for linear ODE-hyperbolic PDE–ODE systems. *Automatica*, 162:111503, 2024.

[RCMDL18] E. Rocha Campos, S. Mondié, and M. Di Loreto. Necessary stability conditions for linear difference equations in continuous time. *IEEE Transactions on Automatic Control*, 63(12):4405–4412, 2018.

[RDPD12] T. Richard, F. Dagrain, E. Poyol, and E. Detournay. Rock strength determination from scratch tests. *Engineering Geology*, 147:91–100, 2012.

[RGD07] T. Richard, C. Germay, and E. Detournay. A simplified model to explore the root cause of stick–slip vibrations in drilling systems with drag bits. *Journal of Sound and Vibration*, 305(3):432–456, aug 2007.

[RH03] M. Rausand and A. Hoyland. *System reliability theory: models, statistical methods, and applications*, volume 396. John Wiley & Sons, 2003.

[Ric56] P. Richards. Shock waves on the highway. *Operations research*, 4(1):42–51, 1956.

[RIH92] J. Rector III and B. Hardage. Radiation pattern and seismic waves generated by a working roller-cone drill bit. *Geophysics*, 57(10):1319–1333, 1992.

[RMDL17] E. Rocha, S. Mondié, and M. Di Loreto. On the Lyapunov matrix of linear delay difference equations in continuous time. *IFAC-PapersOnLine*, 50(1):6507–6512, 2017.

[RNM15] D. Rager, R. Neumann, and H. Murrenhoff. Simplified fluid transmission line model for pneumatic control applications. In *Proc. 14th Scandinavian International Conference on Fluid Power (SICFP15). Tampere, Finland*, 2015.

[Ros14] S. Ross. *Introduction to probability models*. Academic press, 2014.

[Rus72] D.L. Russell. Control theory of hyperbolic equations related to certain questions in harmonic analysis and spectral theory. *Journal of Mathematical Analysis and Applications*, 40(2):336–368, 1972.

[Rus78a] D.L. Russell. Canonical forms and spectral determination for a class of hyperbolic distributed parameter control systems. *Journal of Mathematical Analysis and Applications*, 62(1):186–225, 1978.

[Rus78b] D.L. Russell. Controllability and stabilizability theory for linear partial differential equations: recent progress and open questions. *Siam Review*, 20(4):639–739, 1978.

[Rus91] D.L. Russell. Neutral PDE canonical representations of hyperbolic systems. *The Journal of Integral Equations and Applications*, pages 129–166, 1991.

[RZLGM17] H. Ramirez, H. Zwart, Y. Le Gorrec, and A. Macchelli. On backstepping boundary control for a class of linear port-Hamiltonian systems. In *2017 IEEE 56th Annual Conference on Decision and Control*, pages 658–663. IEEE, 2017.

[SABA21] M. Schwenzer, M. Ay, T. Bergs, and D. Abel. Review on model predictive control: An engineering perspective. *The International Journal of Advanced Manufacturing Technology*, 117(5-6):1327–1349, 2021.

[SB18] R. S. Sutton and A. G. Barto. *Reinforcement learning: An introduction*. MIT press, 2018.

[SBO19] M. Sadeghpour, D. Breda, and G. Orosz. Stability of linear continuous-time systems with stochastically switching delays. *IEEE Transactions on Automatic Control*, 64(11):4741–4747, 2019.

[SBS17] M. Safi, L. Baudouin, and A. Seuret. Tractable sufficient stability conditions for a system coupling linear transport and differential equations. *Systems & Control Letters*, 110:1–8, 2017.

[SDHC15] R. J. Shor, M. W. Dykstra, O. J. Hoffmann, and M. Coming. For better or worse: applications of the transfer matrix approach for analyzing axial and torsional vibration. In *SPE/IADC Drilling Conference and Exhibition*. Society of Petroleum Engineers, 2015.

[SDMKR13] C. Sagert, F. Di Meglio, M. Krstic, and P. Rouchon. Backstepping and flatness approaches for stabilization of the stick-slip phenomenon for drilling. *IFAC Proceedings Volumes*, 46(2):779–784, 2013.

[SIH21] J. Sun, K. A. Innanen, and C. Huang. Physics-guided deep learning for seismic inversion with hybrid training and uncertainty analysis. *Geophysics*, 86(3):R303–R317, 2021.

[SK04] A. Smyshlyaev and M. Krstic. Closed-form boundary state feedbacks for a class of 1-D partial integro-differential equations. *IEEE Transactions on Automatic Control*, 49(12):2185–2202, 2004.

[Sle71] M. Slemrod. Nonexistence of oscillations in a nonlinear distributed network. *Journal of Mathematical Analysis and Applications*, 36(1):22–40, 1971.

[SLY+22] Y. Shi, Z. Li, H. Yu, D. Steeves, A. Anandkumar, and M. Krstic. Machine learning accelerated PDE backstepping observers. In *2022 IEEE 61st Conference on Decision and Control (CDC)*, pages 5423–5428. IEEE, 2022.

[SMLR11] B. Saldivar, S. Mondié, J.-J. Loiseau, and V. Rasvan. Stick-slip oscillations in oillwell drilstrings: Distributed parameter and neutral type retarded model approaches. *IFAC Proceedings Volumes (IFAC-PapersOnline)*, 18(PART 1):284–289, 2011.

[SOB10] R. Sipahi, N. Olgac, and D. Breda. A stability study on first-order neutral systems with three rationally independent time delays. *International Journal of Systems Science*, 41(12):1445–1455, 2010.

[SPSF21] S. Siri, C. Pasquale, S. Sacone, and A. Ferrara. Freeway traffic control: A survey. *Automatica*, 130:109655, 2021.

[SS08] P. Sharma and T. Singh. A correlation between p-wave velocity, impact strength index, slake durability index and uniaxial compressive strength. *Bulletin of Engineering Geology and the Environment*, 67(1):17–22, 2008.

[SvdSB11] R. Serban, A.J van der Schaft, and B. Besselink. Modelling and control of fluid power systems using the port-Hamiltonian approach. *International Journal of Fluid Power*, 12(1):27–38, 2011.

[SWGR13] C. Schmuck, F. Woittennek, A. Gensior, and J. Rudolph. Feed-forward control of an HVDC power transmission network. *IEEE Transactions on Control Systems Technology*, 22(2):597–606, 2013.

[SWS10] T. Stensgaard, C. White, and K. Schiffer. Subsea hardware installation from a FDPSO. In *Offshore technology conference*. OnePetro, 2010.

[Tab07] P. Tabuada. Event-triggered real-time scheduling of stabilizing control tasks. *IEEE Transactions on Automatic Control*, 52(9):1680–1685, 2007.

[TAK05] S. Tliba and H. Abou-Kandil. On the modeling of the electroelastic interaction between a plate and a piezoelectric patch. In ECCOMAS, editor, *International Conference on Computational Methods for Coupled Problems in Science and Engineering, COUPLED PROBLEMS 2005*, page 50, Santorini Islands, Greece, 2005.

[TAKP05] S. Tliba, H. Abou-Kandil, and C. Prieur. Active vibration damping of a smart flexible structure using piezoelectric transducers: $h\infty$ design and experimental results. *IFAC Proceedings Volumes*, 38(1):760–765, 2005.

[THDS15] E. Tzeng, J. Hoffman, T. Darrell, and K. Saenko. Simultaneous deep transfer across domains and tasks. In *Proceedings of the IEEE International Conference on Computer Vision*, pages 4068–4076, 2015.

[TW09] M. Tucsnak and G. Weiss. *Observation and control for operator semigroups*. Springer Science & Business Media, 2009.

[vdSGM02] A. J van der Schaft, P. J Gawthrop, and A. Müller. Port-Hamiltonian formulation of distributed parameter systems: Convective transport and phase transitions. *Journal of Mathematical Analysis and Applications*, 272(1):117–149, 2002.

[vdSM02] A.J. van der Schaft and B.M. Maschke. Hamiltonian formulation of distributed-parameter systems with boundary energy flow. *Journal of geometry and physics*, 42(1):166–194, 2002.

[vdWVvH+18] N. van de Wouw, T. Vromen, M. van Helmond, P. Astrid, A. Doris, and H. Nijmeijer. Experimental validation of torsional controllers for drilling systems. In *Advanced Topics in Nonsmooth Dynamics: Transactions of the European Network for Nonsmooth Dynamics*, pages 291–334. Springer, 2018.

[vdZP20] S. van der Zwan and I. Pothof. Operational optimization of district heating systems with temperature limited sources. *Energy and Buildings*, 226:110347, 2020.

[Vid72] M. Vidyasagar. Input-output stability of a broad class of linear time-invariant multivariable systems. *SIAM J. Control*, 10(1):203–209, 1972.

[Vil07] J.A Villegas. A port-Hamiltonian approach to distributed parameter systems, 2007.

[VK17] R. Vazquez and M. Krstic. Taking a step back: A brief history of PDE backstepping. *IFAC Proceedings Volumes*, 2017.

[VKC11] R. Vazquez, M. Krstic, and J.-M. Coron. Backstepping boundary stabilization and state estimation of a $2\times$ 2 linear hyperbolic system. In *Decision and Control and European Control Conference (CDC-ECC), 2011 50th IEEE Conference on*, pages 4937–4942. IEEE, 2011.

[VSP+17a] A. Vaswani, N. Shazeer, N. Parmar, J. Uszkoreit, L. Jones, A. Gomez, L. Kaiser, and I. Polosukhin. Attention is all you need. *Advances in neural information processing systems*, 30, 2017.

[VSP+17b] A. Vaswani, N. Shazeer, N. Parmar, J. Uszkoreit, L. Jones, A. Gomez, Ł. Kaiser, and I. Polosukhin. Attention is all you need. *Advances in neural information processing systems*, 30, 2017.

[WK20] J. Wang and M. Krstic. Delay-compensated control of sandwiched ODE–PDE–ODE hyperbolic systems for oil drilling and disaster relief. *Automatica*, 120:109131, 2020.

[WK21] J. Wang and M. Krstic. Event-triggered output-feedback backstepping control of 2x2 hyperbolic PDE-ODE systems. *IEEE transaction on automatic control*, 67(1):220–235, 2021.

[WK22] J. Wang and M. Krstic. Delay-compensated event-triggered boundary control of hyperbolic PDEs for deep-sea construction. *Automatica*, 138:110137, 2022.

[WKP18] J. Wang, M. Krstic, and Y. Pi. Control of a $2\times$ 2 coupled linear hyperbolic system sandwiched between 2 ODEs. *International Journal of Robust and Nonlinear Control*, 28(13):3987–4016, 2018.

[Woi13] F. Woittennek. Flatness based feedback design for hyperbolic distributed parameter systems with spatially varying coefficients. *IFAC Proceedings Volumes*, 46(26):37–42, 2013.

[WS17] Z.-G. Wu and S. Swei. Port-Hamiltonian modeling and control of beam vibration. *Mechanical Systems and Signal Processing*, 90:322–336, 2017.

[WWP21] S. Wang, H. Wang, and P. Perdikaris. Learning the solution operator of parametric partial differential equations with physics-informed DeepONets. *Science Advances*, 7(40):8605, October 2021.

[XLKF23] X. Xu, L. Liu, M. Krstic, and G. Feng. Stabilization of chains of linear parabolic pde–ode cascades. *Automatica*, 148:110763, 2023.

[XS02] C.-Z. Xu and G. Sallet. Exponential stability and transfer functions of processes governed by symmetric hyperbolic systems. *ESAIM: Control, Optimisation and Calculus of Variations*, 7:421–442, 2002.

[YAK20a] H. Yu, J. Auriol, and M. Krstic. Output-feedback PDE control of traffic flow on cascaded freeway segments. *IFAC-PapersOnLine*, 53(2):7623–7628, 2020.

[YAK20b] H. Yu, J. Auriol, and M. Krstic. Simultaneous stabilization of traffic flow on two connected roads. In *2020 American control conference (ACC)*, pages 3443–3448. IEEE, 2020.

[YAK22] H. Yu, J. Auriol, and M. Krstic. Simultaneous downstream and upstream output-feedback stabilization of cascaded freeway traffic. *Automatica*, 136:110044, 2022.

[YCBL14] J. Yosinski, J. Clune, Y. Bengio, and H. Lipson. How transferable are features in deep neural networks? In *Advances in neural information processing systems*, pages 3320–3328, 2014.

[YGBK21] H. Yu, Q. Gan, A. Bayen, and M. Krstic. PDE traffic observer validated on freeway data. *IEEE Transactions on Control Systems Technology*, 29(3), 2021.

[YK18] H. Yu and M. Krstic. Varying speed limit control of Aw-Rascle-Zhang traffic model. *Proceedings of the 21st International conference on Intelligent Transportation Systems (ITSC)*, pages 1846–1851, 2018.

[YK19] H. Yu and M. Krstic. Traffic congestion control for Aw-Rascle-Zhang model. *Automatica*, 100:38–51, 2019.

[YK23] H. Yu and M. Krstić. *Traffic Congestion Control by PDE Backstepping*. Springer, 2023.

[Yos60] K. Yoshida. *Lectures on differential and integral equations*, volume 10. Interscience Publishers, 1960.

[YSLL20] J. Yu, P. Shi, J. Liu, and C. Lin. Neuroadaptive finite-time control for nonlinear mimo systems with input constraint. *IEEE Transactions on Cybernetics*, 2020.

[Zha02] H.M. Zhang. A non-equilibrium traffic model devoid of gas-like behavior. *Transportation Research Part B: Methodological*, 36(3):275–290, 2002.

[ZHS16] D. Zhao, S. Hovda, and S. Sangesland. Abnormal Down Hole Pressure Variation by Axial Stick-Slip of Drillstring. *Journal of Petroleum Science and Engineering*, 145:194–204, 2016.

[ZLLP21] L. Zhang, H. Luan, Y. Lu, and C. Prieur. Boundary feedback stabilization of freeway traffic networks: ISS control and experiments. *IEEE Transactions on Control Systems Technology*, pages 1–12, 2021.

[ZP17] L. Zhang and C. Prieur. Stochastic stability of Markov jump hyperbolic systems with application to traffic flow control. *Automatica*, 86:29–37, 2017.

[ZPQ19] L. Zhang, C. Prieur, and J. Qiao. PI boundary control of linear hyperbolic balance laws with stabilization of ARZ traffic flow models. *Systems & Control Letters*, 123:85–91, 2019.

[ZW19] L. Zhang and K. Wang. PI boundary feedback control for freeway traffic networks. In *2019 Chinese Control Conference (CCC)*, pages 5297–5302. IEEE, 2019.

université PARIS-SACLAY

ÉCOLE DOCTORALE
Sciences et technologies de l'information et de la communication (STIC)

Titre: Contributions à la stabilisation robuste de réseaux de systèmes hyperboliques.
Mots clés: EPDs hyperboliques, réseaux, backstepping, équations à retards intégrales, systèmes à retards, équations intégrales.

Résumé:

Les réseaux de systèmes hyperboliques, éventuellement couplés à des équations différentielles ordinaires (ODE), constituent une représentation essentielle pour décrire une grande variété de systèmes complexes, pouvant modéliser la propagation d'ondes, des systèmes de trafic routier, des dispositifs de forage ou des réseaux de communication. Le contrôle et l'estimation d'état pour de tels systèmes sont des problèmes difficiles en raison de la nature distribuée des différents sous-systèmes composant le réseau (dépendance temporelle et spatiale), de la structure de graphe possiblement intriquée du réseau et de l'impossibilité physique/économique de placer des capteurs et actionneurs en tout point du domaine spatial. Ce manuscrit présente quelques contributions récentes concernant la stabilisation robuste des réseaux de systèmes hyperboliques. Nous montrons d'abord qu'en utilisant des transformations de backstepping appropriées, la classe de réseaux que nous considérons peut-être réécrite comme un ensemble d'équations à retards intégrales. Sous certaines hypothèses structurelles, cette nouvelle forme se prête mieux à la synthèse de lois de commande stabilisantes. Nous nous concentrons ensuite sur les réseaux avec une structure de chaîne afin de proposer de nouvelles méthodologies dépassant les limitations structurelles rencontrées précédemment. Nous considérons dans un premier temps le cas où les actionneurs et les capteurs sont disponibles à une extrémité de la chaîne. En introduisant des prédicteurs d'état, nous présentons une approche récursive permettant de stabiliser l'ensemble de la chaîne. Nous nous intéressons ensuite au cas où les actionneurs et capteurs ne sont disponibles qu'à la jonction entre deux sous-systèmes composant la chaîne. Nous montrons qu'une telle configuration ne garantit pas systématiquement la contrôlabilité de la chaîne. À l'aide de conditions de contrôlabilité/observabilité adéquates, nous proposons des lois de commande stabilisantes simples en utilisant un nouveau type de transformation intégrale. Enfin, nous illustrons comment nos résultats s'appliquent à deux cas d'étude : l'estimation de la vitesse d'une tête de forage et la stabilisation de deux segments d'autoroute en cascade. Nous concluons le manuscrit en donnant quelques perspectives générales.

Title: Contributions to the robust stabilization of networks of hyperbolic systems.
Keywords: hyperbolic PDEs, networks, backstepping, integral delay equations, time-delay systems.

Abstract: Networks of hyperbolic systems, possibly coupled with ordinary differential equations, constitute an essential paradigm to describe a wide variety of large complex systems, including wave propagation, traffic network systems, drilling devices, or communication networks. Controlling and monitoring networks of hyperbolic systems are difficult control engineering problems due to the distributed nature of the different subsystems composing the network (time and space dependency), the possibly involved graph structure of the network, and the physical/economic infeasibility of placing sensors and actuators everywhere along the spatial domain.

This manuscript presents some recent contributions to the robust stabilization of networks of hyperbolic systems. We first show that using appropriate backstepping transformations, the class of networks under consideration can be rewritten as a set of Integral Delay Equations. This new form is more amenable to the design of stabilizing output feedback control laws under structural assumptions. We then focus on networks with a chain structure to derive new methodologies that overcome the previously encountered structural limitations. We first consider the case where the actuators and sensors are available at one end of the chain. Using appropriate state predictors, we present a recursive approach to stabilize the whole chain. Then, we focus on the case where the actuators and sensors are only available at the junction between two subsystems composing the chain. We show that such a configuration does not always guarantee the controllability of the chain. Under appropriate controllability/observability conditions, we will design simple stabilizing control laws using a new type of integral transformation. Finally, we illustrate how our results apply to two test cases: estimating the drill bit source signature in a drilling device and stabilizing two cascaded freeway segments. We conclude the manuscript by giving some general perspectives.